

**Discovery of BACE-1 inhibitors using an integrated computational and
experimental approach**

Giorgia Magnatti

Submitted in accordance with the requirements for the degree of
Doctor of Philosophy

The University of Leeds

School of Chemistry

July 2014

The candidate confirms that the work submitted is her own and that appropriate credit has been given where reference has been made to the work of others.

This copy has been supplied on the understanding that it is copyright material and that no quotation from the thesis may be published without proper acknowledgement.

© 2014 The University of Leeds and Giorgia Magnatti

The right of Giorgia Magnatti to be identified as Author of this work has been asserted by her in accordance with the Copyright, Designs and Patents Act 1988.

Acknowledgements

I am very proud to have concluded my PhD studies after three and half long years. At the beginning I found myself lost in deep personal and professional doubts and I was brave in carrying on. Gradually I found my place in the Nelson lab, thanks to my determination and my hard-working attitude. I have to thank many people who supported me in many different ways during my PhD journey and who believed in me.

My first thanks go to my main supervisor Prof. Adam Nelson and to my co-supervisors Prof. Colin Fishwick and Prof. Nigel Hooper. Adam's suggestions and methodical approach to PhD progression was very important. Colin and Nigel contributed in the development of my medicinal chemistry project, showing different point of views which enriched my computational and biological knowledge. My second thanks go to past and present members of Adam Nelson's group, for intellectual discussion, sharing of knowledge, proof reading and moral support. Being in the Nelson lab is a unique experience, I feel I learnt much and I am aware there is always much more to learn.

Among the Nelson group I would like to thank Francesco for the initial (and tricky) help during the first year of my PhD; Charles-Hugues for his friendship (mon ami), his proof reading and his lesson of accuracy and attention to detail (I will never forget the difference between a minus symbol and a dash, while the difference between the apostrophe and the prime symbol will always be a mystery to me); Tom James for his unexpected and gratifying support in learning organic chemistry mechanisms; Richard for the delicate managing of lab maintenance (it is a nightmare, I know!) and for his proof reading; George B. for having showed the use of the semi-prep HPLC; Phil for having proof-read major chapters of my thesis and Raj for having read parts of my experimental chapter. I would like to thank also Steven for his squash lessons, his attempts in learning Italian and his help in using Microsoft Word; George K. for his support in discussing, analysing and interpreting my biological results, his company at the ISACS11 conference in Boston and at many evenings spent with Maria and Keeran; Alun for his talent in doing beautiful impersonations (they often made my day!) and Rong for her tasty cakes.

A big thank goes to all the Italian friends I met in Leeds since December 2010, with whom I shared a flat/house and personal life outside the lab in different occasions. In

particular I would like to mention Chiara (important for my initial staying in Leeds), Pier, Giulio, Bianca, Carlo, Elisa, all great friends! I want to thank also all the beautiful people I met in the School of Chemistry at the University of Leeds, Valeria, Phil, Dave, Roberta, Andrea, George P. and Kerya, thanks for coffee breaks and chats.

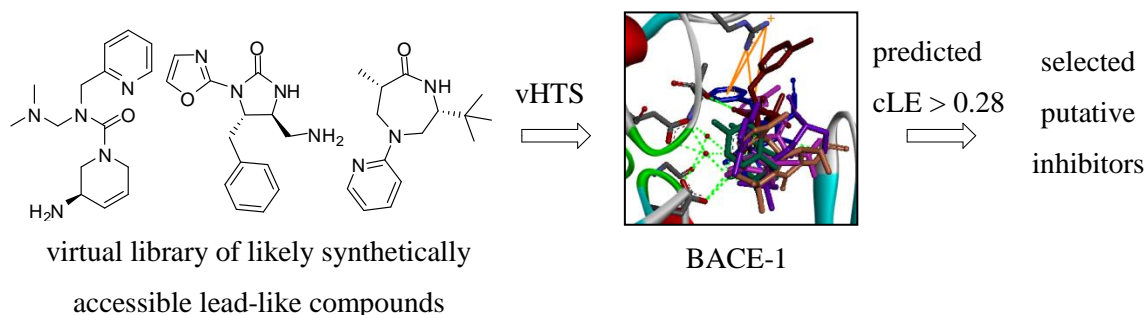
I want to dedicate a very special thanks to Keeran, my German-Yorkshire boyfriend, who made my life happier and much more enjoyable in Leeds and who was an incredible point of reference in many moments. (Dankeschön mein Lieber Cruccoman!) Finally I cannot forget to thank my marvellous and inimitable family and my incredible and fantastic close friends from Rome who followed my PhD journey from the other side of the English Channel, being always as present as possible. The following few lines in Italian are for them.

Questa dedica e' per la mia famiglia, favolosa, unica e inimitabile. Mamma, papa; sorella e nonna siete delle belle persone, piene di vita, gioiose e dolcissime. Vi sento sempre vicino e mi avete fatto sentire il vostro affetto e la vostra carica anche da lontano. Sono dispiaciuta di non aver potuto seguire da vicino alcuni cambiamenti familiari e sono stata sorpresa con la semplicita' con cui tutto e' avvenuto, mantenendo i rapporti tra di noi sempre uguali ed intensi. Mamma, sei una bomba, il tuo spirito di vita e' un esempio. Ilaria, sei una donna grandiosa che ha affrontato da sola molte situazioni difficili e che ha assistito mamma e papa' nelle loro decisioni mentre io ero lontano. Grazie!! Prometto che mi rifaro' e trovero' il modo di starti piu' vicina! A voi amici (Daria, Noemi, Gabriele, Michela, Laura, Mary Christine, Claudio) voglio dire che siete un dono meraviglioso e siete stati bravissimi a non dimenticarvi di me e a farmi sentire sempre tra di voi! Grazie di cuore. Spero di avervi reso tutti voi, amici e parenti, orgogliosi di me.

Abstract

There are numerous complementary approaches to facilitate the identification of novel inhibitors for biological targets, including high throughput screening and fragment-based drug discovery. Computational tools are often employed to predict binding pose and affinity of the new inhibitors. In this thesis an integrated computational and experimental approach to identify novel inhibitors is described. The approach involves the design of a virtual library of likely synthetically accessible lead-like molecules, followed by virtual high throughput screening (vHTS) against target protein. To exemplify the approach, BACE-1 was selected as an example target protein. BACE-1 is responsible for the formation of amyloid plaque in brains affected by Alzheimer's disease and therefore is a potential target for the treatment of the disease.

A virtual library of lead-like molecules was generated based on diversity-oriented synthesis methods established in our laboratory. The library underwent virtual high throughput screening (vHTS) against BACE-1 by using eHiTS and two families of putative inhibitors were identified with high predicted ligand efficiency (cLE). The *in silico* approach employed to identify novel putative BACE-1 inhibitors is schematically represented as follows.



A focused library based on the selected putative inhibitors was designed and synthesised, and biological activity was assessed *via* a fluorimetric assay. Structure-activity relationship (SAR) studies were conducted to rationalise the activity of the inhibitors and to confirm the validity of the integrated approach in identifying new inhibitors for biological targets. A novel series of BACE-1 inhibitors was identified and is herein described.

Table of Contents

Abstract	v
Abbreviations and nomenclature	x
Chapter 1. Introduction	1
1.1 Drug discovery process: from leads to drug candidates	1
1.2 Approaches to identify lead compounds	3
1.2.1 High throughput screening	3
1.2.2 Fragment-based design	4
1.2.3 Virtual screening	5
1.2.3.1 Criteria for ligand selection: ligand efficiency	7
1.2.4 Diversity-oriented synthesis	9
1.2.5 Combining diversity oriented synthesis and virtual screening	13
1.3 BACE-1	14
1.3.1 Involvement in Alzheimer's disease	14
1.3.2 Structure and catalytic mechanism	16
1.3.3 Specificity for the APP substrate	20
1.4 Overview of BACE-1 inhibitors	22
1.4.1 The first peptidomimetic inhibitor: compound OM99-2	23
1.4.2 Inhibitors incorporating a transition state isostere as a central core	24
1.4.3 Reducing inhibitor peptidic character, towards macrocyclic inhibitors	26
1.4.4 Discovery of non-peptidomimetic inhibitors	29
1.4.5 An interesting spiro piperidine iminohydantoin inhibitor	31
1.4.6 Inhibitor designed through computational methods	33
1.4.7 Challenges of BACE-1 inhibitor design, failure in clinical trials	35
1.5 Project outline	35

Chapter 2. Structure-based design of putative bioactive molecules for BACE-1	37
2.1 Overview of the computational approach	37
2.1.1 Pipeline Pilot	38
2.1.2 eHiTS	40
2.1.3 Ligand selection	41
2.2 Testing the applicability of eHiTS to BACE-1	43
2.3 Design of a virtual library of likely synthetically accessible lead-like compounds	47
2.3.1 Identification of promising ligands	49
2.3.2 Optimisation of <i>library A</i> and identification of two families of putative BACE-1 inhibitors	50
2.4 Analysis of the predicted binding poses of the putative inhibitors	54
2.4.1 Validation of the predicted binding poses with additional docking software	57
2.4.2 Design of a focused library of putative inhibitors	62
2.5 Summary	63
Chapter 3. Synthesis of a library of imidazolidinones	65
3.1 Identification of two possible synthetic routes	65
3.2 Synthetic route to the target imidazolidinones based upon a Pd-catalysed aminoarylation	66
3.2.1 Synthesis of substrates for the Pd-catalysed aminoarylation	67
3.2.2 Investigation of the Pd-catalysed aminoarylation	72
3.2.2.1 Determination of the stereochemical outcome of the Pd-catalysed aminoarylation	74
3.2.2.2 Rationalisation of the stereochemical outcome of the Pd-catalysed aminoarylation	75
3.2.2.3 Proposed mechanism for the formation of the <i>N</i> -arylated imidazolidinone 27	76

3.2.3 Practicability of the route based upon the Pd-catalysed aminoarylation	77
3.3 Synthetic route to the target imidazolidinones based upon an iodine-mediated cyclisation reaction	78
3.3.1 Exploration of synthetic route from benzylallylic amine	79
3.3.2 Synthesis of the target imidazolidinones	80
3.3.2.1 Synthesis of substrates for the iodine-mediated cyclisation	81
3.3.2.2 Synthesis of a focused library of imidazolidinones	83
3.3.2.3 Determination of the relative configuration of products	86
3.3.2.4 Rationalisation of the stereochemical outcome of the urea ring formation	87
3.4 Summary	88
Chapter 4. Biological activity evaluation of BACE-1 imidazolidinone putative inhibitors	89
4.1 Assay for biological activity evaluation against BACE-1	89
4.2 Biological activity measurements	90
4.2.1 Analysis of structure-activity relationship	96
4.3 Design of structural analogues of active compounds	101
4.3.1 Synthesis of monosubstituted analogues	102
4.3.2 Synthesis of bisubstituted analogues	103
4.3.3 Biological evaluation of a second generation of analogues	104
4.4 Assessing inhibitor selectivity for BACE-1	108
4.4.1 Biological activity measurements	108
4.5 Summary	110
4.6 Conclusion and future directions	112
Chapter 5. Experimental	119
5.1 General experimental	119
5.2 General experimental procedure	121

5.3 Experimental procedures for compounds	124
5.4 General procedure for biological fluorimetric assay	180
5.4.1 Protocol to assess the optimal concentration of BACE-2 to use in a fluorimetric assay	182
Appendix 1. Virtual library generation supplementary information	183
1.1 Virtual reactants employed in the virtual synthesis protocol to enumerate virtual library A (Section 2.3)	183
1.1.2 Electrophile building blocks	185
1.1.3 Derivatisation reagents	186
1.2 Virtual reactants employed in the virtual synthesis protocol to enumerate virtual library B (Section 2.3.2)	187
1.3 Virtual reactions employed in the virtual synthesis protocol for the enumeration of <i>libraries A</i> and <i>B</i> (Section 2.3 and 2.3.2)	188
Appendix 2. Virtual screening supplementary information	193
2.1 Predicted binding pose of representative ligands in the BACE-1 catalytic site, free from water molecules (Section 2.4)	193
2.2 H-bond length evaluation (Section 2.4.1)	195
Appendix 3. Stereochemical assignment of the synthesised imidazolidinones (Section 3.2.2.1 and 3.3.2.3)	197
Appendix 4. Biological data supplementary information	201
4.1 Dose responses curves of active imidazolidinones (Section 4.2)	201
4.2 Assessing the optimal concentration of BACE-2 for biological fluorimetric assay	202
Reference	205

Abbreviations and nomenclature

°C	Celsius degrees
2D	two dimensional
3D	three dimensional
Å	Ångström
A (Ala)	alanine
A β	amyloid β
Ac	acetyl
App	apparent
APP	amyloid precursor protein
Ar	aromatic
BACE	β -site amyloid precursor protein cleaving enzyme
Bn	benzyl
Boc	<i>tert</i> -butyloxycarbonyl
b.p.	boiling point
br	broad
Bu	butyl
<i>ca.</i>	circa; about
CTF-99	carboxy-terminal fragment of 99 amino acids
δ	chemical shift
d	doublet
D (Asp)	aspartate
DBU	1,8-diazabicyclo[5.4.0]undec-7-ene
<i>de novo</i>	anew
DEAD	diethyl azodicarboxylate
dd	double doublet
ddd	double double of doublet

dddd	double double double of doublet
ddt	double doublet of triplet
DIBAL	diisobutylaluminium hydride
DIPEA	<i>N,N</i> -diisopropylethylamine
^F DIPES	diisopropyl(3,3,4,4,5,5,6,6,7,7,8,8,9,9,10,10,10-heptafluorodecyl)silyl
DMB	3,4 dimethoxy benzyl
DMF	<i>N, N</i> -dimethylformamide
DMSO	dimethyl sulfoxide
DOS	diversity-oriented synthesis
DPPA	diphenylphosphoryl azide
dq	double quadruplet
dt	double triplet
dtd	double triplet of doublet
<i>E</i>	<i>entgegen</i>
E (Glu)	glutamate
<i>e.g.</i>	exempli gratia; for example
Et	ethyl
<i>et al.</i>	et alii; and others
eHiTS	electronic high-throughput screening
EI	electron impact
ELISA	enzyme-linked immunosorbent assay
eq.	equivalent
ES	electron spray
F (Phe)	phenylalanine
FBDD	fragment-based drug design
FGI	functional group interconversion
F.U.	fluorescence unit

g	grams
G (Gly)	glycine
h	hours
H(His)	histidine
hept	heptuplet
(v)HTS	(virtual) high-throughput screen
HE	hydroxyethylene
HEA	hydroxyethylamine
HPLC	high-performance liquid chromatography
HRMS	high-resolution mass spectrometry
Hz	Hertz
I (Ile)	isoleucine
IC ₅₀	50% inhibitory concentration
<i>in silico</i>	performed by computer simulation
<i>in situ</i>	in place
IR	infrared
ⁱ Pr	<i>isopropyl</i>
K (Lys)	lysine
K _i	constant of inhibition
<i>J</i>	spin-spin coupling constant
L (Leu)	leucine
LC/MS	liquid chromatography–mass spectrometry
(c)LE	(computational) ligand efficiency
log	logarithm in base 10
m	multiplet
M (Met)	methionine
Me	methyl

mg	milligram
mL	millilitre
mM	milli mole
MOM	methoxymethyl
m.p.	melting point
μL	microlitre
Ms	mesyl
M.W.	molecular weight
<i>m/z</i>	mass to charge ratio
n	number
N (Asn)	asparagine
N/A	not available
n-Bu	normal butyl
nHA	number of heavy atoms
NIS	<i>N</i> -iodosuccinimide
nM	nanomolar
NMR	nuclear magnetic resonance
nOe	nuclear Overhauser effect
Ns	<i>o</i> -nitrophenylsulfonyl
Ns'	<i>p</i> -nitrophenylsulfonyl
P	partition coefficient
pdb	protein data bank
Petrol	petroleum spirit (b.p. 40-60 °C)
PG	protecting group
pH	potential of hydrogen
Ph	phenyl
ppm	parts per million

Pr	propyl
Py	pyridine
q	quadruplet
Q (Gln)	glutamine
R (Arg)	arginine
R_F	solvent front
r.t.	room temperature
σ	standard deviation
s	singlet
S (Ser)	serine
SAR(s)	structure-activity relationship(s)
SBDD	structure-based drug design
t	triplet
T (Thr)	threonine
td	triple doublet
tdd	triple double doublet
tt	triple triplet
^t Bu	<i>tert</i> -butyl
<i>tert</i>	tertiary
Tf	triflate; trifluoromethanesulfonate
TFA	trifluoroacetic acid
THF	tetrahydrofuran
TLC	thin layer chromatography
TMS	trimethylsilyl or trimethylsilane
TR-FRET	time-resolved fluorescence resonance energy transfer
V (Val)	valine
v/v	volume solute/volume solution

<i>via</i>	by way of
v	wavelength
W (Trp)	tryptophan
w/v	weight/volume
Y (Tyr)	tyrosine
Z	<i>zusammen</i>

Chapter 1. Introduction

This introductory Chapter is composed of two parts. The first part gives an overview of the drug discovery process (Section 1.1) and of methods to identify and generate lead molecules for biological targets (Section 1.2). The second part introduces the protein BACE-1, the biological target chosen for this project (Section 1.3) and gives an overview of known BACE-1 inhibitors (Section 1.4). Finally an outline of the project is provided (Section 1.5).

1.1 Drug discovery process: from leads to drug candidates

The discovery of drugs for biological targets is a long process, which starts by identifying initial molecules, called hits or leads, having affinity for a specific biological target. Lead molecules can be identified by a variety of screening methods (Section 1.2); once a lead is identified, studies of its properties are performed in order to understand the role that different functional groups have in binding the target. Structure-activity relationship (SAR) studies facilitate lead optimisation and ultimately a drug candidate is nominated.

The physico-chemical properties of optimal oral drugs can be described by the Lipinski “rule of five”. This rule provides guidance of the ideal molecular weight (M.W. ≤ 500) and lipophilicity ($\log P^a \leq 5$), and of the number of H-bonding atoms (number of H-bond donors ≤ 5 , number of H-bond acceptors ≤ 10)¹ that a drug should have to allow for oral bioavailability, absorption and permeation. Since drug candidates are developed from leads, physico-chemical properties of leads have been defined as well. Good leads generally have molecular weight between $200 \leq \text{M.W.} \leq 350$, lipophilicity value in the range of $-1 \leq \log P \leq +3$,² number of H-bonding donors ≤ 4 , number of H-bond acceptors ≤ 8 .³

^aP is the partition coefficient which expresses the solubility of a unionised compound in two immiscible solvents, *n*-octanol and water. $P = [\text{solute}]_{\text{octanol}} / [\text{solute}]_{\text{water}}$. $\log P$ is used as a measurement of lipophilicity.

A clearer visual representation of lead development into drug candidates is provided by Nadin *et al.*² (Figure 1). The chemical space of bioactive small molecules can be represented by lipophilicity and molecular weight. Typically, the drug discovery process results in a progression towards higher molecular weight and lipophilicity values. Drug candidates space is represented below $M.W. \leq 400$, $\log P \leq 4$, since it is often observed that molecules with these physico-chemical properties have more chance of becoming successful drugs.⁴ In Nadin's representation it is also shown that fragments, defined as small molecules having a molecular weight between $100 \leq M.W. \leq 300$ and low lipophilicity, $-1.5 \leq \log P \leq 1.5$, are a good starting point to develop leads.

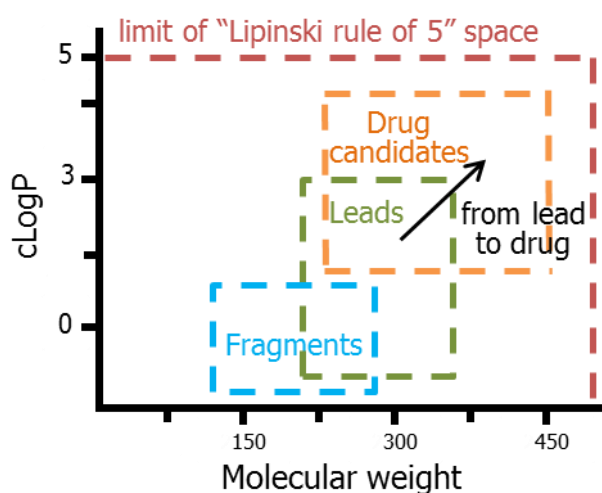


Figure 1. Chemical space of drug candidates, leads, and fragments. Representation of the chemical space explored during drug discovery process. $clogP$ is a predicted measurement of $\log P$ estimated from a computed algorithm which sum $\log P$ values of small parts of a molecule.⁵ Adapted from Nadin *et al.*²

A summary of physico-chemical properties of drug-like, lead-like and fragment-like molecules is given in Table 1. It is worth mentioning that lead-likeness criteria were defined in a broader way ($M.W. \leq 460$ and $\log P \leq 4$ ⁶) before Nadin's definition in 2012. Nadin's chemical space definition can be considered an up-to-date guideline to develop and design optimal leads (Section 1.2.4).

Table 1. Guidelines of physico-chemical properties of drug-like, lead-like and fragment-like molecules

Drug-like molecules ¹	Lead-like molecules ²	Fragment-like molecules ²
M.W. \leq 500	200 \leq M.W. \leq 350	100 \leq M.W. \leq 300
logP \leq 5	-1 \leq logP \leq +3	-1.5 \leq logP \leq +1.5
n H-bond donors \leq 5	n H-bond donors \leq 4 ³	n H-bond donors \leq 3 ⁷
n H-bond acceptors \leq 10	n H-bond acceptors \leq 8 ³	n H-bond acceptors \leq 3 ⁷
n aromatic rings \leq 5 ⁸	n aromatic rings \leq 3 ⁸	- ^a
- ^a	16 \leq nHA ^b \leq 26	- ^a

^aNot defined ^bnHA: number of heavy atoms, corresponding to number of non-hydrogen atoms. nHA is related to the molecular weight, therefore is not always defined.

1.2 Approaches to identify lead compounds

1.2.1 High throughput screening

Approaches to identify leads can be categorised as: high throughput screening (HTS), fragment-based design and virtual high throughput screening (vHTS). HTS refers to screening of large compound libraries (up to 100.000 per day⁹) against a biological target by means of established and validated biochemical (*e.g.* ELISA¹⁰), biophysical (*e.g.* TR-FRET¹¹) or biological assays (*e.g.* cell based¹²) which can measure compound binding affinity. HTS has been widely used by pharmaceutical companies since the mid-1990s.⁹ The screening is generally automated, molecules are assayed in a μ M concentration or lower, and up to 1536 compounds are screened in a run. It is useful to apply when there is no knowledge about the structure of a biological target, as any identified hits can give indication about relevant structure features. When information about the structure of likely active molecules is available, HTS is also applied to focused library subsets. This approach was successful for a range of biological targets, *e.g.* protein kinases, transferases, proteases and nuclear hormone receptors.¹³

1.2.2 Fragment-based design

Fragment-based approaches were developed with the idea of identifying key fragment-sized molecules, able to bind discrete sites of a biological target, and to link them in order to build a lead molecule. These approaches have the potential to combine active fragments in many possible ways, building a variety of potentially active leads. Physico-chemical properties of fragments, have been defined according to the “rule of three”: $M.W. \leq 300$, $\log P \leq 3$, number of H-bond donors and acceptors ≤ 3 (Table 1).⁷ The “rule of three” is used as a good guideline to prepare libraries of fragments, which can be also chosen for their commercial availability and solubility at high concentrations (mM range). Methods of screening fragments include: directed binding assays (*e.g.* ELISA), NMR¹⁴, mass-spectrometry^{15,16} and X-ray.¹⁷ Once active fragments are identified, they can be linked with chemical spacers known from previous inhibitors;¹⁸ alternatively a technique of “*in situ* assembly” can be employed. This technique consists of adding reactive fragments in the presence of the biological target and analysing the higher affinity products obtained.¹⁹

The process of growing fragments into leads is often assisted by computational docking programs, which contain virtual library of linkers. The so-called *de novo* generation software use the coordinates of a known binding pose of a fragment in a target binding site and connect this fragment to virtual linkers and other fragments directly in the target binding site. The resulting virtual leads are docked and ranked according to predicted binding affinity values²⁰ or ligand efficiency, which expresses the affinity per heavy atom (see Section 1.2.3.1). Examples of *de novo* generation software are shown in Table 2.²¹ Due to the potential of combining fragments in different ways, fragment-based approaches enable efficient coverage of chemical space.

Table 2. Examples of *de novo* generation software.²¹

Examples of software	Characteristic
LUDI	<p>Fragments are selected according to the hydrogen bond interactions formed in the protein binding site and to the hydrophobic pocket filling. Fragments are scored, linked together and collected in a library.</p> <p>The protein binding site is classified in areas of directional interactions: lipophilic-aliphatic, lipophilic-aromatic, hydrogen donor and hydrogen acceptor.</p> <p>The library of fragments is matched with the four binding site areas to identify a new potential ligand.</p>
GROW	<p>An initial fragment is placed in the protein binding site and is grown by peptide bond formation.</p> <p>The molecule obtained is scored according to a function of energies parameters: van der Waals, electrostatic, conformational and solvation.</p>
SPROUT	<p>Fragments are sorted according to shape and molecular properties. The target site is divided in different hydrogen-bonding, electrostatic and hydrophobic areas. Fragments are docked in all the binding site areas according to their shape and are linked together.</p> <p>Atoms with the same hybridisation are interchanged in the fragment structures to optimise the interactions. Fragments are scored according to enthalpy and entropy factors to identify the potential ligand.</p>

1.2.3 Virtual screening

Virtual screening is used in drug discovery to predict binding affinity of virtual or known compounds against a specific biological target or to design variations of known active molecules. Virtual screening can help to identify putative leads; therefore the software predictions of lead binding affinity need to be proven by established assays. Virtual screening methods can be differentiated into structure-based and ligand-based methods.

Structure-based virtual screening requires knowledge of the binding site of a biological target to predict binding poses of ligands and to estimate their binding affinity through scoring functions.²² The prediction of binding poses can be performed according to different docking programs; using stochastic or systematic methods.²³ Stochastic methods perform random simulations of ligand binding poses until

convergence criteria are met. In the Monte Carlo method, for example, a ligand is randomly placed in the binding site and its degree of thermal motion is gradually decreased, until a stable state with minimum energy is reached.²⁴ Systematic methods decompose ligands into fragments and dock them independently in a protein binding site; then the final binding pose is built on the basis of those docking results. The reconstruction of a ligand structure from fragments is performed through incremental construction or conformational search algorithm (for more details, see Table 3).²³

The estimation of binding affinity for the predicted ligand binding poses is made using scoring functions. Scoring functions are based on mathematical models and can be categorised as force-field, empirical and knowledge based.²⁵ Force-field scoring functions assess the free energy of binding by deriving the enthalpy of binding at gas phase as sum of van der Waals and electrostatic intramolecular interactions. Intramolecular strain energy (angle, torsional, steric strain), entropic and desolvation energies are also included. Empirical scoring functions estimate the binding affinity from a series of energy terms: van der Waals, ionic, hydrogen bond, hydrophobic interactions and surface complementarity. The knowledge-based scoring function uses databases of known inhibitor-protein complexes to compare distance between ligand and protein atom types and to derive a favourable interaction. The ligand binding energy is derived from a function of distribution of atom pair interactions. The mathematical models, on which scoring functions are based, do not always consider entropic or flexibility factors in the estimation of binding affinity. Scoring functions are therefore limited and implementations of their mathematical models are still challenging.²⁵

Ligand-based virtual screening aims to enrich active compounds. Libraries of (virtual or real) ligands are compared with an active compound of reference according to structural and pharmacophoric similarity. The similarity search algorithm can perform a structure comparison by superimposing each ligand with the compound of reference (small molecule alignment search), or by considering electrostatic and conformational properties (pharmacophore similarity search).²⁴ As an outcome, ligands are ranked according to similarity to the active compounds.

Table 3. Summary of virtual screening method.²³

Stochastic method	Characteristic	Examples of software
Monte Carlo	Cycles of simulations of ligand poses in the protein binding site are applied. The initial thermal motion of a ligand is gradually decreased until reaching a minimum energy.	Autodock, ICM
Genetic algorithm	Initial ligand states are defined according to conformation and orientations, and then they are modified by random gene-fashion crossover and mutation. The resulting new ligands are selected according to their fit. ²⁶	DOCK, GOLD
Systematic method	Characteristic	Examples of software
Incremental construction algorithm	Ligands are broken into fragments by cutting at rotating bond positions. Set of rigid fragments, called anchors, are docked against the binding site. Flexible fragments are matched to anchors and docked considering different torsion angles.	DOCK 4.0, FlexX, Hammerhead
Conformational search	Ligands are broken into fragments and a set of rigid fragments are docked. Only fragment poses which correspond to the original ligand structure are kept and flexible chains are added to these specific rigid fragment poses.	eHiTS, FLOG

1.2.3.1 Criteria for ligand selection: ligand efficiency

Ligand efficiency (LE)²⁷ is widely employed in the literature to evaluate the binding quality of ligands of different sizes to a target protein. LE is defined as the free energy of binding, ΔG° , of a ligand divided by its number of heavy atom, nHA (Equation 1). LE helps to identify ligands which bind to a target protein efficiently. Ligands with a large number of heavy atoms can show a high binding affinity, but they are less efficient than ligands showing the same binding affinity and having a smaller number of heavy atoms (Figure 2).²⁸

$$LE = \frac{\Delta G^\ominus}{nHA}$$

Equation 1. Ligand efficiency definition.

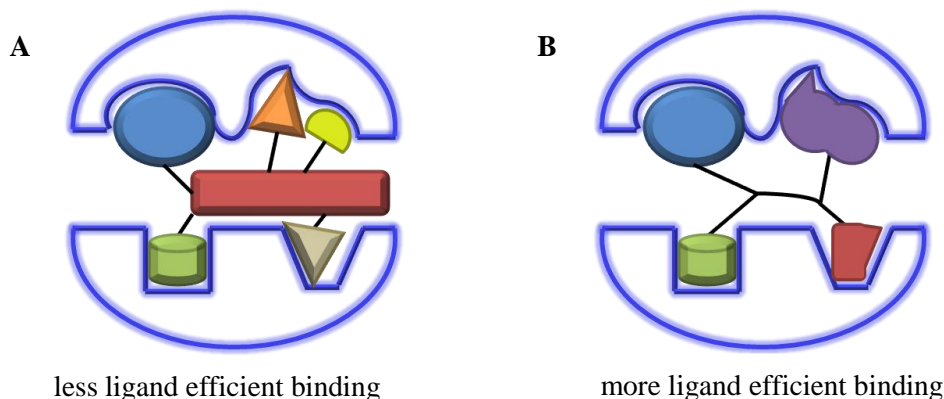


Figure 2. Representation of the ligand efficiency concept. Cartoon of a protein binding site occupied by two ligands with the same binding affinity but of different sizes. A) The ligand is filling all the cavities of the protein binding site by interacting with five different groups, two of them with low-quality binding (orange and brown colour elements). B) The ligand is filling all the cavities of the protein binding site by interacting with four groups, each giving high-quality binding. Adapted from Kitchen *et al.*²⁸

It is often reported in the literature^{29, 30} that when values of K_i and IC_{50} of ligands are available, they can be used in their logarithmic forms (\log) to calculate LE, in place of ΔG^\ominus , according to Equation 2.³¹ The difference between ΔG^\ominus and $\log(K_i)$ is, in fact, a factor of 1.37, as shown in Equation 3.³² Therefore the LE' values calculated with $\log(K_i)$ would only differ from the LE values calculated with ΔG^\ominus by the same factor (Equation 4).

$$LE' = -\frac{\log(K_i)}{nHA} \approx -\frac{\log(IC_{50})}{nHA}$$

Equation 2. Ligand efficiency calculated with $\log(K_i)$ and $\log(IC_{50})$.^{b, 31}

^b In Equation 2 the difference between K_i and IC_{50} is taken in account²⁹

$$\Delta G^\ominus = -2.30 \times RT \times \log(K_i) = -1.37 \times \log(K_i) \approx -1.37 \times \log(IC_{50})$$

Equation 3. Correlation between ΔG^\ominus and $\log(K_i)$ or $\log(IC_{50})$.

$$LE = 1.37 \times LE'$$

Equation 4. Difference between LE and LE'

The definitions of LE and LE', as expressed in the **Equation 1** and **2**, can also be applied to assess the quality of binding of the virtual ligands. Docking software predict the binding affinity of virtual ligands giving a score which expresses $\log(K_i)$; therefore this score can be used to calculate computed/ predicted ligand efficiency, cLE or cLE', according to Equation 5. In this report LE' and cLE' will be used to compare quality of binding of known BACE-1 inhibitors (Section 1.4) or predicted inhibitors (Section 2.1.3)

$$cLE = -1.37 \times \frac{\text{score}}{nHA}; \quad cLE' = -\frac{\text{score}}{nHA}$$

Equation 5. Computed ligand efficiency, cLE and cLE'.

1.2.4 Diversity-oriented synthesis

Combinatorial libraries of compounds of biological interest and large compound collections of pharmaceutical companies tend to lack diversity in shape and in structure, being mainly populated by flat compounds (2-D shape) which differ by their appendages, rather than their skeleton.³³ An analysis of ten commercially available libraries, performed by Baell in 2012,³ showed that vendor libraries of *ca.* 400,000 compounds contained only 6,000 lead-like molecules, which lack diversity. Since the biological activity of compounds depends on their structural features, compound libraries with a high degree of structural diversity increase the probability of interaction with different biological targets.³⁴ Therefore a demand for developing more structurally diverse libraries of lead-like molecules has risen in drug discovery.

It has been demonstrated that a convenient strategy to create a library of skeletally diverse compounds is to start from a range of different chemotypes, rather than

extending or varying the structure of a single chemotype.³⁵ A successful synthetic approach towards diversity enriched libraries is that of diversity-oriented synthesis (DOS). The principle of DOS is to generate multiple scaffolds by performing parallel modification of starting materials to access a series of structurally diverse building blocks/chemotypes. These are able to undergo further diversification. A schematic representation of the DOS approach is given Figure 3.

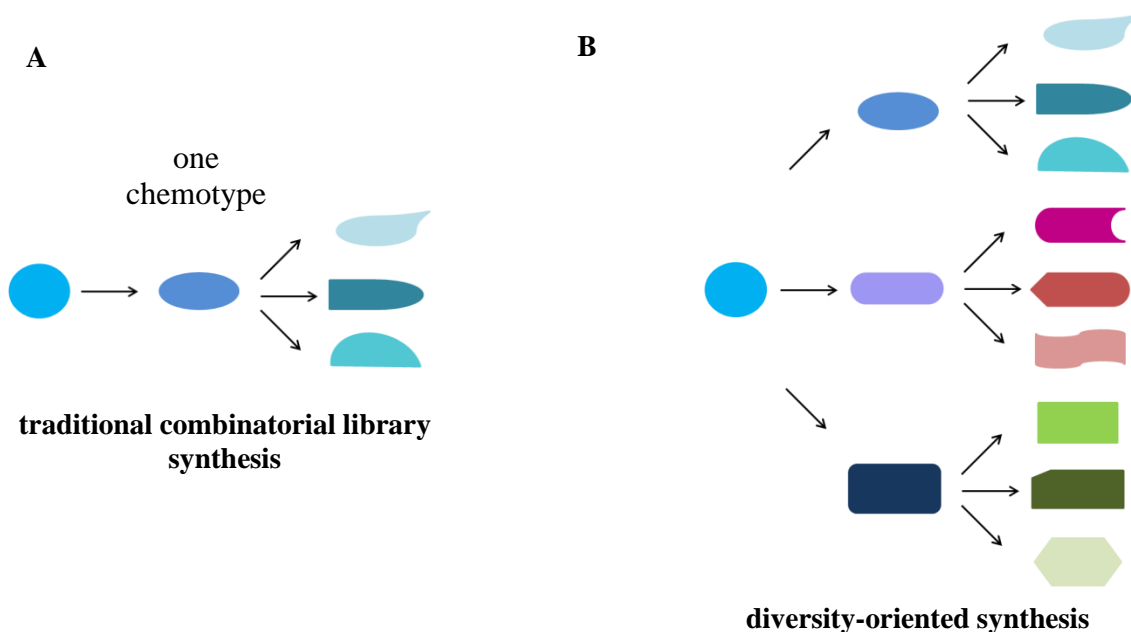
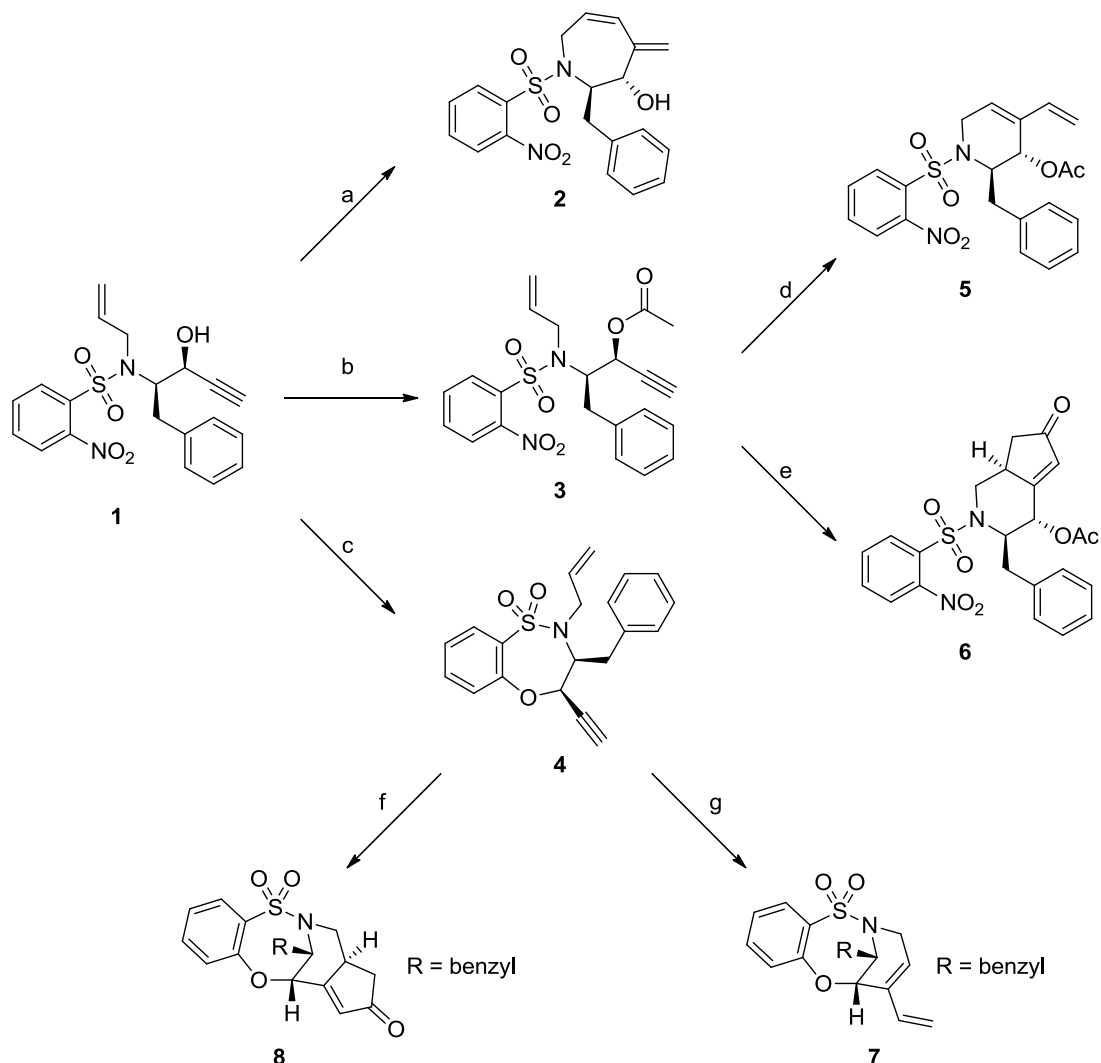


Figure 3. Diversity-oriented synthesis vs combinatorial library synthesis approach.

A) A traditional approach in combinatorial library synthesis is based on variation of one chemotype, to obtain structure variations able to address a specific biological target. B) Diversity-oriented synthesis approach is based on a series of parallel modifications of an initial starting material to achieve a range of chemotypes leading to structurally diverse scaffolds. Adapted from Galloway *et al.*³³

A DOS strategy which uses a “reagent-based” approach was developed by Pizzarini *et al.*³⁶ (Scheme 1). The strategy employed one poly-functionalised starting material, the aminopropargylic alcohol **1**, which was exposed to a series of different reagents to give three different chemotypes, compounds **2**, **3** and **4**, respectively *via* enyne metathesis, derivatisation with acetyl anhydride and intramolecular nucleophilic aromatic substitution. The resulting chemotypes contained different pairs of functional groups which were reacted intramolecularly under different conditions to give diverse cyclic scaffolds. For example, compound **3** was modified *via* enyne metathesis and the Pauson-Khand reaction,³⁷ giving scaffolds **5** and **6**; while compound **4** underwent two

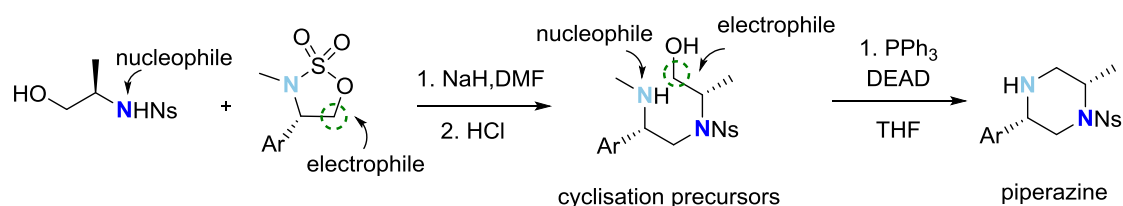
different cyclisation *via* Pauson-Khand reaction and enyne metathesis to lead to scaffolds **7** and **8**.



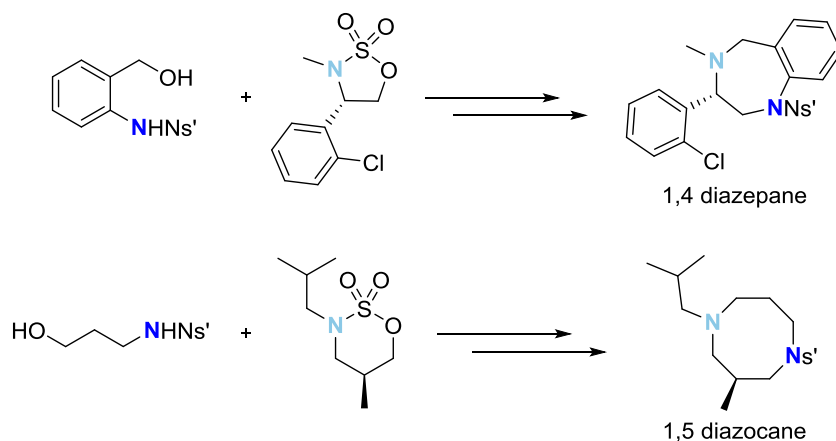
Scheme 1. Example of reagent-based DOS, applied to the poly-functionalised aminopropargylic alcohol **1.** Synthetic pathway developed by Pizzirani *et al.*³⁶ Conditions: a) Hoveyda-Grubbs second-generation catalyst, ethylene, toluene, r.t.; b) acetic anhydride, Et₃N, DMAP, CH₂Cl₂, 0 °C; c) NaH, THF, -10 °C; d) Hoveyda-Grubbs second-generation catalyst, ethylene, toluene, 45 °C; e) and f) [Co(CO)₈], triethylamine *N*-oxide, THF, r.t.; g) Hoveyda-Grubbs first-generation catalyst, CH₂Cl₂, r.t., then Pb(OAc)₄.

In our research group, DOS methodologies have been developed extensively to prepare lead-like molecules following a “substrate-based approach”.³³ This approach uses a range of starting materials to couple under the same conditions, to form key

building blocks. Those building blocks contain functional groups, able to pair together and provide skeletally diverse molecules. This methodology was employed to prepare a variety of heterocyclic scaffolds based on piperazine, 1,4-diazepanes and 1,5 diazocanes,³⁸ and a series of alkaloid-like scaffolds.³⁹ In the case of heterocyclic scaffolds, a series of commercially available aminoalcohols was protected and then reacted with a range of cyclic sulfamidates to give cyclisation precursors. These precursors underwent to cyclisation to lead to a variety of heterocyclic scaffolds (Scheme 2).



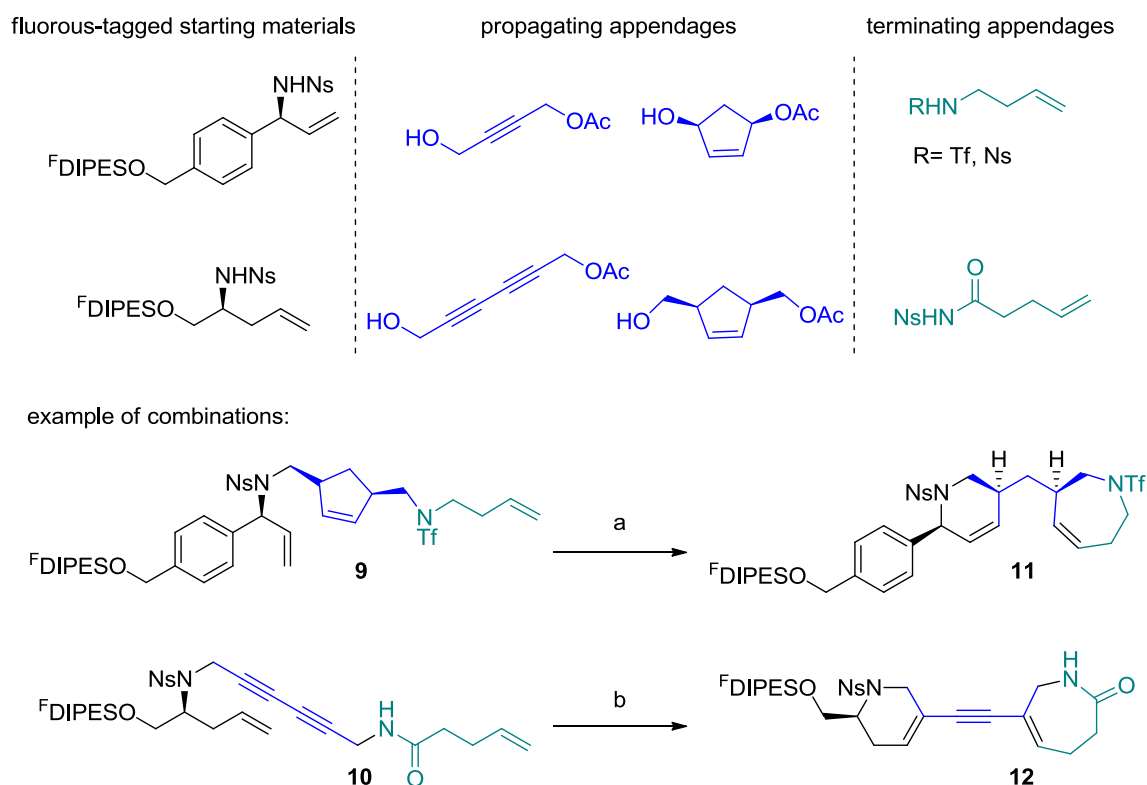
application to different substrates:



Scheme 2. Example of substrate-based DOS to prepare lead-like heterocycles.

Coupling of a range of *N*-nosyl amino alcohols with cyclosulfamidates led to the preparation of cyclisation precursors, able to cyclise to give diverse heterocyclic scaffolds. Ns: *o*-nitrophenylsulfonyl, Ns': *p*-nitrophenylsulfonyl. Adapted from James *et al.*³⁸

For the preparation of alkaloid-like molecules, a range of unsaturated building blocks was synthesised by attachment of propagating and terminating appendages to initial starting materials. The resulting cyclisation precursors underwent metathesis cascade reactions to yield skeletally diverse scaffolds. The initial building blocks were attached to a fluororous-tagged linker which facilitated the purification of the final scaffolds *via* fluororous solid-phase extraction (Scheme 3).



Scheme 3. Example of substrate-based DOS, using propagating and terminating appendages to prepare cyclisation precursors. Compounds **9** and **10** were prepared *via* coupling of starting materials with propagating groups *via* Mitsunobu reaction, followed by deacetylation. The resulting substrates were coupled with terminating groups again *via* Mitsunobu reaction, followed by deacetylation. Mitsunobu reaction condition: starting material or substrate (1.0 eq.), propagating group or terminating group (4.0 eq.), PPh₃ (4.0 eq.), DEAD (4.0 eq.), CH₂Cl₂, 0 °C–r.t.; deacetylation condition: NH₃ in MeOH (0.025 M). Compounds **11** and **12** were synthesised *via* metathesis cascade. Conditions: a) Hoveyda-Grubbs second-generation catalyst, CH₂Cl₂, 50 °C then Et₃N (86 eq.), P(CH₂OH)₃ (86 eq.) then silica. PhSH (1.2 eq.), K₂CO₃ (3.0 eq.), DMF; b) Hoveyda-Grubbs second-generation catalyst, methyl tert-butyl ether, 50 °C then Et₃N (86 eq.), P(CH₂OH)₃ (86 eq.) then silica. PhSH (2.4 eq.), K₂CO₃ (6.0 eq.), DMF. ^FDIPESO is a fluorous-tagged linker. Adapted from Maurya *et al.*³⁹

1.2.5 Combining diversity oriented synthesis and virtual screening

In this thesis a new approach to design novel bioactive lead molecules is described. To demonstrate the validity of the approach, it was applied to the BACE-1 protein. The approach combined *in silico* generation of a library of skeletally diverse lead-like

scaffolds, with virtual screening of this library against BACE-1. The generation of skeletally diverse lead-like scaffolds was obtained by designing a synthetic protocol based on DOS methodology. The aims in developing such an approach was, on one hand, to explore the chemical space of lead-like molecules by means of computer-aided design of DOS protocols; and on the other hand, to identify novel active leads, able to inhibit BACE-1, a target of pharmaceutical interest. Moreover, it was hoped to contribute in implementing lead discovery approaches, by combining the prediction of activity of lead-like scaffolds with information of their synthetic accessibility. An overview of the project is described in Section 1.5. In the following Section 1.3 the protein BACE-1 is introduced.

1.3 BACE-1

1.3.1 Involvement in Alzheimer's disease

BACE-1 is a transmembrane human aspartic protease, known as ' β -site amyloid precursor protein cleaving enzyme' (BACE), which is expressed in high levels in the brain, mostly by neurons, and also in the peripheral tissues and in the pancreas^{14,15} in low level. BACE-1 enzymatic activity is displayed only in the brain,¹⁵ where it is involved in the early stage of formations of β -amyloid plaques, insoluble accumulations of neurotoxic amino acidic fragments recognised as the major symptoms of Alzheimer's disease. Alzheimer's disease is a neurodegenerative disease which affects memory, cognitive functions and behaviour. The causes of Alzheimer's disease are still unknown, but the molecular mechanism associated with the disease is believed to start with the "amyloid cascade".⁴⁰ The amyloid cascade is a process which leads to the formation of neurotoxic peptides of 40/42 amino acids, called β -amyloid peptides $A\beta_{40}$ and $A\beta_{42}$, from the amyloid precursor protein (APP). APP is a substrate for different proteases, but its cleavage by BACE-1 starts an amyloidogenic pathway.

APP is cleaved by BACE-1 at the M-D bond contained in the sequence KMDAE, producing two fragments: an $A\beta$ N-terminus soluble fragment, called APPs β , and a C-terminus fragment, called CTF99.⁴⁰ The CTF99 fragment is then heterogeneously cleaved by γ -secretase, releasing neurotoxic peptides $A\beta_{40}$ and $A\beta_{42}$. In the metabolism

of APP another alternative and ‘non-amyloidogenic’ pathway is initiated by the zinc metalloproteinase α -secretase; this pathway prevails in most cell types (Figure 4).⁴¹

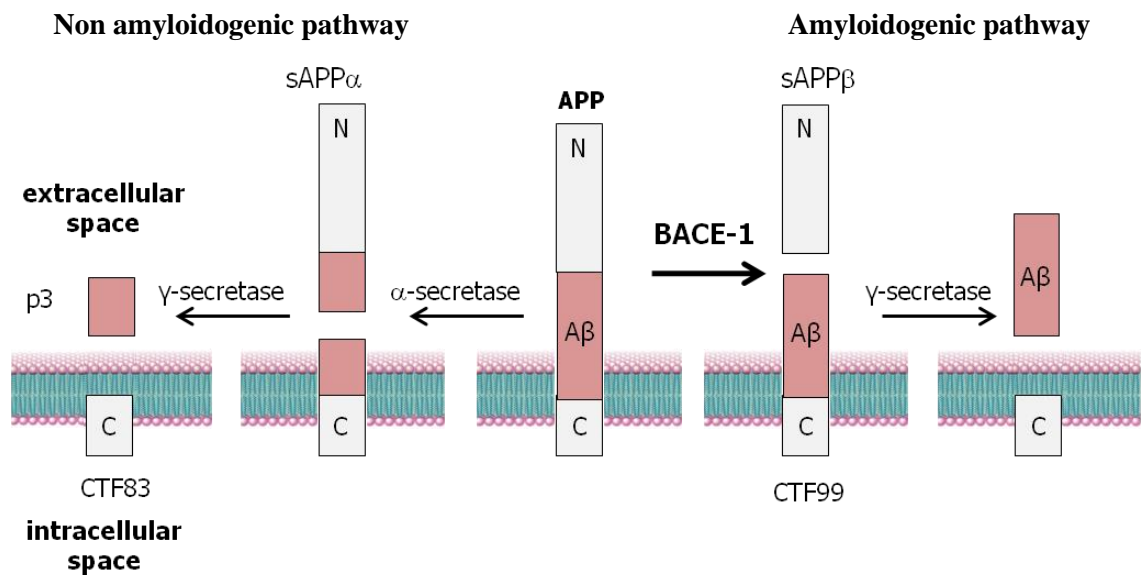


Figure 4. Amyloidogenic and non-amyloidogenic pathway of APP substrate. The APP can undergo two alternative and competing metabolic pathways. The major and non-amyloidogenic pathway, on the left, is started by α -secretase and precludes the formation of Alzheimer’s A β peptide. The amyloidogenic pathway, on the right, is started by β secretase. Adapted from Cole *et al.*⁴⁰

A β_{40} and A β_{42} are insoluble peptides which aggregate to form β -amyloid plaques; they are formed in the brain cells, but they can be transported outside spreading their damaging effect.⁴² According to the amyloid cascade hypothesis, the formation of β -amyloid plaques has two main consequences: the activation of an inflammatory response and the hyperphosphorylation of Tau protein. The inflammatory response relies principally on the activation of brain glial cells, which degenerate and produce oxygen free radicals causing damage and neurons death.⁴³ The hyperphosphorylation of Tau protein induces pairing of helical filaments of the protein which accumulate, resulting in the so called toxic “neurofibrillary tangles”.⁴⁴

It has been demonstrated that BACE-1 inhibition reduces A β peptide levels in mouse brain and up-regulates the α -secretase non amyloidogenic pathway.⁴⁵ While BACE-1 total inhibition caused development of cognitive dysfunctions in mice,⁴⁶ since

BACE-1 is necessary for specific hippocampal memory processes,⁴⁷ its partial inactivation may not affect normal learning and memory processes. Therefore BACE-1 has been considered a good therapeutic target for the disease.

1.3.2 Structure and catalytic mechanism

Due to its pharmaceutical interest, BACE-1 has been targeted and studied widely in the last three decades. There are more than 250 crystal structures of BACE-1 in complex with inhibitors,⁴⁸ and BACE-1 structural features and catalytic mechanism have been disclosed. The main characteristics of BACE-1 are: a flexible region, located in front of the substrate binding cleft, and the presence of two conserved water molecules in its catalytic site. These characteristics are in common with other aspartic proteases, with which BACE-1 shows from 24 to 52% of sequence identity (*e.g.* 29% with cathepsin D, 52% with BACE-2, 24% with renin, 27% with pepsin).⁴⁹

The BACE-1 flexible region, called “flap”, is a β hairpin structure composed of 14 residues (from Lys65 to Glu79) and a sequence of 7 amino acids (from Ala101 to Lys107) connected by antiparallel H-bond interactions and forming three strands which cover the binding cleft.⁵⁰ The role of this flexible region in other aspartyl proteases is unclear; while X-ray structures of numerous of BACE-1 complexes^{51,52} revealed that this flexible region induces a conformational change in the protein, from an open and closed position, allowing the insertion of APP substrate in the catalytic site. The substrate-free BACE-1 structure (apo-structure) adopts an open conformation in which the flap is distant from the binding cleft and APP substrate can access into the active site. A closed conformation has been observed when BACE-1 is in complex with inhibitors and the flap residues move up to *ca.* 4.5 Å closer to the binding cleft (Figure 5).⁵⁰

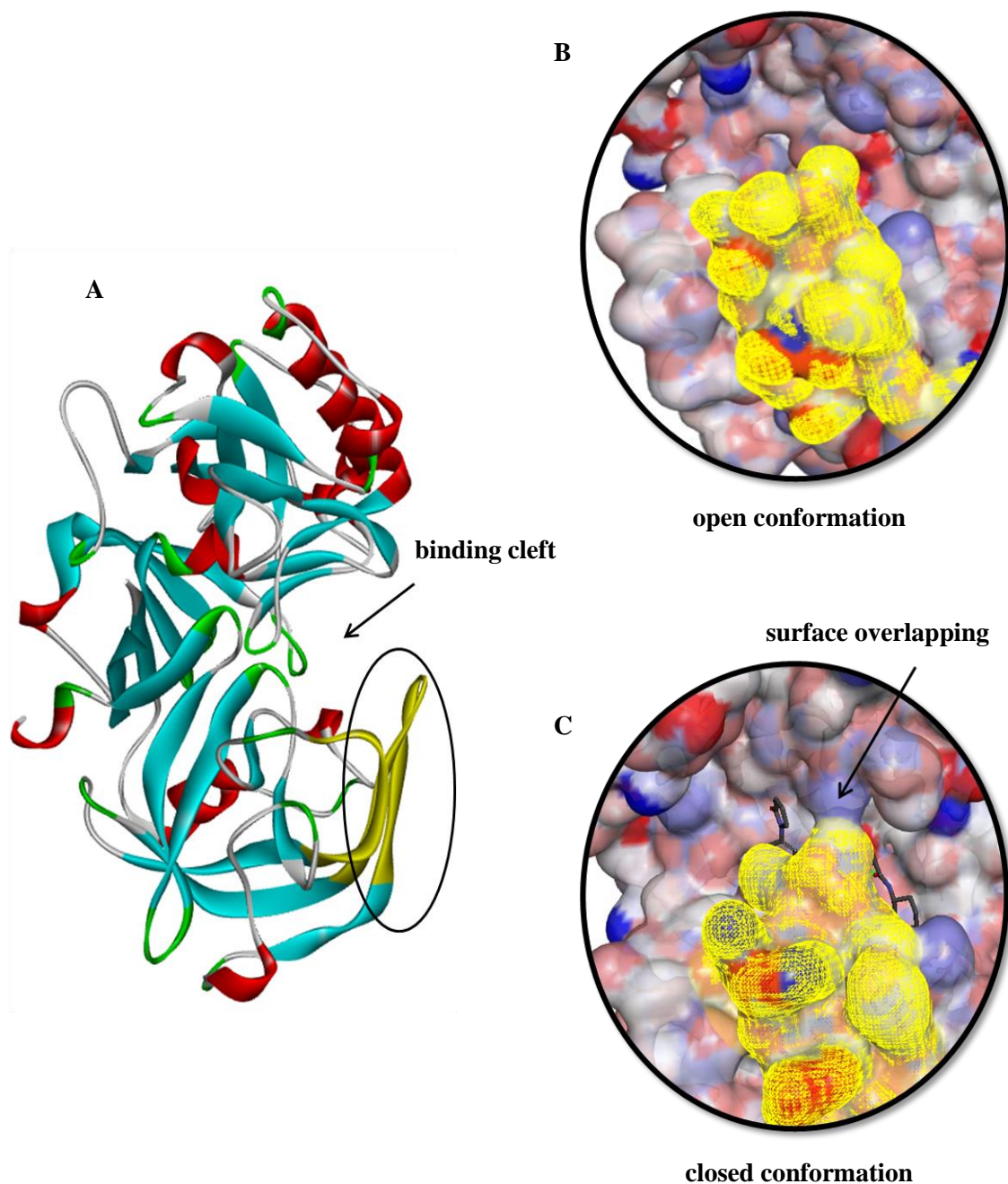


Figure 5. Features and conformations of the flexible region of BACE-1, called “flap”. A) Apo-structure of BACE-1 (pdb code 1W50) with the flexible region, flap, highlighted in yellow. The flap is covering the binding cleft. B) Example of protein adopting open flap conformation (pdb code: 1W50). C) Example of closed flap conformation: BACE-1 is in complex with an inhibitor (pdb code 2XJT) and the flap surface is overlapping with the top surface of the protein, which limits the binding cleft. Visualised with Discovery Studio 3.0.

In the flap region Tyr71 is involved in key H-bond interactions which determine the protein conformational change. In the open conformation, Tyr71 forms a H-bond (CO backbone) with Gly74 (NH backbone) of *ca.* 2.8 Å of length,⁵² in the closed conformation, Tyr71 can be oriented towards Trp76⁵² or towards Lys107⁵³ and can form new H-bonds with the O atom of the OH group of Tyr71 side chain (Figure 6).

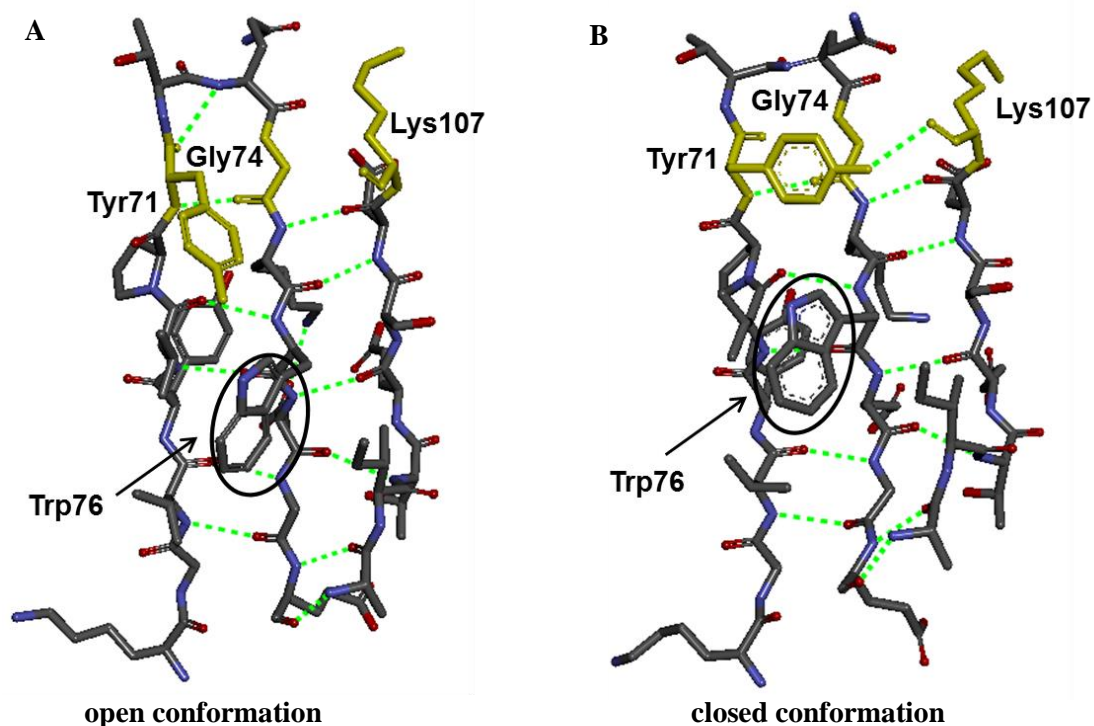


Figure 6. Example of H-bond interactions formed in the flap regions of BACE-1. 14 amino acids (from Lys65 to Glu79) and 7 amino acid sequences (from Ala101 to Lys107) connected by antiparallel H-bonds, which constitutes the flap region. A) H-bonds formed in a flap open conformation; Tyr71 and Gly74 (yellow colour) form a characteristic H-bond between Tyr71 (CO backbone) and Gly74 (NH backbone) (pdb code 1W50). B) H-bonds formed in a flap closed conformation (pdb code 2XJT). A new H-bond is formed between Tyr71 (OH) and Lys107 (CO backbone). Visualised with Discovery Studio 3.0.

As with other aspartyl proteases, BACE-1 contains two proximal aspartyl residues, Asp228 and Asp32, and two conserved water molecules in the catalytic site. One water molecule (Wat1) is located between Asp32 and Asp228 and seems to assist the catalytic process of the natural substrate. The second molecule (Wat2) is part of a conserved network of hydrogen-bonds which involves Ser35 (Figure 7). The proteolysis mechanism of BACE-1 is an acid-base catalysed mechanism mediated by Wat1 and by the Asp228/Asp32 pair (see Figure 8).⁵⁴

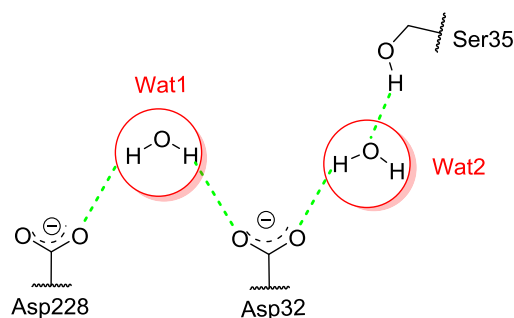


Figure 7. Water molecules located in the catalytic site of BACE-1. The two conserved water molecules, Wat1 and Wat2, form a network of H-bond (green) with the proteolytic Asp228 and Asp32, and with Ser35.

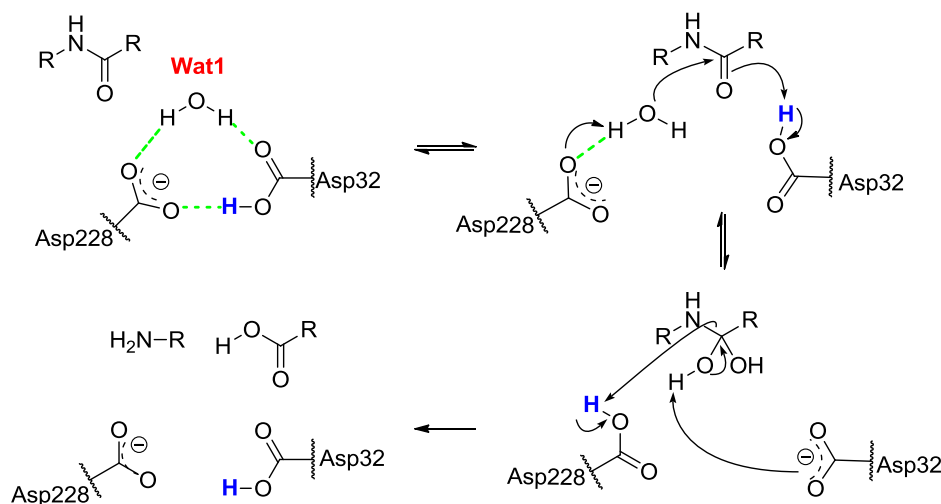


Figure 8. Catalytic mechanism of BACE-1. The conserved water molecule Wat1, located between the two catalytic aspartates, takes part in the proteolytic mechanism of APP substrate. Asp32 is represented in its mono-protonated form, which is likely to be assumed at pH 4.5, at which BACE-1 is active.⁵⁵

As shown in Figure 8, one catalytic aspartate, Asp32, seems to assume a monoprotonated state where the inner oxygen contains the proton.⁵⁵ It has been reported that BACE-1 optimal activity is at pH 4.5.⁵² The binding of the inhibitor resulted to be pH dependent: at pH 5.0 the inhibitor binding seems to occur simultaneously with protein conformational switching, whilst at pH 4.5 proteolysis of the inhibitor occurs.

1.3.3 Specificity for the APP substrate

The specificity of BACE-1 for APP has been explained from studies of mutations of APP. The cleavage point of APP is the M596-D597 bond of the EVKMDAEF sequence. According to the standard nomenclature of proteases, these residues are labelled P4-P3-P2-P1*P1'-P2'-P3'-P4' and the cleavage point is indicated by * (Figure 9).

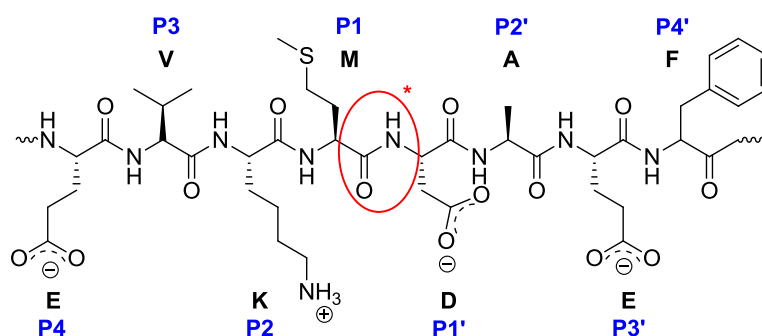


Figure 9. Amino acids sequence of BACE-1 APP substrate, flanking the cleavage point. The cleavage point between M and D is in highlighted in red. The amino acids are represented according to the charge state likely assumed at pH 4.5, at which BACE-1 is active.

Mutations of KM \rightarrow NL at P2-P1, the so-called Swedish mutation, are associated with early onset of Alzheimer's disease.⁵⁶ The sequence EVNL*DAEF of the Swedish mutant is very efficiently hydrolysed by BACE-1; while a mutation of M596 with V at P1 position reduces the cleavage.⁵⁷ Sauder *et al.*⁵⁸ explained this difference of substrate preference by modelling interactions formed by P1*P1' residues of APP substrates with BACE-1 residues located in the catalytic site. The P1' residue of APP can form a salt bridge with Arg235 of BACE-1; while hydrophobic contacts can be established by the P1 residue with Leu30 and Ile118 of BACE-1, located in hydrophobic pocket of the

protein, and with Tyr71 located in the flap region. These interactions could show BACE-1 specificity for a negative charge at P1' and for a hydrophobic residue at P1. They also reveal a difference with most aspartyl proteases, which have a preference for hydrophobic residues at P1' (Figure 10).

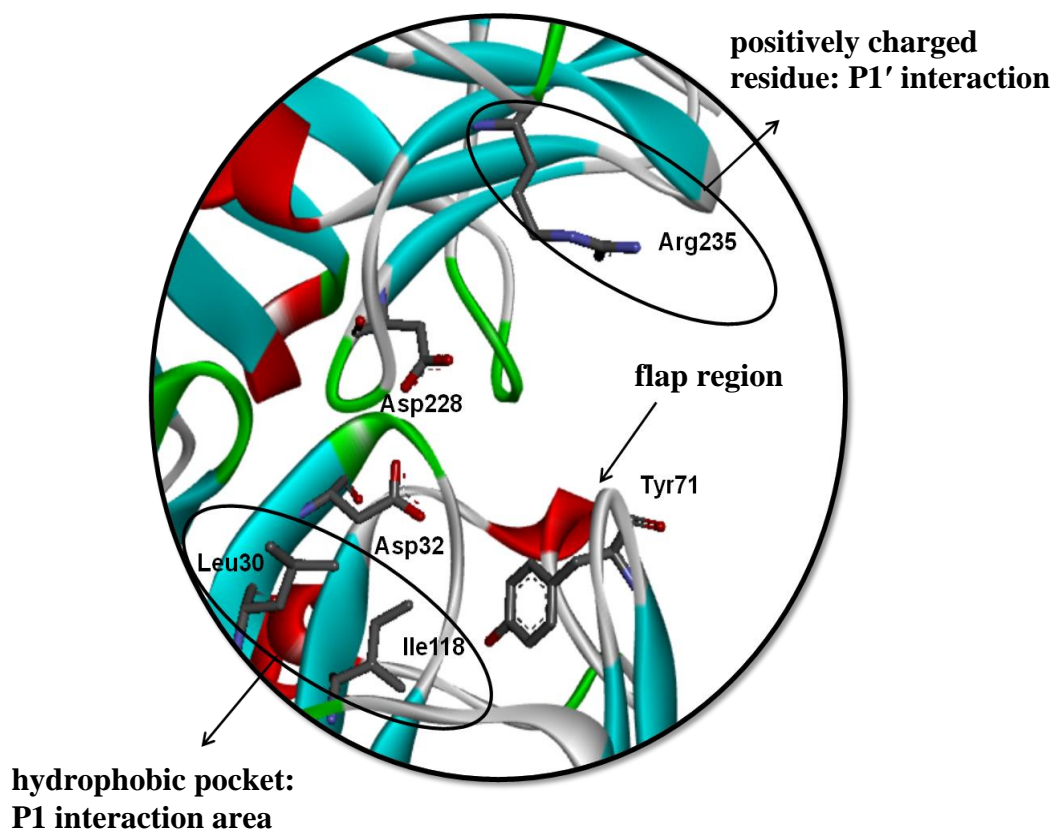


Figure 10. BACE-1 region of interactions with P1 and P1' residue of APP substrate. A hydrophobic region containing Leu30 and Ile118 interacts with P1 lipophilic residue of APP, M, together with the lipophilic Tyr71, located in the flap. A positively charged region, containing Arg235, shows preference for interaction with negatively charged P1' residue of APP, D. Visualised with Discovery Studio 3.0.

The Swedish mutant substrate, containing Leu at P1, can maintain hydrophobic contacts with Leu30, Ile118 and Tyr71 of BACE-1. When the P1 residue of APP is mutated to V, one of the methyl groups of V can be oriented towards the catalytic Asp32 of BACE-1 and interferes with the catalytic activity; at the same time hydrophobic interactions with Leu30, Ile118 and Tyr71 would be suppressed. This could explain why BACE-1 hydrolyses the Swedish mutant substrate more efficiently.

The BACE-1 specificity for APP is also determined by other interactions with APP residues P2, P3, P2' and P3'. These residues seem to occupy specific pockets of BACE-1, which are named according to the contacts made with APP residues (Figure 11). The study of pocket interactions was important in the development of BACE-1 inhibitors.

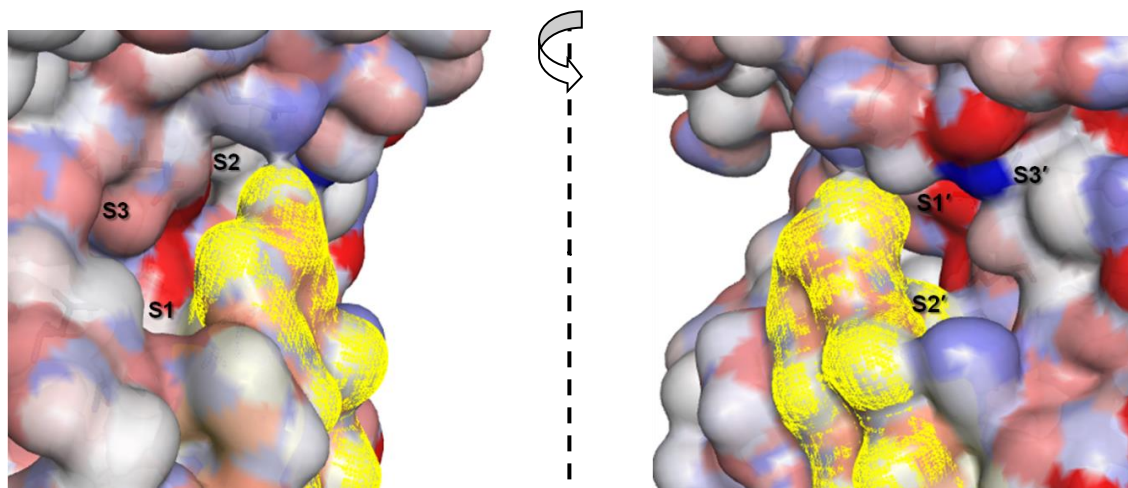


Figure 11. BACE-1 pockets. BACE-1 pockets are separated by the flap region (in yellow) and are numbered according to the interactions made with residues P1, P2, P3 and P1', P2', P3' of APP substrates. Visualised with Discovery Studio 3.0.

1.4 Overview of BACE-1 inhibitors

BACE-1 inhibitors can be separated into two major categories: peptidomimetic inhibitors and non-peptidomimetic inhibitors. The first attempts to design BACE-1 inhibitors were based on structural modifications of the APP substrate which led to a series of peptides containing a transition state isostere modification in the substrate backbone. Further research was directed to the discovery of a series of potent and lower molecular weight peptidomimetic inhibitors (M.W. ~700), but the need to improve the inhibitor brain penetration forced the investigation towards a series of small non-peptidomimetic inhibitors (M.W. <500). The design of these inhibitors has proven to be extremely difficult due to the large size of the active site of BACE-1 ($> 10000\text{\AA}$).^{59, 60}

1.4.1 The first peptidomimetic inhibitor: compound OM99-2

The first peptidomimetic inhibitor, OM99-2, reported by Tang and co-workers⁵⁷ was based on an octapeptide sequence of EVNL*AAEF in which the L-A bond was substituted by a hydroxyethylene transition-state isostere (Figure 12). The design of the inhibitor was based on the substitution of the P1' residue of the Swedish mutant EVNL*DAEF. The crystal structure of BACE-1 in complex with OM99-2 shows that the inhibitor forms a network of H-bonds in the active site, which involves the catalytic Asp32 and Asp228. OM99-2 is a nanomolar inhibitor of BACE-1 ($K_i=1.6$ nM).⁶¹

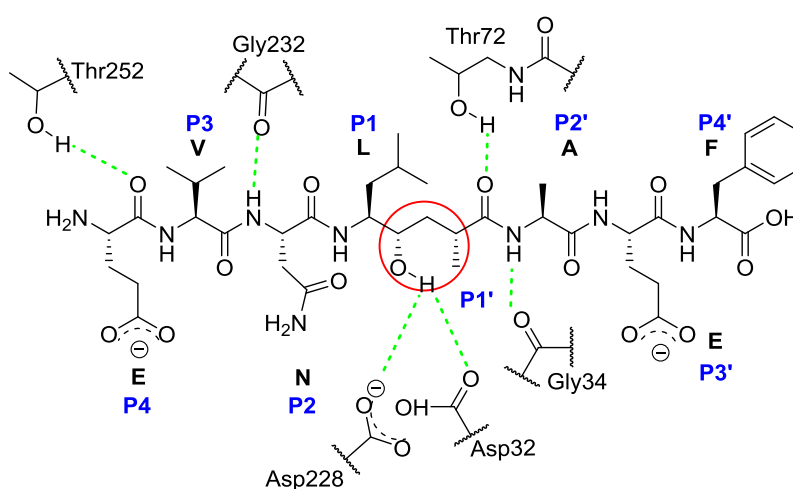


Figure 12. Structure of the OM99-2 inhibitor. 2D structure and representation of H-bonds formed between the OM99-2, first BACE-1 inhibitor,⁵⁷ and BACE-1 residues in the catalytic site. The inhibitor structure is based on a reduced form of the Swedish mutant peptide, having only eight amino acids. A hydroxyethylene isostere group is contained at the centre of the sequence (highlighted in red) in replacement of the peptidic bond L-D, in position P1 and P1'. The amino acids are represented according to the likely charge state assumed at pH 4.5, at which BACE-1 is active.

Improvement of the OM99-2 structure led to the peptide analogue ELDL*AVEF. This inhibitor, OM00-3, forms three new H-bonds with NH and CO groups of the backbone of residue E and with the NH of the backbone of residue F in P3' and P4' position. Its K_i value is 0.3 nM (Figure. 13).⁵⁰ In the BACE-1 complex formed with OM99-2 and with OM00-3 inhibitor, the water molecule Wat1, located between the two catalytic aspartates, is displaced by the inhibitor in the binding site.⁶²

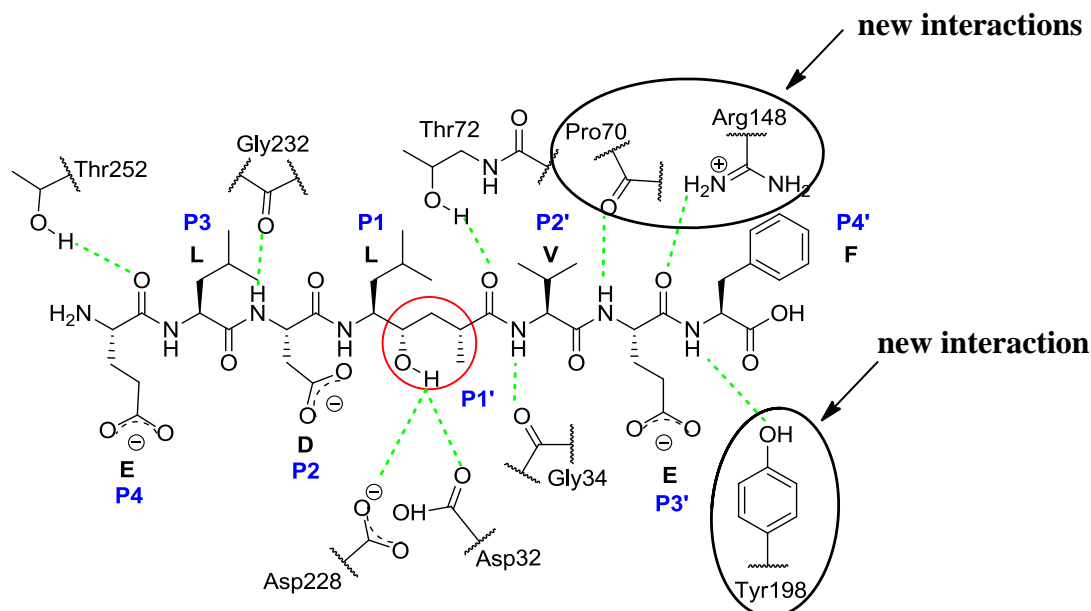


Figure. 13. Structure of the OM00-3 inhibitor. 2D structure and representation of H-bonds formed between the OM00-3 inhibitor and BACE-1 residues in the catalytic site. The OM00-3 inhibitor contains an hydroxyethylene bond between P1-P1' residue (in evidence in red). The E and F residues of the inhibitor are involved in new H-bonds with BACE-1.

1.4.2 Inhibitors incorporating a transition state isostere as a central core

Peptide analogues containing a transition state isostere were proven to be effective inhibitors of the BACE-1 enzyme. A key structural feature of these compounds is the hydrogen bonds formed between the secondary hydroxyl group with the Asp32 and Asp228 residues of BACE-1 in the catalytic site (as shown in Figures 12 and 13). A series of BACE-1 inhibitors containing this hydroxyl group has been reported;^{63,64} the structures are based on statine, *tert*-hydroxy motif,⁶⁵ hydroxyethylene (HE),^{51, 66} aminoethylene⁶⁷ and hydroxyethylamine (HEA),⁶⁸ units that are non-cleavable isosteres of the transition state (Figure 14).

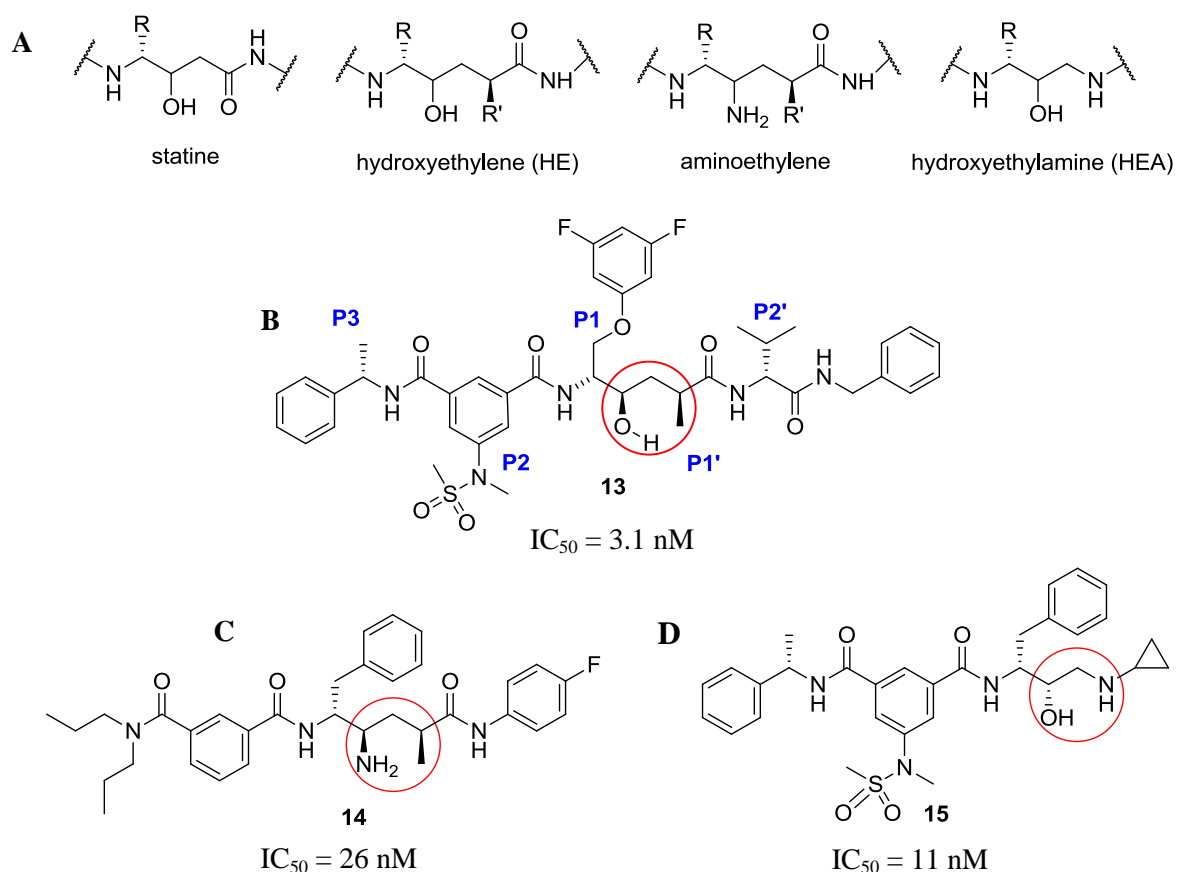


Figure 14. Inhibitors incorporating a transition state isostere. A) Representation of the central core of transition state isostere-type inhibitors. The hydroxyl group or the primary amine is incorporated in replacement of a peptide bond. B) HE isostere inhibitor designed by Wångsell *et al.*⁶⁵ C) Aminoethylene isostere inhibitor designed by Yang *et al.*⁶⁷ D) HEA isostere inhibitor designed by Stachel *et al.*⁶⁸ Red circles highlight the isostere central core of the inhibitors.

The inhibitors presented in Figure 14 show a higher lipophilic character in comparison with the peptidomimetic inhibitors OM99-2 and OM00-3. The aromatic groups were introduced in the structure to fill BACE-1 hydrophobic pockets. In the case of the inhibitor **13**, an interaction in the S1 pocket of BACE-1 was established by increasing the size of a lipophilic group at P1; while the S2 pocket was occupied by the sulfonyl groups, and the S2' was filled with a benzylic group (Figure 15).⁶⁵

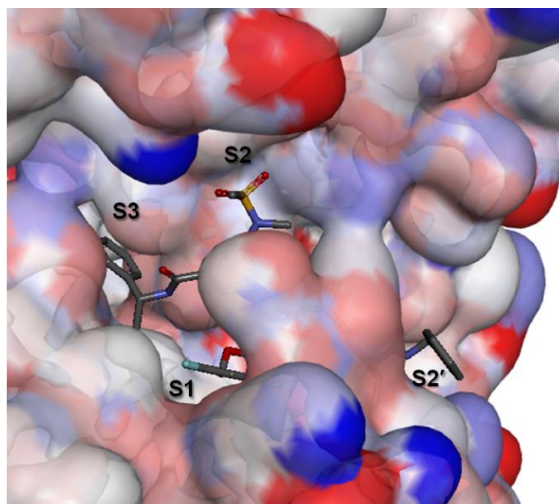
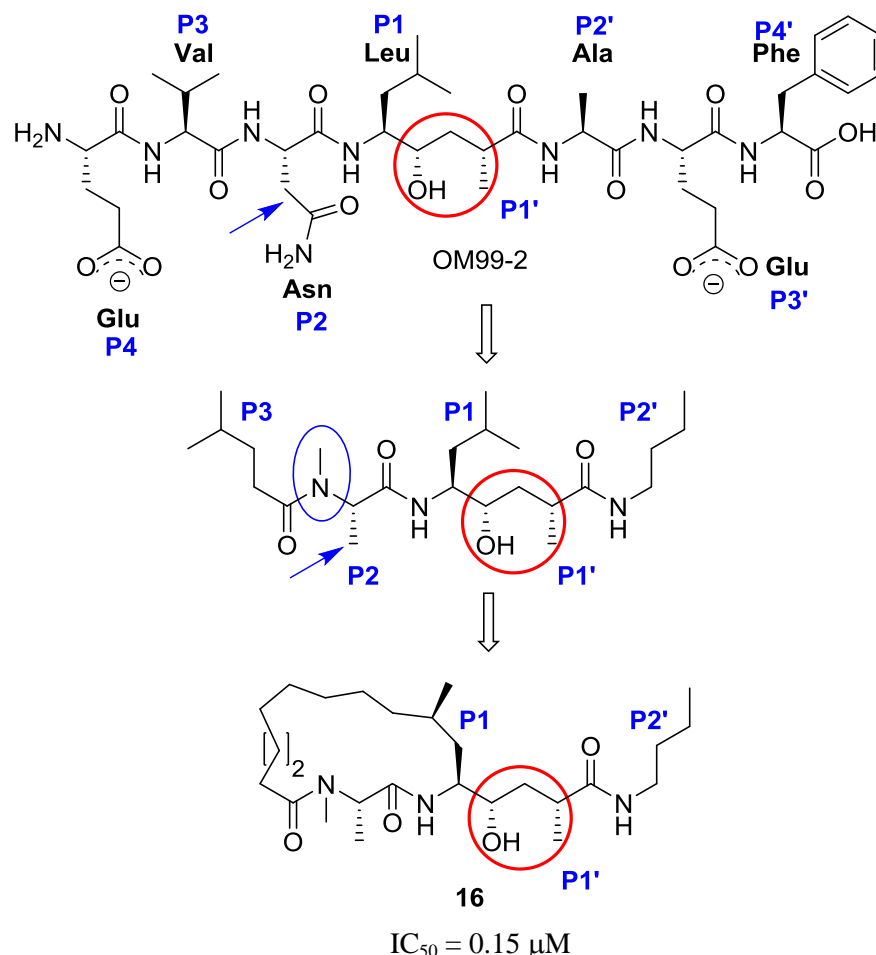


Figure 15. Example of interactions of the HE inhibitor 13 in BACE-1 pockets. 3D representation of the conformation assumed by BACE-1 in complex with the HE inhibitor **13**. S1, S2 and S3 pockets of BACE-1 are occupied by the aryl group at P1, the sulfonyl group at S2 and the benzylic group at P3. Another benzyl group at P2' occupies S2' pocket of BACE-1. Adapted from Wångsell *et al.*⁶⁶ (pdb code 3IXK). Visualised with Discovery Studio 3.0.

1.4.3 Reducing inhibitor peptidic character, towards macrocyclic inhibitors

Most of the peptide-like BACE-1 inhibitors showed a limited brain penetration due to their large molecular weight and their affinity for P-glycoprotein.⁶⁹ Some structural adjustments were made to reduce molecular weight and peptide character, such as removing the P3-P4 amide segment and modifying the P2-P3 positions. Machauer *et al.*⁷⁰ modified the structure of the inhibitor OM99-2 by: replacing Asn chain at P2 with a methyl group, methylating the N atom at P2-P3 bond, and ring closing the P1-P3 extremities. A macrocyclic inhibitor was derived, compound **16**, which displayed a sub-micromolar activity, $IC_{50} = 0.15 \mu\text{M}$ (Scheme 4).



Scheme 4. Example of a macrocyclic inhibitor derived from OM99-2 inhibitor structure. Gradual modifications of the inhibitor OM99-2, which led to the macrocyclic inhibitor **16**. The length of the amino acid chain of OM99-2 was reduced by eliminating P3-P4 and P3'-P4' fragments and by methylation of N atom at P2-P3 bond. Cyclisation of lateral chain in P1-P3 gave the macrocycle **16**. The isostere central core (highlighted in red) was kept in the macrocycle structure. Adapted from Machauer *et al.*⁷⁰

Macrocyclic inhibitors demonstrated a low molecular weight, potential for high cell permeability and good proteolytic stability.⁷¹ Structural differences of these inhibitors relied on the lateral chain linked to the ring (which contains the isostere unit); on the number of atoms contained in the ring (generally between 15 and 17 membered) and on the rigidity of the ring. Examples are provided in Figure 16.^{72,73}

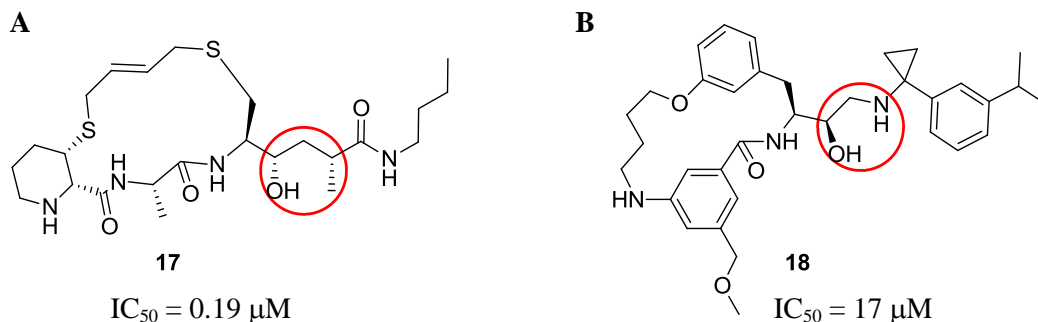


Figure 16. Other macrocyclic inhibitors. A) Inhibitor designed by Hanessian *et al.*⁷², containing a HE unit in the later chain (highlighted in red). B) Inhibitor designed by Lecher *et al.*⁷³, containing a HEA unit in the later chain (highlighted in red) and a longer and more rigid ring structure.

Further structural development brought to eliminate of the isostere core, as shown in the macrolactone inhibitor **19**. Compound **19** contains a primary amine which forms key H-bond interactions with the catalytic Asp32 and Asp228.⁷⁴ The macrolactone **19** occupies S1, S2 and S3 pockets of BACE-1 (Figure 17).

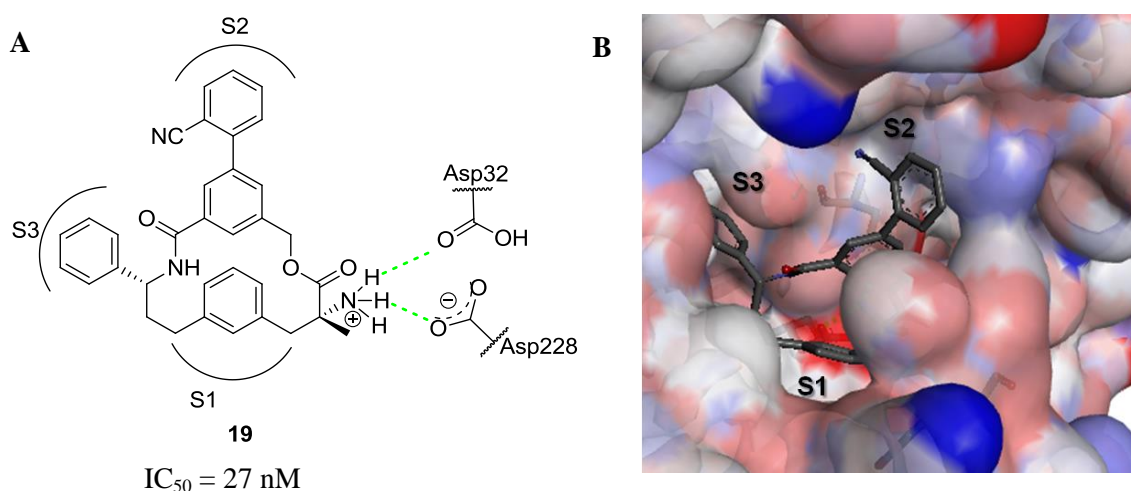


Figure 17. Macrolactone inhibitor 19. A) 2D structure and representation of the key H-bonds (green dotted line) formed by the inhibitor **19** with Asp32 and Asp228 of BACE-1. The inhibitor does not contain an isostere core; the primary amine is responsible for forming key H-bond interactions. B) 3D representation of the conformation assumed by BACE-1 in complex with the inhibitor **19**: S1, S2 and S3 pockets are filled by aromatic groups (pdb code 2QZK). Adapted by Moore *et al.*⁷⁴ Visualised with Discovery Studio 3.0.

1.4.4 Discovery of non-peptidomimetic inhibitors

Since 2006, many BACE-1 non-peptidomimetic inhibitors were discovered by fragment-based screening and optimised by computer modelling and SAR studies. These inhibitors have different structures but they all contain a heterocyclic unit and a central primary amine, which forms key H-bond interactions with the Asp32 and Asp228 in the BACE-1 catalytic site. These inhibitors can be divided into: pyridinyl aminohydantoin,⁷⁵⁻⁷⁷ aminopyridine,^{78, 79} acylguanidine,^{80, 81} dihydroquinazoline,⁸² aminoimidazole,⁸³ and spiropyrrolidine⁸⁴ inhibitors. X-ray structures of BACE-1 in complex with these inhibitors revealed that BACE-1 adopts an open or semi-closed flap conformation. The water molecule located between the two catalytic aspartates, Wat1, is displaced by the inhibitors. Examples of interactions formed by these heterocyclic inhibitors in the BACE-1 catalytic site are reported in Figures 18-21. Value of activity against BACE-1 and respective LE' are shown; values of activity against BACE-2, a homologue of BACE-1 with 52% of sequence similarity, are also shown when available.

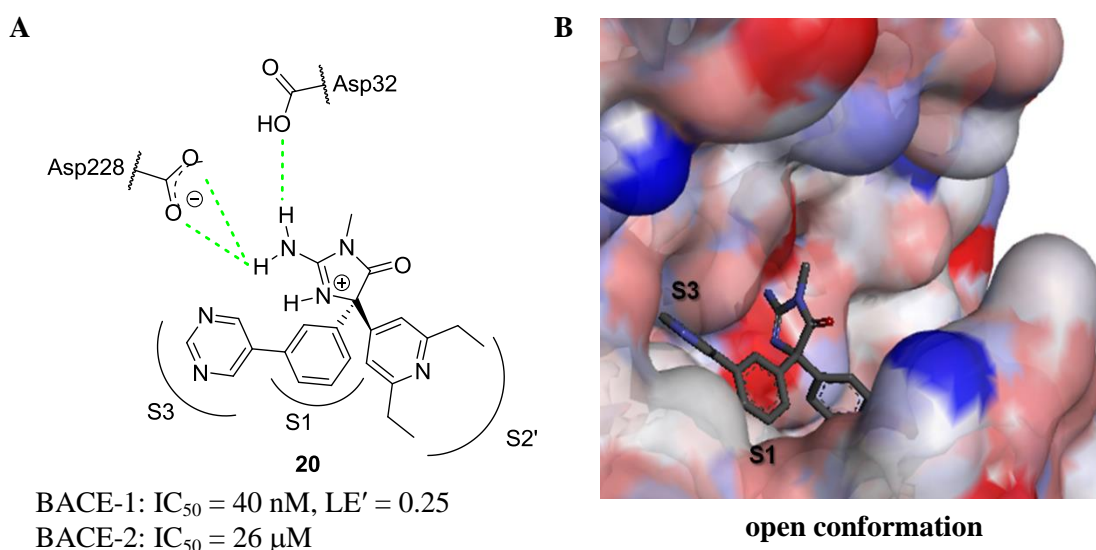


Figure 18. Pyridinyl aminohydantoin inhibitor 20. A) 2D structures and representation of key H-bond (green dotted line) formed by the inhibitor **20** with Asp32 and Asp228 of BACE-1. B) 3D representation of the conformation assumed by BACE-1 in complex with the inhibitor **20**: S1, S3 pockets are filled by aromatic groups. The flap is open (pdb code 3IN4), adapted from Malamas *et al.*⁷⁵ Visualised with Discovery Studio 3.0.

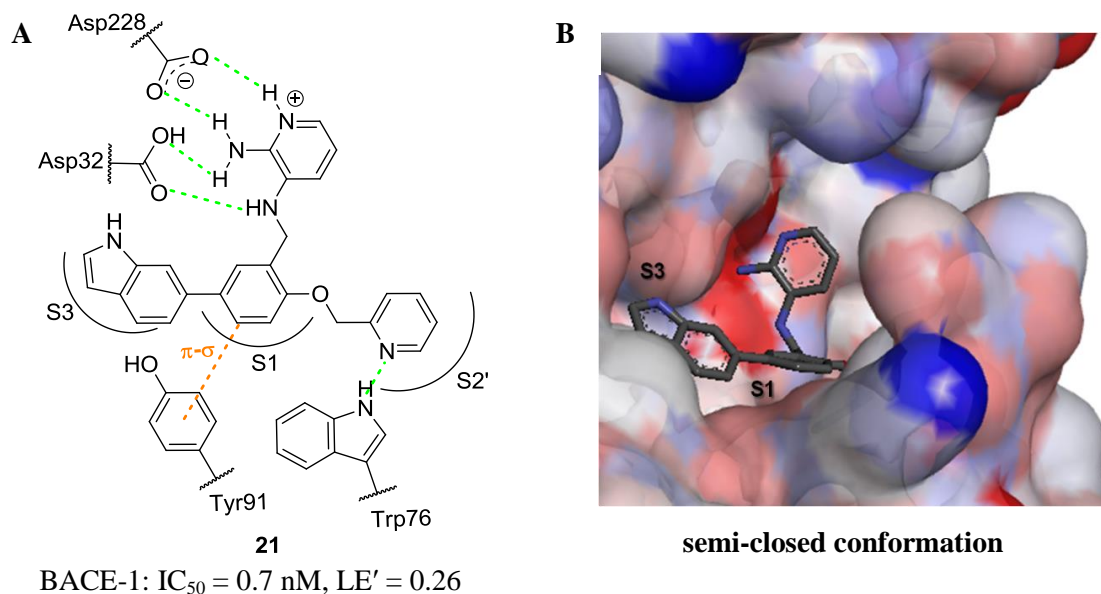


Figure 19. Aminopyridine inhibitor 21. A) 2D structures and representation of key H-bond (green dotted line) and π interactions (orange dotted line) formed by inhibitor **21** with BACE-1 residues in the catalytic site. B) 3D representation of the conformation assumed by BACE-1 in complex with the inhibitor **21**: S1, S3 pockets are filled by aromatic groups. The flap is semi-closed (pdb code 2OHU), adapted from Congreve *et al.*⁷⁸ Visualised with Discovery Studio 3.0.

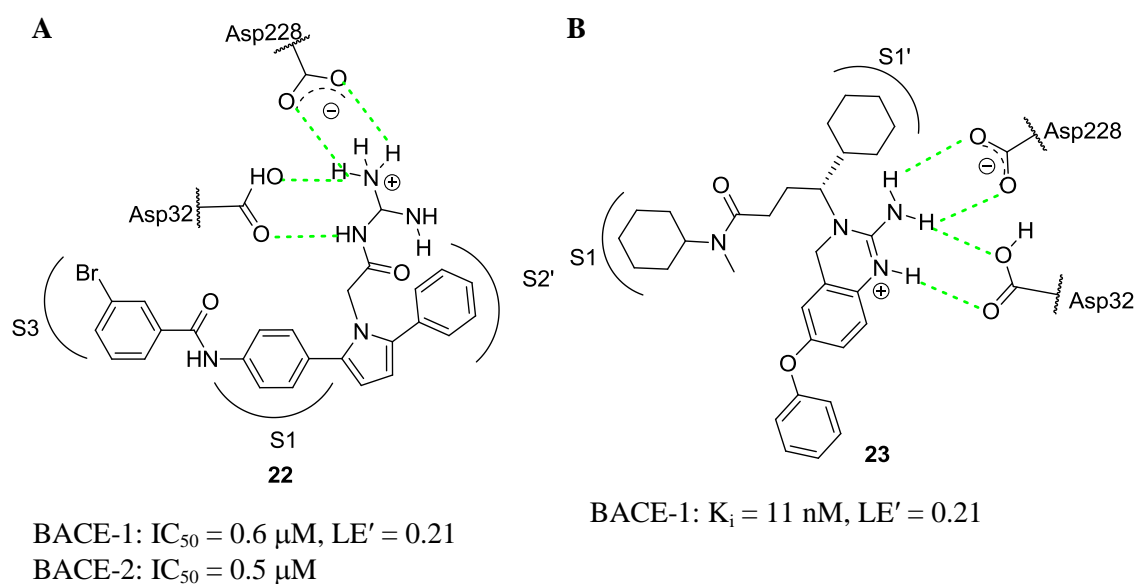


Figure 20. Acylguanidine inhibitor 22 and dihydroquinazoline inhibitor 23. 2D structures and representation of key H-bond interactions (green dotted line) formed by inhibitors **22** and **23** in with BACE-1 residues in the catalytic site. A) Acylguanidine inhibitor **22** designed by Cole *et al.*⁸¹ B) Dihydroquinazoline inhibitor **23** designed by Baxter *et al.*⁸²

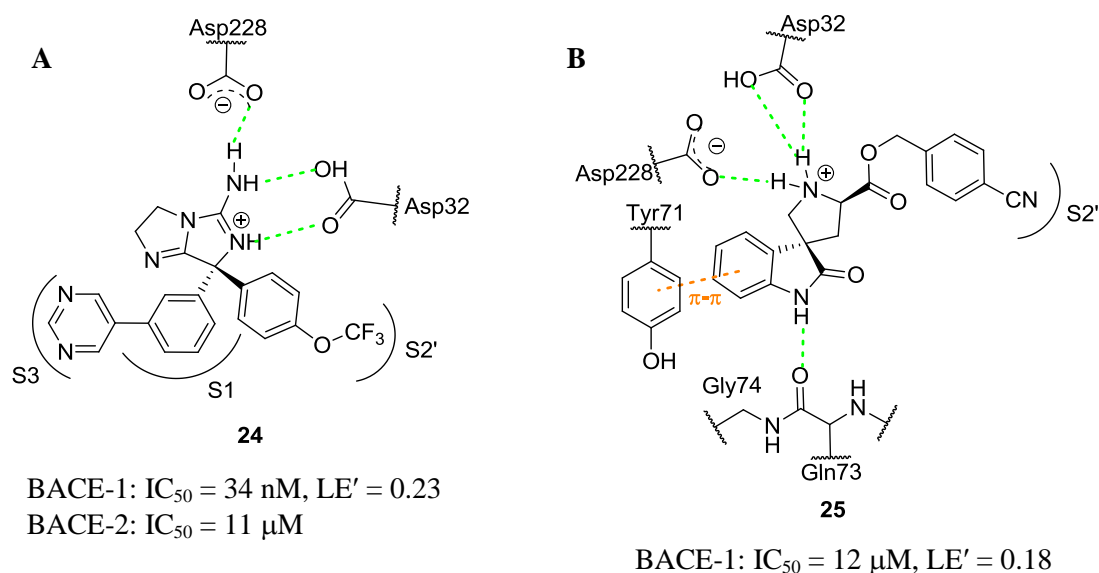
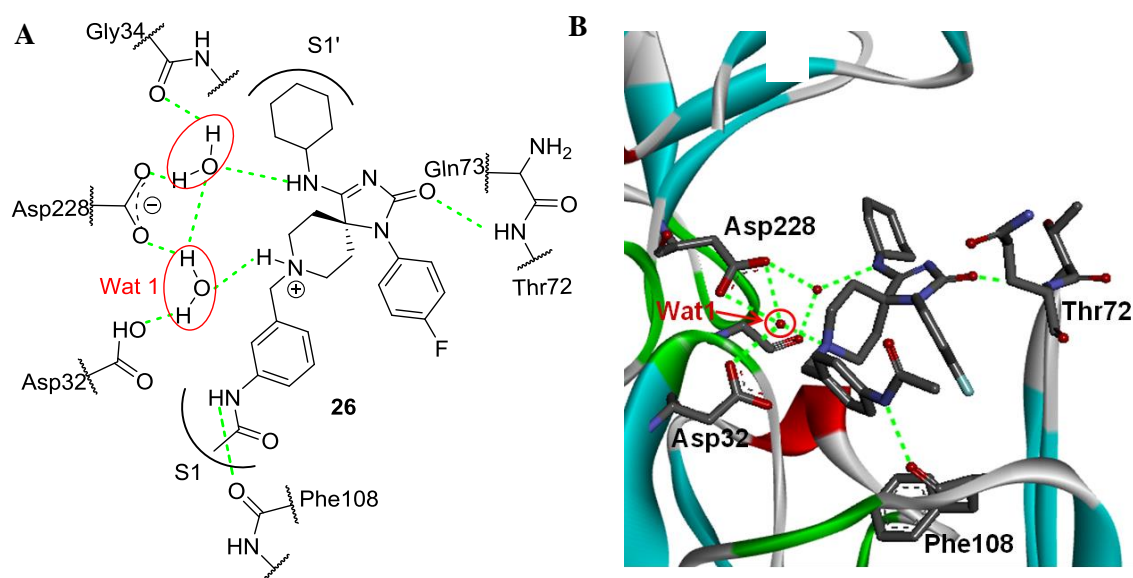


Figure 21. Aminoimidazole inhibitor 24 and spiropyrrolidine inhibitor 25. 2D structures and representation of key H-bond (green dotted line) and π interactions (orange dotted line) formed by inhibitors **24** and **25** with BACE-1 residues in the catalytic site. A) Aminoimidazole **24** designed by Malamas *et al.*⁸³ B) Spiropyrrolidine inhibitor **25** designed by Efremov *et al.*⁸⁴

1.4.5 An interesting spiropiperidine iminohydantoin inhibitor

Among the series of non-peptidomimetic BACE-1 inhibitors identified by fragment-based drug design, there is the interesting spiropiperidine iminohydantoin inhibitor **26**.⁸⁵ The X-ray structure of the inhibitor **26** in complex with BACE-1 showed a particular feature of H-bond interactions. The water molecule located between the two catalytic aspartates, Wat1, is not displaced but forms a H-bond network with the N of the piperidine group of the inhibitor and with the BACE-1 catalytic aspartates. Another water molecule forms H-bonds with the secondary amine group of the inhibitor and with Gly34 and Asp228. This type of inhibition through water molecules is a new mode of inhibition (Figure 22). The inhibitor **26** also forms H-bonds with Phe108 and Thr72, located in the flap region, locking the protein in an open conformation.



BACE-1: $IC_{50} = 3.0 \mu M$, $LE' = 0.18$

Figure 22. Spiropiperidine iminohydantoin inhibitor 26. 2D (A) and 3D (B) representation of the binding pose of the inhibitor **26** in the BACE-1 catalytic site. H-bond interactions are represented as green dotted line, water molecules are highlighted in red. The characteristic of the spirocyclic inhibitor **26** is to inhibit BACE-1 through a network of H-bonds with two bridge water molecules, one of which is the conserved water molecule Wat1. Adapted from Barrow *et al.*⁸⁵ (pdb code 3FKT). Visualised with Discovery Studio 3.0.

Inspired by this kind of water bridge inhibition mode, Brodney *et al.*⁸⁶ designed a series of a spirocyclic sulfamide inhibitors. Among those, the inhibitor **27** assumes a binding pose similar to the previously shown inhibitor **26**. Wat1 is involved in a H-bond with the N of the piperidine group of the inhibitor and forms a network of H-bonds with the catalytic aspartates of BACE-1. Another water molecule forms a H-bond with Asp228. The X-ray structure shows also another H-bond formed by the *O*-alkyl group of the aromatic substituent of the inhibitor with a third water molecule (Figure 23).

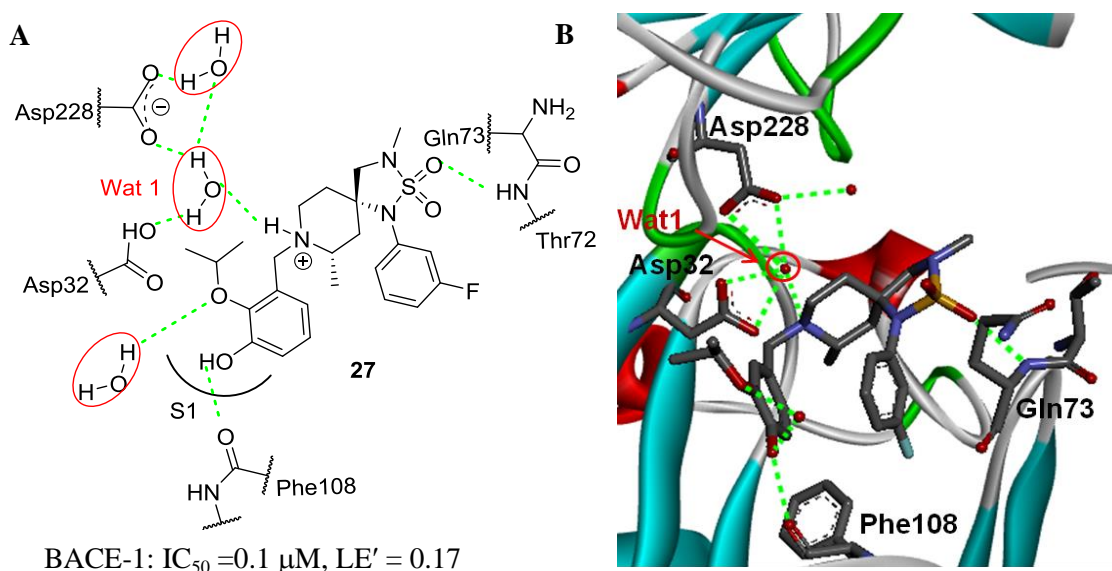


Figure 23. Spirocyclic sulfamide inhibitor 27. 2D (A) and 3D (B) representation of the binding pose of the inhibitor **27** in the BACE-1 catalytic site. H-bond interactions are represented as green dotted line, water molecules are highlighted in red. The inhibitor has a binding pose similar to inhibitor **26** (Figure 22). The conserved water molecule Wat1 is involved in a bridge network of H-bonds. Two other water molecules are present in the catalytic site region. The sulfamide ring is involved in a H-bond with the NH (backbone) of Gln73 in the flap region. Adapted from Brodney *et al.*⁸⁶ (pdb code 4FM7). Visualised with Discovery Studio 3.0.

1.4.6 Inhibitor designed through computational methods

Virtual screening was also successful in discovering new structures for BACE-1 inhibitors. In 2010 Xu *et al.*^{87, 88} identified two new BACE-1 inhibitors by screening *in silico* libraries of commercially available compounds with lead-like properties (Section 1.1). One inhibitor was based on a pyrazole-derived central core and the other on a benzothiazole central core (Figure 24).

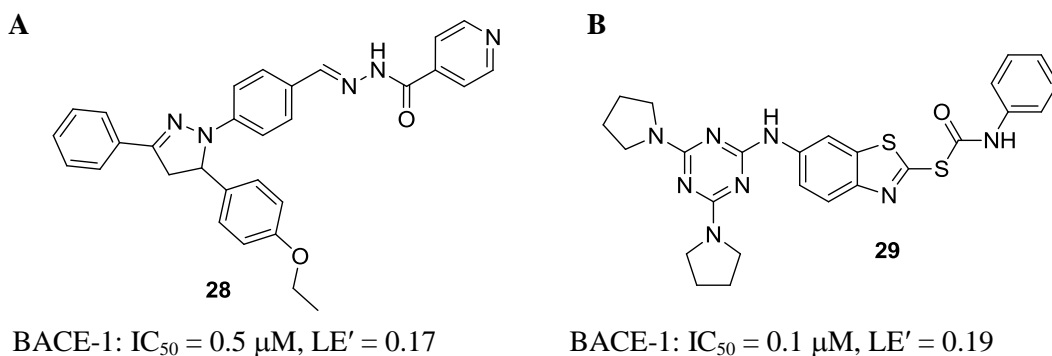


Figure 24. Inhibitors identified via virtual screening by Xu *et al.*^{87, 88} A) Inhibitor **28** contains a pyrazole-derived central core. B) Inhibitor **29** contains a benzothiazole central core.

In 2013 Mok *et al.*⁸⁹ employed a *de novo* generation software, SPROUT, to design a series of biphenylacetamide BACE-1 inhibitors. Among those, the inhibitor **30** showed an IC_{50} of 33 μM (Figure 25). In 2014 Viklund *et al.*⁹⁰ generated novel cores for BACE-1 inhibitors based on *de novo* design of lead molecules and computational prediction of their affinity, permeability and synthetic feasibility. They derived and synthesized seven active cores, containing variation elements from known cores (Figure 26).

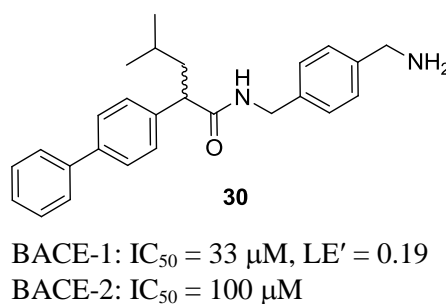
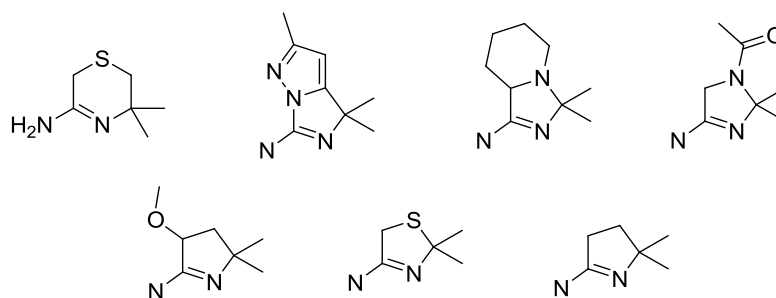


Figure 25. Inhibitors designed through de novo generation software. Inhibitor design by Mok *et al.*⁸⁹ using SPROUT.



BACE-1: IC₅₀ from 100 to 1 μM

Figure 26. Cores for BACE-1 inhibitors identified by de novo design. Seven cores designed by Viklund *et al.*⁹⁰

1.4.7 Challenges of BACE-1 inhibitor design, failure in clinical trials

Despite the wide range of BACE-1 inhibitors designed, only few of them entered into clinical trials. To enter a phase I clinical trial BACE-1 inhibitors require good cellular potency (nM range) and selectivity for BACE-1 *vs* BACE-2 and *vs* cathepsin D (100-fold). Inhibitors designed by Eli Lilly, AstraZeneca and Roche from 2009 onwards failed phase I studies due to the poor blood-brain barrier permeability. Currently only two inhibitors are in phase II and phase III trials, one is **E2609** of Eisai (phase II) and the other is **MK-8931** of Merck (phase III).

Due to the failure of clinical studies, a new approach based on antibody therapies was proposed in 2011 to target BACE-1. A human antibody, able to target BACE-1 and to induce conformational changes on residues 157-170 of the protein, was developed by Atwal *et al.*⁹¹ Residues 157-170 of BACE-1 normally adopt α -helical structure when the protein binds APP substrate. In the antibody-BACE-1 complex these residues assume a random loop structure, which seems to prevent APP substrate to reach the catalytic site of the protein. The anti BACE-1 antibody therapy showed in mice high selectivity and effective reduction of β -amyloid peptides.

1.5 Project outline

The project described herein was directed to develop a novel computational and experimental approach to design lead-like bioactive molecules by generating a virtual library of likely synthetic accessible lead-like compounds based on DOS strategy. To

investigate the approach, BACE-1 protein was chosen as biological target, and the virtual library of lead-like compounds was screened *in silico* against BACE-1.

A virtual library of likely synthetic accessible lead-like compounds was generated by following DOS methodologies developed in the Nelson group. A protocol of synthesis was designed on the basis of known chemical reactions and commercially available reactants, and was built using Pipeline Pilot software. The virtual library was screened *in silico* against BACE-1 using eHits software. Putative BACE-1 inhibitors were identified from the virtual screening according to criteria of ligand efficiency (cLE') and were selected for synthesis. Two synthetic routes were investigated to prepare a focused library of putative inhibitors. The biological activity of the focused library was assessed *via* a fluorimetric assay.

This report is composed as follows. Chapter 2 describes computational tools (Pipeline Pilot and eHiTS) and strategy envisaged to design lead-like putative BACE-1 inhibitors. Chapter 3 describes two synthetic routes towards a focused library of putative BACE-1 inhibitors. Chapter 4 presents results of the biological activity of putative BACE-1 inhibitors; describes further SAR studies and provides a discussion of the obtained results.

Chapter 2. Structure-based design of putative bioactive molecules for BACE-1

The following Chapter describes a novel computational approach to identify new putative bioactive molecules for BACE-1. The approach involved the design of a virtual library of likely synthetically accessible lead-like compounds based on diversity-oriented synthesis (DOS) and the virtual screening of this library against BACE-1. An overview of the approach, including a description of the computational tools employed for the enumeration of a virtual library (Pipeline Pilot) and for virtual screening (eHiTS), is presented in Section 2.1. Demonstration of the validity of the virtual screening method is given in Section 2.2. A detailed description of the performed computational process is shown in Section 2.3 and analysis of the identified putative inhibitors is presented in Section 2.4.

2.1 Overview of the computational approach

The proposed computational approach combined the *in silico* enumeration of likely synthetically accessible compounds using DOS and virtual high-throughput screening (vHTS). The approach was directed towards the identification of novel small cyclic BACE-1 inhibitors, able to interact with the catalytic aspartates, Asp32 and Asp228, and/or with two water molecules located in the catalytic site of BACE-1 (similarly to the inhibitor **26**, Section 1.4.5).

Two libraries of cyclic molecules were generated using Pipeline Pilot. The first library, *library A*, was optimised after analysing the results of an initial vHTS round against BACE-1. The optimisation of *library A* led to the generation of the more focused *library B*. From each library, lead-like molecules were selected according to specific structural and lipophilicity parameters: number of heavy atoms, $16 \leq \text{nHA} \leq 23$ for *library A* and $16 \leq \text{nHA} \leq 27$ for *library B*; number of aromatic rings ≤ 2 ; value of the atomic-based prediction partition coefficient,⁹² $0 \leq \text{AlogP}^c \leq 3.5$. The number of saturated rings > 0 was also considered as a parameter for the selection of molecules in

^cAlogP is an algorithm estimation of the partition coefficient, $P_{\text{octanol/water}}$, based on the contribution of different atoms according to their physicochemical properties.

order to verify that only cyclic molecules were generated from the enumeration of the two virtual libraries.

The selected lead-like molecules underwent vHTS using two BACE-1 structures: one containing two water molecules in the catalytic site and the other one without water molecules. After the vHTS of *library B*, putative inhibitors were chosen for synthesis. The overall computational approach is shown in Figure 27.

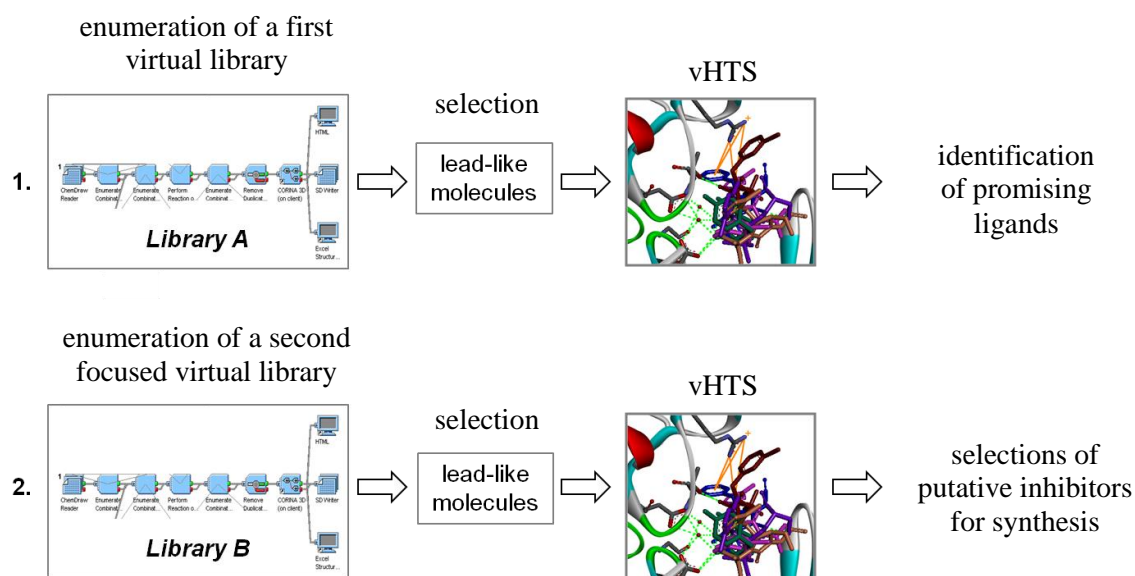


Figure 27. Summary of the computational approach which led to the identification of novel putative BACE-1 inhibitors. 1) The approach starts with the enumeration of a virtual library of likely synthetically accessible molecules, *library A*. The generated library was filtered according to lead-like parameters and the resulting molecules were screened *in silico* against the target protein BACE-1. Promising ligands were identified and analysed. 2) The initial *library A* was optimised and the more focused *library B* was obtained. *Library B* underwent the same computational process to identify putative inhibitors of BACE-1.

2.1.1 Pipeline Pilot

Pipeline Pilot^{93, 94} is a scientific informatics platform which can be used to generate virtual compound libraries. Pipeline Pilot allows the creation of configurable protocols to manage, order and analyse scientific data, and to enumerate combinatorial processes. Configurable protocols can be built by assembling specific components which store,

manipulate, filter, and display data. The chemistry components in Pipeline Pilot are able to: perform virtual reactions, modify chemical structures, enumerate libraries, calculate different molecular properties, search molecules according to substructures and similarities, and cluster and filter compounds. An example of a configurable protocol designed in Pipeline Pilot to enumerate a virtual library of structurally diverse compounds is illustrated in Figure 28.

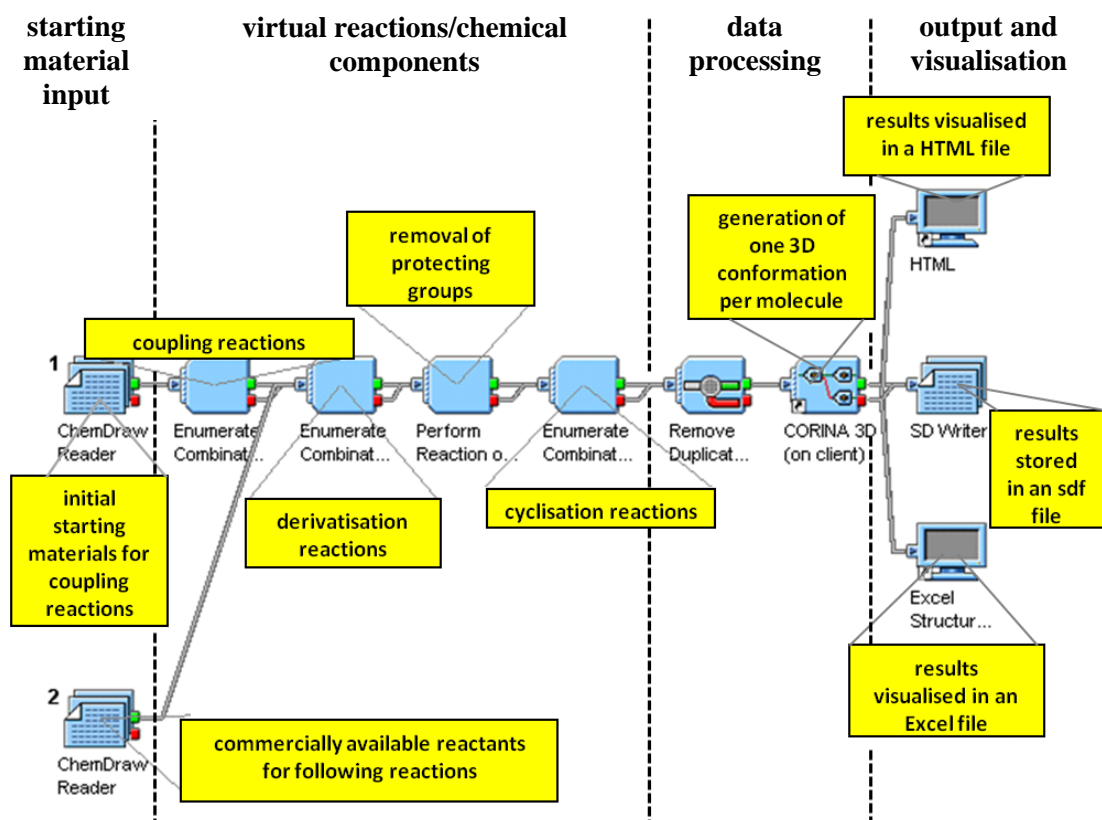


Figure 28. Configurable protocol designed in Pipeline Pilot to enumerate a virtual library of structurally diverse compounds. The protocol was built with a series of components. Firstly starting materials and reactants are read in the form of a ChemDraw file (components “Reader” 1 and 2, on the left), then a series of virtual reactions are performed through chemistry components. The data are then processed (removing duplicates and generating a 3D conformation per molecule) and stored in the form of SD file. The resulting molecules are then visualised as HTML and Excel File (components on the right).

2.1.2 eHiTS

eHiTS²³ (electronics **H**igh **T**hroughput **S**creening) is one of the many docking programs (Section 1.2.3) employed in the virtual screening of molecules. eHiTS contains a systematic structure search algorithm to predict the binding pose of a ligand in a protein target site,²³ and an empirical scoring function to estimate binding affinity. The structure search algorithm in eHiTS identifies rigid fragments and flexible chains contained in the ligand structure, and docks rigid fragments separately in any available location of the protein binding site. The docked poses of the fragments which are in proximity to each other are considered “pose sets” and are combined together through a graph matching algorithm. The ligand flexible chains are connected to the “pose sets”, without changing their original conformation, and the overall structure of the ligand is then reconstructed. The reconstructed ligand structure is then optimised by considering low energy rotamers or by resolving steric clashes. The predicted ligand pose is scored according to an empirical scoring function.

The scoring function detects interactions between surface points of a ligand’s rigid fragments and of a protein binding site to determine the initial score. Surface points are classified according to chemical properties and are divided into 23 different types: metals, H-bond donors, weak H-bond donors, lone pairs, π -electrons, halogens, positively charged hydrogens, *etc.* An estimation of the binding affinity of a ligand is derived from a statistic sum of the ligand surface point types and it is expressed as a negative value on a logarithmic scale.²³ The estimated ligand binding affinity can be correlated with the ligand inhibition constant for the target protein, K_i , as follows: an eHiTS score of -7.0 would correspond to an estimated 10^{-7} M inhibitor.

Protonation states of the ligand and the protein binding site are important factors in predicting the ligand binding pose and its affinity. eHiTS scores all possible protonation states of the ligand and the protein in one run and selects the best protonation state for each single interaction. eHiTS can screen thousands of molecules in one run, enabling virtual high throughput screening.

2.1.3 Ligand selection

As shown in Figure 1 (Section 2.1), promising ligands were selected from virtual screening of library *A* and putative inhibitors were selected from virtual screening of library *B*. The criteria of selection of promising ligands and putative inhibitors were based on values of cLE' (Section 1.2.3.1) and molecular weight: $cLE' \geq 0.27$ or 0.28 and $200 \leq M.W. \leq 460$. The cLE' was calculated from the eHiTS score according to Equation 6. The limiting value of cLE' was chosen according to the distribution of data, in order to focus on the best 1-2% of cLE'.

$$cLE' = -\frac{\text{eHiTS score}}{nHA}$$

Equation 6. Computed ligand efficiency calculated from eHiTS scores.

The range of molecular weight and lipophilicity chosen to select promising ligands and putative BACE-1 inhibitors ($200 \leq M.W. \leq 460$ and $0 \leq AlogP \leq 3.5$) respects the lead-likeness criteria suggested by Monge *et al.*⁶ ($M.W. \leq 460$ and $\log P \leq 4$). According to the chemical space definition of Nadin *et al.*² (Section 1.1), instead, this range includes mostly lead-like compounds and a small part of drug like-compounds (Figure 29). The selection of promising ligands and putative inhibitors selection was performed by using a specific protocol designed in Pipeline Pilot (Figure 30).

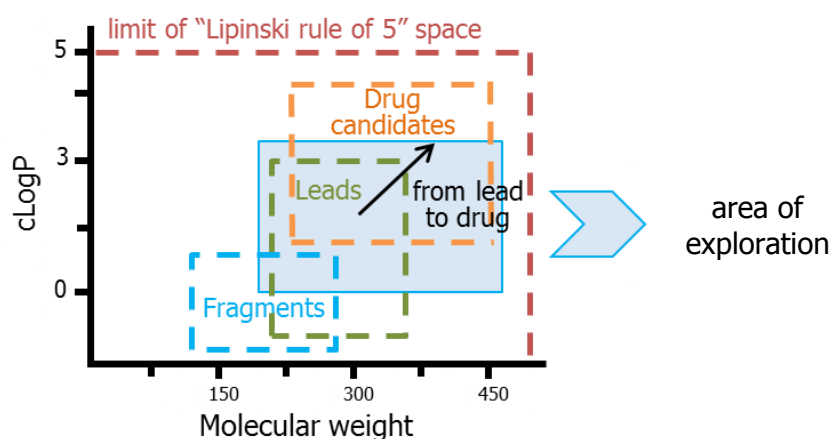


Figure 29. Chemical space explored in the identification of putative bioactive molecules. The blue area shows the chemical space explored in the proposed approach to identify bioactive molecules. According to the representation of chemical space of Nadin *et al.*,² this area includes mostly lead-like and part of drug -like molecules.

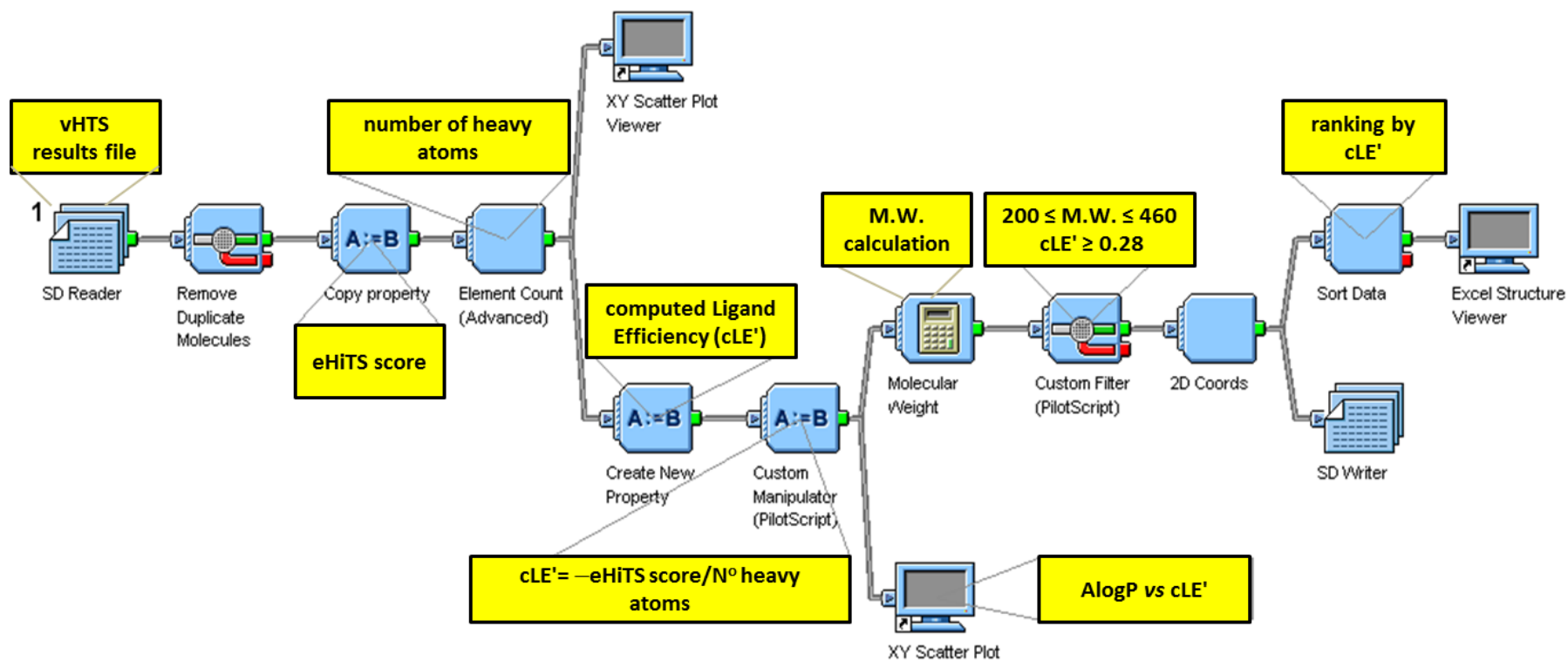


Figure 30. Protocol designed in Pipeline Pilot to select virtual ligands identified by vHTS against BACE-1. The results files of any vHTS rounds, containing eHiTS scores, are used to calculate cLE'. The results are filtered according to cLE' and M.W. values, and are visualised in a scatter plot of AlogP vs cLE'.

2.2 Testing the applicability of eHiTS to BACE-1

The docking method employed by eHiTS was validated before being applied to the virtual screening of *libraries A* and *B*. To verify the applicability of eHiTS to BACE-1 and to confirm the validity of eHiTS in predicting ligand binding poses, a docking test was performed. The test consisted of reproducing the binding pose of a known inhibitor in the catalytic site of BACE-1 using eHiTS. The known co-crystal structure of the spiropiperidine iminohydantoin inhibitor **26** bound to BACE-1,⁸⁵ referred as 3FKT^a hereafter, was chosen for the docking test (Figure 31). The compound **26**, a 3 μM inhibitor, inhibits BACE-1 *via* a hydrogen bonding network with the conserved water molecule Wat1, located between the catalytic aspartates, and another water molecule contained in the protein catalytic site (Section 1.4.5).

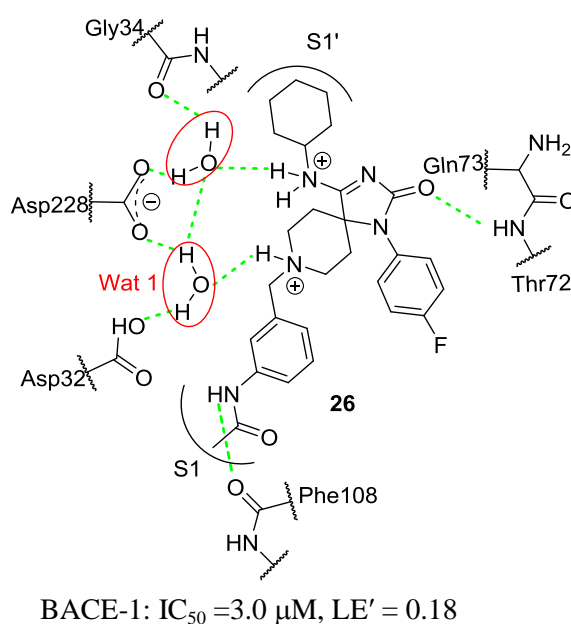


Figure 31. 2D representation of the inhibitor **26** in complex with BACE-1. The H-bond network formed in the catalytic site of BACE-1 is represented in green dotted lines.

^a3FKT corresponds to the PDB access number of the complex formed between the inhibitor **26** and BACE-1.

To reproduce the mode of interaction of the inhibitor **26** with BACE-1, a compatible structure had to be derived from 3FKT. The coordinates corresponding to the inhibitor **26**, as well as the coordinates corresponding to all water molecules, except for the two in proximity to the catalytic aspartates, were removed. The resulting structure is shown in Figure 32.

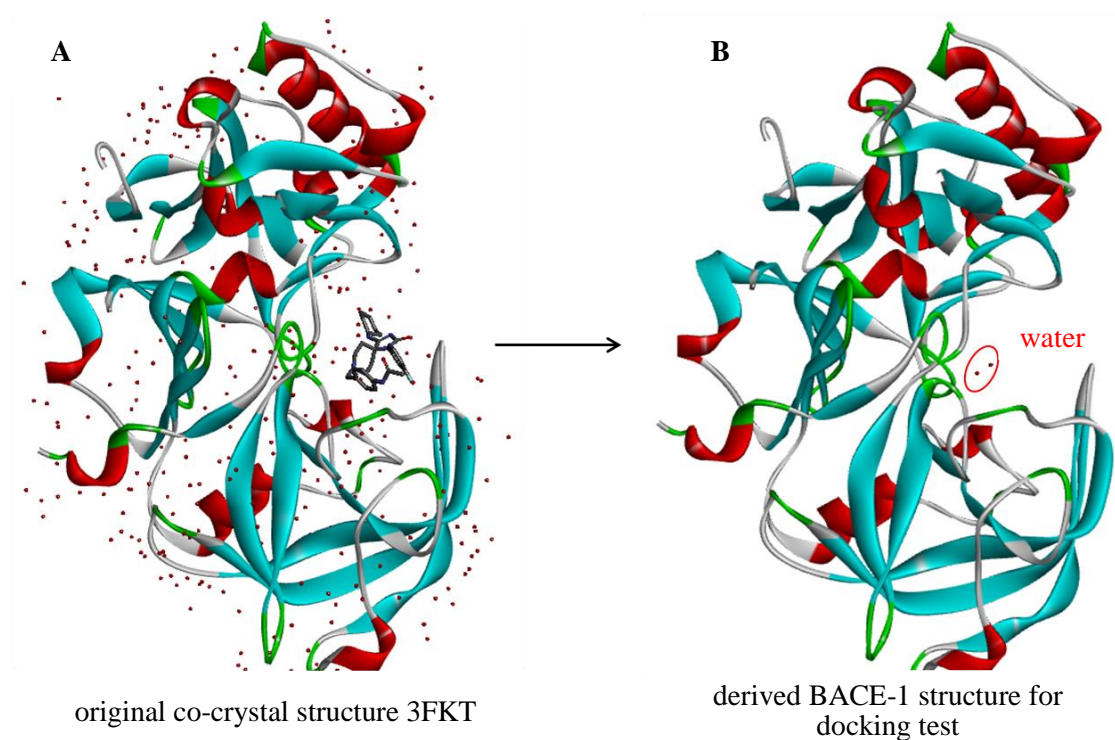
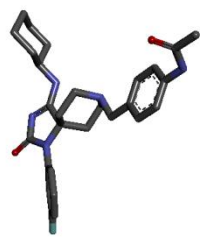
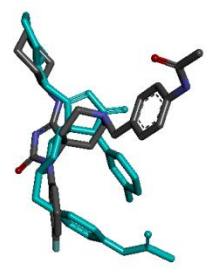
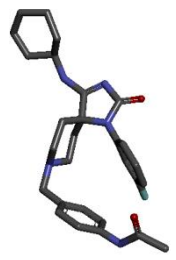
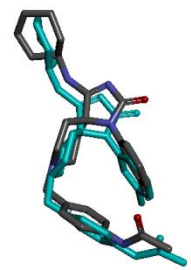
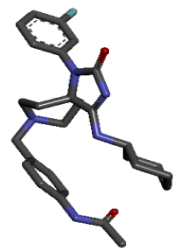
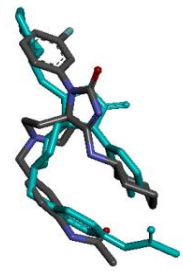
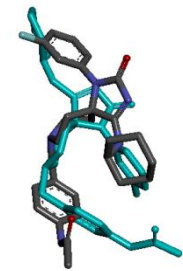
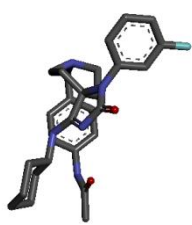
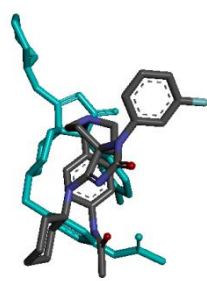


Figure 32. Derived BACE-1 structure for docking test. A) Original X-ray co-crystal structure of the 3FKT (1.90 Å). B) Derived BACE-1 structure used for docking test. The coordinates of the ligand and the water molecules, except for the ones in proximity to the catalytic aspartates, were removed. Structures visualised with Discovery Studio 3.0.

25 different three-dimensional conformations of the inhibitor **26** were generated^{a, 95} and docked against BACE-1. The resulting binding poses were analysed and sorted according to their eHiTS score. The top five binding poses predicted by eHiTS are reported in Table 4.

^aThe three-dimensional conformations of the inhibitor **26** were generated using Corina⁹⁵

Table 4. Top scoring poses of inhibitor 26 predicted by eHiTS software.

Entry	eHiTS predicted pose	eHiTS score	Predicted (grey) vs experimental (blue) pose ^a
1		-7.05	
2		-7.03	
3		-6.89	
4		-6.88	
5		-6.82	

^aBinding poses visualised with Discovery Studio 3.0

The predicted binding pose ranked as second, according to its eHiTS score, was in good agreement with the pose of the inhibitor **26** (Table 4, entry 2). The root mean square deviation (RMSD) of heavy atom position between this predicted binding pose and the co-crystal structure pose of the inhibitor **26** was of 1.36 Å; in line with the accepted limited value of Å ≤ 2.0 for reliable prediction.⁹⁶ This predicted binding pose forms one H-bond between the piperidine-N atom of the inhibitor **26** and Wat1 in the catalytic site of BACE-1 (Figure 33).

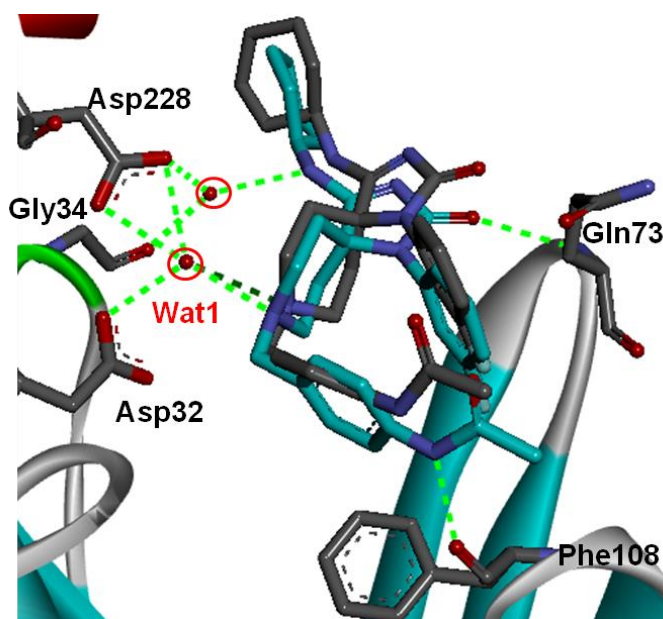


Figure 33. Superimposed binding poses of the spiropiperidine iminohydantoin inhibitor **26** in the catalytic site of BACE-1. Predicted (grey) and experimental (blue) binding poses of the inhibitor **26** in complex with BACE-1.^a The green dotted lines show the network of H-bond interactions for the experimental binding pose, red circles indicate the water molecules. The inhibitor binding pose predicted by eHiTS forms a H-bond with Wat1 (dark green dotted line), while the inhibitor **26** in complex with BACE-1 forms other three main H-bonds: one with another water molecule in proximity of Asp228, one with Phe108 and another one with NH (backbone) of Gln73. Visualised with Discovery Studio 3.0.

^a PDB access number 3FKT

The H-bond between the secondary amino group of the inhibitor and the water molecule in proximity of Asp228, observed in 3FKT (Figure 31), was not detected. Other two H-bonds with BACE-1 residues, Gln73 and Phe108, located in the flap region (Section 1.3.2) were also missed. Nevertheless, the orientation of the inhibitor **26** in the catalytic site of BACE-1 was correctly reproduced and the reliability of eHiTS was therefore demonstrated.

2.3 Design of a virtual library of likely synthetically accessible lead-like compounds

A virtual library of likely synthetically accessible lead-like molecules was enumerated using Pipeline Pilot. In each case, it was envisaged that a scaffold might be assembled from an initial coupling of two main building blocks and the resulting intermediate could be varied by a sequence of established reactions. The virtual synthesis of each scaffold was performed in parallel from a range of different building blocks and a library of structurally diverse scaffolds was generated according to the DOS principle (Section 1.2.4).

In order to ensure synthetic accessibility as far as possible, a toolbox of previously established reactions and a pool of commercially available reagents were applied to the protocol. The protocol started with a series of virtual coupling reactions between nucleophile and electrophile building blocks (*e.g.* nucleophilic opening of cyclic sulfamidates,⁹⁷ Ir-catalysed asymmetric amination of an allylic carbonate⁹⁸), and then proceeded with virtual derivatisation reactions on the resulting intermediates with isocyanates or aryl bromide reagents. The resulting compounds underwent one or two virtual cyclisation reactions (*e.g.* metathesis,⁹⁹ Pd-catalysed aminoarylation¹⁰⁰) followed by virtual removal of protecting groups. A series of virtual skeletally diverse molecules was obtained and further modified by virtual derivatisation reactions. The list of virtual reactions and building blocks employed to enumerate the library, *library A*, is reported in Appendices 1.1 and 1.3.

The resulting compounds were filtered according to lead-like parameters (Section 2.1) and a library of *ca.* 85,000 likely synthetically accessible compounds, *library A*,

was obtained. Examples of cyclic compounds obtained from the enumeration of *library A* are represented in Figure 34.

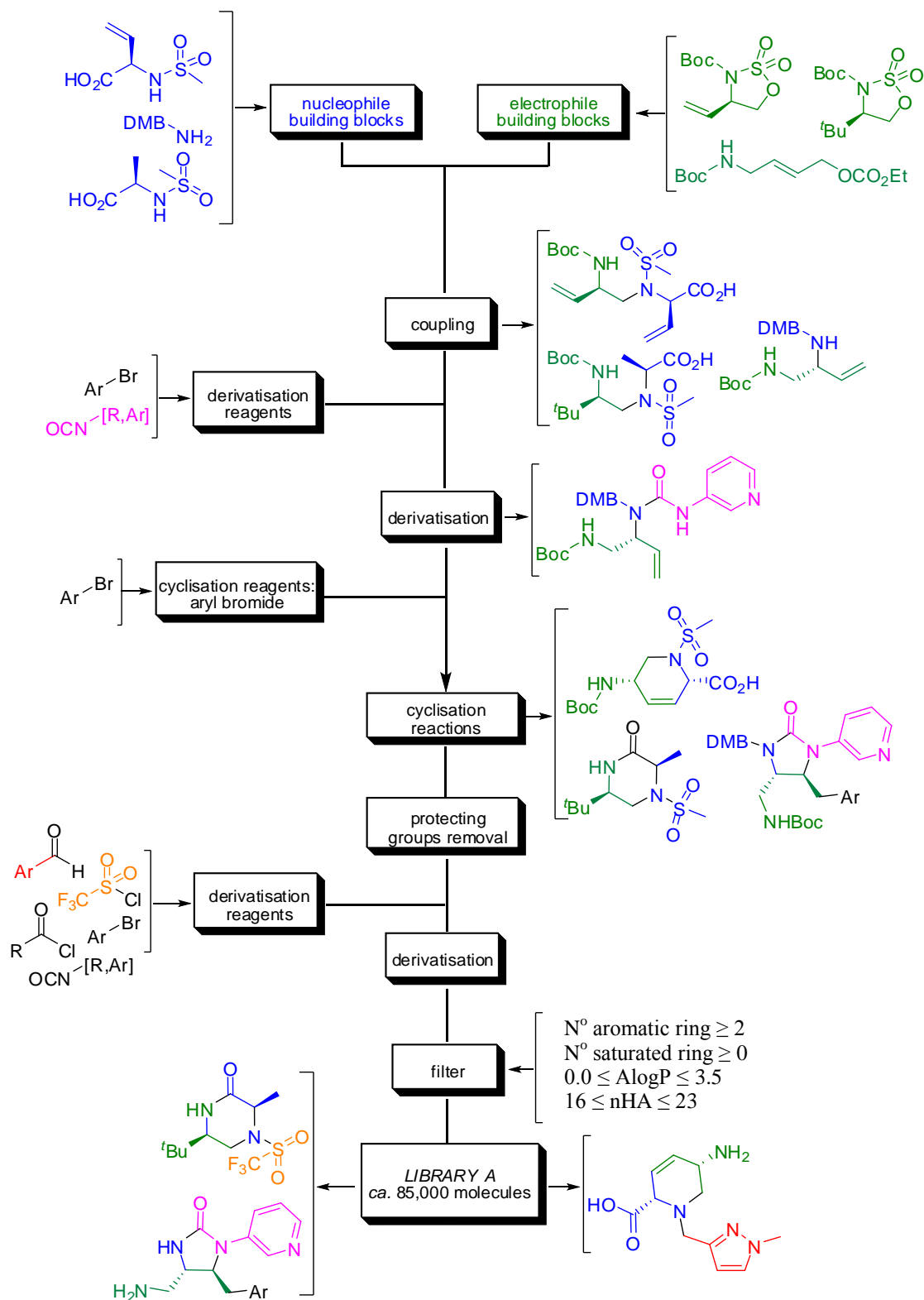


Figure 34. Protocol of virtual synthesis employed to enumerate virtual *library A*. Examples of virtual products obtained at each stage are shown.

2.3.1 Identification of promising ligands

Library A was docked against BACE-1 in order to identify putative ligands. A first vHTS was conducted using a randomly-selected sample of 10% of the molecules,^a in order to identify representative classes of molecules contained in the library. The resulting eHiTS scores were used to calculate the cLE'. The most promising putative ligands were chosen on the basis of cLE' value, $cLE' \geq 0.27$.^b The structures of those ligands were analysed and clustered into eight main substructures (Figure 35).

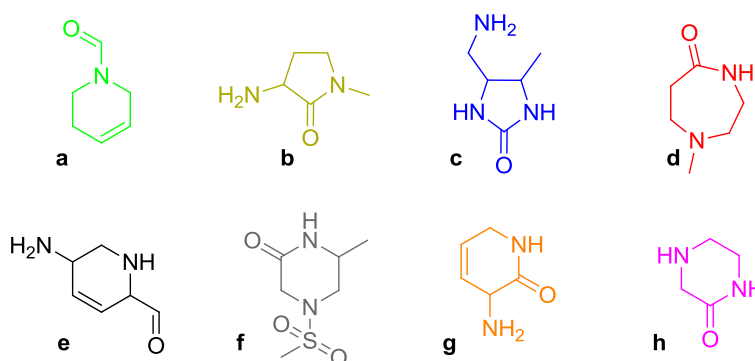


Figure 35. Eight main substructures of the most promising virtual ligands of *library A*. The substructures were identified by vHTS a randomly-selected sample of 10% of library A against BACE-1.

All the compounds in *library A* that contained one of the above substructures were selected. The resulting 29,084 molecules were docked against BACE-1. The 131 most promising compounds, with $cLE' \geq 0.28$,^b were analysed: 68% of the compounds contained the substructure **e**, 35% the substructure **c** and 7% the substructures **d** and **h**. Examples of those compounds and their distribution according to lipophilicity (AlogP) and cLE', values are reported in Figure 36.

^aThe three-dimensional conformations of the representative 10% sample of *library A* were generated using Corina⁹⁵ (one three-dimensional conformation for each molecule).

^bThe limiting value of cLE' was chosen according to the distribution of data, in order to focus on the best 1% of cLE'.

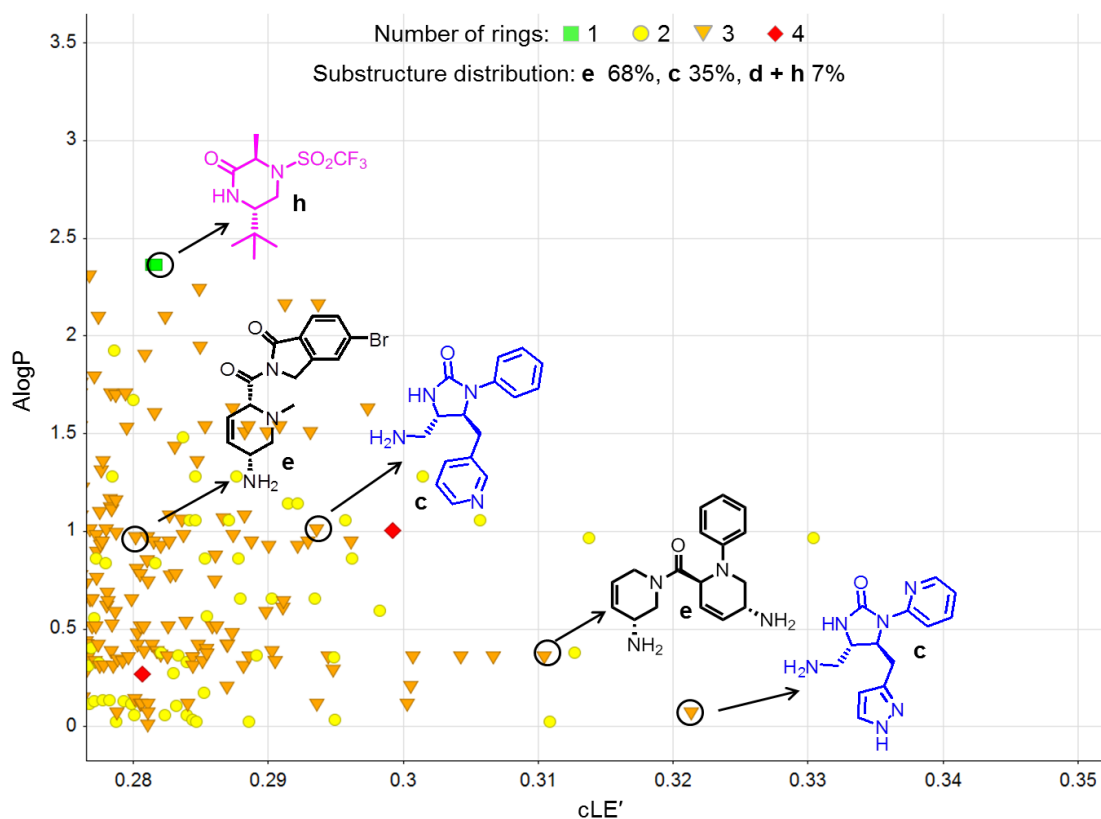


Figure 36. Promising putative BACE-1 ligands with $cLE' \geq 0.28$ contained in *library A*. Each symbol represents a single ligand described by AlogP and cLE' . Representative ligands are coloured according to their substructure defined in Figure 35. 131 ligands were identified following vHTS of 29,084 molecules. The substructures **c** and **e** contained mainly 2 or 3 saturated or aromatic rings, while the substructure **d** and **h** contained 1 or 2 saturated or aromatic rings. Graph reproduced with Dotmatics Vortex.

2.3.2 Optimisation of *library A* and identification of two families of putative BACE-1 inhibitors

The protocol used for the generation of *library A* was modified in order to create a more focused virtual library of putative BACE-1 inhibitors. A further series of virtual derivatisation reactions, performed with a variety of secondary amines, was added at the end of the protocol and a broader variety of virtual derivatisation reagents (aryl bromide and isocyanates) was used. The list of virtual derivatisation reactions and of the reagents employed is provided in Appendices 1.2 and 1.3.

Five million molecules were generated and filtered according to the established lead-like parameters (Section 2.1) and a virtual library of ca. 55,000 molecules was derived; *library B*. The overall protocol for the generation of the virtual *library B* is illustrated in Figure 37. It was observed that molecules generated from *library B* showed more substituted structures than members of *library A* (Figure 38).

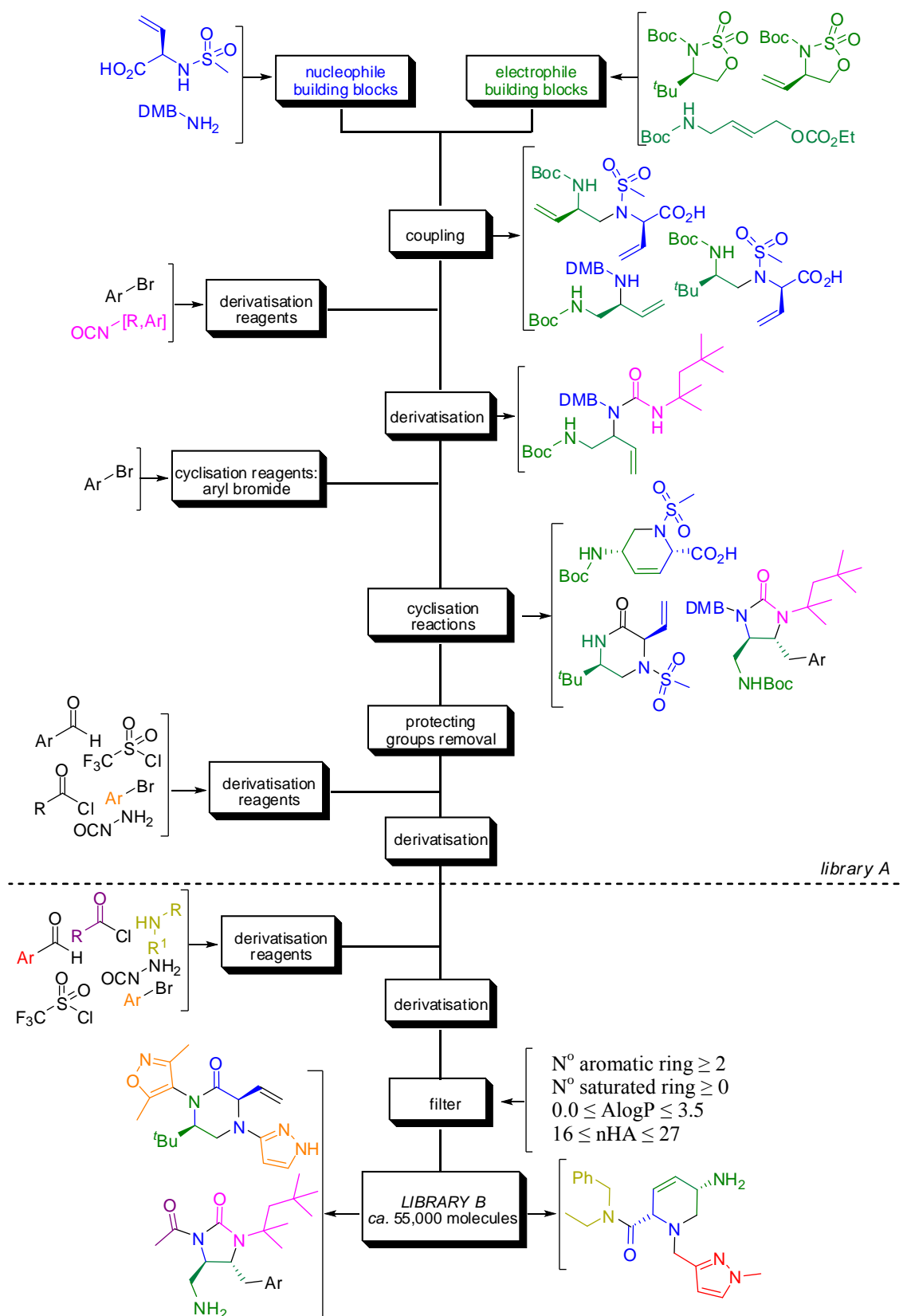


Figure 37. Protocol of virtual synthesis employed to enumerate virtual library B. Examples of virtual products obtained at each stage are shown. The protocol of virtual synthesis of library A was implemented with additional virtual derivatisation reactions (below the dotted line) to give more substituted structures ($16 \leq n\text{HA} \leq 27$).

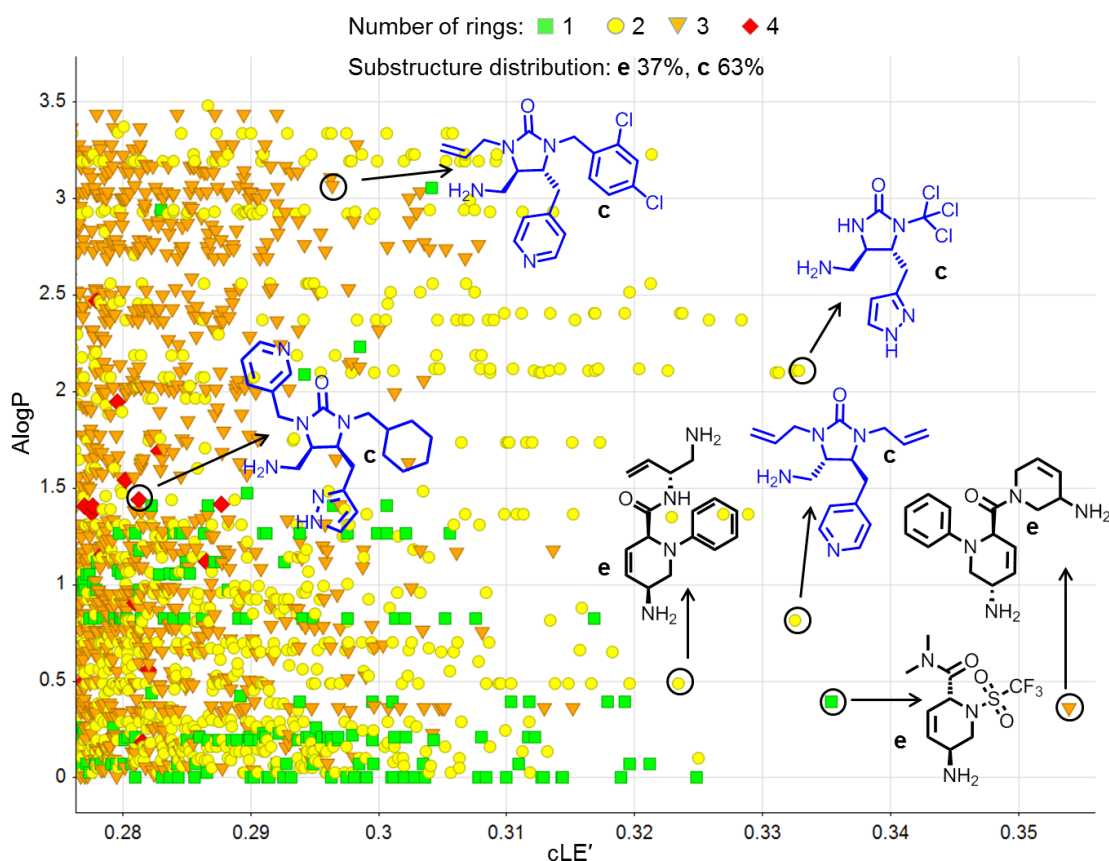


Figure 39. Putative BACE-1 inhibitors, $cLE' \geq 0.28$ identified from *library B*. Each symbol represents a single ligand described by AlogP and cLE' . Representative ligands are coloured according to their substructure defined in Figure 35. 900 ligands were identified following vHTS of *ca.* 55,000 molecules. The amino tetrahydropyridine family of putative inhibitors (substructure **e**) contained mainly 1 or 2 saturated or aromatic rings, while the imidazolidinone family of putative inhibitors (substructure **c**) contained mainly 2 to 4 saturated or aromatic rings. Graph reproduced with Dotmatics Vortex.

2.4 Analysis of the predicted binding poses of the putative inhibitors

The predicted binding poses of the two identified families of putative inhibitors for BACE-1 were analysed. For both families the key predicted interactions with the catalytic site of BACE-1 were H-bond interactions formed through the primary amine contained in the putative inhibitor structures. The predicted H-bond interactions were directed towards the water molecules and/or the catalytic aspartates, Asp32 and Asp228. The primary amine is predicted to be protonated at the pH at which BACE-1 is active

(pH 4.5). Other predicted H-bond interactions were formed with Lys107 and Phe108 contained in the flap region of BACE-1 or with Arg235. Examples of the predicted binding poses of the two main families of putative inhibitors are shown in Figure 40.

When docking was conducted without including the water molecules in the catalytic site of BACE-1, the H-bond interactions between the putative inhibitor's protonated primary amine, NH_3^+ , and the catalytic aspartate residues, Asp32 and Asp228, were still predicted (illustrations given in the Appendix 2.1). The binding pose prediction was therefore consistent, orienting the putative inhibitors in the catalytic site of BACE-1 in the same direction, either in presence or in absence of the water molecules.

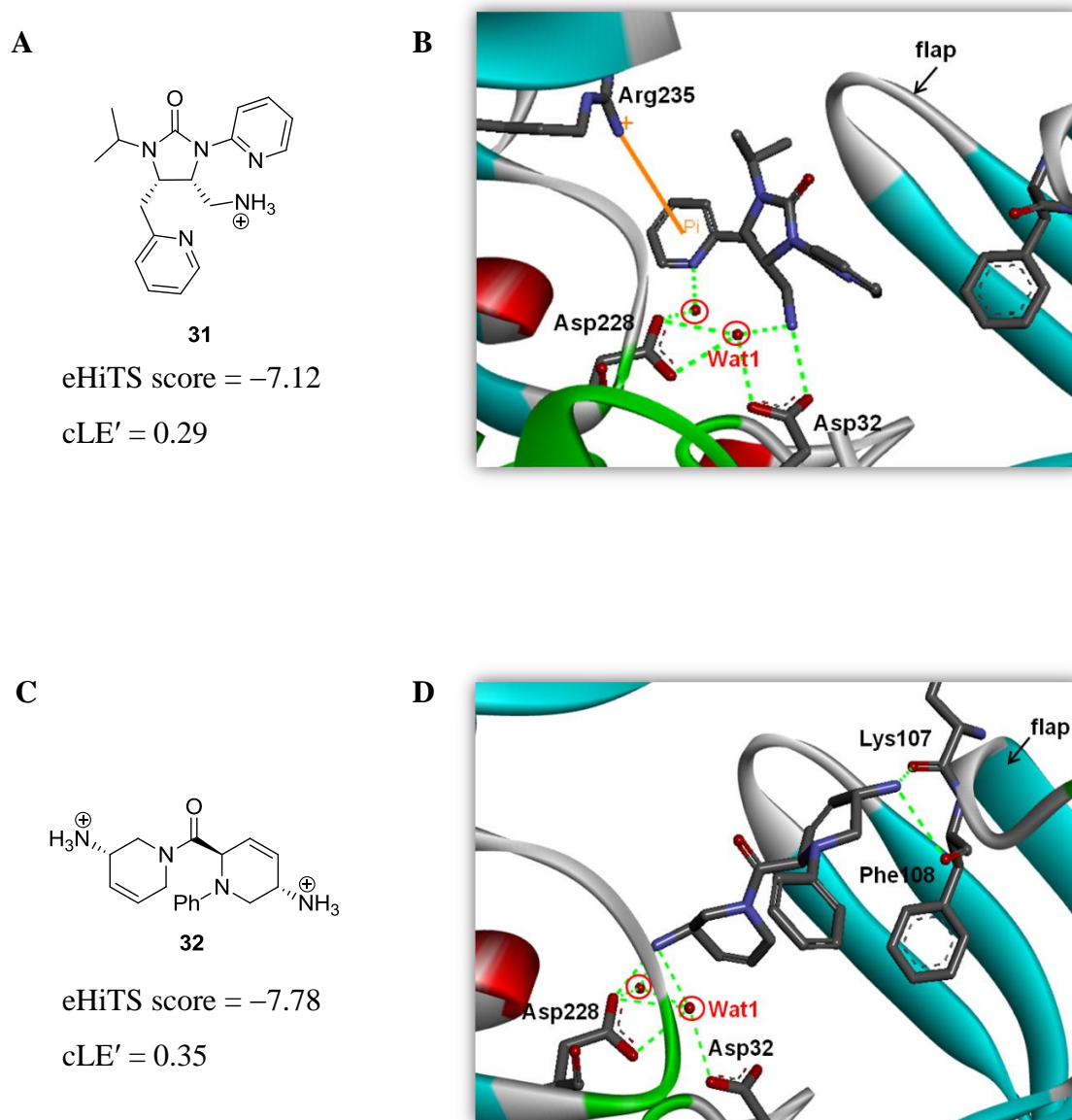


Figure 40. Predicted binding pose of representative members of the identified families of BACE-1 putative inhibitors. A) and C) 2D structure of the imidazolidinone putative inhibitor **31** (A) and of the amino tetrahydropyridine putative inhibitor **32** (C) in their protonated state. B) and D) 3D image of the predicted binding pose of the inhibitors **31** (B) and **32** (D). The predicted H-bond interactions are shown with green dotted lines, π -cation interactions are shown in orange line, and red circles indicate water molecules. The water molecules, Asp228 and Asp32 form H-bonds with the protonated primary amine, NH_3^+ , of the putative inhibitor **31** (B) and **32** (D). Arg235 forms a π -cation interaction with one pyridine ring of the putative inhibitor **31** (B). Lys107 and Phe108, both located in the flap region form H-bond with the other protonated primary amine, NH_3^+ , of the putative inhibitor **32** (D). Visualised with Discovery studio 3.0.

2.4.1 Validation of the predicted binding poses with additional docking software

A representative set (eight molecules) of the two identified families of putative BACE-1 inhibitors was studied using the Maestro suite (Schroedinger).¹⁰¹ The lengths of the predicted H-bonds formed in the catalytic site of BACE-1 were measured. The predicted length range was of 2.4-2.9 Å for H-bonds formed with Asp32 and Asp228, and 2.2-2.5 Å for H-bonds formed with the water molecules. These lengths were in agreement with the range of 2.5-3.2 Å reported in the literature for H-bonds formed in the catalytic site of BACE-1.^{77, 86} Representative examples are provided in Appendix 2.2.

The predicted binding poses of the representative putative inhibitors were analysed using Macromodel, a specific component within Maestro, in order to assess their conformational energy. Macromodel was used to minimise the conformational energy of raw eHiTS binding poses inside the catalytic site of BACE-1. Macromodel applied a force field method to calculate the putative energy of a ligand, using an iterative function of distances and angles between atoms and keeping the coordinates of the protein unchanged. Representative examples of energy-minimised binding poses of the putative inhibitors are represented in Figure 41. The root-mean square deviation (RMSD) of heavy atom positions between raw and minimised conformations was in the range of $1.8 \leq \text{Å} \leq 1.3$, in line with the accepted limited value of $\text{Å} \leq 2.0$ for reliable prediction.⁹⁶

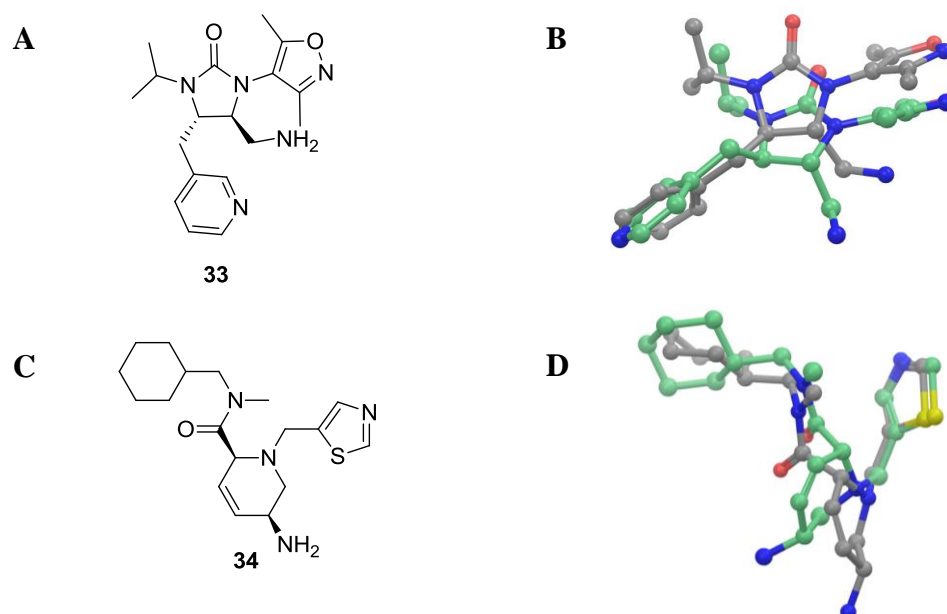


Figure 41. Evolution of raw binding poses upon conformational energy minimisation for selected putative inhibitors. A) and C) 2D structure representation of the imidazolidinone and the amino tetrahydropyridine putative inhibitors **33** and **34**. B) and D) Superimposed structures of the energy-minimised (grey) and raw (green) binding poses for the putative inhibitors **33** and **34**.

The binding poses obtained after the minimisation of their conformational energy were compared with the raw eHiTS binding poses using SPROUT. SPROUT is a fragment-based ligand design program that identifies protein binding regions, favourable protein hydrogen bonding and hydrophobic sites.^{102, 103} In SPROUT, the ALIGATOR module (Algorithms for **LIG**And **T**esting and **O**rding of **R**esults) contains a scoring function which can help investigating the ligand binding poses generated by other *in silico* docking software (*e.g.* eHiTS). The scoring function of SPROUT has a logarithmic scale and hydrophobic interactions represent the main score parameter. The scores have a negative value and represent the predicted $\log(K_i)$ of the ligand for the protein.^a The binding poses of the eight representative putative inhibitors, predicted by eHiTS and Maestro, were scored using SPROUT.

^a A score of -7.0 would correspond to an estimated 10^{-7} M inhibitor.

The resulting SPROUT scores for selected putative inhibitors are illustrated in Table 5 and in Table 6. As a general outcome, the SPROUT scores of binding poses with minimised conformational energy were similar to the raw ones (Table 5 and 6, column 3). Only one exception was observed (Table 5, entry 1). This similarity in the SPROUT scores for raw and energy minimised binding poses showed that the binding poses predicted by eHiTS were reliable.

It was noticed that the SPROUT scores were higher by 3.5 logarithm units than the eHiTS scores (Table 5 and 6 column 3 and 4); thus predicting 10^{-4} M inhibitors. These differences could be attributed to the different scoring functions employed by the two docking programs: H-bonding and π -cation interactions are weighted more in eHiTS, while lipophilic interactions and cavity filling are weighted more in SPROUT. Despite the scores differences, the interactions predicted by eHiTS were confirmed by SPROUT. A summary of the predicted non-covalent interactions formed by representative ligands of the two promising families in the catalytic site of BACE-1 is given in Table 5 and 6.

Table 5. eHiTS and SPROUT scores and predicted non-covalent interactions of selected imidazolidinone putative inhibitors in BACE-1.

Entry	2D representation of predicted non-covalent interactions	Score			Main H-bond interactions				Other interactions
		SPROUT ^a (SPROUT) ^b	eHiTS	cLE ^c	Wat1	Other water	Asp228	Asp32	
1		-3.99 (-5.06)	-7.59	0.29	✓	✓	x	x	Thr329 (H-bond interaction) Arg235 (π -cation interaction)
2		-3.90 (-4.02)	-7.78	0.30	✓	x	x	✓	Arg235 (π -cation interaction)

^aRaw eHiTS binding poses scored by SPROUT; ^benergy-minimised binding poses (Macromodel/Maestro) scored by SPROUT; ^ccalculated with eHiTS score

Table 6. eHiTS and SPROUT scores and predicted interactions of selected amino tetrahydropyridine putative inhibitors in BACE-1.

Entry	2D representation of predicted non-covalent interactions	Score			Main H-bond interactions				Others interactions
		SPROUT ^a (SPROUT) ^b	eHiTS	cLE ^c	Wat1	Other water	Asp228	Asp32	
1		-4.58 (-4.50)	-7.08	0.31	✓	x	x	✓	Thr232 (H-bond interaction)
2		-3.37 (-3.30)	-7.45	0.30	✓	✓	x	x	Thr231 (H-bond interaction) Arg235 (π-cation interaction)

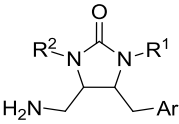
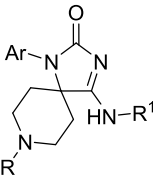
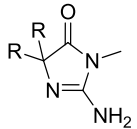
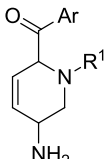
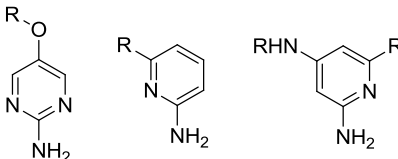
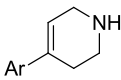
^aRaw eHiTS binding poses scored by SPROUT; ^benergy-minimised binding poses (Macromodel/Maestro) scored by SPROUT; ^ccalculated with eHiTS score

2.4.2 Design of a focused library of putative inhibitors

The two families of putative inhibitors identified by vHTS showed similar interactions with the catalytic site of BACE-1. The selection of one family over the other for synthesis was determined by their respective chemical structural features. An evaluation of their structural novelty, potential for diversification, and chemical stability were made.

To assess the novelty of the putative BACE-1 inhibitors, structures were compared with the ones of known BACE-1 inhibitors. Elements of novelty were found in both putative inhibitor scaffolds. The imidazolidinone scaffold (Table 7 entry 1) differed from the spiro piperidine imihydantoin inhibitor **26** and from the 2-aminoimidazole-4-one inhibitors⁷⁷ in the position of the amino group and the number of substituent groups around the cyclic urea ring. The amino tetrahydropyridine scaffold entry (Table 7, entry 2) differed from known aminopyridine inhibitors^{78, 104, 105} for the position in the N atom, and the number of double bonds in the ring; and from a tetrahydropyridine inhibitor¹⁰⁶ for the position and type of substituent groups on the ring. As a consequence, both putative inhibitor scaffolds were considered novel chemotypes for BACE-1.

Table 7. Comparison of structure features of putative BACE-1 inhibitors with known BACE-1 inhibitors.

Entry	Putative BACE-1 inhibitors ^a	Known BACE-1 inhibitors ^a	
1	 imidazolidinone scaffold	 spiro piperidine iminohydantoin inhibitor 26	 2-aminoimidazole-4-one inhibitors
2	 amino tetrahydropyridine scaffold	 aminopyridine inhibitors	 tetrahydropyridine inhibitor ^b

^aThe central core of the molecules is shown; ^bOnly one example in the literature¹⁰⁶

In terms of potential for diversification, the imidazolidinone scaffold represented the most diverse family of putative BACE-1 inhibitors. In this scaffold the central core can be diversified at three different positions, allowing for a broad investigation of binding effect of substituent groups. In the case of the amino tetrahydropyridine scaffolds, only two positions of diversification can be considered (Figure 42).

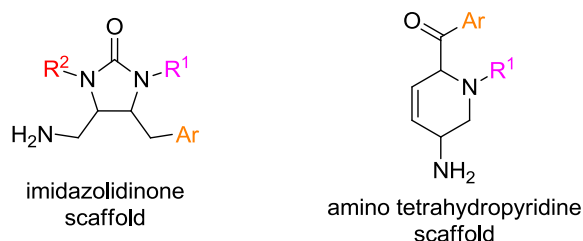


Figure 42. Positions of diversification in the structures of the two families of putative inhibitors.

Regarding chemical stability, it was noticed that the amino tetrahydropyridine scaffold can be subjected to tautomerisation into the α,β unsaturated ketone, giving a reactive Michael acceptor. From those considerations, the more potentially diverse and stable family of imidazolidinone compounds was chosen for synthesis. A focused library of these compounds was designed (Figure 43). Binding pose predictions, hydrophilicity, and variation of geometry and length of the substituent groups were considered in the library design.

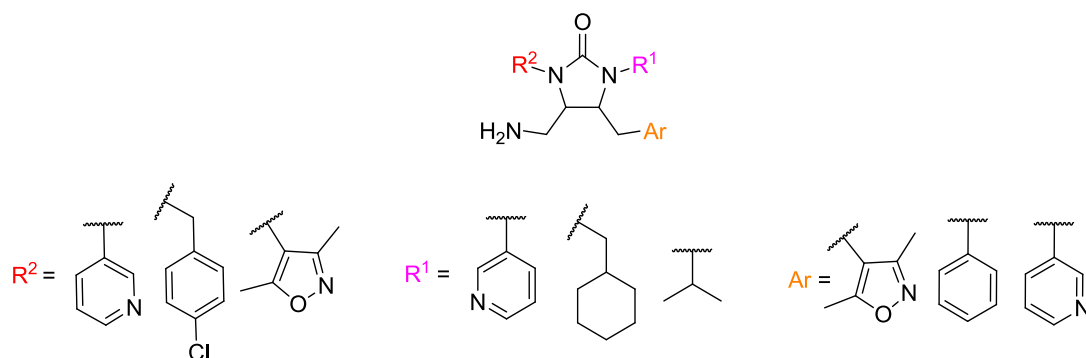


Figure 43. Focused library of putative BACE-1 inhibitors.

2.5 Summary

The design of a library of putative BACE-1 inhibitors was presented in this Chapter. The design approach consisted of enumerating a virtual library of lead-like

compounds and screening those compounds *in silico* against BACE-1. The virtual library enumeration was based on diversity oriented synthesis, to generate skeletally diverse molecules from an initial pool of building blocks. The protocol employed for the virtual library enumeration included established chemical reactions and commercially available reactants to ensure synthetic accessibility as far as possible.

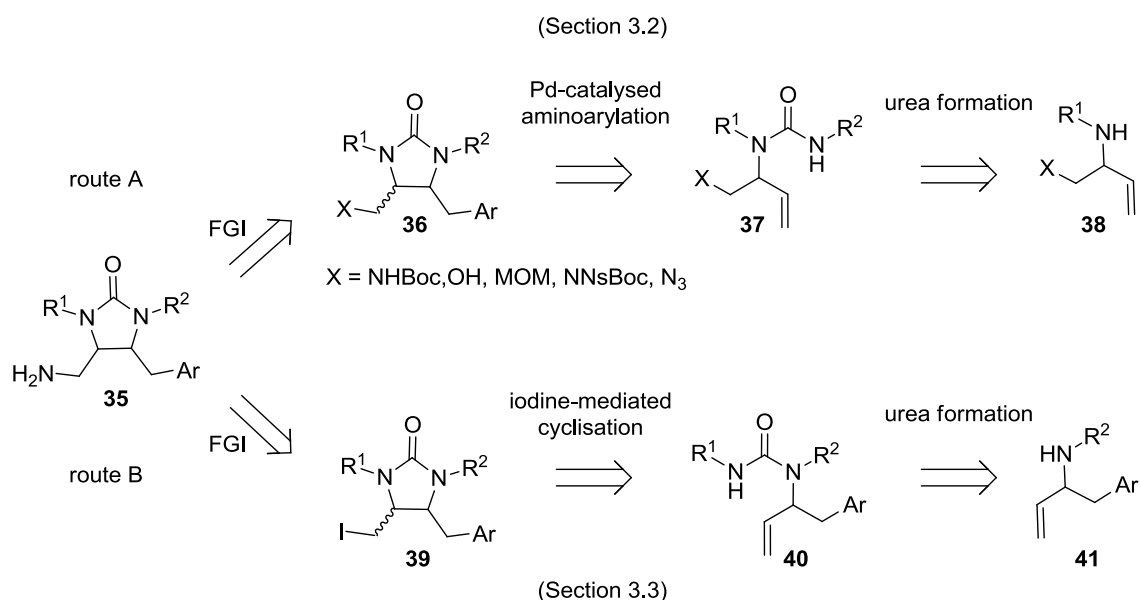
The virtual screening of the library was performed using eHiTS. The eHiTS screening method was validated and the predicted binding poses of the putative BACE-1 inhibitors were also analysed using Maestro Macromodel and SPROUT. The non-covalent interactions predicted by eHiTS were confirmed. Two families of putative BACE-1 inhibitors were identified, both containing elements of novelty in comparison to known BACE-1 inhibitors. One family was chosen over the other for synthesis, on the basis of potential points of diversification and chemical stability. A focused library of imidazolidinone putative inhibitors was then designed; the synthesis of these compounds is discussed in Chapter 3.

Chapter 3. Synthesis of a library of imidazolidinones

The following Chapter describes the synthetic routes to a library of BACE-1 putative inhibitors based on the imidazolidinone structure. Two different potential synthetic routes are presented, both including a cyclisation reaction on a series of *N*-allyl urea substrates to lead to the imidazolidinone scaffold (Section 3.1). The first synthetic route is based upon a Pd-catalysed aminoarylation and is described in Section 3.2; the second synthetic route is based upon an iodine-mediated cyclisation and is described in Section 3.3.

3.1 Identification of two possible synthetic routes

A variety of imidazolidinones was identified as putative inhibitors for the BACE-1 by virtual high throughput screening. A generic representation of the putative inhibitors is given by structure **35** (Scheme 5). Two possible synthetic routes were envisaged for the imidazolidinone **35**. The synthetic route **A** was suggested by the protocol of virtual reactions employed for the enumeration of virtual *libraries A* and *B* (Section 2.3); while the synthetic route **B** was envisaged from literature precedence. The two routes lead to two different starting materials: the allylic amines **38** and **41**.

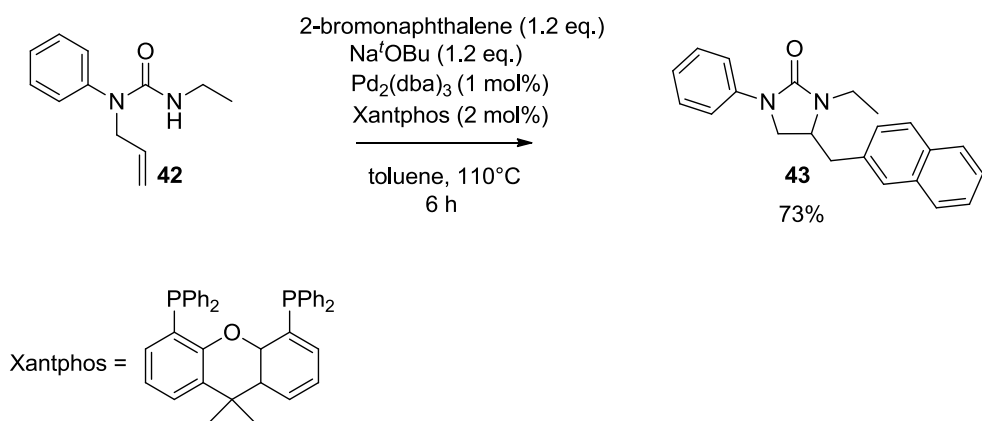


Scheme 5. Retrosynthetic analysis of target imidazolidinones. The groups R¹, R² and Ar were chosen according to the virtual library hits (see Figure 43, Section 2.4.2).

Following route A, the target imidazolidinone **35** might be obtained by functional group interconversions (FGIs) of cyclic precursor **36**, itself be prepared by Pd-catalysed aminoarylation of the *N*-allyl urea **37**. The *N*-allyl urea **37** might be synthesised from the allylic amine **38**. According to route B, two FGIs of imidazolidinone **35** might lead to the precursor **39**. Compound **39** might be formed *via* iodine-mediated cyclisation of the *N*-allyl urea **40**, derived from the allylic amine **41**. The investigation of the viability of these two routes is described in Sections 3.2 and 3.3.

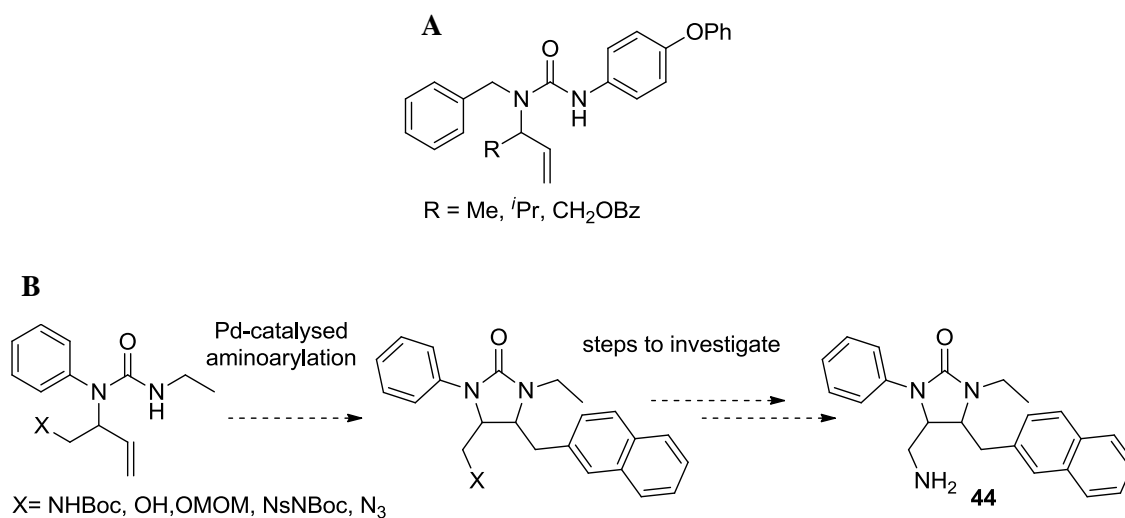
3.2 Synthetic route to the target imidazolidinones based upon a Pd-catalysed aminoarylation

The synthesis of a first imidazolidinone was planned on the basis of literature examples of a Pd-catalysed aminoarylation. Wolfe *et al.* reported the use of the phenylurea **42** as substrate for the aminoarylation (Scheme 6).¹⁰⁷ Here the formation of the new C-N bond provided the cyclic urea system and a 2-naphthalenyl was concomitantly introduced.



Scheme 6. Example of a Pd-catalysed aminoarylation

Wolfe *et al.* also applied the Pd-catalysed aminoarylation to a series of *N*-allyl phenylureas containing an alkyl group at the allylic position (Scheme 7, A). Following these examples, the reaction scope was extended and adapted to our synthetic purpose. A variety of *N*-allyl phenylureas containing different functional group substitutions at the allylic position was chosen for synthesis, keeping the target imidazolidinone **44** in mind (Scheme 7, B).

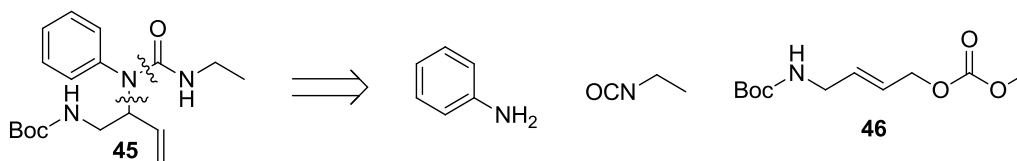


Scheme 7. Other substrates for Pd-catalysed aminoarylations. A) Substituted *N*-allyl ureas employed in the literature. B) Designed *N*-allylureas to investigate Pd-catalysed aminoarylation in order to achieve the final amine **44**.

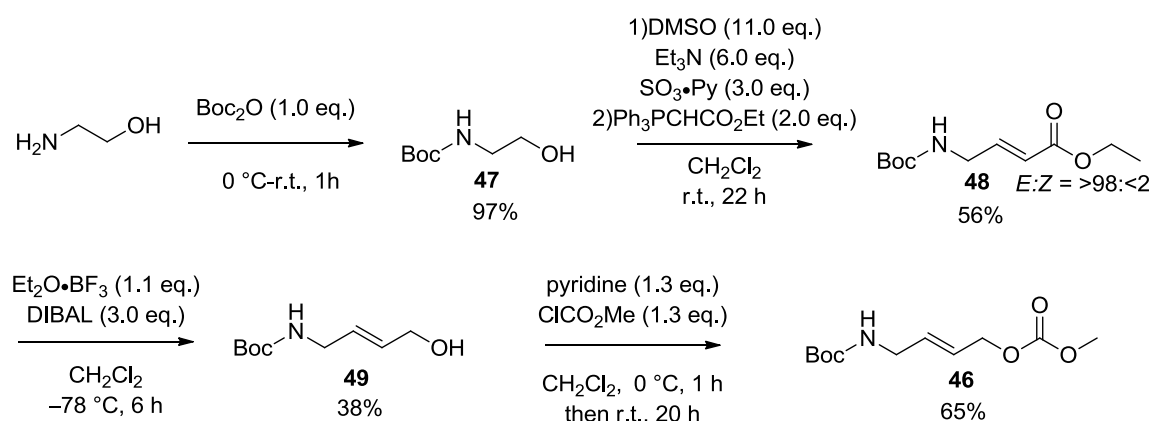
3.2.1 Synthesis of substrates for the Pd-catalysed aminoarylation

A first substrate for the Pd-catalysed aminoarylation, compound **45**, was synthesised starting from the allylic carbonate building block **46** (Scheme 8). The allylic

carbonate **46** was prepared in four steps from 2-aminoethanol following a literature procedure (Scheme 9).¹⁰⁸



Scheme 8. Allylcarbonate **46**, precursor of compound **45**, substrate for Pd-catalysed aminoarylation.



Scheme 9. Synthesis of the allylic carbonate **46**.

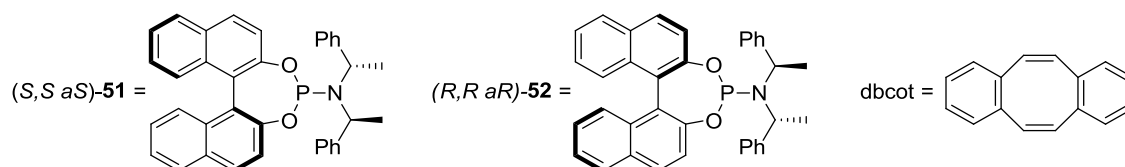
2-Aminoethanol was treated with di-*tert*-butyl dicarbonate under solvent free conditions to form the carbamate **47**. The carbamate **47** then underwent an one pot Parikh–Doering oxidation¹⁰⁹/Wittig reaction¹¹⁰ by treatment with sulfur trioxide pyridine, triethylamine and dimethylsulfoxide (DMSO) in CH₂Cl₂, followed by addition of the triphenylphosphorane Ph₃PCHCO₂Et. The resulting unsaturated ester **48** was obtained with >98:<2 *E:Z* selectivity. The reduction of the ester **48** to the corresponding alcohol **49** was achieved by treatment with diisobutylaluminium hydride (DIBAL) and borontrifluoride diethyletherate in CH₂Cl₂ at –78 °C. Finally, treatment of the alcohol **49** with methylchloroformate and pyridine in CH₂Cl₂ gave the allylic carbonate **46**.

The allylic carbonate **46** was then employed in the synthesis of the allylic amine **50**, precursor of the substrate for the Pd-catalysed aminoarylation. The conversion of the allylic carbonate **46** into the allylic amine **50** was achieved *via* an Ir-catalysed allylic amination (Table 8).⁹⁸ The allylic carbonate **46** was treated with aniline in DMSO or THF as solvent in presence of 2 mol% of each of the precatalyst [Ir(*dbcot*)Cl]₂,^{111,112}

phosphoramidite chiral ligands (*S,S aS*)-**51** and (*R,R aR*)-**52**¹¹³ and *n*-butyl amine.^a The active catalyst was formed *in situ*.¹¹⁴ The reaction was performed using a 1:1 mixture of the two chiral ligands (*S,S aS*)-**51** and (*R,R aR*)-**52** in order to obtain the product as a racemate. The reaction was attempted in DMSO and THF;¹¹⁵ similar yields were obtained in both solvents (**Table 8**) and, as a general trend, the yield improved with the scale of the reaction (entry 1 and 3 and entry 2, 4).

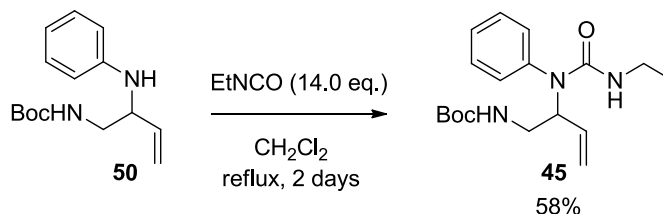
Table 8. Synthesis of the allylic amine 50.

Entry	Scale 46 (mmol)	Solvent	Yield (%)
1	0.50	DMSO	49
2	0.50	THF	43
3	0.75	DMSO	61
4	1.2	THF	69



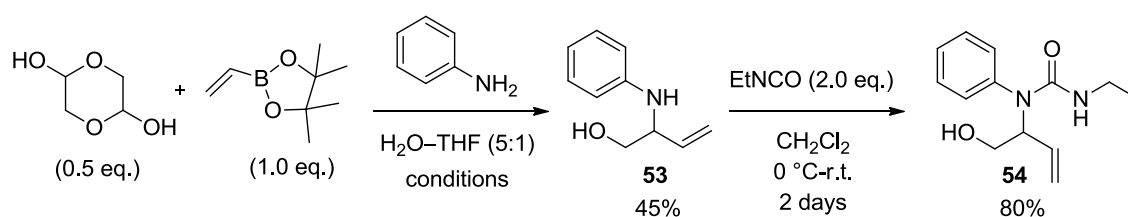
^aThe dbcot ligand, the precatalyst [Ir(dbcot)Cl]₂ and the phosphoramidite ligands (*S,S aS*)-**51** and (*R,R aR*)-**52** were prepared according to literature procedures.

The allylic amine **50** was ultimately converted into the *N*-allyl urea **45**. The formation of the *N*-allyl urea **45** required the treatment of **50** with an excess of ethylisocyanate in CH₂Cl₂, stirring at reflux for 2 days (Scheme 10). The urea **45** was prepared in 58% yield.



Scheme 10. Synthesis of the *N*-allyl urea **45.**

To prepare other substituted *N*-allyl ureas, an alternative concise approach was subsequently adopted. The synthesis of the *N*-allyl urea **54** was accomplished in two steps consisting of a Petasis multicomponent reaction,¹¹⁶ followed by an urea formation (Scheme 11). The allylic amine **53** was isolated as a racemate after combining glycoaldehyde dimer, vinyl boronic acid pinacol ester and aniline in H₂O–THF. A range of conditions was investigated (Table 9) and ultimately the best yield was obtained at 30 °C over 4 days. The conversion of the allylic amine **53** into the respective urea **54** was performed by treatment with an excess of ethylisocyanate in CH₂Cl₂ in 80% yield.

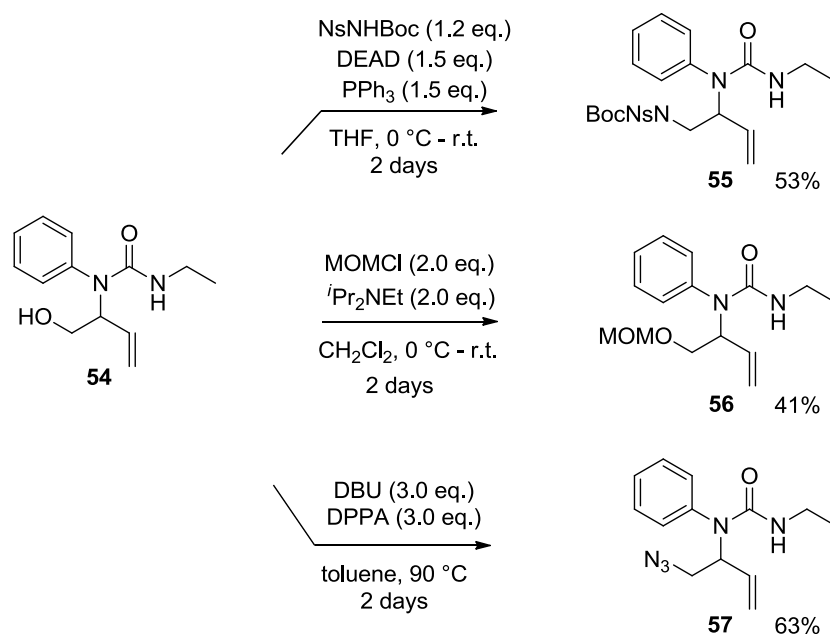


Scheme 11. Preparation of the substituted *N*-allyl urea **54.**

Table 9. Reaction conditions employed in the preparation of the allylic amine 53.

Entry	Scale PhNH ₂ (mmol)	Time (days)	Temperature (°C)	Yield (%)
1	1.5	2	50	18
2	2.0	3	50	30
3	20	4	30	45

Three additional substrates for the Pd-catalysed aminoarylation were prepared from the *N*-allyl urea **54**. The *N*-allyl urea **54** was converted into the NsBoc-protected amine **55**, the MOM-protected alcohol **56** and the azide **57** (Scheme 12).

**Scheme 12. Conversion of the *N*-allyl urea **54** into the *N*-allyl ureas **55**, **56** and **57**.**

The NsBoc protected amine **55** was prepared under Fukuyama–Mitsunobu¹¹⁷ conditions in 53% yield, by treating the *N*-allyl urea **54** with NsNH₂Boc, triphenylphosphine and DEAD. The protected alcohol **56** was obtained in a 41% yield stirring the alcohol **54** with methyl chloromethyl ether (MOMCl) and *N,N*-diisopropylethylamine (DIPEA) base in CH₂Cl₂. The formation of the azide **57** was achieved from compound **54** using 1,8-diazadicyclo[5.4.0]undec-7-ene (DBU) and diphenylphosphoryl azide (DPPA).¹¹⁸ Initially the reaction was conducted in DMF stirring from 1 to 3 days obtaining up to 34% yield (entry 1 and 2, Table 10). When toluene was employed as solvent, the yield improved to 63% (entry 3, Table 10).

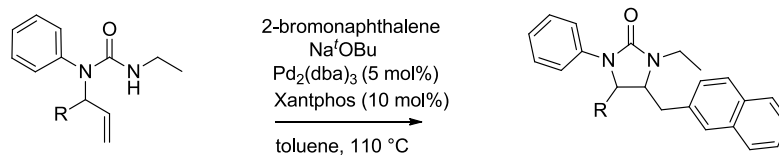
Table 10. Study of the formation of the azide 57 from the alcohol 54.

Entry	DBU, DPPA (eq.)	solvent	Time (days)	Yield (%) ^a
1	3.0	DMF	1	21
2	6.0	DMF	3	34
3	3.0	toluene	3	63

3.2.2 Investigation of the Pd-catalysed aminoarylation

The Pd-catalysed aminoarylation reaction was initially reproduced using the known substrate **42**¹ and then it was investigated using the prepared *N*-allyl urea substrates **45**, **54**, **55**, **56** and **57**. In each case, the relevant substrate was treated with 2-bromonaphthalene and NaO^tBu in the presence of a 5 mol% of Pd₂(dba)₃ complex and 10 mol% of phosphine ligand Xantphos in toluene, stirring the resulting mixture at reflux for 2-3 days (Table 11).

Table 11. Results of the Pd-catalysed aminoarylations performed on different *N*-allyl ureas.



Entry ^b	<i>N</i> -allyl urea	R	ArBr ^a (eq.)	NaO ^t Bu (eq.)	product	yield (%)
1	42	H	2.0	1.8		48
2	45	CH ₂ NHBoc	1.5	2.5		4
					<i>trans:cis</i> = >98: <2	
3	54	CH ₂ OH	2.0	1.8		10 ^c
4	55	CH ₂ NsNBoc	2.0	1.8		13
5	56	CH ₂ OMOM	2.0	1.8		35
					<i>trans:cis</i> = >98: <2	
6	57	CH ₂ N ₃	3.0	1.8		5
					<i>trans:cis</i> = >98: <2	

^aAr = 2-naphthyl; ^bAll the substrates were reacted for 3 days, only in the case of entry 2 the reaction lasted 2 days; ^cThe starting material was recovered in 15% yield.

From the *N*-allyl ureas **42**, **56** and **57**, the expected imidazolidinones **43**, **60** and **61** were obtained (entry 1, 5 and 6). In the case of the *N*-Boc substrate **45**, the *N*-arylated imidazolidinone **58** was isolated in 4% yield (entry 2). In this reaction, an excess of base was employed since no product was recovered by using one equivalent of NaO^tBu. From the *N*-allyl urea **55**, containing Nosyl-*N*-Boc amino group, a product of the competing Heck reaction,¹¹⁹ compound **59**, was obtained in 13% yield (entry 4). The starting material and the amine precursor, compound **53**, were recovered from the reaction of the *N*-allyl urea **54** (entry 3). A mechanistic rationalisation of these reactions is provided in Sections 3.2.2.2 and 3.2.2.3.

3.2.2.1 Determination of the stereochemical outcome of the Pd-catalysed aminoarylation

The 500 MHz ¹H-NMR spectrum of the imidazolidinone **43** was studied to help assign the relative configuration of the other imidazolidinone products. A nOe experiment of the imidazolidinone **43** was performed (Figure 44). A nOe enhancement (6%) of the proton 5-H_A was recorded when the proton 4-H was irradiated and *vice versa*, while no nOe enhancement was recorded between proton 4-H and 5-H_B. Therefore a *syn* relationship was assigned between the proton 4-H and 5-H_A.

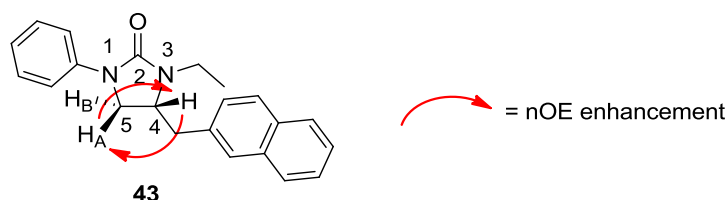


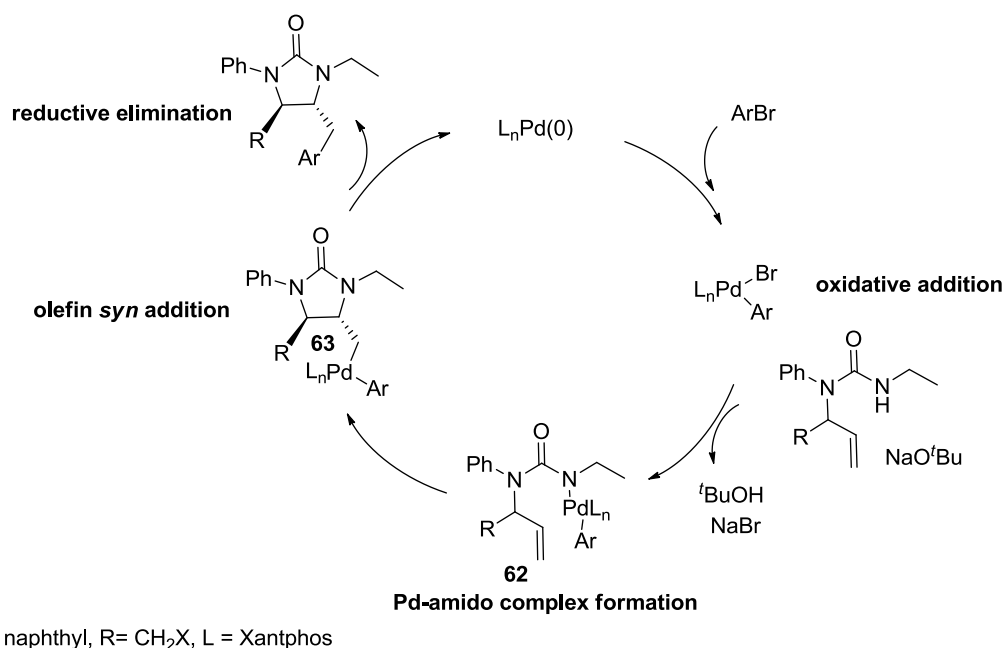
Figure 44. Results of the nOe experiment on the imidazolidinone **43**. No nOe was observed between proton 4-H and 5-H_B.

The relative configuration of the imidazolidinones **58**, **60** and **61** was assigned on the basis of the magnitude of the coupling constant, *J*, of the diagnostic proton signals in the urea ring system, protons 4-H and 5-H. The protons 4-H and 5-H_A of the imidazolidinone **43** in *syn* relationship showed a *J* value of 8.9 Hz, while the protons 4-H and 5-H_B in *anti* relationship showed a *J* value of 6.0 Hz. Proton 4-H in the imidazolidinones **58**, **60** and **61** all showed a *J* value between 3.0-4.0 Hz, therefore the

relative configuration assigned was *trans*. The magnitude of the observed coupling constants was in accordance with the Karplus relation.¹²⁰ A summary of the *J* values of all the synthesised imidazolidinones is provided in the Appendix 3 (Table 24).

3.2.2.2 Rationalisation of the stereochemical outcome of the Pd-catalysed aminoarylation

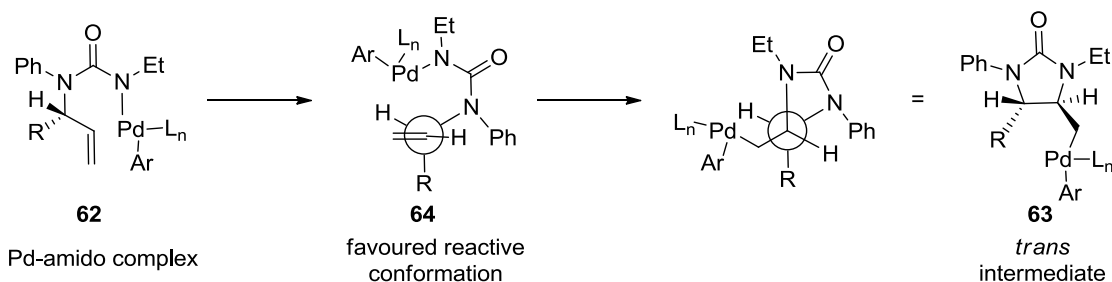
The stereochemical outcome of the Pd-catalysed aminoarylation may be rationalised using the mechanism reported by Wolfe *et al* (Scheme 13).¹⁰⁷ The Pd-phosphine complex, formed *in situ*, is proposed to undergo oxidative addition to 2-bromonaphthalene to start the catalytic cycle of the reaction. Once the urea substrate is deprotonated by NaO^tBu, an Ar-Pd-amido complex **62** is formed, followed by *syn* insertion across the alkene. From the resulting cyclic urea species **63**, the formation of the aryl-C bond occurs *via* a reductive elimination leading to the product and to the regeneration of the Pd⁽⁰⁾ catalyst.



Scheme 13. Catalytic cycle of the Wolfe reaction. Adapted from Wolfe *et al.*¹

According to the mechanism, the stereo-determining step is the olefin *syn* addition across the alkene which leads to the intermediate **63**. The substituent R at the allylic position in the imidazolidinones **58**, **60** and **61** determines the facial selectivity of the reaction. The N-Pd bond would attack the olefin from the opposite side to the R group,

through the favoured conformation **64**, favouring the formation of the *trans* imidazolidinones (Scheme 14).

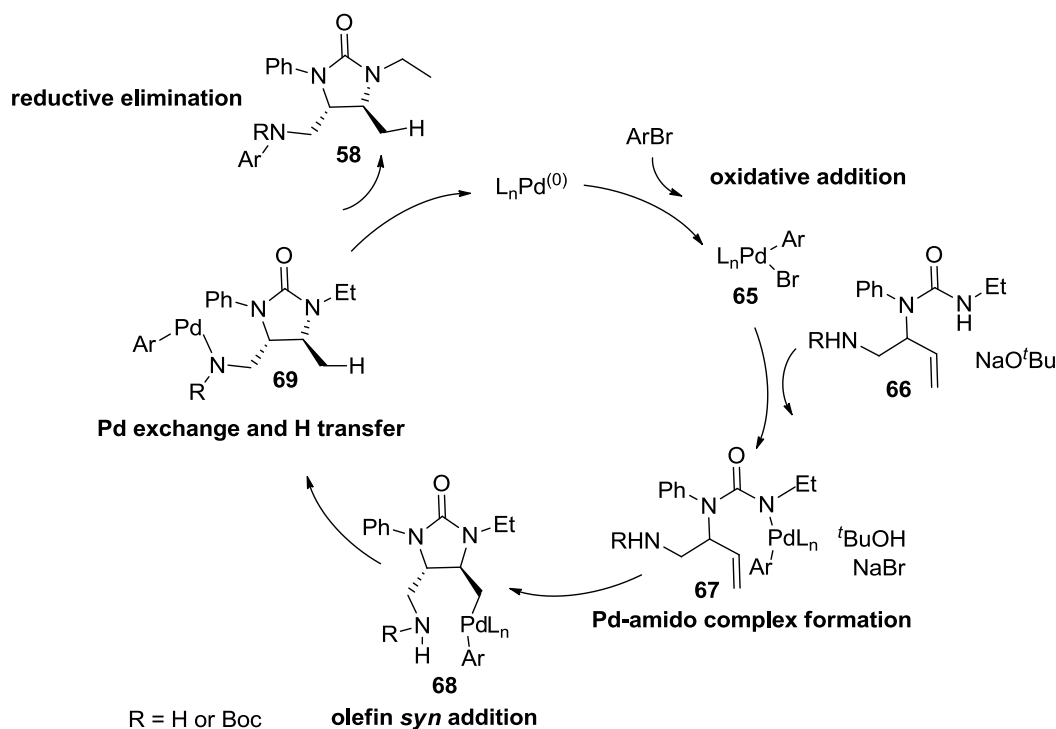


Scheme 14. Rationalisation of the stereochemical outcome of the Pd-aminoarylation.

3.2.2.3 Proposed mechanism for the formation of the *N*-arylated imidazolidinone

27

A mechanism for the formation of the *N*-arylated imidazolidinone **58**, obtained from the *N*-allyl urea **45**, is here proposed (Scheme 15). Under the high temperature of the reaction the Boc group was removed^{121,122} either before or after the product formation, therefore, in the Scheme 15 the R group can represent either the Boc group or a proton.

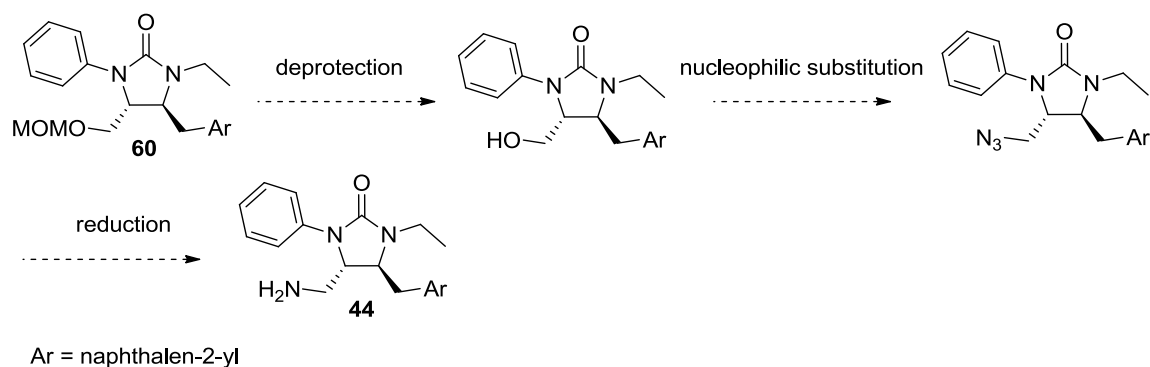


Scheme 15. Proposed mechanism for the formation of the imidazolidinone 58.

According to the mechanism proposed, after the formation of the Pd-amido complex **67** from the allylurea **66** and the Pd active species **65**, the *syn* addition of the olefin would occur. The resulting cyclic intermediate **68** would undergo a hydrogen transfer and a concomitant Pd exchange, between the amino group and the carbon attached to the Pd, to give a new Pd-N complex **69**. The species **69** would undergo a reductive elimination to provide the compound **58** and regenerate the catalyst.

3.2.3 Practicability of the route based upon the Pd-catalysed aminoarylation

The investigation of the Pd-catalysed aminoarylation on different *N*-allyl ureas showed that the protected alcohol **56** was tolerated under the reaction conditions, giving the imidazolidinone **60** in 35% yield. A possible synthetic pathway towards the synthesis of the final imidazolidinone **44**, starting from the precursor **60** was envisaged (Scheme 16).



Scheme 16. Envisaged synthetic steps towards the preparation of the target imidazolidinone 44.

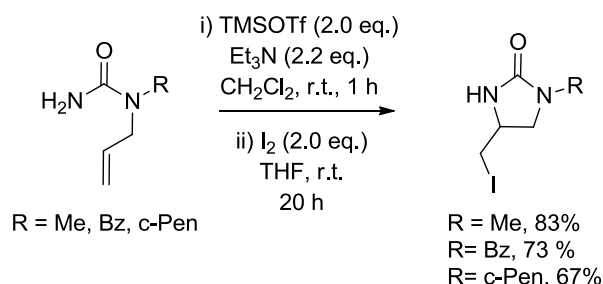
The synthesis of the final imidazolidinone **44** would consist of three steps: deprotection of the alcohol group, subsequent displacement with azide and final reduction to the amino group. The envisaged synthetic pathway would have to be applied to each desired compound, making the synthetic route longer and not necessarily practical. Moreover, the Pd-catalysed aminoarylation is not known with heteroaromatic-containing ureas and the insertion of a heteroaryl group is limited to the 2-pyridyl group.¹ Contextually the preparation of the heteroaromatic *N*-allyl urea substrates would need to be planned differently. In Section 3.2.2, the alcohol **53**, precursor of the *N*-allyl urea **54**, was prepared using the Petasis reaction from aniline, but the use of amines containing a heteroaromatic group is not known for the Petasis reaction.^{116,123} Due to these considerations, the synthetic route based upon the Pd-catalysed aminoarylation was not pursued. A potentially more viable synthetic route based upon an iodine-mediated cyclisation was investigated (Section 3.3).

3.3 Synthetic route to the target imidazolidinones based upon an iodine-mediated cyclisation reaction

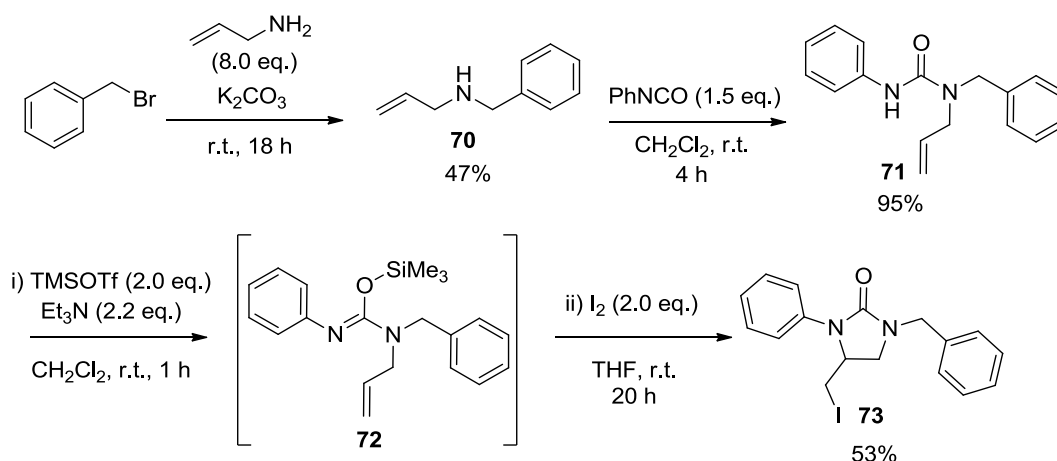
An alternative synthesis of the target imidazolidinones was investigated according to the envisaged retrosynthetic route B (Section 3.1). In this synthesis, the key urea ring system would be prepared through an iodine-mediated cyclisation of the *N*-allyl urea substrate. The synthesis was first explored using benzylallylamine, expanding the scope of a literature procedure (Section 3.3.1),¹²⁴ and then was extended to the specific *N*-allyl urea substrates (Section 3.3.3).

3.3.1 Exploration of synthetic route from benzylallylamine

The synthesis of imidazolidinones *via* an iodine-mediated cyclisation of *N*-allylurea was firstly reported by Moody *et al.* in 2010.¹²⁴ The reaction, performed on three different *N*-allylurea substrates, gave yields between 67 and 83% (Scheme 17). In order to expand the scope of the iodine-mediated cyclisation for our synthetic purpose, the preparation of the imidazolidinone **73** was initially attempted (Scheme 18).



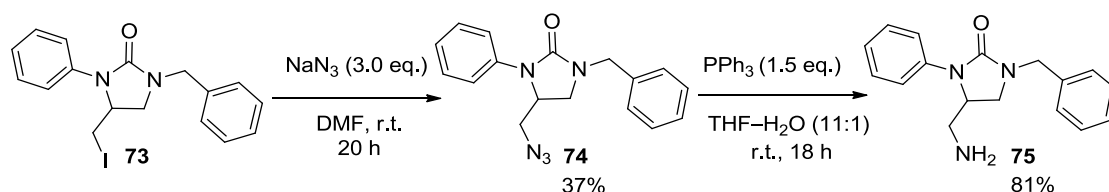
Scheme 17. Literature example of iodine-mediated cyclisation of *N*-allylureas.



Scheme 18. Study of the iodine-mediated cyclisation on benzylallylamine.

Benzylallylamine **70** was prepared in 47% yield by treating benzyl bromide with an excess of allylamine and potassium carbonate. The *N*-allyl urea **71** was then obtained in 95% yield by treatment of the benzylallylic amine **70** with phenylisocyanate in CH_2Cl_2 . The imidazolidinone **73** was synthesised by treatment of the urea **71** with trimethylsilyl trifluoromethanesulfonate and triethylamine in CH_2Cl_2 and then with iodine in THF. The cyclic urea **73** was isolated in 53% yield. Presumably, the reaction proceeds *via* an *O*-silyl imidate species **72**.

Subsequently, the synthetic steps for the transformation of the imidazolidinone **73** into the amine **75** were undertaken (Scheme 19). The iodide **73** was treated with sodium azide in DMF to give the azide **74** in a 37% yield. The azide **74** was used without further purification in the following reduction. The imidazolidinone **75** was obtained in 81% yield following a Staudinger reaction, using triphenylphosphine in THF–H₂O (11:1) with stirring at r.t. for 18 h.¹²⁵



Scheme 19. Conversion of the imidazolidinone **73** into the amine **75**.

3.3.2 Synthesis of the target imidazolidinones

This synthetic route was then extended to a series of *N*-allyl urea substrates containing a substituent at the allylic position. The choice of the heteroaromatic and alkyl groups to incorporate in the *N*-allyl ureas was determined by the commercial availability of the reactants. As a consequence, the initial design of a focused library of imidazolidinones (Figure 43, Section 2.4.2) was readapted, taking in consideration computational predictions of binding affinity of the new substituent groups against BACE-1. The resulting diverse *N*-allyl ureas selected for the synthesis are illustrated in Figure 45. An *N*-allyl urea substrate without substitution at the allylic position was also included in the series.

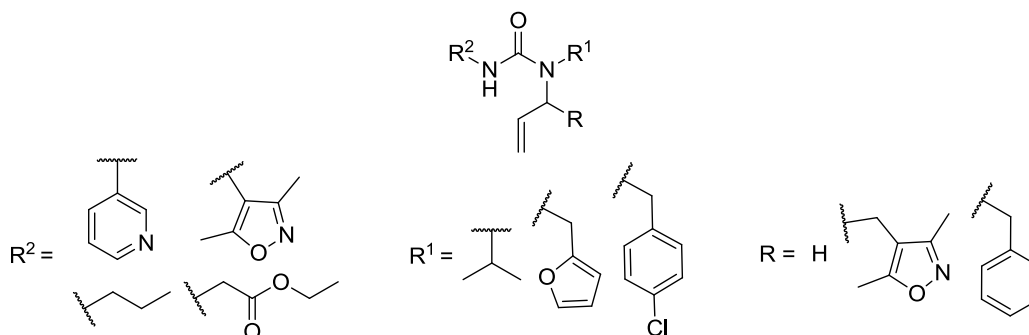
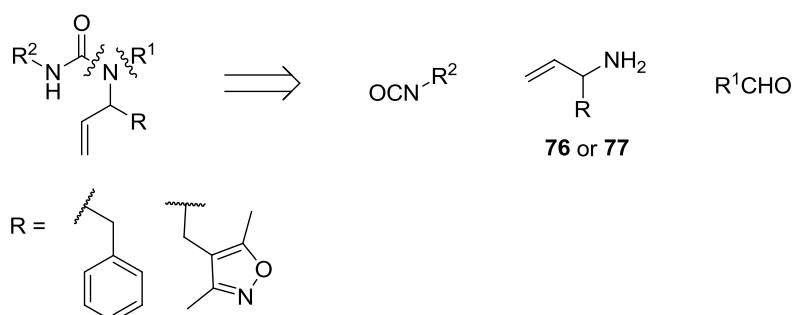


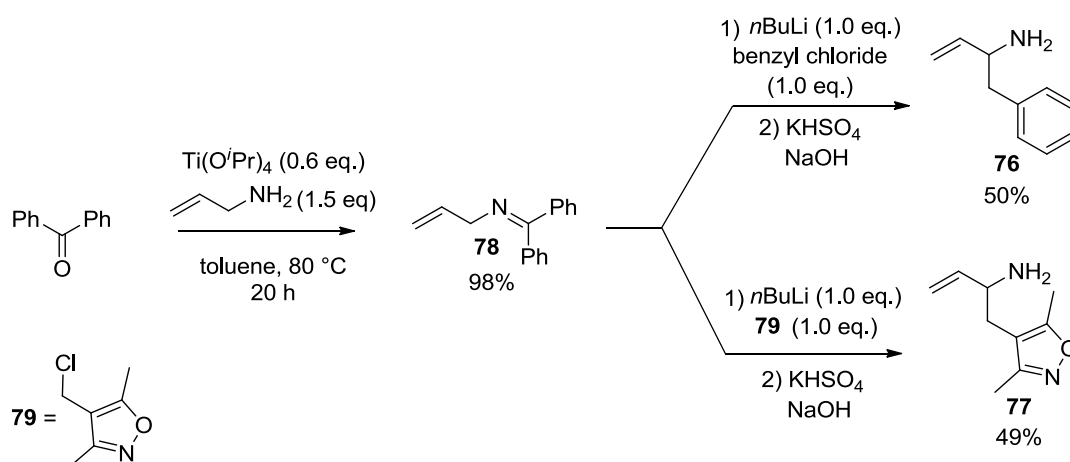
Figure 45. Structure of the designed *N*-allyl urea substrates for the iodine-mediated cyclisation reaction.

3.3.2.1 Synthesis of substrates for the iodine-mediated cyclisation

The use of the building blocks **76** and **77**, containing respectively a benzyl and isoxazole group at the allylic position, was envisaged for the preparation of the designed substituted *N*-allyl ureas (Scheme 20). The substituted allylic amine **76** was prepared in two steps following a literature precedence.¹²⁶ Then, the same reaction conditions were applied to prepare the amine **77** (Scheme 21).



Scheme 20. Allylic amines building block **76** and **77** for *N*-allyl ureas.



Scheme 21. Synthesis of the substituted allylic amines **76** and **77**, building blocks for a variety of *N*-allyl ureas.

Benzophenone was condensed with allylamine in presence of titanium isopropoxide in toluene at 80 °C to give the resulting imine **78** in 98% yield. Deprotonation of the imine **78** by *n*-butyl lithium, followed by addition of the relevant electrophile (chloroisoxazole **79** or benzyl chloride), led to formation of the substituted imine intermediate which was hydrolysed to give the substituted allylic amine **76** and **77** in 50% and 49% yield respectively.

Reductive amination was employed to prepare a series of secondary amines from compounds **76** and **77** and from allylamine (Table 12). In the majority of cases, the relevant aldehyde was reacted with the relevant amine in MeOH at r.t. and the resulting imine was reduced with sodium borohydride. The products did not require purification. The secondary amines **80-83** were obtained in 98%, 45%, 65% and 43% yield respectively (entry 1-4). The secondary amine **84** (entry 5) was prepared by treating the allylic amine **76** with acetone and magnesium sulfate in EtOH at r.t. and the resulting imine was reduced with sodium borohydride to yield the amine **84** in 61% yield.

Table 12. Synthesis of the secondary amines 80-84, precursors of the *N*-allyl urea substrates for the iodine-mediated cyclisation reaction.

Entry	aldehyde	product	R	R ¹	Yield (%)
1		80			98
2		81			45
3		82			65
4		83	H		43
5		84			61 ^a

^aReaction conditions: 1) Acetone (4 eq.), MgSO₄, EtOH, r.t., 2 days; 2) NaBH₄ (3.0 eq.), 0 °C-r.t., 1 day

The secondary amines **80-84** were converted into a range of *N*-allyl ureas (**85-92**) by refluxing with the relevant isocyanate in CH₂Cl₂ for 1 or 2 days (Table 13). The *N*-allyl ureas **85**, **88**, **89**, **90** and **91** (entry 1, 4, 5, 6, 7) were obtained in similar yield,

between 77-87%; lower yields, between 58-70%, were achieved with the *N*-allyl ureas **86**, **87** and **92** (entry 2, 3 and 8).

Table 13. Preparation of a variety of *N*-allyl ureas from the amine 85-92.

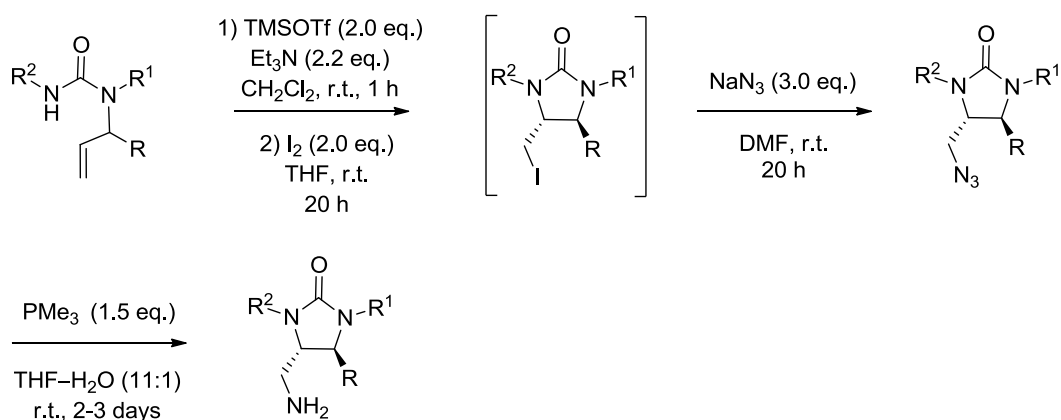
Entry	Product	R	R ¹	R ²	Yield (%)
1	85				77
2 ^a	86				70
3	87				58
4	88	H			82
5	89				87
6	90				80
7	91				81
8 ^a	92				68

^aReaction time extended to 2 days

3.3.2.2 Synthesis of a focused library of imidazolidinones

The iodine-mediated cyclisation and the final steps of the synthesis of the target imidazolidinones were initially investigated using the *N*-allyl urea **85** and then were applied to the *N*-allyl ureas **86** and **87** (Scheme 22). The relevant *N*-allyl urea was first

treated with trimethylsilyl trifluoromethanesulfonate and triethylamine in CH_2Cl_2 at r.t. and then with iodine in THF. Due to concerns about the stability of these products, the crude products were used in the next step without further purification. The displacement of the iodide with sodium azide was achieved by stirring in DMF at r.t. overnight. The azide product was obtained with *trans* relative configuration. The final imidazolidinones were obtained by reducing the relative azides under Staudinger¹²⁵ conditions, by treating the relevant azide with trimethylphosphine in THF- H_2O (11:1).



Scheme 22. Final steps of synthesis of a focused library of imidazolidinones.

The azide compounds prepared from the *N*-allyl urea **85**, **86** and **87** contained traces of triethylamine salt and in some cases the final imidazolidinones contained traces of trimethylphosphonium oxide. Therefore the iodine-mediated cyclisation on the next *N*-allyl urea substrates, **88-92**, was performed using DBU base instead of triethylamine, and triphenylphosphine was employed in the azide reduction instead of trimethylphosphine. The imidazolidinone **96**, prepared from the *N*-allyl urea **86**, gave the lactam **97** after purification (Figure 46). The results of the synthesis are summarised in Table 14.

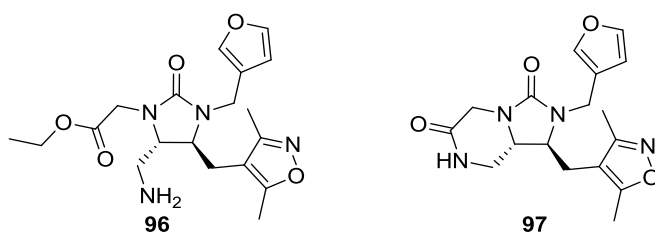
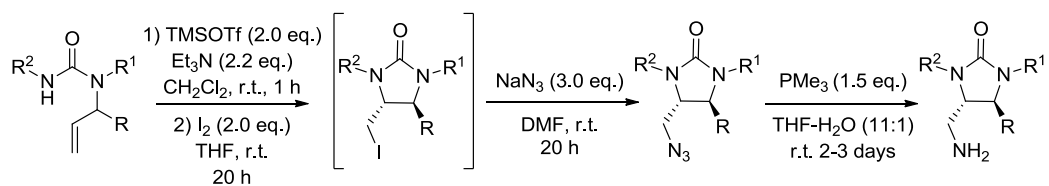


Figure 46. Imidazolidinone **96** and lactam **97**. The lactam **97** was recovered after purification by ion exchange column of compound **96**.

Table 14. Summary of synthesis of a focused library of imidazolidinones.



Entry	<i>N</i> -allyl urea	R	R ¹	R ²	Azide formation yield (%) [<i>trans</i> : <i>cis</i>] ^a	Final product yield (%)
1	85				93 , 16 ^d [> 98: < 2] <i>trans</i> ^d	94 , 18 <i>trans</i> ^d
2	86				95 , 20 [> 98: < 2] <i>trans</i>	lactam 97 8 ^e
3	87				98 , 20 [> 98: < 2] <i>trans</i>	99 , 9 ^f
4 ^b	88	H			100 , 18 [> 98: < 2] <i>trans</i>	101 , 7
5 ^b	89				102 , 7 [> 98: < 2] <i>trans</i>	- ^g
6 ^{b,c}	90				103 , 18 [> 98: < 2] <i>trans</i>	104 , 27 ^h
7 ^{b,c}	91				105 telescoped	106 , 2.5 over three steps ^h [> 98: < 2] <i>trans</i>
8 ^{b,c}	92				107 , 13 ⁱ [> 98: < 2] <i>trans</i>	<1 mg ^{h,i} obtained

^aYield of purified product over two steps; ^bDBU was employed in place of Et₃N; ^cPPh₃ was used in place of PMe₃; ^dA trace of triethylamine salt was present; ^eTrimethylphosphonium oxides was contained in 10%; ^fThe imidazolidinone **99** was purified by HPLC; ^gReaction not attempted; ^hThe products **104**, **106** and **107** were purified by column chromatography; ⁱInsufficient material for full characterisation.

In general, the yields of the preparation of the azides and amines from the substituted *N*-allyl ureas were surprisingly lower compared to that obtained during the synthesis of the imidazolidinone **75** (Section 3.3.1). Presumably the poor yields obtained in the synthesis of the azide were affected by the outcome of the iodine-mediated cyclisation. The iodine-mediated cyclisations were monitored by LCMS and TLC and were not quenched until the *N*-allyl urea starting material was completely consumed, but the 500 MHz ¹H-NMR analysis of the reaction mixture of the iodide or of the azide crude revealed the presence of the *N*-allyl urea precursors in 20-35%. This could be explained by the hydrolysis of the *O*-silyl imidate species, which could lead to the *N*-allyl urea precursors, preventing the formation of the iodide compounds.

The final amines were also obtained in low yields. The purification of the amines through analytical methods, HPLC and mass directed chromatography, gave yields between 8-18% (entry 1-4). Better yields, ~28%, were obtained when the amines were purified *via* column chromatography (entry 6-7). Despite the low yields, the synthetic route based upon the iodine-mediated cyclisation allowed the preparation of a focused library of imidazolidinones to test against the biological target, BACE-1.

3.3.2.3 Determination of the relative configuration of products

By analogy to the analysis reported in Section 3.2.2.1, the relative configuration of the imidazolidinones in Table 7 was assigned on the basis of *J* values of the diagnostic proton 4-H/5-H. Firstly the protons of the imidazolidinone **75** were assigned by a nOe experiment. A nOe enhancement (1.6%) of the proton 5-H_A was recorded when the proton 4-H was irradiated and *vice versa*, while no nOe enhancement was showed between proton 4-H and 5-H_B (Figure 47). Therefore a *syn* relationship was assigned between the proton 4-H and 5-H_A.

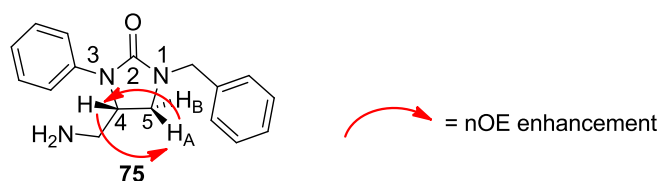
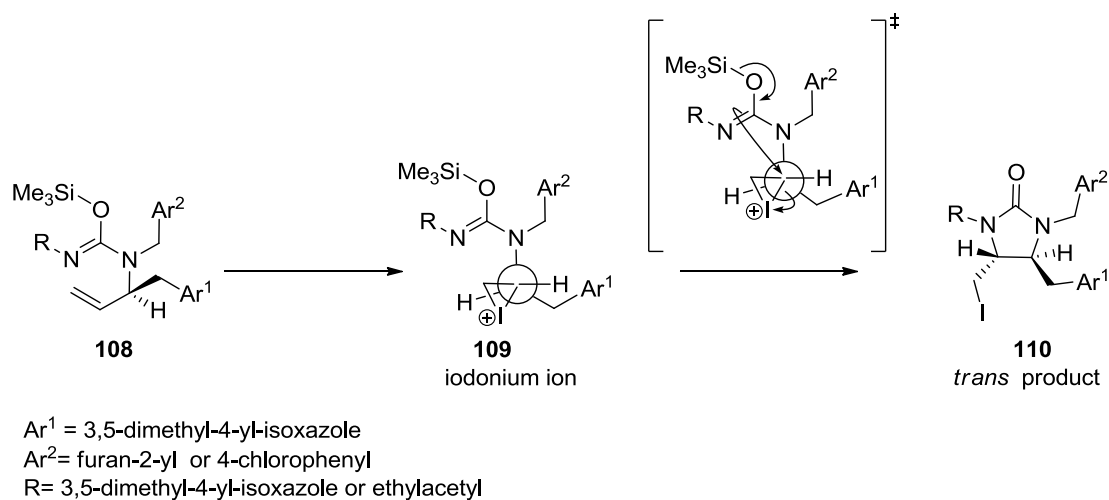


Figure 47. Results of the nOe experiment on the imidazolidinone 75. No nOe enhancement was observed between protons 4-H and 5-H_B.

The imidazolidinone **75** had a J value of 9.0 Hz between the *syn*-related protons 4-H/5-H_A, while the J value between the *anti*-related protons 4-H/5-H_B was 5.1 Hz.¹²⁴ The protons 4-H/5-H of all the imidazolinone products had J values in the range of 3.5-6.0 Hz, as a consequence, the relative configuration of those compounds was assigned as *trans*. A summary of the diagnostic J values of all the synthesised imidazolidinones is provided in the Appendix 3 (Table 24).

3.3.2.4 Rationalisation of the stereochemical outcome of the urea ring formation

The stereochemical outcome of the synthesised imidazolidinones is controlled by the formation of the respective cyclic iodine precursors from the *N*-allyl urea substrates; therefore the mechanism of the iodine-mediated cyclisation can provide a rationalisation of the stereochemical outcome. The substituted *N*-allyl urea substrates were first treated with triethylamine and trimethylsilyl trifluoromethanesulfonate to presumably form the *O*-silyl imidate species **108** (Scheme 23).



Scheme 23. Rationalisation of the stereochemical outcome of the iodine-mediated cyclisation.

Treatment with iodine is believed to trigger iodonium ion formation, species **109**. The formation of the iodonium ion species is considered reversible;¹²⁷ therefore the stereochemistry of the reaction is likely determined by the intramolecular nucleophilic attack of the nitrogen of the urea system onto the iodonium ion. The attack would favour the formation of a five-membered ring and the new formed C-I bond would be

oriented to the opposite side in respect to the methyl-aryl substituent, avoiding clashing interactions. The resulting compound **110** would have *trans* geometry.

3.4 Summary

Two synthetic routes towards the imidazolidinone compounds, putative inhibitors of BACE-1, were described in this Chapter. The first one was based upon the Pd-catalysed aminoarylation on *N*-allyl ureas, containing different functional groups at the allylic position: NHBoc, NsBocN, OH, N₃, OMOM. The second one was based upon the iodine-mediated cyclisation of *N*-allyl ureas containing different aromatic group at the allylic position.

The investigation of the Pd-catalysed aminoarylation showed that the *N*-allyl urea **56**, containing the MOM protected alcohol at the allylic position, was a suitable substrate for the reaction, giving the imidazolidinone **60** in 34% yield. Further studies to convert the imidazolidinone **60** into the target one, compound **44**, containing a primary amino group, or to prepare a range of MOM substituted *N*-allyl ureas, containing different heteroaromatic and alkylic group at N atoms, were not carried on.

The route based upon the iodine-mediated cyclisation was applied to eight different *N*-allyl urea substrates and led to the synthesis of a small family of six target imidazolidinones and seven azide precursors. Surprisingly, the yields of the iodine-mediated cyclisation and of the final two steps of synthesis were low. The biological activity of those compounds will be discussed in Chapter 4.

An analysis of the relative configuration of the imidazolidinones, prepared through both synthetic routes, was also described in the Chapter. A summary of the diagnostic *J* value of those compounds is reported in Appendix 3, Table 24. Mechanisms to rationalise the stereochemical outcomes of the Pd-catalysed aminoarylation and the iodine-mediated cyclisation were also discussed.

Chapter 4. Biological activity evaluation of BACE-1 imidazolidinone putative inhibitors

The following Chapter presents results of the biological activity of the synthesised imidazolidinone compounds against BACE-1. The biological activity evaluation was performed through an *in vitro* assay based on fluorescence quenching (Section 4.1). Initially, measurements of biological activity at single concentration were performed; subsequently dose responses were carried out for selected molecules (Section 4.2). After a discussion of the biological results, new structural analogues of active inhibitors were synthesised and tested against BACE-1 (Section 4.3). Studies of biological selectivity were also performed by assessing the biological activity of selected inhibitors against BACE-2, a homologue of BACE-1 (Section 4.4).

4.1 Assay for biological activity evaluation against BACE-1

The biological activity of the synthesised imidazolidinone compounds against BACE-1 was assessed using an *in vitro* fluorescent competitive inhibition assay. The assay uses a Swedish mutant of BACE-1 natural substrate containing a fluorescent tag, FAM, and a quencher, TAMRA, at its two extremities (Figure 49). The distance between the fluorescent tag and quencher is such that, under UV light excitation, the fluorescence of the donor is quenched.

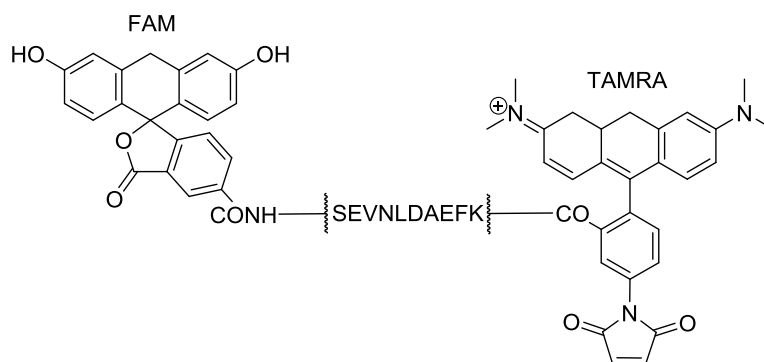


Figure 48. Swedish mutant of BACE-1 natural substrate containing a fluorescent tag and a quencher at its extremities. The peptide sequence of the Swedish mutant at the centre of the figure is represented by amino acid symbols.

When BACE-1 cleaves the substrate, the fluorescent tag is separated from the quencher and a fluorescence signal is emitted. In presence of a BACE-1 inhibitor, the substrate cleavage is partially or totally inhibited; as a consequence, the fluorescence signal emission is also reduced or suppressed. The difference between the signal observed in absence and in presence of a BACE-1 inhibitor is used to assess the inhibition. A schematic illustration of the fluorescence quenching assay is provided in Figure 49.

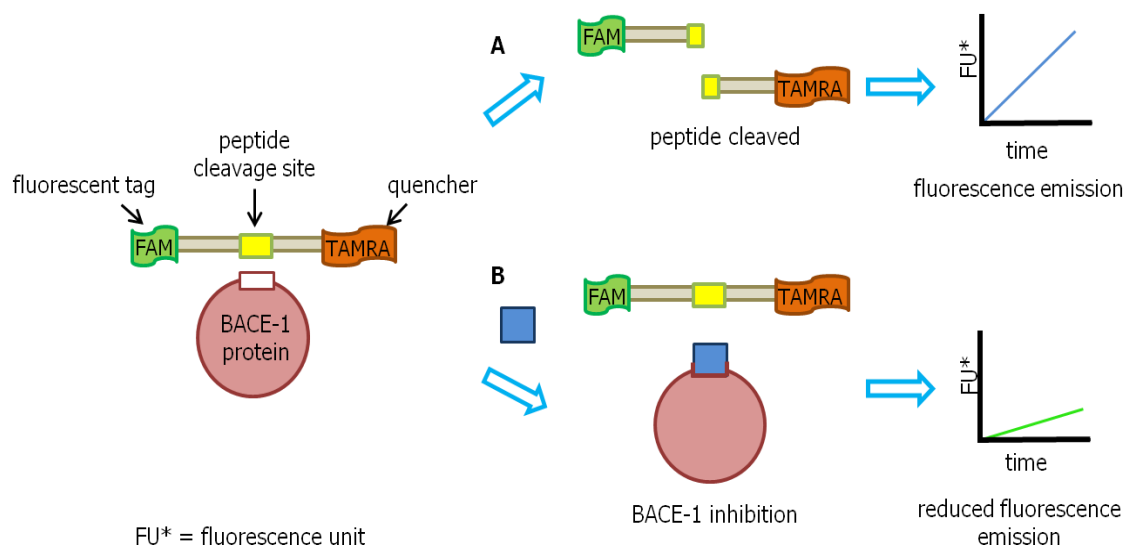


Figure 49. Fluorescent quenching assay illustration. A) BACE-1 cleaves the substrate, the fluorescent tag, FAM, is separated from the quencher, TAMRA, and it emits a fluorescence signals. B) An inhibitor competes with the substrate in interacting with BACE-1, therefore the substrate cleavage is partially inhibited and a reduced fluorescent emission is observed.

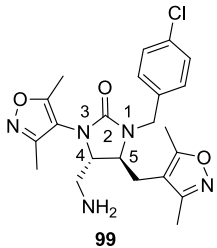
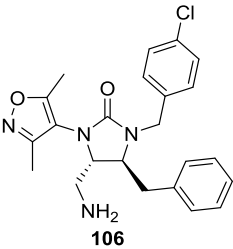
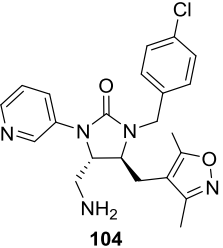
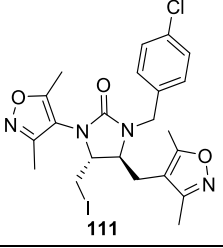
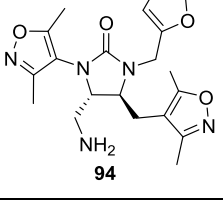
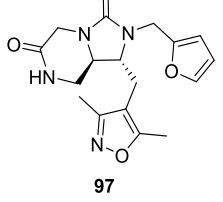
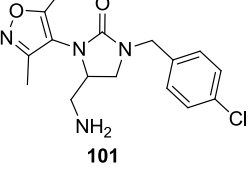
4.2 Biological activity measurements

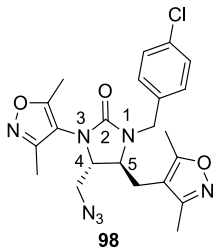
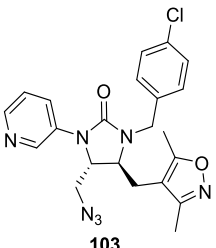
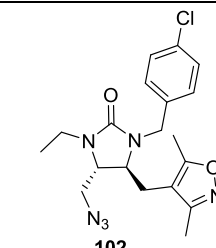
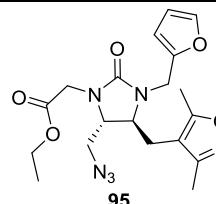
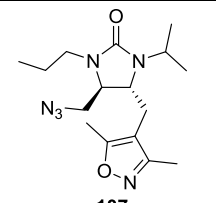
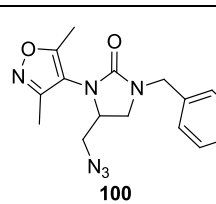
The biological activity of imidazolidinone putative inhibitors was measured at the initial concentration of 100 μ M in DMSO. The commercially-available inhibitor β -secretase IV (10 μ M in DMSO) was used in the assay as a positive control; DMSO-only (5-10%) was used as a negative control. Details regarding the protocol of the fluorescent quenching assay are provided in Section 5.4. The designed imidazolidinone compounds **94**, **97**, **99**, **101**, **104** and **106**, their azide precursors and an

iodo precursor, **111**,^a were assayed. The lipophilic imidazolidinone **43**, **60**, **73**, **74** and **75**, which were not included in the putative inhibitor design but were prepared to establish the synthetic route of target compounds, were also assayed. The imidazolidinones showing $\geq 25\%$ inhibition were also assayed for a dose response to determine their IC_{50} . The ligand efficiency, LE' was calculated from the IC_{50} values (see Equation 2, Section 1.2.3.1, page 8). The results of these *in vitro* assays are summarised in Table 15 and Table 16. In cases in which was not possible to determine the full dose response, due to solubility or stability issues, the concentration of the putative inhibitor at 50% of inhibition was reported. Examples of dose response curves are illustrated in Figure 50 further data are reported in Appendix 4.1.

^a Intermediate of the synthesis of the imidazolidinone **99**.

Table 15. Biological activity of amino and azido imidazolidinones against BACE-1.

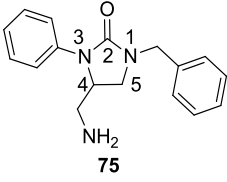
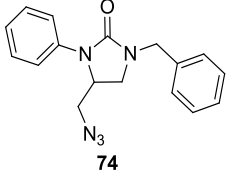
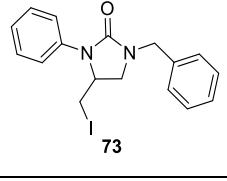
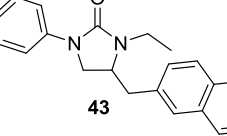
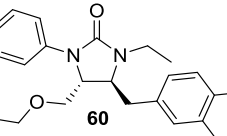
Entry	Compound	Inhibition at 100 μ M (%)	IC ₅₀ (μ M)	LE' ^a
1	 99	33 \pm 11	250 \pm 4	0.12
2	 106	39 \pm 2	720 \pm 20	0.10
3	 104	17 \pm 2	- ^b	- ^b
4	 111	13 \pm 4	- ^b	- ^b
5	 94	9 \pm 5	- ^b	- ^b
6	 97	12 \pm 4	- ^b	- ^b
7	 101	6 \pm 1	- ^b	- ^b

Entry	Compound	Inhibition at 100 μM (%)	IC ₅₀ (μM)	LE' ^a
8	 98	28 \pm 5	750 \pm 20 ^c	- ^d
9	 103	30 \pm 3	590 \pm 20	0.10
10	 102	10 \pm 2	- ^b	- ^b
11	 95	8 \pm 5	- ^b	- ^b
12	 107	no inhibition observed	- ^b	- ^b
13	 100	7 \pm 2	- ^b	- ^b

^aLE' calculated as $-\log(\text{IC}_{50})/n\text{HA}$ (see Equation 2, Section 1.2.3.1); ^bNot determined;

^cConcentration at 50% inhibition, ^dNot calculated, IC₅₀ value not available

Table 16. Biological activity of lipophilic imidazolidinones against BACE-1.

Entry	Compound	Inhibition at 100 μ M (%)	IC ₅₀ (μ M)	LE' ^a
1	 75	34 \pm 12	260 \pm 20	0.17
2	 74	28 \pm 1	805 \pm 13 ^c	- ^d
3	 73	15 \pm 7	- ^b	- ^b
4	 43	16 \pm 1	- ^b	- ^b
5	 60	27 \pm 5	260 \pm 5 ^c	- ^d

^aLE' calculated as $-\log(\text{IC}_{50})/n\text{HA}$ (see Equation 2, Section 1.2.3.1); ^bNot determined;

^cConcentration at 50% inhibition, ^dNot calculated, IC₅₀ value not available

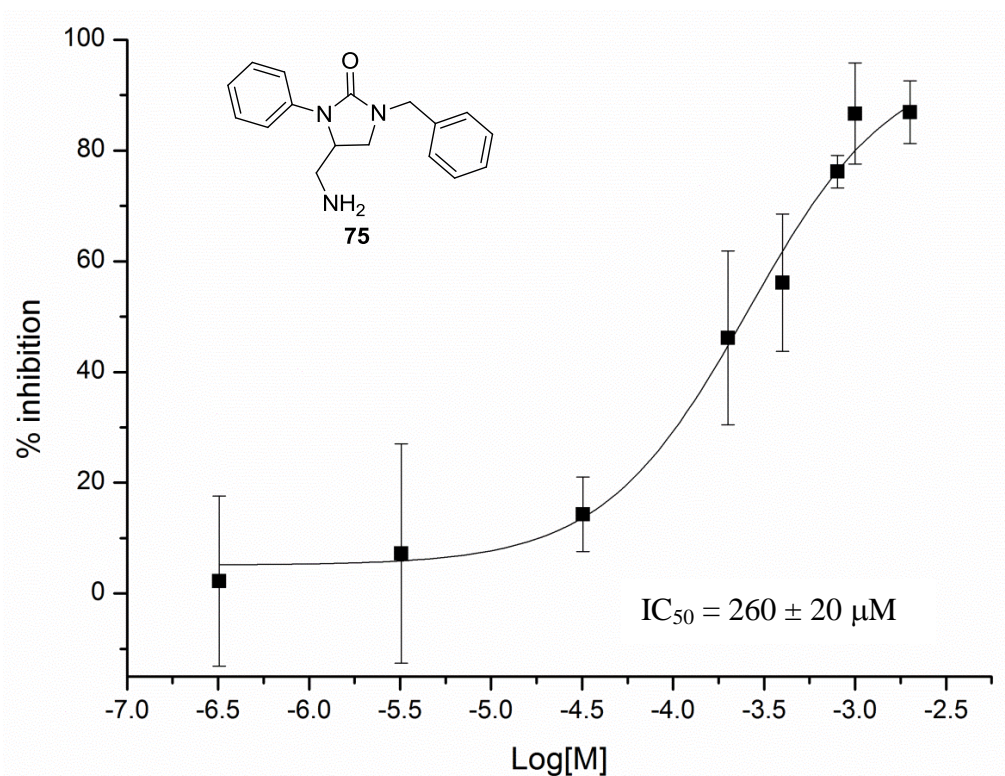
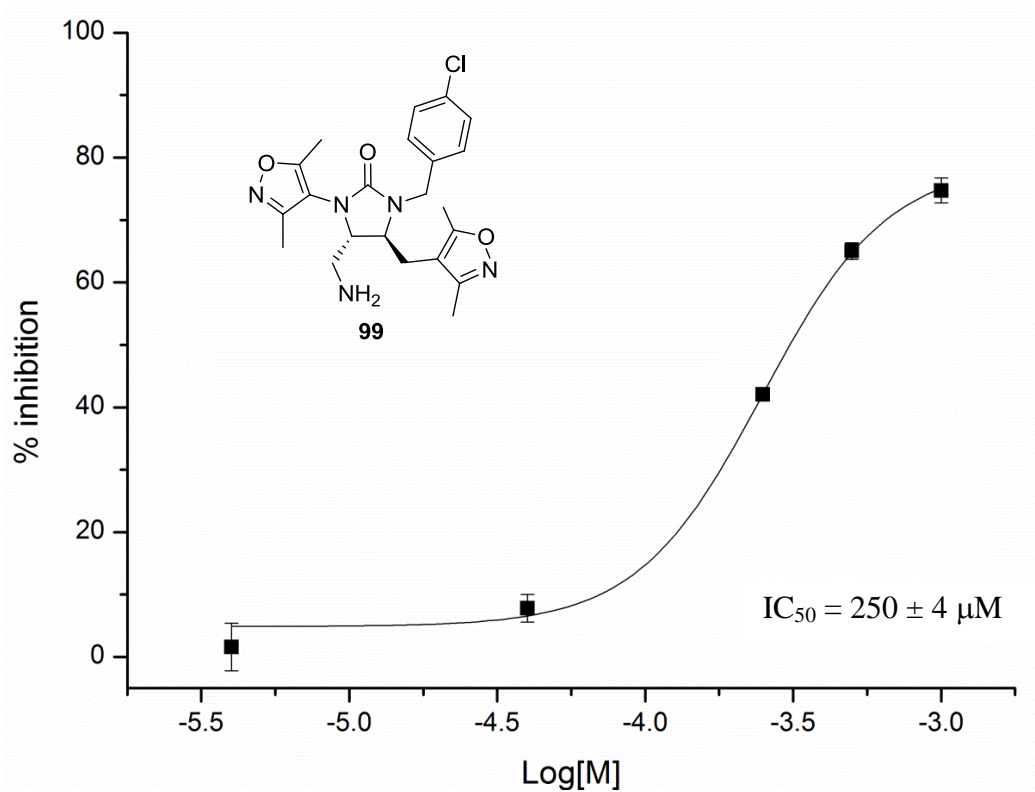


Figure 50. Dose response curves of imidazolidinone 99 and 75 against BACE-1.
Data fitted with a sigmoidal dose response model using Origin Pro 8.6.

4.2.1 Analysis of structure-activity relationship

The biological results obtained with the designed series of imidazolidinones, summarised in Table 15, showed that the imidazolidinone **99** (entry 1, $IC_{50} = 250 \mu\text{M}$) is the most active compound of the series and contains the best combination of substituent groups around the cyclic urea ring. In this compound, the two dimethyl isoxazole groups seem to be important for the activity observed. Replacing the dimethyl isoxazole at the *N*-3 with a pyridyl ring (entry 3, compound **104**) resulted in an inhibition value at single concentration below the 25% threshold (17%). Replacing the dimethyl isoxazole at *C*-5 with a phenyl group (entry 2, compound **106**) decreases the activity of 3-fold ($IC_{50} = 720 \mu\text{M}$), and removing the dimethyl isoxazole at *C*-5 (entry 7, compound **101**) causes a drastic fall of activity (6% inhibition at $100 \mu\text{M}$).

A comparison of the azides **98** (entry 8, $IC_{50} = 750 \mu\text{M}$) with the amines **99** (entry 1) shows that the azide group could be a viable surrogate of the primary amine, maintaining a moderate activity. This was shown also by the azide **103** (entry 9, $IC_{50} = 590 \mu\text{M}$) to compare with the amine **106** (entry 2, $IC_{50} = 720 \mu\text{M}$). The presence of an iodide group (entry 4, compound **111**) or of a more constrain cyclic amidic bond (entry 6, compound **97**) reduces significantly the activity (*ca.* 13% inhibition at $100 \mu\text{M}$).

The importance of the dimethyl isoxazole groups at the *N*-3 and at *C*-5 was observed also in the azide compounds (entry 8-13). The substitution of the dimethyl isoxazole at the *N*-3 (entry 10, compound **102**) and the removal of the dimethyl isoxazole at the *C*-5 (entry 13, compound **100**) bring the activity below the 25% threshold (*ca.* 10% inhibition at $100 \mu\text{M}$) in comparison with compound **98** (entry 8). Regarding the *p*-chlorobenzyl substituent, it appears to be preferred in comparison to the furan ring or the isopropyl group, as shown by the difference of activity between compound **99** (entry 1) and compounds **94** (entry 5, *ca.* 10% inhibition at $100 \mu\text{M}$); and between compound **102** (entry 10, *ca.* 10% inhibition at $100 \mu\text{M}$) and compound **107** (entry 12, no inhibition observed).

Among the lipophilic series of imidazolidinones, Table 2, the compound **75** (entry 1) resulted surprisingly active ($IC_{50} = 260 \mu\text{M}$), showing an activity similar to the designed imidazolidinone **99** in Table 1 (entry 1). The azide analogue (entry 2) of the

imidazolidinone **74** demonstrated a lower level of activity (concentration at 50% inhibition = 805 μM), and the iodide analogue **73** (entry 3) did not show any activity (15% inhibition at 100 μM); confirming the trend of the imidazolidinones **99**, **98**, **111** in Table 1 (entry 1, 4, 7). It was interesting to note that the compound **60** (entry 5), containing a MOM protected alcohol group instead of the primary amine and a bulkier aromatic lipophilic substituent at the C-5, was active (27% inhibition at 100 μM). Unfortunately due to solubility issues, it was not possible to obtain the full dose response curve. As expected, the monosubstituted analogue **43** (entry 4) did not display any activity (15% inhibition at 100 μM).

In terms of ligand efficiency, the active compounds **99**, **106** and **103** (Table 15, entry 1, 2 and 9) had similar ligand efficiency values ($\text{LE}' = \mathbf{99}: 0.12$, **106** and **103}: 0.10). The lipophilic compound **75** (Table 16, entry 1) was the most ligand efficient, $\text{LE}' = 0.17$; as generally occurred with lipophilic compounds^{b,32} The ligand efficiency values were generally lower than the predicted ones ($\text{cLE}' = \mathbf{99}: 0.23$, **106}: 0.21**, **103}: 0.20** and **75}: 0.26**) and the activity values as well (eHiTS prediction of 10^{-7} M inhibitors).**

The structures of the most active compounds were analysed in order to rationalise the activity results. As mentioned, the biological results revealed that in the case of the imidazolidinone **99** the two dimethyl isoxazole substituents seemed to be fundamental for activity (Figure 51). This might suggest that the two dimethyl isoxazoles could be involved either in key interactions in BACE-1 catalytic site or that their geometry could be more efficient in filling BACE-1 pockets, in comparison to phenyl or pyridine groups.

^bLipophilic compounds generally show higher ligand efficiency but less specific interactions with a biological target.

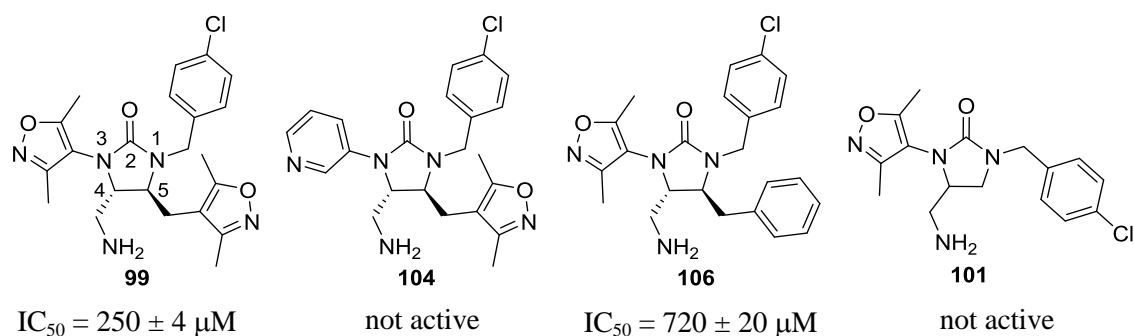


Figure 51. Structure activity relationship relevant to the imidazolidinone 99.

In order to shed light on this outcome, an analysis of the predicted binding poses of the imidazolidinones **99** was performed. According to the binding pose predicted by eHiTS, the dimethyl isoxazole attached to *N*-3 of the urea central core could be involved in a H-bond with Wat1, positioned between the two catalytic aspartates; while the primary amine could act as an H-bond donor and form a H-bond with Glu124 located in the flexible region of the protein, called flap (Section 1.3.2). At the same time the carbonyl group of the urea could act as a H-bond acceptor and be involved in an H-bond with Thr231 (Figure 52, panel A). In terms of protein surface interactions, the dimethyl isoxazole group at *C*-5 is predicted to be accommodated in the S3 pocket of BACE-1 (Section 1.3.3); the *p*-chlorobenzyl group is predicted to occupy the S2 pocket, and the H-bond with Glu124 is predicted to lock the protein in a semi-closed conformation (Figure 52, panel B).

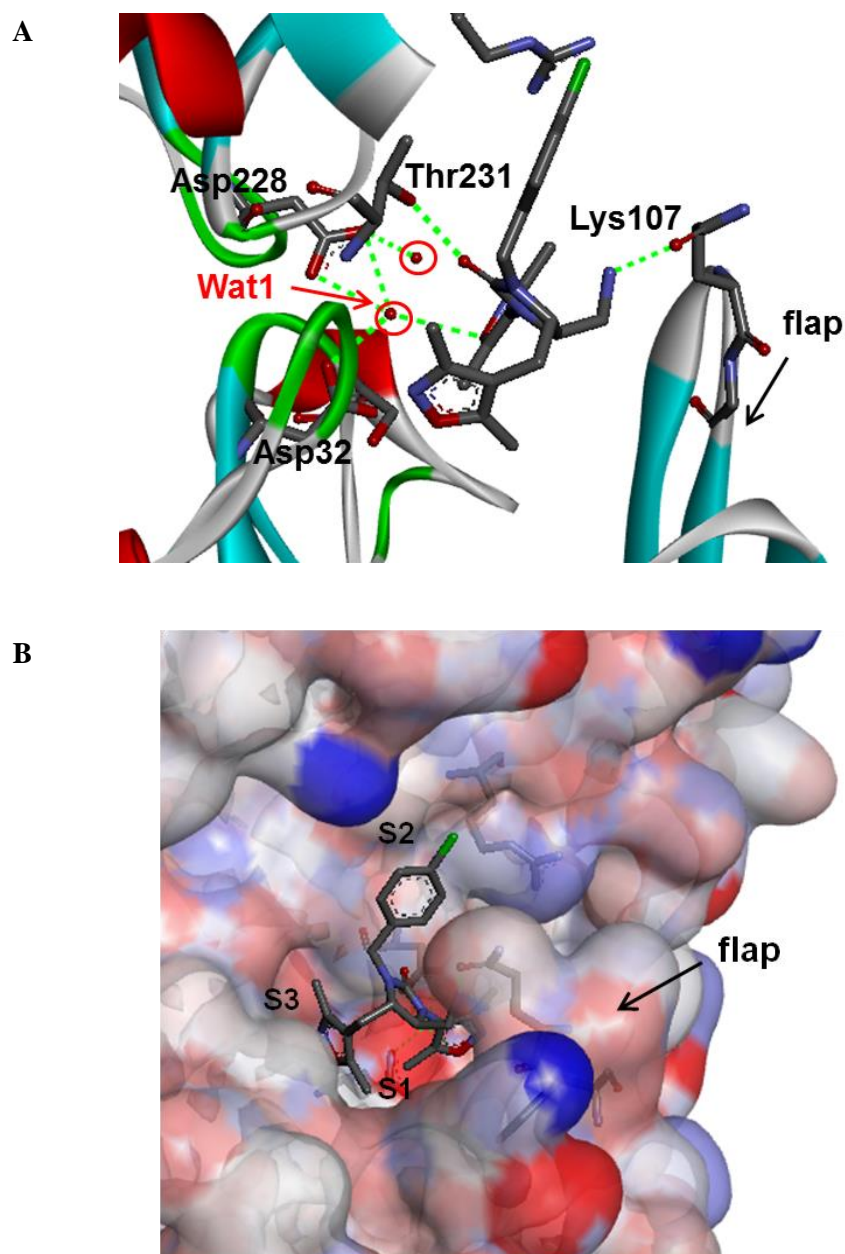


Figure 52. Predicted binding pose of the imidazolidinone **99 in BACE-1.** A) Representation of the predicted H-bonds (green dotted lines) formed with aminoacidic residues in the catalytic site. The primary amine is predicted to form a H-bond with Glu124, located in the flexible region of BACE-1, while the O atom of the isoxazole at *N*-3 is predicted to form an H-bond with Wat1. B) Representation of the predicted surface interaction. The imidazolidinone **99** is predicted to fill S3 and S2 pockets of BACE-1 respectively with the dimethyl isoxazole at *C*-5 and with the *p*-chlorobenzyl group. Images correspond to the 4*S*, 5*S* enantiomer of the imidazolidinone **99**, visualised by Discovery Studio 3.0.

The predicted binding pose of the imidazolidinone **99** seems to help rationalising the role of the isoxazoles. Keeping in mind limitations of computational prediction, it can still be stated that a dimethyl isoxazole group could interact with the conserved water molecule in BACE-1 catalytic site, forming H-bonds with its N or O atoms. Furthermore, it is known that heteroaromatic and aromatic groups can often be accommodated in BACE-1 pockets (See examples in Section 1.4.4); therefore it is plausible that the dimethyl isoxazole group can assume a similar role, and that the two methyl groups can contribute to occupy the pockets more extensively in comparison to pyridine and phenyl group (Figure 53).

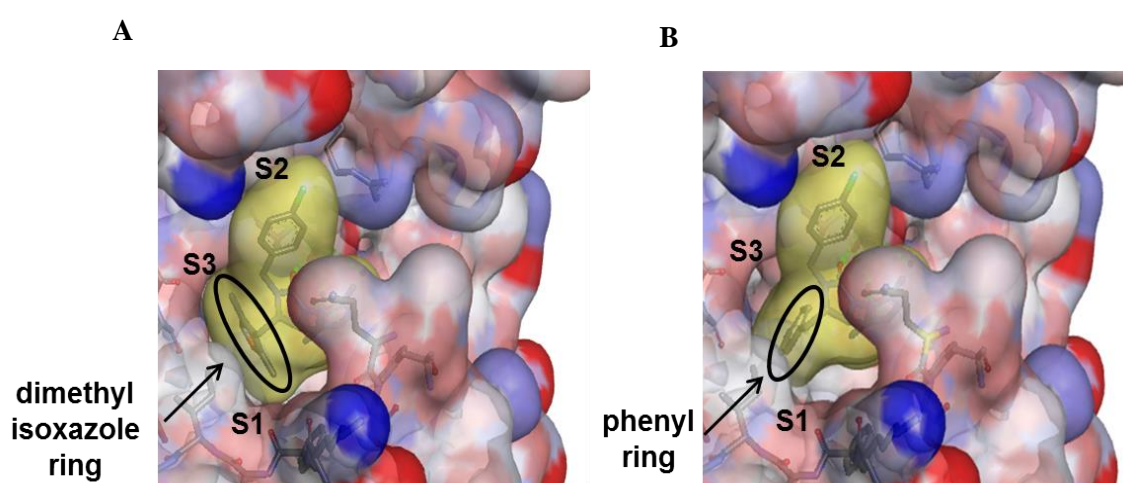


Figure 53. Comparison of surface interactions between the imidazolidinone **99** and imidazolidinone **105** in BACE-1 catalytic site. A) Representation of surface interaction of the imidazolidinone **99** containing the dimethyl isoxazole group. B) Representation of surface interaction of the imidazolidinone **99**, containing the phenyl group. The more extended surface of the dimethylisoxazole ring (A) occupies S3 pocket and partially S1 pocket, while the phenyl group (B) occupies only a part of S3 pocket. Visualised with Discovery Studio 3.0.

Regarding the lipophilic monosubstituted imidazolidinone **75** (Table 16, entry 1), it was interesting to note that the main structure difference with the inactive analogue **101** (Table 15, entry 7) was the *N*-aryl substituent group (Figure 54). This difference might suggest that, in this case, the isoxazole group is not involved in critical binding interactions. Other type of interactions, such as lipophilic one, might determine the activity of the monosubstituted imidazolidinone **75**, which might assume a different binding pose in BACE-1 catalytic site, in respect to the imidazolidinone **99**.

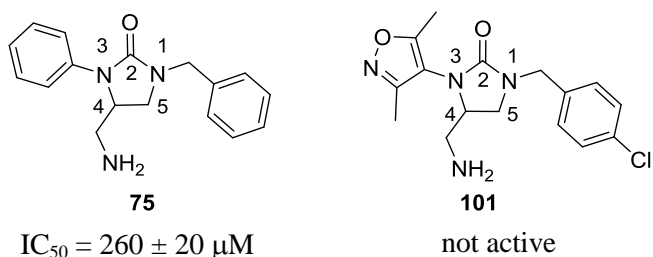


Figure 54. Comparison of two monosubstituted imidazolidinone analogues. The active imidazolidinone **75** differs from the not active imidazolidinone **101** mainly for the substituent group at *N*-3. This seems to suggest that lipophilic interactions have an important role for the activity of the imidazolidinone **75**.

Moreover, a comparison between the monosubstituted imidazolidinones **75** and the more lipophilic bisubstituted imidazolidinone **60** (Table 16, entry 5), both containing a phenyl group, revealed that lipophilic aromatic groups at the “right side” of the urea core might play an important role for the activity (Figure 55). In order to investigate those lipophilic interactions and to understand the role of the OMOM group, the synthesis of a series of analogues of those molecules was designed and prepared (Section 4.3).

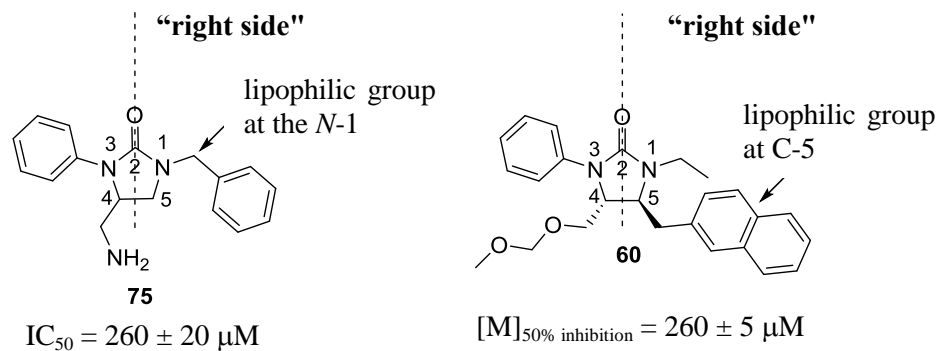


Figure 55. Comparison of the imidazolidinone 75 with the lipophilic compound 60.

4.3 Design of structural analogues of active compounds

A small library of analogues of lipophilic imidazolidinones was designed varying the structure of compounds **75** and **60**. The analogues were designed in order to identify an alternative group to the primary amine and to evaluate the importance of the lipophilic interactions (Figure 56).

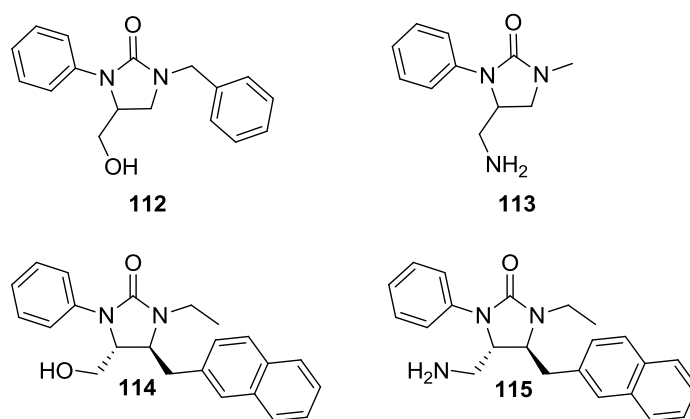
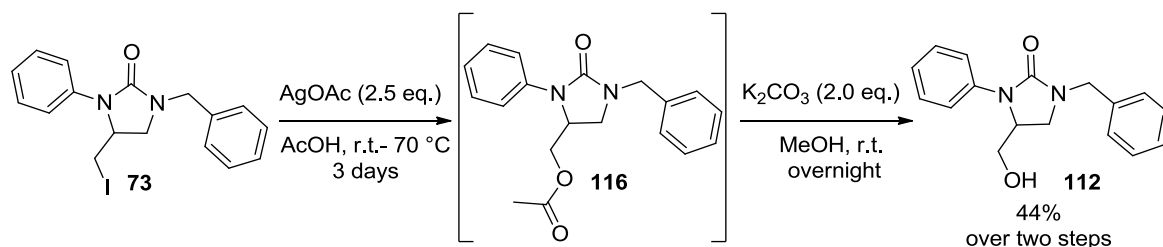


Figure 56. Analogues of lipophilic imidazolidinones selected for synthesis.

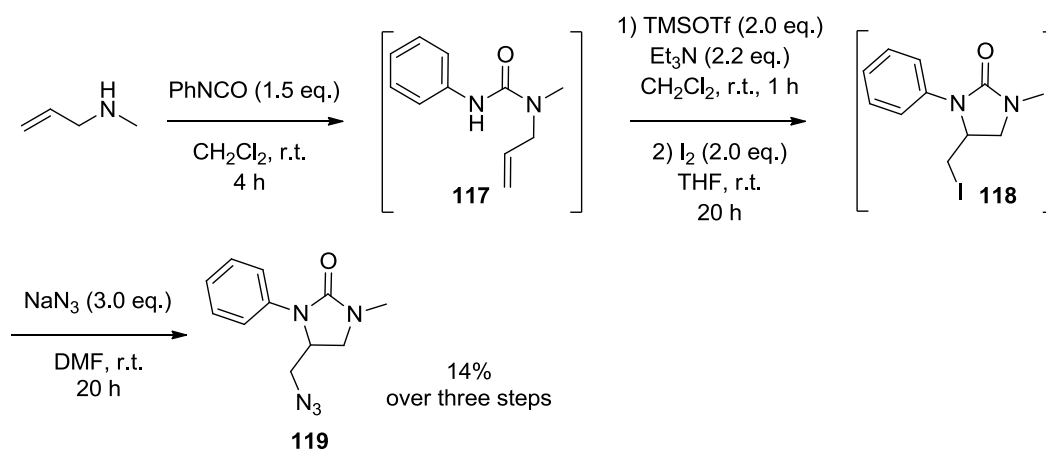
4.3.1 Synthesis of monosubstituted analogues

The alcohol **112** was prepared in two steps from the iodide **73** via displacement of iodide with acetate (Scheme 24). The iodide **73** was treated with silver acetate in acetic acid to give the intermediate **116** which was used without further purification. The intermediate **116** was converted into the alcohol **112** by treatment with potassium carbonate in MeOH. The alcohol **112** was obtained in 44% yield over two steps.



Scheme 24. Synthesis of the alcohol **112**.

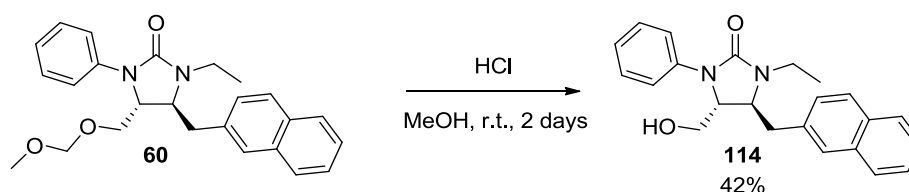
The synthesis of the imidazolidinone **113** was attempted using the established iodine-mediated cyclisation (Section 3.3.1). Commercially-available methyl allylamine was treated with phenylisocyanate in CH_2Cl_2 to give the urea **117**, which was used without further purification. The urea **117** was first treated with trimethylsilyl trifluoromethanesulfonate and triethylamine in CH_2Cl_2 at room temperature, and then with iodine in THF. The resulting iodide intermediate **118** was mixed with sodium azide in DMF at room temperature overnight, giving the azide **119** in 14% yield over three steps. Treatment of the azide **119** with triphenylphosphine and water in THF did not give the expected product (Scheme 25).



Scheme 25. Synthetic route towards the preparation of the amine **113**.

4.3.2 Synthesis of bisubstituted analogues

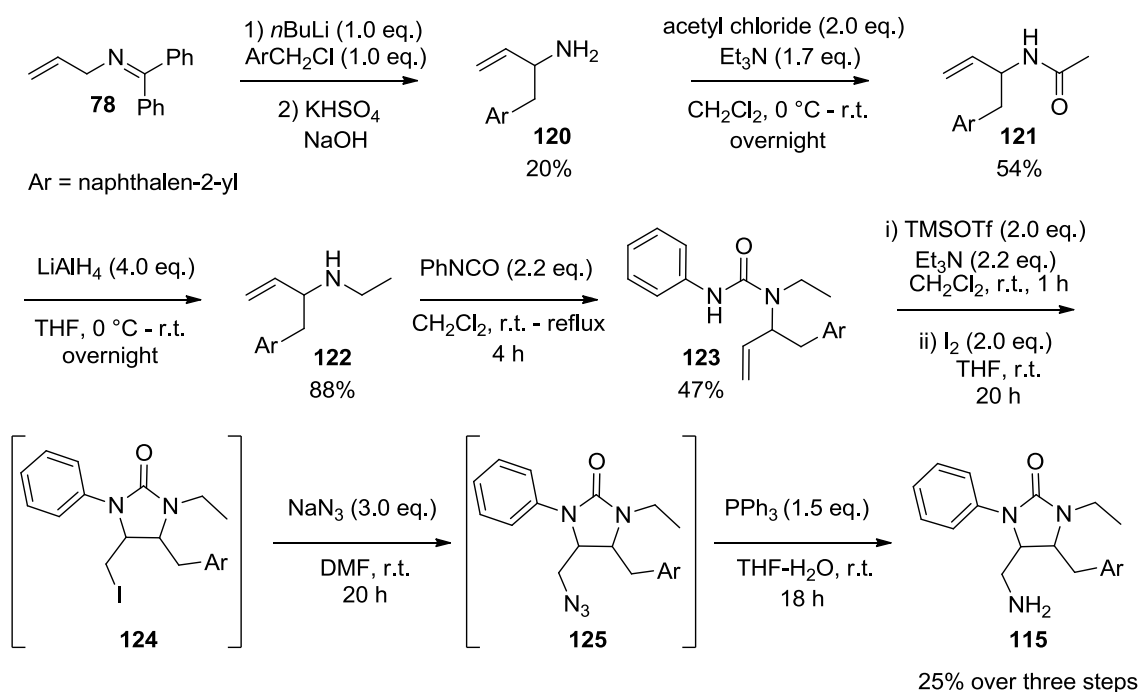
The imidazolidinone **114** was prepared from the precursor **60** (Section 3.2.2) in one step, *via* deprotection of the MOM group. The compound **60** was treated with few drops of hydrochloric acid in MeOH stirring at r.t., giving the alcohol **114** in 42% yield (Scheme 26).



Scheme 26. Preparation of the alcohol **114**.

The imidazolidinone **115** was prepared from the amine building block **120** (Scheme 27). The amine building block **120** was synthesised in 54% yield from the imine **78**, using a similar methodology to the amines **76** and **77** (Scheme 21, Section 3.3.2.1), by treatment with *n*-butyl lithium and 2-(chloromethyl)naphthalene, followed by base hydrolysis. The amine **120** was then treated with acetylchloride and triethylamine in CH₂Cl₂, to give the acetamide **121**. The acetamide **121** was reduced to give the ethyl allylamine **122** in 88% yield by treatment with lithium aluminium hydride in THF. The urea **123** was prepared from the allylamine **122** and phenyl isocyanate in CH₂Cl₂ in 47% yield and was employed in the iodine-mediated cyclisation to give imidazolidinone **124**. The urea **123** was treated with trimethylsilyl trifluoromethanesulfonate and triethylamine in CH₂Cl₂ at r.t. and then with iodine in THF. The resulting iodine

intermediate was treated with sodium azide in DMF at r.t. overnight to give the azide **125**, which was used without further purification. The azide **125** was treated with triphenylphosphine and water in THF to give the final imidazolidinone **115** in 25% yield over three steps.

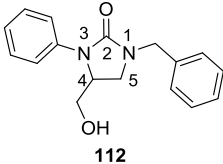
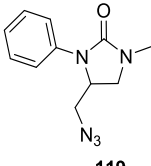
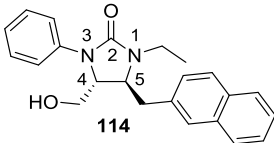
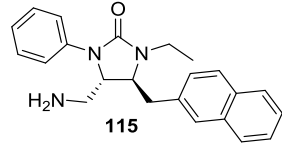


Scheme 27. Synthesis of the imidazolidinone 115.

4.3.3 Biological evaluation of a second generation of analogues

The synthesised analogues of lipophilic imidazolidinones, compounds **112**, **114** and **115**, and the azide compound **119** were tested against BACE-1 through the established *in vitro* assay. The results are summarised in Table 17. In cases in which it was not possible to obtain the full dose response curve, due to solubility issues, the concentration at 50% of inhibition observed was reported.

Table 17. Biological activity of analogues of lipophilic imidazolidinones against BACE-1.

Entry	Compound	Inhibition at 100 μ M (%)	IC ₅₀ (μ M)	LE' ^a
1	 112	10 \pm 1	- ^b	- ^b
2	 119	no inhibition observed	- ^b	- ^b
3	 114	41 \pm 12	1170 \pm 83 ^c	- ^d
4	 115	25 \pm 3	724 \pm 12	0.12

^aLE' calculated as $-\log(\text{IC}_{50})/\text{nHA}$, (see Equation 2, Section 1.2.3.1); ^bNot determined; ^cValue of concentration at 50% inhibition, ^dNot calculated, IC₅₀ value not available

The biological results showed that the alcohol group is not a suitable surrogate of the primary amine; since the monosubstituted analogues **112** (entry 1, 10% inhibition at 100 μ M) and the bisubstituted analogues **114** (entry 3, concentration at 50% inhibition = 1170 μ M) demonstrated lower activity than the respective amino compounds **75** (Table 16, entry 1, IC₅₀ = 260 μ M) and **115** (Table 3, entry 4, IC₅₀ = 724 μ M). The benzyl group at the *N*-1 of the urea central core seems to be critical for the activity of the monosubstituted series of imidazolidinones. Replacement of the benzyl group with a methyl group (compound **119**, entry 2) suppressed any activity in comparison with the more lipophilic azide **74**, (Table 16, entry 2, 28% inhibition at 100 μ M). These results seem to indicate that, in this series of compounds, lipophilic groups at both side of the urea central core play a significant role in inhibiting BACE-1.

Regarding the series of bisubstituted imidazolidinones, the analogue **114**, containing the alcohol group at C-4 (entry 3) displayed activity at single concentration above the threshold; but, once again, it was not possible to determine the full dose response due to solubility issues. A comparison of the concentrations at 50% inhibition revealed that the analogue **114** (entry 3) is *ca.* 5-fold less active than the analogue **60** containing the MOM group (Table 16, entry 5, concentration at 50% inhibition = 260 μM). The imidazolidinone **115**, containing the amino group (entry 4), displayed modest activity: *ca.* 2.8-fold less than the monosubstituted compound **75** (Table 16, entry 1, IC_{50} =260 μM). This might suggest that the best position to incorporate a lipophilic group is at N-1, at the “right side” of the urea central core.

Illustrations of the predicted binding poses of the imidazolidinone **75** are provided in Figure 57. The imidazolidinone **75** is predicted to be involved in H-bond and π -cation interactions with Arg235, located at the top of BACE-1 catalytic site. The H-bond is formed through the carbonyl group, while the π -cation interactions are formed through both benzyl and phenyl group. These interactions seem to direct the primary amine towards the water molecules, allowing the formation of H-bonds (Figure 57, panel A). In terms of protein surface interactions, the phenyl group is predicted to occupy the S1' pocket of BACE-1, while the benzyl group is predicted to be oriented towards the inner without occupying any pocket (Figure 57, panel B).

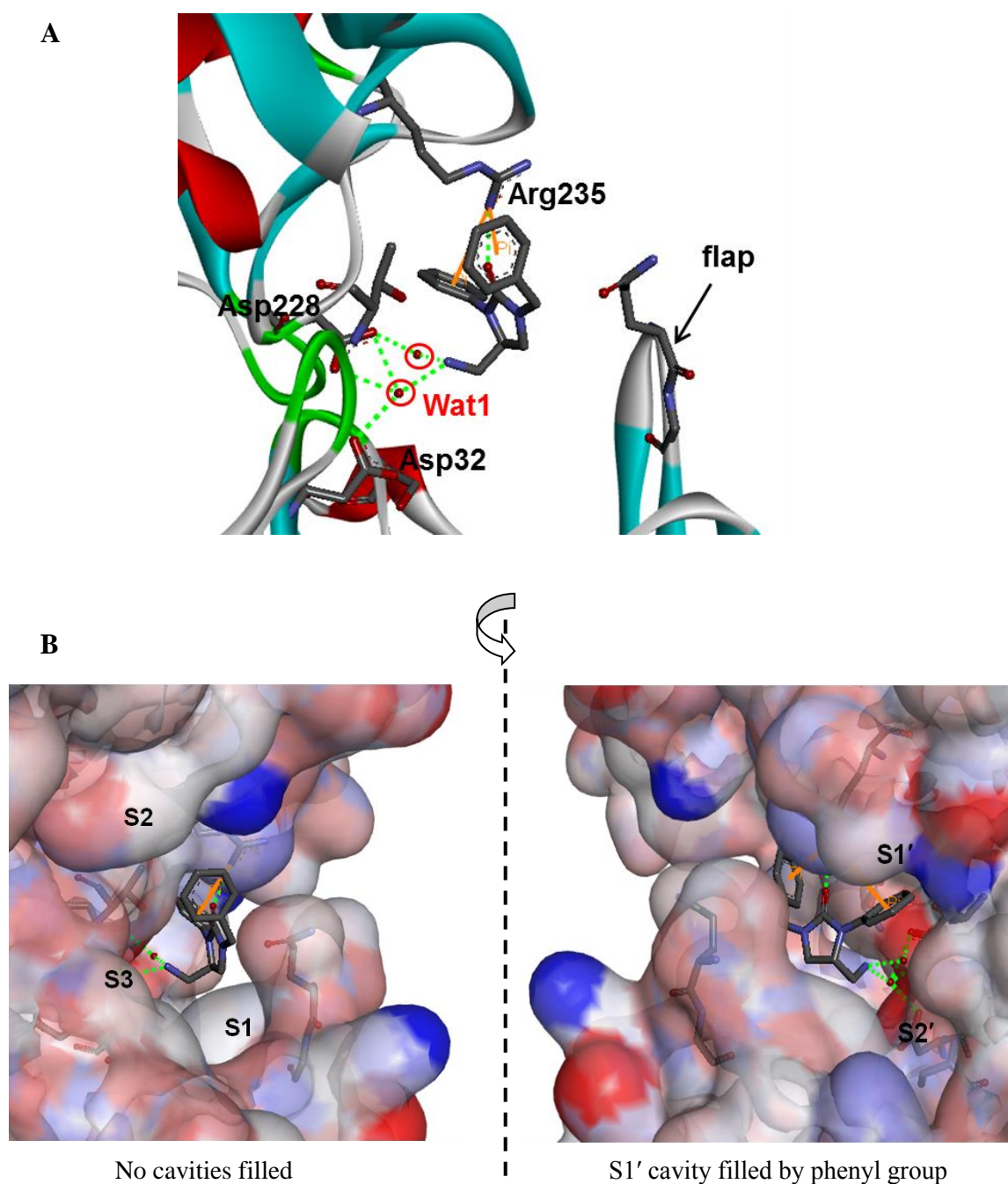


Figure 57. Predicted binding pose of the imidazolidinone 75. A) Representation of the predicted H-bonds (green dotted-lines) and π -cation interactions (orange dotted lines) in BACE-1 catalytic site. B) Representation of the predicted surface interactions: the benzylic group is not oriented towards the available pockets (right), the phenyl group is accommodated into S1' pocket (left). Figures represented for the *R* enantiomer of the imidazolidinone 75. Visualised with Discovery Studio 3.0.

The predicted binding pose of the imidazolidinone **75** might suggest a possible explanation about the importance of the aromatic groups for the activity against BACE-1. When both benzyl and phenyl group are attached to the two *N* of the urea core, they could be oriented in the same direction in BACE-1 catalytic site and be involved in common binding interactions (*e.g.* π -sigma, π - π or π -cations interactions or pocket filling); which might act as an “anchor point” to direct the rest of the molecule towards the catalytic aspartates or Wat1, where the primary amine can form H-bonds. When the benzyl group is replaced with an alkyl group (in the case of the imidazolidinone **113**, Table 17, entry 2) or when a bulkier aromatic group is incorporated in another position around the cyclic urea central core (in the case of the imidazolidinone **60**, Table 16, entry 5), such as a common interaction cannot occur and the imidazolidinone scaffold might assume a less effective binding pose.

4.4 Assessing inhibitor selectivity for BACE-1

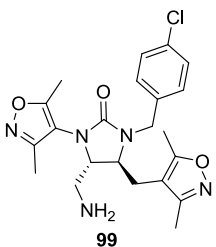
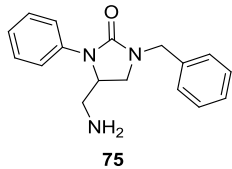
BACE-2 is an homolog of BACE-1, with 75% homology and 45% gene coding sequence identity.¹²⁸ BACE-2 is expressed in low level in brain and competes with BACE-1 for the same substrate, acting as an antagonist for BACE-1, similar to α -secretase¹²⁹ (Section 1.3.1). The role of BACE-2 in Alzheimer’s disease is not fully understood yet, but seems to be marginal in comparison to BACE-1.¹³⁰ BACE-1 inhibitors are generally tested against BACE-2 in order to determine their selectivity for BACE-1. Therefore the two identified BACE-1 inhibitors, the imidazolidinone **99** and **75**, were assayed *in vitro* against BACE-2 protein to determine their selectivity for either protein.

4.4.1 Biological activity measurements

The described *in vitro* fluorescent competitive inhibition assay (Section 4.1) was employed to determine the activity of the imidazolidinone **99** and **75** against BACE-2. The biological activity was initially measured at 100 μ M (5-10% of DMSO in buffer); then a dose response assay was performed. As for BACE-1, the commercially-available inhibitor β -secretase IV (100 μ M in DMSO) was employed as a positive control DMSO-only (5-10%) was employed as a negative control. Details regarding the execution of the fluorescent quenching assay for BACE-2 are provided in Section 5.4.1.

The results of the *in vitro* assays are summarised in Table 18; dose response curves are illustrated in Figure 58 and Figure 59.

Table 18. Biological activity of imidazolidinones 99 and 75 against BACE-2.

Entry	Compound	Inhibition at 100 μM (%)	IC ₅₀ (μM)
1	 99	10 \pm 3	- ^a
2	 75	8 \pm 4	647 \pm 20

^aNot determined, dose-response not observed.

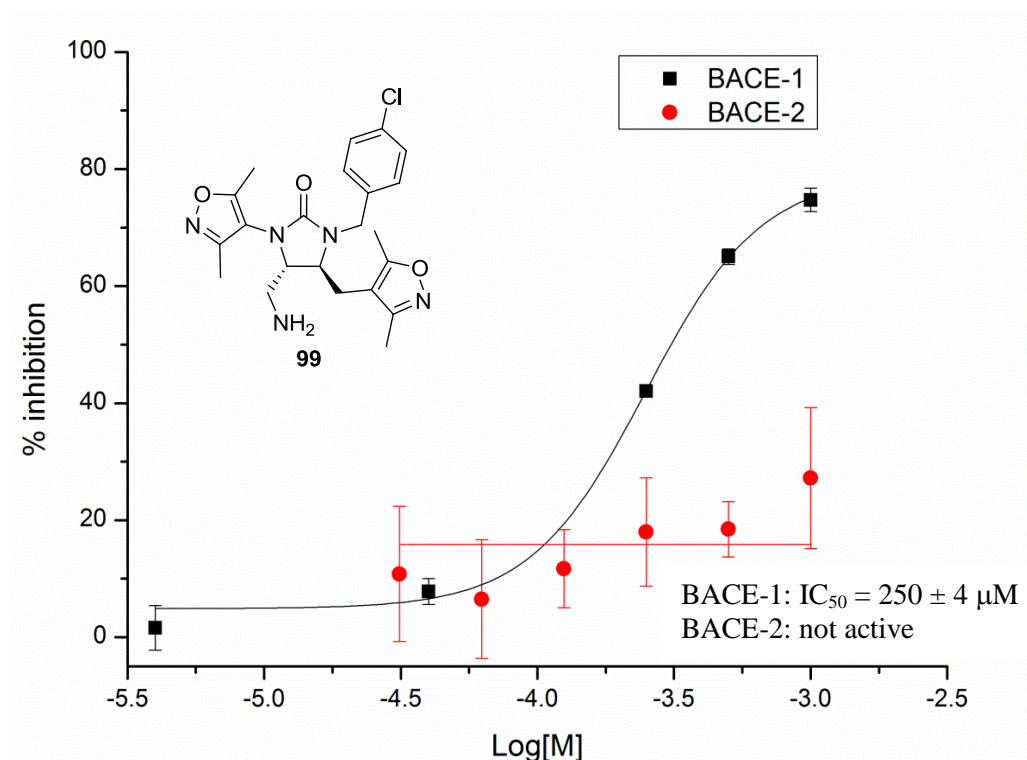


Figure 58. Comparison of activity of the imidazolidinone 99 against BACE-1 and BACE-2. Data fitted with a sigmoidal dose response model using Origin Pro 8.6.

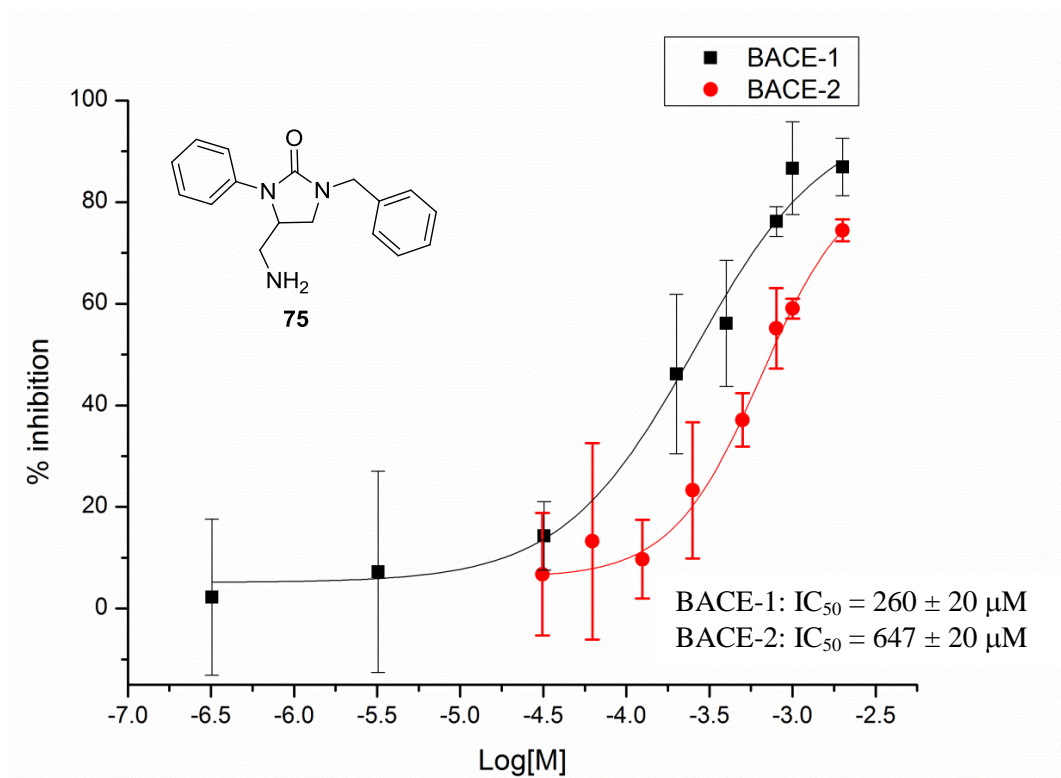


Figure 59. Comparison of the dose response curves of the imidazolidinone **75 against BACE-1 and BACE-2.** Data fitted with a sigmoidal dose response model using Origin Pro 8.6.

The imidazolidinone **99** and **75** displayed a similar value of inhibition against BACE-2 at single concentration, *ca.* 10%; but the dose response revealed different outcome. The imidazolidinone **75** showed an activity of *ca.* 647 μ M, only 2.5-fold less active than against BACE-1, suggesting that the activity may stem from non-specific interactions. Regarding the imidazolidinone **99**, although the IC_{50} could not be determined with BACE-2, the compound showed at least 10-fold selective for BACE-1.

4.5 Summary

This Chapter described the evaluation of biological activity of a focused library of imidazolidinone putative inhibitors of BACE-1, and of a series of lipophilic analogues. The compounds were assayed at a single concentration (100 μ M) and IC_{50} values of the promising inhibitors were also determined. The best BACE-1 inhibitors, amongst the imidazolidinones assayed, were compounds **75** and **99**, showing an IC_{50} value of *ca.* 250 μ M.

The inhibitor **99**, belonging to the designed focused library of compounds, showed the following key structure features: an hydrophilic dimethyl isoxazole ring at *N*-3 of the urea system, a *p*-chlorobenzyl group at *N*-1, another dimethyl isoxazole ring at the *C*-4 position and a primary amine at the *C*-5 position (Figure 60, panel A). The lipophilic imidazolidinone **99**, which did not belong to the designed focused library of putative inhibitors, contained lipophilic substituents (benzyl and phenyl) at both the *N* atoms of the urea system and a primary amine at the *C*-4 position (Figure 60, panel B).

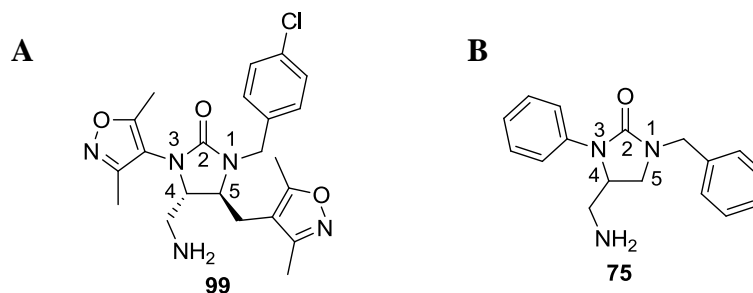


Figure 60. Structures of the identified imidazolidinone BACE-1 inhibitors. A) Designed imidazolidinone **99**, $IC_{50} = 250 \mu M$, dimethyl isoxazole groups seem to be critical for activity. B) Lipophilic imidazolidinone **75**, $IC_{50} = 260 \mu M$, aromatic groups at the *N* atoms seem to be critical for activity.

The designed imidazolidinone **99** demonstrated a good selectivity for BACE-1 vs the homolog BACE-2, being at least 10-fold less active against BACE-2. The lipophilic imidazolidinone **75**, instead, was only 2.5-fold more active against BACE-1 than against BACE-2, suggesting that it might bind BACE-1 through non-specific lipophilic interactions. Given the good selectivity of the imidazolidinone **99**, it can be considered a good novel lead molecule to be developed into a more potent BACE-1 inhibitor.

4.6 Conclusion and future directions

In this thesis a novel approach to design inhibitors was described and validated. The approach started with a computational design of a virtual library of skeletally diverse virtual lead-like compounds, which was screened *in silico* against a target protein, BACE-1. From the virtual screening, identified putative inhibitors were selected for synthesis and tested *in vitro* through a fluorimetric assay.

A virtual library of skeletally diverse lead-like compounds was generated on the basis of the diversity oriented synthesis approach (DOS) developed within the Nelson group. The approach used a virtual protocol of synthesis, in which an initial pool of virtual electrophile and nucleophile building blocks underwent a combinatorial virtual coupling, followed by a series of virtual chemical reactions: derivatisation, cyclisation and further derivatisation (Section 2.3, Figures 34 and 37). The virtual chemical reactions employed were previously established experimentally, and only commercially available reactants were included in the virtual library enumeration, in order to ensure synthetic accessibility as far as possible. A virtual library of *ca.* 55,000 cyclic lead-like molecules was generated. The virtual library was screened against BACE-1 using eHiTS software.

Two families of putative inhibitors of BACE-1 were identified after the vHTS with eHiTS: the amino tetrahydropyridine and the imidazolidinone family. Both families contained elements of novelty with respect to known BACE-1 inhibitors. The most potentially diverse family of imidazolidinone was selected for synthesis (Section 2.4.2). A focused library of this family was designed. The key features of the structure of imidazolidinones were a primary amine and a series of heteroaromatic or alkyl substituent positioned around the cyclic urea central core (Figure 61). According to the computational prediction of binding poses of this family, the primary amine would form key H-bond interactions with the catalytic Asp32 and Asp228 in BACE-1 catalytic site; while heteroaromatic group could fill pockets in BACE-1.

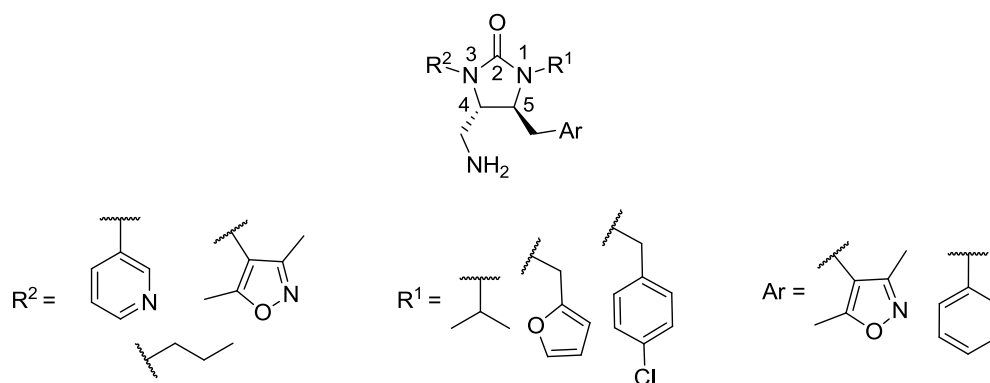


Figure 61. Features of the designed library of imidazolidinones putative inhibitors of BACE-1.

Two synthetic routes were envisaged for the synthesis of the imidazolidinone putative inhibitors of BACE-1, both based on a key cyclisation reaction of *N*-allyl ureas, to obtain the cyclic central core of the imidazolidinones. The first synthetic route was suggested by the virtual protocol of synthesis employed to enumerate a virtual library of lead-like compounds. The route was based upon the Pd-catalysed aminoarylation on *N*-allyl ureas containing different functional groups at the allylic position. The second synthetic route was based upon the iodine-mediated cyclisation of *N*-allyl ureas containing different aromatic groups at the allylic position (see Scheme 5, Section 3.1, page 66).

The investigation of the Pd-catalysed aminoarylation led to the identification of the imidazolidinone **60** (Figure 62), containing the MOM protected alcohol at the 4-CH₂ position, as a precursor of the final imidazolidinone, containing a primary amine at the same position. To apply this route to the designed imidazolidinones (Figure 61), further investigations regarding the synthesis of specific *N*-allyl urea substrates, containing heteroaromatic groups, were required. At the same time, chemical reactions to convert the MOM protected alcohol into a primary amine needed to be explored. As a consequence the route was abandoned.

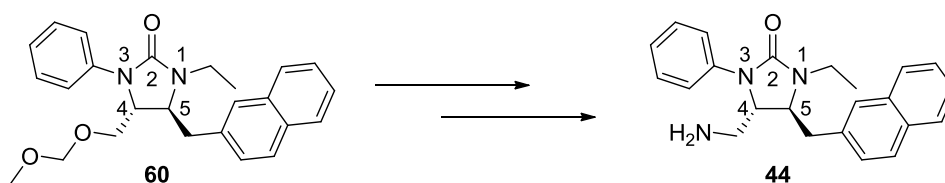


Figure 62. Imidazolidinone 60, synthesised through the Pd-catalysed aminoarylation. The imidazolidinone **60** was identified as a possible precursor of a final imidazolidinone, containing a primary amine at 4-CH₂ position.

The second synthetic route, based upon the iodine-mediated cyclisation, was applied to eight different *N*-allyl urea substrates and led to the synthesis of a small library of six target imidazolidinones (Figure 63) and seven azide precursors. Surprisingly, the yields of the iodine-mediated cyclisation and of the final two steps of synthesis were low. The six target imidazolidinones, the azide precursors and a series of lipophilic imidazolidinones (synthesised during the exploration of the two synthetic routes) were assayed against BACE-1 through an established *in vitro* fluorimetric assay.

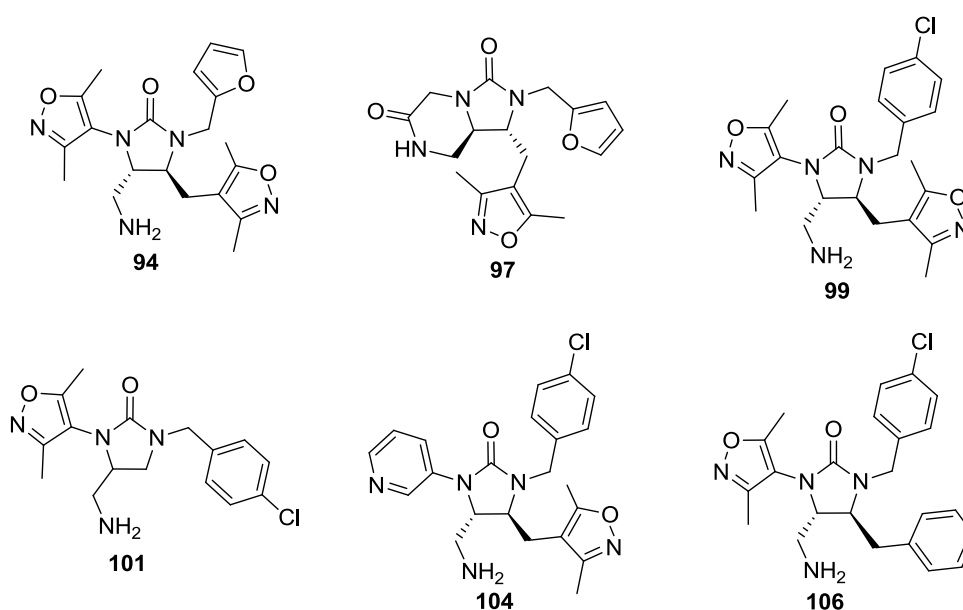


Figure 63. Focused library of six imidazolidinones, putative inhibitors of BACE-1.

Two compounds showed inhibitory capacity against BACE-1, with IC₅₀ value of *ca.* 250 μ M (Figure 60, Section 4.5). The imidazolidinone **99**, belonging to the designed library of putative inhibitors, showed a good selectivity (10-fold) for BACE-1 over its homologue BACE-2. The imidazolidinone **75**, belonging to the series of lipophilic

compounds, was surprisingly active, but it did not show good selectivity for BACE-1 over BACE-2; being only 2.5-fold more active against BACE-1. These results suggested that the imidazolidinone **99** is likely to interact through promiscuous interactions, while the designed imidazolidinone **75** is likely to form specific interactions in BACE-1 catalytic site.

In conclusion, the biological results validated the computational approach employed to design a focused library of BACE-1 inhibitors. A novel imidazolidinone inhibitor, compound **99**, exhibited a μM inhibitory capacity, 3-fold lower than the one predicted by the eHiTS, nevertheless it showed a good selectivity for BACE-1 over BACE-2. Therefore, it can be considered a good lead to be developed in a more potent BACE-1 inhibitor. Suggestions towards the optimisation of **99** are herein indicated.

A common strategy employed to develop initial leads of μM activity into potent BACE-1 inhibitor is to increase the length of alkyl substituents or adding lipophilic groups.⁴⁹ These modifications generally aim to occupy BACE-1 pockets. Following this strategy, similar modifications can be suggested to further develop the imidazolidinone **99**. Keeping the two dimethyl isoxazoles in the structure, critical for the activity, and the *p*-chloro benzyl group, which is preferred above a furan ring of an alkyl group (Section 4.2), the imidazolidinone **99** could be modified at the primary amine. The primary amine could be converted into an amide, by reaction with amino acids containing aromatic groups. Alternatively it could be modified by simple arylation (Figure 64). The aromatic group and the amino acid chains could occupy S2' or S1' BACE-1 pockets, which are predicted not to be occupied by the imidazolidinone **99** (Section 4.2.1, Figure 52).

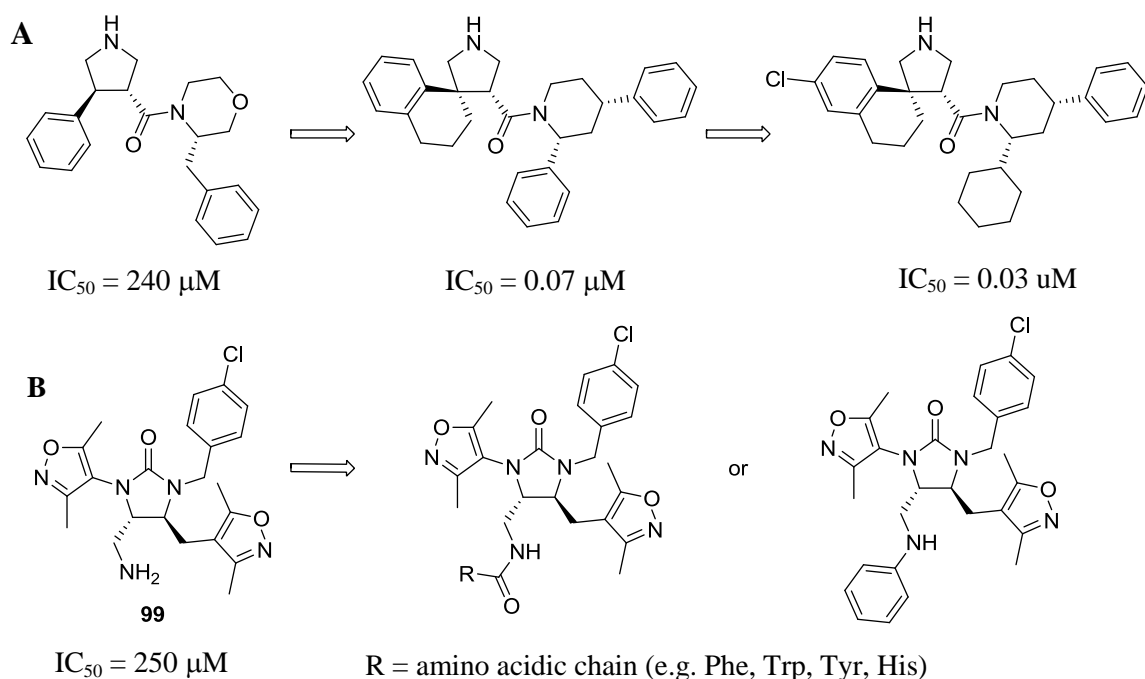


Figure 64. BACE-1 μM inhibitor as lead molecule to develop into more potent inhibitors. A) Pyrrolidine compound discovered by Stachel *et al.*¹³¹ in 2012, and developed in a spiro-pyrrolidine inhibitor of 0.03 μM . B) Imidazolidinone inhibitor **99**, to be develop in a more potent inhibitors by addition of alkyl or aromatic groups.

The described computational approach had two main limitations: the difficulty of predicting both synthetic accessibility and inhibitory activity of the designed molecules. Regarding the synthetic accessibility, the protocol of synthesis designed in Pipeline Pilot was based on Pd-catalysed aminoarylation and was not successful. The investigation of the Pd-catalysed aminoarylation showed that functional groups such as azide, NHBoc, NsNBoc are not compatible with the reaction conditions. *N*-Allylurea substrates containing those functional groups at the allylic position did not give the expected product, or gave it in very low yield (Section 3.2.2, Table 11). Therefore a new synthetic route based on the iodine-mediated cyclisation was employed to prepare a focused library of imidazolidinones. Unfortunately, apart from few exceptions (compound **104**, Section 3.3.2.2, Table 14, entry 6, and compound **115**, Section 4.3.2, Scheme 27), the yield of the iodine-mediated cyclisation were poor. In order to improve the value of virtual libraries of structurally diverse compounds, designed *in silico* according to our computational approach, it is necessary to refine them as the scope of the reactions included in the protocol of synthesis is defined. In our group, Richard Doveston has recently exemplified the synthesis of structurally diverse lead-like

scaffolds using a robust toolkit of reactions. This toolkit of reactions would be a good basis for the design a virtual library of compounds, having a greater of successful results in synthesis.

Regarding the prediction of inhibitory activity of novel molecules against biological target, the employed eHiTS software overestimated the potency of the imidazolidinone library. The predicted potency of compounds was of 10^{-7} M, while the measured potency was of *ca.* 10^{-4} M. eHiTS was reliable in reproducing the binding pose of the known inhibitor **26** (Section 1.4.4 and 2.2) and in predicting its activity (predicted activity of 10^{-7} M, real activity 3 μ M) therefore it seemed to be a good choice to perform the vHTS of virtual libraries. As eHiTS requires a reference inhibitor to identify protein binding site and to orient new ligands in the protein, it is possible that scores of ligand binding poses, which are oriented similarly to the inhibitor of reference in the binding site, can be overestimated. It is worth mentioning that SPROUT prediction of potency for the imidazolidinone library was more accurate, 10^{-4} M. SPROUT scoring function differs from eHiTS scoring functions; in SPROUT pocket filling and lipophilic interactions weighted more than H-bond interactions. Therefore it is possible that given the characteristic of BACE-1 target, with six pockets available to be filled (Section 1.3.3), SPROUT could be more appropriate to predict a more reliable score.

The literature confirmed that prediction of activity of library of compounds against specific biological targets is still challenging. It has been reported that many docking software are able to reproduce correctly X-ray poses of an inhibitors in a biological target, but a reliable prediction of the free energy of binding is still very difficult.^{132,133} Factors such as protein flexibility and solvent are not always predictable. In this project, vHTS was performed in the presence and absence of two water molecules, located in the proximity of the catalytic Asp32 and Asp228 residues, and in both cases similar docking predictions were obtained. The similarity of outcomes, for displaceable water molecules, occurred often with most biological targets.¹³⁴ As general advice, the use of more than one docking software can be advantageous in achieving a good prediction of potency, and verifying predicted ligand binding poses through X-ray and H^1 NMR could be a good source of information to assess the quality of docking.

Despite the discussed limitations of the investigated approach, a novel lead molecule with μM potency against BACE-1, compound **99**, has been successfully identified. The importance of the dimethyl isoxazole groups for the compound activity is an interesting factor, which has not yet been acknowledged in the literature. Moreover the approach opens a new pathway towards ligand identification, which differs from the currently used approach of fragment based-drug design or high throughput screening.

Chapter 5. Experimental

5.1 General experimental

All non-aqueous reactions were performed under an atmosphere of nitrogen unless otherwise stated. Water sensitive reactions were performed in oven dried glassware, cooled under nitrogen before use, or flame dried, and cooled under vacuum if stated. Solvents were removed under reduced pressure using a Büchi rotary evaporator and a Vacuubrand PC2001 Vario diaphragm pump, or a Genevac HT-4 evaporation system.

Tetrahydrofuran, dichloromethane, toluene, ethanol and acetonitrile were dried and purified by means of a PureSolv MD solvent purification system (Innovative Technology Inc.). Anhydrous *N,N*-dimethylformamide and 1,4-dioxane was obtained in Oxford sure/seal™ bottles from Sigma–Aldrich. All other solvents used were of chromatography or analytical grade. Ether refers to diethyl ether and petrol refers to petroleum spirit (b.p. 40-60 °C). Commercially available starting materials were obtained from Sigma–Aldrich, Fluka, Lancaster, Alfa Aesar or Acros Organics and used without further purification unless stated.

Thin layer chromatography was carried out on aluminium backed silica (Merck silica gel 60 F254) plates supplied by Merck. Visualisation of the plates was achieved using an ultraviolet lamp ($\lambda_{\text{max}} = 254 \text{ nm}$), KMnO_4 , anisaldehyde or ninhydrin. Flash column chromatography was carried out using silica (35-70 μm particles)¹³⁵ with crude reaction mixtures loaded in dichloromethane (CH_2Cl_2) or the initial solvent system, or pre-absorbed onto silica. Where specified, flash column chromatography was carried using Isolera flash purification system of Biotage SNAP cartridge Kp-Sil instrument (Isolera four, version 1.3.3). SNAP cartridge columns of 25 g were used for 1.0-1.5 g of crude and SNAP cartridge column 50 g for 3-4 g of crude.

Mass-directed HPLC purifications were run on an Agilent 1260 Infinity Preparative HPLC system equipped with a Waters XBridge™ Prep C18 19 × 100 mm column, 5 μm particle size, on an acetonitrile or methanol/water gradient (5-95% acetonitrile or methanol over 8 minutes) and an Agilent 6120 Quadrupole system equipped with a quadrupole MS detector, using electrospray (ES) ionisation. Semipreparative HPLC

purifications were run on a Gynkotec system equipped with a Phenomenex® Hyperclone ODS-C18 250 × 10 mm column, 5 μm particle size, on an acetonitrile/water gradient (5-95% acetonitrile, 0.1% TFA, over 30 minutes).

All optical rotations were carried out at room temperature on a Perkin-Elmer AA-1000 with a path length of 1 dm; concentrations are g/100 mL, the optical rotations are given in 10^{-1} deg cm² g⁻¹ and units are omitted for clarity. Infrared spectra were recorded on a Perkin-Elmer One FT-IR spectrometer, the wavenumbers (ν_{\max}) are given in cm⁻¹ and units are omitted for clarity.

Proton and carbon NMR data were combined on an Avance 500, Bruker DPX500 and DPX300 spectrometer. All shifts were recorded against an internal standard of tetramethylsilane (TMS). Solvents (CDCl₃, DMSO-*d*₆ and MeOH-*d*₄) used for NMR experiments were obtained from Sigma-Aldrich. Splitting patterns in this report have been recorded in an abbreviated manner; app. (apparent), s (singlet), d (doublet), t (triplet), q (quartet), m (multiplet). NMR data was recorded in the following format; ppm (*number of protons, splitting pattern, coupling constant (Hz), proton ID*). Signal assignments were made with the aid of COSY, DEPT 90 and 135, HMQC and HMBC. NMR spectra were recorded at 300 K, unless stated.

Low resolution mass spectra data were recorded on a system comprising an Aligent 1200 series LC system comprising and a Bruker HCT Ultra ion trap mass spectrometer using electrospray (ES) ionisation. The system used two solvent systems; MeCN/H₂O + 0.1% formic acid with a Phenomenex Luna C18 50 × 2 mm 5 micron column or MeCN/H₂O with a Phenomenex Luna C18 50 × 2 mm 5 micron column.

Nominal and accurate mass spectrometry was routinely performed by Mrs Tanya Marinko-Covell on a Waters-Micromass GCT spectrometer using electron impact (EI) or on a Bruker Daltronics micrOTOF using ES ionisation. Accurate mass spectrometry was also carried out using ES ionization with a Bruker Maxis Impact spectrometer. For each compound, data of the most abundant isotope are reported.

In the experimental procedures for compounds, Session 5.3, novel compounds are indicated in italics according to the handbook for postgraduate research students of the University of Leeds. References of the preparation are indicated after the name of the compounds.

5.2 General experimental procedure

A. General procedure for the preparation of the chiral phosphoramidites (*S,S* a*S*)-**51** and (*R,R* a*R*)-**52**.¹¹³

Triethylamine (4.0 mL, 28.0 mmol) was added slowly to a solution of phosphorus trichloride (0.6 mL, 7.0 mmol) in CH₂Cl₂ (15 mL) at 0 °C, then a solution of the relevant amine (bis[*(R)*-1-phenethyl]amine or bis[*(S)*-1-phenethyl]amine) (1.6 mL, 7.0 mmol) in CH₂Cl₂ (25 mL) was added by dropping funnel over 1 h at 0 °C. The reaction mixture was allowed to warm to r.t. and stirred for 18 h, then a solution of the relevant naphthol [*(R)*-BINOL or *(S)*-BINOL] (2.0 g, 7.0 mmol) in CH₂Cl₂ (25 mL) was added followed by triethylamine (3.0 mL, 21.6 mmol) by dropping funnel over 1 h at 0 °C. The reaction mixture was allowed to warm to r.t., stirred for 5 h and quenched with cold water (30 mL) at 0 °C. The phases were separated, the aqueous phase was extracted with CH₂Cl₂ (3 × 25 mL), the combined organic phases were dried (MgSO₄) and concentrated under reduced pressure to give a crude product.

B. General procedure for the preparation of the ureas **42**, **45**, **54**, **71**, **85-92** and **123**.¹⁰⁰

The relevant isocyanate (2.0-10 eq.) was added slowly to a solution of the relevant amine (from 0.4 to 15.0 mmol) in CH₂Cl₂ (0.20 M) and the reaction mixture was heated under reflux and stirred. The reaction was monitored by TLC and LC/MS and, when judged complete, the mixture was concentrated under reduced pressure to give a crude product.

C. General procedure for the Pd-catalysed aminoarylation of the *N*-allyl ureas, to give the imidazolidinones **43**, **58**, **60** and **61**.¹⁰⁰

Pd₂(dba)₃ (5 mol%), Xantphos (10 mol%), NaO^tBu (1.8 eq.), 2-bromonaphthalen (1.5-3.0 eq.) were loaded in a flame-dried round bottom flask and the reaction vessel was purged with nitrogen and degassed (four times). The *N*-allylphenyl urea substrate (from 0.2 to 1.35 mmol) and toluene (4.0 mL/mmol of the urea substrate) were added and the resulting mixture was stirred at 110 °C for 2-3 days. The reaction was

monitored by TLC and LC/MS and, when judged complete, the reaction mixture was cooled to r.t. Then a saturated aqueous solution of ammonium chloride (5.0 mL/mmol of the urea substrate) was added and the mixture was extracted with EtOAc (3 × 4.0 mL/mmol of the urea substrate). The combined organic phases were dried (Na₂SO₄) and concentrated under reduced pressure to give a crude product.

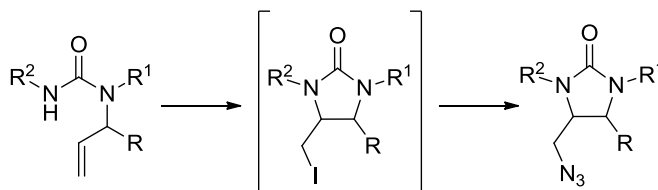
D. General procedure for the preparation of substituted allylic amines 76, 77 and 120.¹²⁶

n-Butyl lithium (1.0 eq.) was added dropwise to a solution of the diphenyl methylene propenamine **78** (from 18.1 to 29.0 mmol) in THF (0.9 M) at –50 °C and the resulting mixture was stirred at –50 °C for 1 h. The relevant electrophile (1.0 eq.) was added portionwise as a solution of THF (6.0 M), the mixture was stirred at –50 °C for 1 h and quenched with EtOH (0.7-1.2 mL). An aqueous solution of KHSO₄ (20% w/v, 1.2 mL/mmol of the propenamine) was added and the mixture was stirred overnight allowing the temperature to warm to r.t. Two phases were formed; the aqueous phase was separated, washed with methyl *tert*-butyl ether (25-35 mL) and CH₂Cl₂ (2 × 25 mL), basified at 0 °C with an aqueous solution of NaOH (50% w/v) until pH 10 then extracted with CH₂Cl₂ (2 × 25 mL). The combined organic phases were washed with brine (2 × 25 mL), dried (Na₂SO₄) and concentrated under reduced pressure to give a crude product.

E. General procedure for the reductive amination of substituted allylic amines, to give compounds 80, 81 and 83.¹³⁶

The relevant aldehyde (1.2-2.4 eq.) was added to a solution of the relevant amine (from 1.2 to 8.0 mmol) in MeOH (0.20 M) and the resulting mixture was stirred at r.t. or heated under reflux for 6-24 h. NaBH₄ (3.0-5.0 eq.) was added at 0 °C and the mixture was stirred at r.t. overnight. The solvent was removed under reduced pressure and the crude material was dissolved in EtOAc (~10-20 ml), washed with H₂O (2 x 10 mL) and brine (2 x 10 mL), dried (MgSO₄) and concentrated under reduced pressure to give a crude product.

F. General procedure for the preparation of the azides 74, 93, 95, 98, 100, 102, 103, 105 and 107^{124,137} from allyl ureas.



The iodo intermediates were prepared from the relevant allyl ureas according to the procedure of Moody *et al.*¹²⁴ Triethylamine or DBU (2.0 eq.) and trimethylsilyltrifluoromethanesulfonate (2.0 eq.) were added to a solution of the relevant allyl urea (0.3-1.5 mmol) in CH₂Cl₂ (0.20 M) and the resulting mixture was stirred for 1 h at r.t., then concentrated under reduced pressure. The crude material was dissolved in THF (0.15 M), I₂ (2.0 eq.) was added and the resulting mixture was stirred at r.t. or heated under reflux overnight. Then the reaction mixture was poured into an aqueous solution of Na₂S₂O₃ (20% w/v) and extracted with EtOAc (3 × 7-20 mL). The combined organic phases were dried (MgSO₄) and concentrated under reduced pressure to give the relevant iodo intermediate as a crude product which was used without further purification.

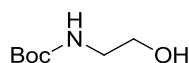
The azide compounds were prepared from the relevant iodo intermediates according to the procedure of Knapp *et al.*¹³⁷ Sodium azide (4.0-6.0 eq.) was added to a solution of the relevant iodo intermediate in DMF (0.1 M) at 0 °C; the resulting mixture was stirred under reflux overnight, allowed to cool at r.t., poured in EtOAc (7-20 mL) and washed with H₂O (3 x 5.0-15 mL) and brine (2 x 5-15 mL). The organic phase was dried (MgSO₄) and concentrated under reduced pressure to give a crude product.

G. General procedure for the reduction of azides, to give the amines 75, 94, 97, 99, 101, 104, 106 and 115.¹³⁸

Trimethylphosphine or triphenylphosphine (1.5 eq.) was added to a solution of the relevant azide in THF (0.1 M), H₂O was added (1/10 of THF volume) and the resulting mixture was stirred under reflux for 2-3 days; then concentrated under reduced pressure to give a crude product.

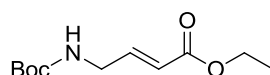
5.3 Experimental procedures for compounds

tert*-Butyl(2-hydroxyethyl)carbamate **47*¹³⁹



The title compound was prepared according to the general method of Jia *et al.*¹³⁹ Di-*tert*-butyl dicarbonate (14.5 g, 66.4 mmol) was added slowly at 0 °C to ethanolamine (4.0 mL, 66.4 mmol) and the resulting mixture was stirred at r.t. for 1 h. Water (40 mL) and EtOAc (40 mL) were added to the reaction mixture and the phases were separated. The aqueous phase was extracted with EtOAc (3 × 20 mL) and the combined organic phases were washed with brine (20 mL), dried (MgSO₄) and concentrated under reduced pressure to yield the title protected amine **47** as a colourless oil (10.4 g, 97%), which was used without further purification. *R*_F: 0.6 (10:1 CH₂Cl₂-MeOH); *v*_{max}/cm⁻¹ (film) 3358, 2978, 2934, 1693, 1530, 1367, 1280, 1172, 1070, 867; *δ*_H (500 MHz; CDCl₃) 4.96 (1H, br s, NH), 3.70 (2H, q, *J* 4.8, 2-H₂), 3.29 (2H, q, *J* 4.8, 1-H₂), 2.47 (1H, br s, OH), 1.45 (9H, s, ^{*t*}Bu); *δ*_C (75 MHz, CDCl₃) *δ* 157.2 (CONH), 79.9 (C(^{*t*}Bu)), 62.9 (C-2), 43.4 (C-1), 28.5 (^{*t*}Bu); *m/z* (ES) 184.1 (100%, [M+Na]⁺). Characterisation data were consistent with those reported in literature.¹³⁹

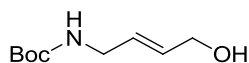
(*E*)- Ethyl 4-(*tert*-butoxycarbonylamino)but-2-enoate **48**¹⁴⁰



The title compound was prepared according to the general method of Crisóstomo *et al.*¹⁴⁰ Dimethyl sulfoxide (26.0 mL), triethylamine (26.5 mL) and (ethoxycarbonylmethylene) triphenylphosphorane (22.0 g, 63.2 mmol) were added to a solution of the carbamate **47** (5.1 g, 31.6 mmol) in CH₂Cl₂ (210 mL). The reaction mixture was stirred until all reactants were solubilised, SO₃·Py complex (15.1 g, 91.8 mmol) was added at 0 °C and the reaction mixture was stirred at r.t. for 36 h. An aqueous solution of HCl (1.00 M) was added until pH ~ 2 and the phases were separated. The aqueous phase was extracted with CH₂Cl₂ (3 × 30 mL) and the combined organic phases were washed with saturated solution of brine (3 × 50 mL), dried

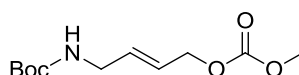
(MgSO₄) and concentrated under reduced pressure. The crude product was purified by chromatographic column (80:20 petrol–EtOAc), to give the unsaturated ester **48** (1.10 g, 56%; *E:Z* >98:< 2) as pale yellow oil. *R*_F: 0.6 (60:40 petrol–EtOAc); $\nu_{\max}/\text{cm}^{-1}$ (film) 3361, 2980, 2933, 1721, 1662, 1523, 1367, 1174, 1042, 867; δ_{H} (500 MHz; CDCl₃) 6.88 (1H, dt, *J* 15.7 and 6.1, 3-H), 5.91 (1H, d, *J* 15.7, 2-H), 4.65 (1H, br. s, NH), 4.19 (2H, q, *J* 7.1, ethyl 1-H₂), 3.92 (2H, app. br s, 4-H₂), 1.45 (9H, s, ^tBu), 1.28 (3H, t, *J* 7.1, ethyl 2-H₃); δ_{C} (75 MHz; CDCl₃) 166.1 (CO₂Et), 155.5 (CONH), 144.7 (C-3), 121.6 (C-2), 80.0 (C(^tBu)), 60.5 (ethyl C-1), 41.5 (C-4), 24.5 (^tBu), 14.3 (ethyl C-2); *m/z* (ES) 252.1 (100%, [M+Na]⁺). Characterisation data were consistent with those reported in literature.¹⁴⁰

(*E*)-tert-Butyl(4-hydroxybut-2-en-1-yl)carbamate **49**¹¹¹



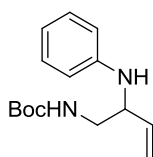
The title compound was prepared according to the general method of Moriwake *et al.*¹¹¹ The unsaturated ester **48** (3.1 g, 13.6 mmol) was dissolved in dry CH₂Cl₂ (31 mL) at –78 °C and trifluoride etherate (1.9 mL, 4.1 mmol) was added. The reaction mixture was stirred at –78 °C for 30 min, then diisobutylaluminium hydride in hexane (41 mL, 41.0 mmol, 1.0 M) was added slowly and the reaction mixture was stirred at –78 °C for 90 min. The reaction mixture was quenched with an aqueous saturated solution of NH₄Cl (30 mL) and filtered on Celite[®] eluting with EtOAc. The phases were separated, the aqueous phase was extracted with EtOAc (3 x 7.0 mL), the combined organic phases were washed with brine (3 x 7.0 mL), dried (MgSO₄) and concentrated under reduced pressure to give a crude product which was purified by column chromatography (50:50 petrol–EtOAc) to yield the alcohol **49** as a yellow oil (0.98 g, 38%). *R*_F: 0.5 (30:70 petrol–EtOAc); $\nu_{\max}/\text{cm}^{-1}$ (film) 3350, 2978, 2930, 1693, 1526, 1366, 1252, 1171, 970; δ_{H} (500 MHz; CDCl₃) 5.78 (1H, dt, *J* 15.7 and 5.0, 2-H), 5.72 (1H, dt, *J* 15.7 and 5.1, 3-H), 4.59 (1H, br s, NH), 4.13 (2H, d, *J* 5.1, 4-H₂), 3.75 (2H, app.br.s, 1-H₂), 1.44 (9H, s, ^tBu); δ_{C} (75 MHz; CDCl₃) 155.9 (CONH), 130.8 (C-2), 129.0 (C-3), 79.6.1 (C(^tBu)), 63.1 (C-4), 42.0 (C-1), 28.7 (^tBu); *m/z* (ES) 210.1 (100%, [M+Na]⁺). Characterisation data were consistent with those reported in literature.¹¹¹

(E)-tert-Butyl(4-methoxycarbonyloxy)but-2-en-1-yl)carbamate 46¹⁴¹



The title compound was prepared according to the general method of Gramm *et al.*¹⁴¹ Methyl chloroformate (0.55 mL, 7.2 mmol) and pyridine (0.58 mL, 7.2 mmol) were added and to a solution of the alcohol **49** (1.0 g, 5.55 mmol) in CH₂Cl₂ (14 mL) at 0 °C. The reaction mixture was stirred for 1 h at 0 °C, allowed to warm up to r.t. and stirred overnight. An aqueous solution of NH₄Cl (1.0 M, 10 mL) was added, the phases were separated, the aqueous phase was extracted with CH₂Cl₂ (3 × 3.0 mL). The combined organic phases were dried (MgSO₄) and concentrated under reduced pressure to give a yellow oil that was purified by flash chromatography (99:1 CH₂Cl₂–MeOH) to give the carbamate **46** as a pale yellow oil (0.88 g, 65%). *R*_F: 0.6 (97:3 CH₂Cl₂–MeOH); *v*_{max}/cm⁻¹ (film) 3351, 1750, 1696, 1236, 1168, 944, 792; δ_H (500 MHz; CDCl₃) 5.82 (1H, dt, *J* 15.3 and 4.8, 2-H), 5.72 (1H, dt, *J* 15.3 and 5.9, 3-H), 4.60 (2H, dd, *J* 5.9 and 0.7, 4-H₂), 4.56 (1H, br.s, NH), 3.78 (3H, s, OMe), 3.56 (2H, app.br.s, 1-H₂), 1.44 (9H, s, ^tBu); δ_C (75 MHz; CDCl₃) 156.1 (CO₂Me), 155.6 (CONH), 132.5 (C-2), 124.9 (C-3), 84.5 (C(^tBu)), 67.7 (C-4), 54.9 (OCH₃), 41.5 (C-1), 28.5 (^tBu); *m/z* (ES) 268.1 (100%, [M+Na]⁺). Characterisation data were consistent with those reported in literature.¹⁴¹

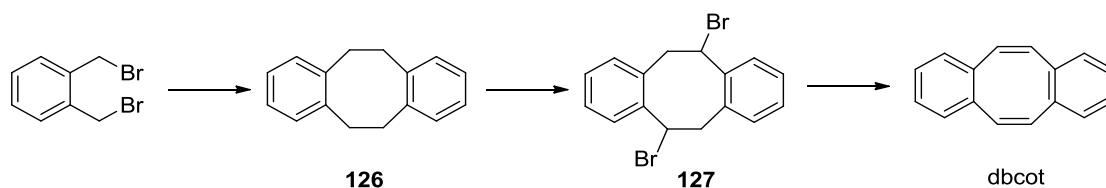
tert-Butyl 2-(phenylamino)but-3-enylcarbamate 50¹¹⁵



THF (2.5 mL) and *n*-butyl amine (4.8 μL, 50 μmol) were added to the [Ir(dbcot)Cl]₂ complex (20.4 mg, 25 μmol), phosphoramidites *S,S aS-51* (13.1 mg, 25 μmol) and *R,R aR-52* (13.1 mg, 25 μmol). The reaction mixture was stirred at 50 °C for 45 minutes, then the allyl carbonate **46** (0.30 g, 1.2 mmol) and aniline (167 μL, 1.8 mmol) were added and the resulting mixture was stirred at 55°C for 18 h. The solvent was removed under reduced pressure and the crude product was purified by flash

chromatography (80:20 petrol–EtOAc) to give *the title allyl phenylamine 50* as a colourless amorphous solid (0.22 g, 69%). R_F : 0.7 (66:33 petrol–EtOAc); $\nu_{\max}/\text{cm}^{-1}$ (film) 3388, 3321, 1667, 1603, 1517, 1498, 1165, 919; δ_{H} (500 MHz; CDCl_3) 7.15 (2H, dd, J 8.5 and 7.3, phenyl 3- and 5-H), 6.70 (1H, app. t, J 7.3, phenyl 4-H), 6.61 (2H, dd, J 8.5 and 0.9, phenyl 2- and 6-H), 5.77 (1H, ddd, J 17.2, 10.5 and 5.3, 3-H), 5.31 (1H, d, J 17.2, 4- H_A), 5.22 (1H, d, J 10.5, 4- H_B), 4.80 (1H, s, NH^tBu), 4.18 (1H, s, NHPh), 3.95 (1H, app. dt, J 7.7 and 5.3, 2-H), 3.40–3.22 (1H, m, 1- H_A), 3.29 (1H, ddd, J 13.8, 7.7 and 6.1, 1- H_B), 1.45 (9H, s, ^tBu); δ_{C} (75 MHz; CDCl_3) 157.7 (CONH), 137.2 (phenyl C-1), 129.4 (phenyl C-3-and C-5), 117.7 (phenyl C-4), 117.1 (C-3), 117.0 (C-4), 113.5 (phenyl C-2 and C-6), 79.9 (C(^tBu)), 57.3 (C-2), 45.1 (C-1), 28.5 (^tBu); m/z (ES) 263.17 (100%, $[\text{M}+\text{H}]^+$), HRMS Found: 263.1743 ($\text{C}_{15}\text{H}_{22}\text{N}_2\text{O}_2$, requires $[\text{M}+\text{H}]$ 263.1754).

Dibenzo[a,e]cyclooctatetraene (dbcot)¹⁴²



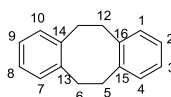
The title compound was prepared from α,α' -dibromo-*o*-xylene according to the general method of Wuld *et al.*¹⁴² Under an atmosphere of argon, lithium (granular dry, high in sodium) (0.79 g, 113.5 mmol) was added to THF (24 mL). α,α' -dibromo-*o*-xylene (5.0 g, 18.4 mmol) was dissolved in THF (7.5 mL) by sonication and added portionwise to the lithium solution at 0 °C, to give a grey suspension that was allowed to warm to r.t. and then sonicated for 3 h. The solution was separated from the residual lithium *via* syringe and the solvent removed under reduced pressure to give a pale yellow oil that was dissolved in EtOAc. Florisil (17.7 g) was added, the solvent was removed under reduced pressure and the resulting mixture was purified eluting through a silica plug (95:5 cyclohexane–EtOAc) to give the 5, 6, 11, 12-tetrahydrodibenzo[a,e]cyclooctadiene **126**, (1.54 g, 40%) as a colourless amorphous solid. R_F : 0.6 (80:20 cyclohexane–ether); $\nu_{\max}/\text{cm}^{-1}$ (film) 3060, 3015, 2933, 2869, 2246, 1490, 1450, 1159, 1047; 909; 720; 690; δ_{H} (500 MHz; CDCl_3) 7.27–7.24 (8H, m, Ar

CH), 7.01-6.97, 3.06 (8H, s, 4 x CH₂); δ_C (75 MHz; CDCl₃)^c 140.2 (C-13, C-14, C-15- and C-16), 129.8 (C-2, C-3, C-8 and C-9), 126.2 (C-1, C-4, C-7 and C-8), 35.4 (C-5, C-6, C-11- and C-12); m/z (EI) 208.1 (100%, [M+H]⁺). Characterisation data were consistent with those reported in literature.¹⁴²

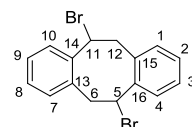
N-Bromosuccinimide (2.96 g, 14.9 mmol), recrystallised (water), was added to a solution of **126** (1.54 mg, 7.4 mmol) in CCl₄ (52 mL) and the resulting mixture was stirred at 90 °C for 24 h under air. The reaction was allowed to reach r.t. and filtered; the solvent was removed under reduced pressure and the crude material was washed with water and sonicated. The water removed by azeotropical drying with toluene to give 5, 11-dibromo-5, 6, 11, 12-tetrahydrodibenzo[a,e]cyclooctene **127**, as an orange amorphous solid (2.4 g, 85%). R_F = 0.5 (80:20 cyclohexane–ether); $\nu_{\max}/\text{cm}^{-1}$ (film) 3063, 2928, 1715, 1601, 1489, 1450, 1146, 908; δ_H (500 MHz; CDCl₃) 7.22-6.84 (8H, m, 8 x Ar CH), 5.34 (2H, dd, J 11.2 and 8.5, CHBr), 4.30 (2H, dd, J 14.2 and 11.3, CH_AH_B), 3.66 (2H, dd, J 14.3 and 8.5, CH_AH_B); δ_C (75 MHz; CDCl₃)^d 138.4 (C-13 and C-16), 136.4 (C-14 and C-15), 130.9 (C-4 and C-10), 130.8 (C-1 and C-7), 129.1 (C-3 and C-9), 127.9 (C-2 and C-8), 52.9 (C-5 and C-11), 43.7 (C-6 and C-12); m/z (EI) 285.0 (30%, [M–Br]⁺), 79.9 (30%, [Br]⁺). Characterisation data were consistent with those reported in literature.¹⁴²

A solution of the dibromide **127** (2.4 g, 6.8 mmol) in THF (67 mL) was added at 0 °C to a suspension of ^tBuOK (12.2 g, 109.3 mmol) in THF (150 mL). The reaction mixture was allowed to warm to r.t., stirred for 18 h and quenched with water (50 mL) at 0 °C. The phases were separated, the aqueous phase was extracted with chloroform (3 × 35 mL), the combined organic phases were dried (MgSO₄) and concentrated under reduced pressure to give a brown solid that was re-dissolved in CHCl₃. Florisil (7.0 g) was added, the solvent was removed under reduced pressure and the crude product was purified by flash chromatography with Biotage instrument (gradient elution petrol–

^c Numbering according to the literature:

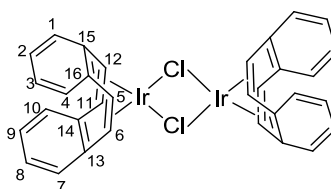


^d Numbering according to the literature:



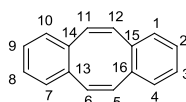
EtOAc 100:0 → 95:5 in 10 column volumes) to give the dbcot as a colourless needle solid (0.34 g, 25%). R_F : 0.3 (petrol–Et₂O); m.p. 107-109 [lit. 109 °C]; $\nu_{\max}/\text{cm}^{-1}$ (film) 3047, 3008, 1950, 1922, 1476, 1446, 1208, 1093, 1041, 976; δ_{H} (500 MHz; CDCl₃) 7.17 (4H, dd, J 5.7 and 3.4, 1-, 4-, 7- and 10-H), 7.07 (4H, dd, J 5.6 and 3.4, 2-, 3-, 8- and 9-H), 6.77 (4H, s, 5-, 6-, 11- and 12-H)^e; δ_{C} (75 MHz; CDCl₃) 137.2 (C-13, C-14, C-15 and C-16), 133.4 (C-5, C-6, C-11 and C-12), 129.3 (C-2, C-3, C-8 and C-9), 126.9 (C-1, C-4, C-7 and C-10); m/z (EI) 204.1 (100%, [M+H]⁺). HRMS Found: 204.0939 (C₁₆H₁₂, M+H requires 204.0950. Characterisation data were consistent with those reported in literature.¹⁴²

Chloro(dibenzo[a,e]cyclooctatetraene)iridium(I)dimer, [Ir(dbcot)Cl₂]¹¹²

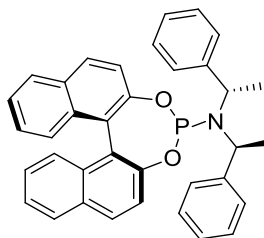


The title compound was prepared according to the general method of Crabtree *et al.*¹¹² A solution of the dbcot (118 mg, 0.57 mmol) in CH₂Cl₂ (4.5 mL) was added by dropping funnel to solution of the [Ir(cod)Cl]₂ complex in CH₂Cl₂ (3.5 mL) and stirred for 20 minutes. The reaction mixture changed from red to yellow colour, the solvent was reduced to *ca.* 3.0 mL under flow of N₂ and cyclohexane (8.0 mL) was added slowly. The precipitated was filtered and dried under reduced pressure to give the Iridium complex [Ir(dbcot)Cl₂] as a yellow amorphous solid (136 mg, 28%). $\nu_{\max}/\text{cm}^{-1}$ (film) 3066, 3020, 2978, 1488, 1462, 1384, 1218, 1003, 916, 829, 747; δ_{H} (500 MHz; CDCl₃) 6.99 (4H, dd, J 5.6 and 3.3, 1-, 4-, 7- and 10-H), 6.85 (4H, dd, J 5.7 and 3.2, 2-, 3-, 8- and 9-H), 5.32 (8H, s, 5-, 6-, 11- and 12-H); δ_{C} (75 MHz; CDCl₃) 145.8 (C-5, C-6, C-11 and C-12), 126.8 (C-2, C-3, C-8 and C-9), 126.2 (C-1, C-4, C-7 and C-10), 63.9 (C-13, C-14, C-15 and C-16); m/z (EI) 864.0 (100%, [M+H]⁺). Characterisation data were consistent with those reported in literature.¹¹²

^e Numbering according to the literature:

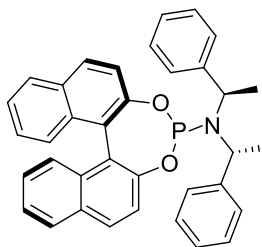


(*S,S* a*S*)-*O,O'*-[1,1'-binaphthyl-2,2'-diyl-*N,N'*-bis[1-phenethyl]phosphoramidite
51^{113,144}



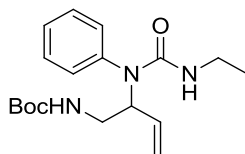
The title compound **51** was prepared in 75% yield according to the general method of Mikhel *et al.*¹¹³ described in **general procedure A**. The crude product was purified by flash chromatography (95:5 petrol–EtOAc) to give a colourless needle solid. R_F : 0.7 (80:20, petrol–EtOAc); m.p. 85–87 °C [lit. 88–89 °C¹⁴⁵]; $[\alpha]_D^{25}$: +16.5° (c. 1, CHCl₃) [lit. $[\alpha]_D^{22}$ +202 (c.0.79, CHCl₃)¹⁴⁶]; $\nu_{\max}/\text{cm}^{-1}$ (film) 3059, 2970, 1591, 1463, 1373, 1327, 1230, 1070, 946, 817; δ_H (500 MHz; CDCl₃) 8.00 (1H, d, J 8.8 Ar CH), 7.92 (1H, dd, J 8.8 Ar CH), 7.81 (1H, d, J 8.4 and 1.2 Ar CH), 7.73 (1H, dd, J 8.7 Ar CH), 7.57 (1H, d, J 8.7 and 0.9 Ar CH), 7.44–7.32 (4H, m, Ar CH), 7.30–7.15 (13H, m, Ar CH), 4.42 (2H, dq, J 11.0 and 7.0 NCH), 1.68 (6H, d, J 7.1, CH₃); δ_C (75 MHz; CDCl₃) 150.9, 150.8 (Ar C), 150.1, 143.5 (Ar CH), 133.3 (2 x Ar C), 133.2 (2 x Ar C), 131.8, 130.8, 130.7, 130.0, 128.7, 128.5 (Ar CH), 128.4 (2 x Ar CH), 128.1 (2 x Ar CH), 127.7, 127.5 (Ar CH), 127.1 (Ar CH), 126.5, 126.3, 125.2, 124.7, 122.9 (Ar CH), 122.8, 122.7 (Ar CH), 121.6, 121.5 (Ar C), 55.0, 54.9 (NCH), 23.5, 23.3 (CH₃); 2 X Ar C not observed; m/z (ES) 540.21 (100%, [M+H]⁺). HRMS Found: 540.2087 (C₃₆H₃₀NO₂P M+H requires 540.2085). Characterisation data were consistent with those reported in literature.¹⁴⁴

(*R,R aR*)-*O,O'*-[1,1'-binaphthyl-2,2'-diyl-*N,N'*-bis[1-phenethyl]phosphoramidite,
52¹¹³



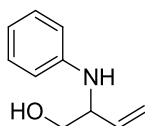
The title compound **52** was prepared in 57% yield according to the general method of Mikhel *et al.*¹¹³ described in **general procedure A**. The crude product was purified by flash chromatography with Biotage instrument (gradient elution petrol–EtOAc 100:0 in 2 column volumes → 80:20 in 6 column volumes, dry loading of crude in 7.0 g of Florisil, loaded in 50 g SNAP cartridge column) to give a colourless needle solid. R_F : 0.7 (80:20, petrol–EtOAc); m.p. 84–86 °C [lit. 88–89 °C¹⁴⁵]; $[\alpha]_D^{25}$: -13.1° (c 1.0, CHCl₃); $\nu_{\max}/\text{cm}^{-1}$ (film) 3058, 2969, 1590, 1463, 1327, 1230, 1117, 1070, 948; δ_H (500 MHz; CDCl₃) 8.00 (1H, d, J 8.8, Ar CH), 7.92 (1H, d, J 8.2, Ar CH), 7.81 (1H, dd, J 8.4 and 0.4, Ar CH), 7.73 (1H, d, J 8.8, Ar CH), 7.58–7.56 (1H, m, Ar CH), 7.44–7.31 (4H, m, Ar CH), 7.29–7.13 (13H, m, Ar CH), 4.42 (2H, dq, J 10.8 and 7.0, NCH), 1.69 (6H, d, J 7.1, CH₃); δ_C (75 MHz; CDCl₃) 151.2, 151.1 (Ar C), 150.4, 143.7 (Ar CH), 133.6, 133.5 (Ar C), 133.4 (2 x Ar C), 132.0, 131.1, 131.0, 130.2, 128.9, 128.8, 128.7, 128.6 (Ar CH), 128.4 (2 x Ar CH), 127.9, 127.8, 127.3, 126.7, 126.5, 125.4, 125.0 (Ar CH), 124.9, 124.8 (Ar C), 123.2, 123.1, 123.0 (Ar CH), 121.9, 121.8 (Ar C), 55.2, 55.1 (NCH), 23.7, 23.6 (CH₃); m/z (ES) 540.21 (100%, [M+H]⁺). HRMS Found: 540.2087 (C₃₆H₃₀NO₂P M+H requires 540.2089). Characterisation data were consistent with those reported in literature.¹¹³

***tert*-Butyl 2-(3-ethyl-1-phenylureido)but-3-enylcarbamate 45¹⁰⁰**



The *title compound* **45** was prepared from allyl amine **50** (0.26 g, 1.0 mmol) and ethylisocyanate (0.6 mL, 5.0 mmol) in CH₂Cl₂ at 35 °C, according to **general procedure B**.¹⁰⁰ The crude product was purified by flash chromatography (petrol–EtOAc 66:33) to give a pale amorphous solid (58% yield). *R*_F: 0.2 (66:33, petrol–EtOAc); *v*_{max}/cm⁻¹ (film) 3344, 2975, 2930, 1710, 1650, 1514, 1274, 1173, 927, 709; δ_{H} (500 MHz; CDCl₃) 7.41 (2H, app. t, *J* 7.4, phenyl 2- and 6-H), 7.36 (1H, app.t, *J* 7.4 phenyl 4-H), 7.18 (2H, d, *J* 7.4 phenyl 3- and 5-H), 5.71 (1H, ddd, *J* 17.4, 10.2 and 7.5, 3-H), 5.17 (1H, dt, *J* 17.4 and 1.1, 4-H_A) 5.13 (d, *J* 10.2, 4-H_B), 5.00 (1H, app.tdd, *J* 7.5, 6.8 and 0.5, 2-H), 4.02 (1H, br. s, *NHEt*), 3.50-3.38 (1H, m, 1-H_A), 3.34-3.10 (3H, m, 1-H_B and ethyl 1-H₂), 1.43 (9H, s, ^{*t*}Bu), 1.01 (3H, t, *J* 7.19, ethyl 2-H₃); δ_{C} (75 MHz; CDCl₃) 162.2 (NCONH) 157.9 (COOtBu), 137.7 (phenyl C-1), 135.6 (C-3), 130.9 (phenyl C-2 and C-6), 130.3 (phenyl C-3 and C-5), 128.8 (phenyl C-4), 118.6 (C-4), 80.2 (C(^{*t*}Bu)₃), 58.8 (C-2), 43.5 (ethyl C-1), 35.9 (C-1), 28.8 (^{*t*}Bu), 15.9 (ethyl C-2); *m/z* (ES) 356.19 (100%, MNa⁺); HRMS Found: 356.1945 (C₁₈H₂₇N₃O₃ M+Na requires 356.1951).

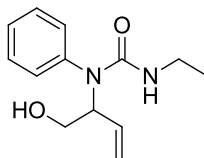
2-(Phenylamino)but-3-en-1-ol 53¹²³



Vinylboronic acid pinacol ester (3.3 mL, 20.0 mmol) was added to a solution of glycoaldehyde dimer (1.20 g, 10.0 mmol) in water (100 mL) and the resulting mixture was stirred at 50 °C for 45 minutes, then allowed to warm to 30 °C. A solution of aniline (1.8 mL, 20.0 mmol) in THF (25 mL) was added and the resulting mixture was stirred for 4 days at 30 °C. An aqueous solution of HCl (1.0 M) was added until pH 1 and the mixture was extracted with CH₂Cl₂ (3 × 50 mL); then the combined aqueous phases were basified with an aqueous solution of NaOH (2.0 M) until pH 12 and extracted with

CH₂Cl₂ (3 × 100 mL). The combined organic phases were dried (Na₂SO₄) and concentrated under reduced pressure to give a crude product which was purified by flash chromatography (petrol–EtOAc 60:20) to give *the title compound 53* as a yellow oil (1.5 g, 45%). *R*_F: 0.6 (20:80, petrol–EtOAc; $\nu_{\max}/\text{cm}^{-1}$ (film); 3392, 2933, 1602, 1504, 1317, 1031, 926, 751; δ_{H} (500 MHz; CDCl₃) 7.17 (2H, dd, *J* 8.5 and 7.3, phenyl 2- and 6-H), 6.74 (1H, dd, *J* 7.3 and 0.9, phenyl 4-H), 6.67 (2H, dd, *J* 8.5 and 0.9, phenyl 3- and 5-H), 5.81 (1H, ddd, *J* 17.3, 10.4 and 5.4, 4-H), 5.32 (1H, d, *J* 17.3, 3-H_A), 5.25 (1H, d, *J* 10.4, 3-H_B), 4.04 (1H, app. q, *J* 6.0, 2-H), 3.95 (1H, br. s, *NH*), 3.8 (1H, dt, *J* 6.9, 5.5, 1-H_A), 3.67-3.61 (1H, m, 1-H_B), 1.80-1.77 (1H, m, *OH*); δ_{C} (125 MHz; CDCl₃) 147.3 (phenyl C-1), 136.3 (C-3), 129.2 (phenyl C-2 and C-6), 118.1 (phenyl C-4), 117.4 (C-4), 113.9 (phenyl C-3 and C-5), 64.9 (C-1), 57.6 (C-2); *m/z* (ES) 146.1 (100%, fragment [C₁₀H₁₁NH]⁺); HRMS Found: 164.1082 (C₁₀H₁₃NO requires *M*+*H* 164.107).

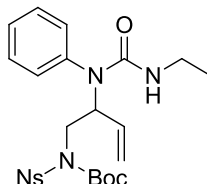
3-Ethyl-1-(1-hydroxybut-3-en-2-yl)-1-phenylurea **54**²



Ethylisocyanate (1.0 mL, 12.8 mmol) was added at 0 °C to a solution allyl amine **53** (1.0 g, 6.4 mmol) in CH₂Cl₂ (27 mL) and the resulting mixture was stirred at 0 °C for 2 hours, then allowed to warm to r.t. and stirred overnight. Another equivalent of the ethylisocyanate was added to the reaction and the resulting mixture was stirred at r.t. for 2 days. The solvent was removed under reduced pressure to give a crude product which was purified by flash chromatography (petrol–EtOAc 60:40) to give the *title compound 54* as a yellow oil (1.2 g, 80%). *R*_F: 0.4 (50:50, petrol–EtOAc); $\nu_{\max}/\text{cm}^{-1}$ (film) 3440, 3368, 2972, 2932, 1643, 1595, 1515, 1282, 1065, 711; δ_{H} (500 MHz; CDCl₃) 7.45-7.43 (2H, m, phenyl 2- and 6-H), 7.40-7.36 (1H, m, phenyl 4-H), 7.26-7.23 (2H, m, phenyl 3- and 5-H), 5.75 (1H, ddd, *J* 17.4, 10.4 and 7.4, 3-H), 5.20 (1H, dt, *J* 17.4 and 1.3, 4-H_A), 5.19-5.18 (1H, m, 4-H_B), 4.83 (1H, ddd, *J* 8.5, 7.4 and 4.1, 2-H), 4.07 (1H, br. s, *NH*), 3.84 (1H, ddd, *J* 11.5, 4.1 and 3.9, 1-H_A), 3.74-3.67 (1H, m, 1-H_B), 3.57 (1H, dd, *J* 8.8 and 3.3, *OH*), 3.19 (2H, dq, *J* 7.2 and 5.6, ethyl 1-H₂), 1.01 (3H, t, *J* 7.2, ethyl 2-H₃); δ_{C} (125 MHz; CDCl₃) 158.4 (*CO*), 139.8 (phenyl C-1), 134.2 (C-3), 130.1 (phenyl C-2

and C-6), 129.9 (phenyl C-3 and C-5), 128.4 (phenyl C-4), 118.2 (C-4), 64.8 (C-1), 62.8 (C-2), 35.6 (ethyl C-1), 15.4 (ethyl C-2); m/z (ES) 257.0 (100%, $[M+Na]^+$); HRMS Found: 257.1268 ($C_{13}H_{18}N_2O$ requires $M+Na$ 257.1260).

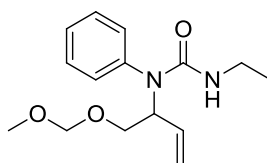
***tert*-Butyl 2-(3-ethyl-1-phenylureido)but-3-enyl(2-nitrophenylsulfonyl)carbamate**
55¹⁴⁷



tert-Butyl 2-nitrophenylsulfonylcarbamate (0.31 g, 1.0 mmol) was added to a solution of the phenyl urea **54** (0.20 g, 0.85 mmol) in THF (8.5 mL) at 0 °C, followed by triphenylphosphine (0.33 g, 1.3 mmol) and by a dropwise addition of diethyl azodicarboxylate (0.2 mL, 1.27 mmol). The resulting mixture was stirred at 0 °C for 3 h then allowed to warm to r.t. and stirred overnight. The reaction mixture was diluted with EtOAc (40 mL), washed with an aqueous solution of HCl (1.0 M) (2 × 15 mL), with a saturated aqueous solution of NaHCO₃ (2 × 15 mL) and brine (2 × 15 mL). The combined organic phases were dried (Na₂SO₄) and concentrated under reduced pressure to give a crude product which was purified by flash chromatography (CH₂Cl₂–MeOH 98.5:1.5) to give the *title compound* **55** as a pale yellow oil (0.2 g, 53%). R_F : 0.55 (98:2, CH₂Cl₂ –MeOH); ν_{max}/cm^{-1} (film) 3508, 3004, 2145, 1704, 1660, 1422, 1367, 1230, 1093, 904; δ_H (500 MHz; CDCl₃) 8.34-8.31 (1H, m, Ns 3-H), 7.74-7.71 (3H, m, Ns 4-, 5- and 6-H), 7.45-7.40 (2H, m, phenyl 2- and 6-H), 7.36-7.34 (1H, m, phenyl 4-H), 7.33-7.31 (2H, m, phenyl 3- and 4-H), 5.99 (1H, ddd, J 17.1, 10.1 and 9.0, 3-H), 5.28 (1H, ddd, J 17.1, 1.4 and 0.9, 4-H_A), 5.22 (1H, dd, J 10.1 and 1.6, 4-H_B), 4.88 (1H, app. m, 2-H), 4.33 (1H, dd, J 14.6 and 7.1, 1-H_A), 4.06 (1H, dd, J 14.6 and 7.4, 1-H_B), 4.02 (1H, t, J 5.2, NH), 3.25-3.16 (2H, app. m, ethyl 1-H₂), 1.37 (9H, s, ^{*t*}Bu), 1.01 (3H, t, J 7.2, ethyl 2-H₃); δ_C (125 MHz; CDCl₃) 156.7 (CO urea), 150.4 (COO^{*t*}Bu), 140.9 (Ns C-2), 140.1 (phenyl C-1), 134.8 (C-3), 133.9 (Ns C-3), 133.8 (Ns C-4 or C-5 or C-6), 133.2 (Ns C-1), 131.7 (Ns C-4 or C-5 or C-6), 130.1 (phenyl C-2 and C-6), 129.9 (phenyl C-3 and C-5), 128.1 (phenyl C-4), 124.3 (Ns C-4 or C-5 or C-6), 119.4 (C-4), 85 (C (^{*t*}Bu)), 61.9 (C-2), 50.2 (C-1), 35.4 (ethyl C-1), 27.8 (^{*t*}Bu), 15.4 (ethyl C-2); m/z

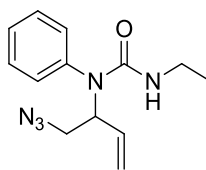
(ES) 541.14 (100% $[M+Na]^+$); HRMS Found: 541.1739 ($C_{24}H_{30}N_4O_7S$ requires $M+Na$ 541.1727).

3-Ethyl-1-[1-(methoxymethoxy)but-3-en-2-yl]-1-phenylurea **56**¹⁴⁸



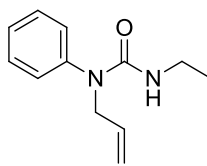
N,N-Diisopropylethylamine (0.11 mL, 0.66 mmol) was added dropwise to a solution of the phenyl urea **54** (0.07 g, 0.33 mmol) in CH_2Cl_2 (2 mL) at 0 °C, followed by portionwise addition of chloromethyl ethyl (50 μ L, 0.66 mmol). The resulting mixture was stirred at 0 °C for 1.5 h, then allowed to warm to r.t. and stirred overnight. The reaction mixture was quenched with brine (2.0 mL) and extracted with CH_2Cl_2 (2 \times 3.0 mL), the combined organic phases were dried (Na_2SO_4) and concentrated under reduced pressure to give a crude product which was purified by flash chromatography (petrol–EtOAc 50:50) to give the *title compound* **56** as a pale yellow oil (40 mg, 41%). R_F : 0.5 (30:70, petrol–EtOAc); ν_{max}/cm^{-1} (film) 3400, 2987, 2212, 1654, 1648, 1508, 1279, 1039, 919, 712; δ_H (500 MHz; $CDCl_3$) 7.42 (2H, app. t, J 7.4, phenyl 2- and 6-H), 7.36 (1H, app. t, J 7.4, phenyl 4-H), 7.25 (2H, d, J 7.2, phenyl 3- and 5-H), 5.79 (1H, ddd, J 17.6, 10.5 and 7.3, 3-H), 5.26–5.16 (3H, m, 4- H_A , 4- H_B , 2-H), 4.67 (1H, d, J 6.6, OCH_AH_BO), 4.59 (1H, d, J 6.6, OCH_AH_BO), 3.96 (1H, br. s, NH), 3.62 (1H, dd, J 10.3 and 6.2, 1- H_A), 3.58 (1H, dd, J 10.3 and 9.1, 1- H_B), 3.35 (3H, s, OCH_3), 3.17 (2H, dq, J 14.5 and 7.0, ethyl 1- H_2), 0.99 (3H, t, J 7.2, ethyl 2- H_3); δ_C (125 MHz; $CDCl_3$) 157.0 (CO), 144.9 (phenyl C-1), 135.3 (C-3), 130.8 (phenyl C-2 and C-6), 129.7 (phenyl C-3 and C-5), 128.3 (phenyl C-4), 117.9 (C-4), 96.4 (OCH_AH_BO), 67.5 (C-1), 57.9 (OCH_3), 53.6 (C-2), 41.8 (ethyl C-1), 18.66 (ethyl C-2); m/z (ES) 301.1 (100%, $[M+Na]^+$); HRMS Found: 301.1532 ($C_{15}H_{22}N_2O_3$ requires $M+Na$ 301.1523).

1-(1'-Azidobut-3'-en-2'-yl)-3-ethyl-1-phenylurea **57**¹⁴⁹



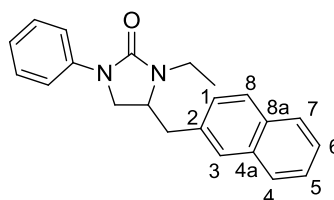
Diphenyl phosphoryl azide (0.7 mL, 3.2 mmol) was added to a solution of the phenyl urea **54** (0.25 g, 1.0 mmol) in toluene (27 mL) followed by DBU 0.5 mL, 3.2 mmol) and the resulting mixture was stirred at 90 °C for 3 days. The solvent was removed under reduced pressure to give a crude material which was partitioned in EtOAc (8.0 mL) and an aqueous solution of HCl (1.0 M, 8.0 mL). The phases were separated and the aqueous phase was extracted with EtOAc (3 x 15 mL), the combined organic phases were washed with water (2 x 15 mL), with a saturated aqueous solution of NaHCO₃ (2 x 15 mL) and brine (15 mL), dried (MgSO₄) and concentrated under reduced pressure. The crude product was purified by flash chromatography (petrol–EtOAc 60:40) to give the *title compound* **57** as an orange oil (0.17 g, 63%). *R*_F: 0.6 (40:60, petrol–EtOAc); *v*_{max}/cm⁻¹ (film) 3368, 2946, 2931, 2878, 1659, 1508, 1494, 1273, 923, 713; *δ*_H (500 MHz; CDCl₃) 7.46-7.42 (2H, m, phenyl 2- and 6-H), 7.40-7.36 (1H, m, phenyl 4-H), 7.26-7.23 (2H, m, phenyl 3- and 5-H), 5.88 (1H, ddd, *J* 17.4, 10.4 and 7.6, 3-H), 5.23 (1H, app. dt, *J* 17.4 and 1.1, 4-H_A), 5.20 (1H, app. dt, *J* 10.4, and 1.1, 4-H_B), 4.91-4.86 (1H, app. m, 2-H), 4.01 (1H, br. s, NH), 3.65 (1H, dd, *J* 12.4 and 8.8, 1-H_A), 3.4 (1H, dd, *J* 12.4 and 6.0, 1-H_B), 3.19 (2H, qdd, *J* 7.2, 5.6 and 1.7, ethyl 1-H₂), 1.01 (3H, t, *J* 7.2, ethyl 2-H₃); *δ*_C (125 MHz; CDCl₃) 156.7 (CO), 139.5 (phenyl C-1), 134.9 (C-3), 130.3 (phenyl C-2 and C-6), 130.0 (phenyl C-3 and C-5), 128.4 (phenyl C-4), 118.6 (C-4), 59.8 (C-2), 52.6 (C-1), 35.5 (ethyl C-1), 15.5 (ethyl C-2); *m/z* (ES) 282.1 (100%, [M+Na]⁺); HRMS Found: 282.1320 (C₁₃H₁₇N₅O requires M+Na 282.1325).

1-Allyl-3-ethyl-1-phenylurea **42**¹⁰⁰



The title compound **42** was prepared according to the general method of Wolfe *et al.*,¹⁰⁰ described in **general procedure B**, from the *N*-allyl-aniline (2.0 g, 15.0 mmol) and ethylisocyanate (6.0 mL, 75.0 mmol) in CH₂Cl₂, stirring for 1 day. The crude product was purified by flash chromatography (petrol–EtOAc 75:25) to give a yellow oil (2.7 g, 88%). *R*_F: 0.2 (66:33, petrol–EtOAc); $\nu_{\text{max}}/\text{cm}^{-1}$ (film) 3445, 3356, 2972, 2873, 1650, 1496, 1271, 1227, 921, 750; δ_{H} (500 MHz; CDCl₃) 7.43-7.38 (2H, m, phenyl 2- and 6-H), 7.31-7.28 (1H, m, phenyl 4-H), 7.24 -7.21 (2H, m, phenyl 3- and 5-H), 5.90 (1H, ddt, *J* 17.7, 9.7 and 6.1, allyl 2-H), 5.08 (1H, app. dt, *J* 17.7 and 1.4 allyl 3-H_A), 5.06 (1H, app. dt, *J* 9.7 and 1.4 allyl 3-H_B), 4.28 (2H, dt, *J* 6.1 and 1.4, allyl 1-H₂), 4.26 (1H, br. s, NH), 3.21 (2H, dq, *J* 7.2 and 5.6, ethyl 1-H₂), 1.03 (3H, t, *J* 7.2, ethyl 2-H₃); δ_{C} (125 MHz; CDCl₃) 156.7 (CO), 141.9 (phenyl C-1), 134.7 (allyl C-2), 129.8 (phenyl C-2 and C-6), 128.4 (phenyl C-3 and C-5), 127.4 (phenyl C-4), 116.7 (allyl C-3), 52.1 (allyl C-1), 35.5 (ethyl C-1), 15.4 (ethyl C-2); *m/z* (ES) 227.2 (100%, [M+Na]⁺); HRMS Found: 227.1152 (C₁₂H₁₆N₂O, requires M+Na 227.1155). Characterisation data were consistent with those reported in literature.¹⁰⁰

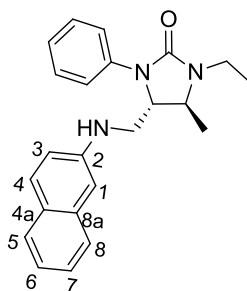
3-Ethyl-4-(naphthalen-2-ylmethyl)-1-phenylimidazolidin-2-one **43**¹⁰⁰



The title compound **43** was prepared according to the general method of Wolfe *et al.*,¹⁰⁰ described in **general procedure C**, from the allyl urea **42** (0.27 g, 1.35 mmol) and 2-bromonaphthalenyl (0.56 g, 2.7 mmol) stirring for 2 days. The crude product was purified by flash chromatography (petrol–EtOAc 80:20 → 70:30) to give a pale yellow

amorphous solid (0.21 g, 48%). R_F : 0.5 (60:30, petrol–EtOAc); $\nu_{\max}/\text{cm}^{-1}$ (film) 3380, 2955, 2926, 2854, 1702, 1597, 1261, 1124, 942, 762, 694; δ_H (500 MHz; CDCl_3) 7.81-7.77 (3H, m, naphthalenyl 7-, 6- and 4-H), 7.63 (1H, s, naphthalenyl 1-H), 7.48-7.43 (4H, m, naphthalenyl 3- and 5-H, phenyl 2- and 6-H), 7.30 (1H, d, J 8.3, naphthalenyl 8-H), 7.26-7.21 (2H, m, phenyl 3- and 5-H), 6.95 (1H, t, J 7.3, phenyl 4-H), 4.08-4.02 (1H, m, 4-H), 3.68 (1H, dq, J 14.7 and 7.4, ethyl 1- H_A), 3.62 (1H, app. t, J 8.9, 5- H_A), 3.46 (1H, dd, J 9.1 and 6.0, 5- H_B), 3.35 (1H, dd, J 13.5 and 4.2, 4- CH_AH_B), 3.21 (1H, dq, J 14.0 and 7.0, ethyl 1- H_B), 2.76 (1H, dd, J 13.4 and 9.8, 4- CH_AH_B), 1.27-1.22 (3H, app. m, ethyl 2- H_3); δ_C (125 MHz; CDCl_3) 157.5 (CO), 140.7 (phenyl C-1), 134.1 (naphthalenyl C-4a), 133.7 (naphthalenyl C-2), 132.3 (naphthalenyl C-8a), 128.9 (phenyl C-2 and C-6), 128.8 (naphthalenyl C-6- or C-7), 127.9 (naphthalenyl C-1), 127.8 (naphthalenyl C-6 or C-7), 127.6 (naphthalenyl C-4), 127.2 (naphthalenyl C-8), 126.5 (naphthalenyl C-3), 126 (naphthalenyl C-5), 122.3 (phenyl C-4), 117.4 (phenyl C-3 and C-5), 53 (C-4), 48 (C-5), 39.5 (4- CH_2), 36.5 (ethyl C-1), 13.2 (ethyl C-2); m/z (ES) 683.4 (100%, $[\text{M}_2+\text{Na}]^+$). Characterisation data were consistent with those reported in literature.¹⁰⁰

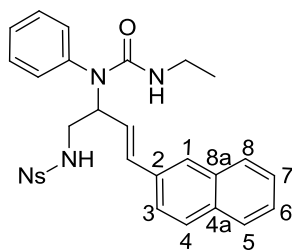
(4*S, 5*S**)-1-Ethyl-5-methyl-4-((naphthalen-2-ylamino)methyl)-3-phenyl imidazolin-2-one **58**¹⁰⁰**



The *title compound* **58** was prepared according to **general procedure C**¹⁰⁰ from the allyl urea **45** (0.18 g, 0.53 mmol) and 2-bromonaphthalenyl (0.16 g, 0.80 mmol) stirring for 2 days in the presence of NaO^tBu (0.13 g, 1.3 mmol). The crude product was purified by flash chromatography (petrol–EtOAc 80:20 \rightarrow 70:30) to give a yellow oil (2.0 mg, 4%). R_F : 0.25 (60:30, petrol–EtOAc); $\nu_{\max}/\text{cm}^{-1}$ (film); 3838, 3753, 2956, 2912, 2852, 1687, 1578, 1219, 1034, 939, 799; δ_H (500 MHz; CDCl_3) 7.66 (1H, dd, J 8.1 and

0.6, naphthalenyl 5-H), 7.62 (1H, d, *J* 8.8, naphthalenyl 4-H), 7.57 (1H, dd, *J* 8.3 and 0.6, naphthalenyl 8-H), 7.50-7.48 (2H, dd, *J* 8.7 and 1.1, phenyl 2- and 6-H), 7.39-7.34 (3H, m, phenyl 3- and 5-H, naphthalenyl 7-H), 7.21 (1H, ddd, *J* 8.1, 6.8 and 1.2, naphthalenyl 6-H), 7.12 (1H, app. t, *J* 7.4, phenyl 4-H), 6.81 (1H, dd, *J* 8.7 and 2.4, naphthalenyl 3-H), 6.77 (1H, app. br. s, naphthalenyl 1-H), 4.04 (1H, td, *J* 5.2 and 3.4, 4-H), 3.77-3.72 (1H, m, 5-H), 3.58 (1H, dq, *J* 14.3 and 7.3, ethyl 1-*H_AH_B*), 3.47 (1H, dd, *J* 13.2 and 5.1, 4-*CH_AH_B*), 3.43 (1H, dd, *J* 13.1 and 3.4, 4-*CH_AH_B*), 3.16 (1H, dq, *J* 14.2 and 7.2, ethyl 1-*H_AH_B*), 1.35 (3H, d, *J* 6.2, methyl), 1.17 (3H, t, *J* 7.2, ethyl 2-*H₃*), *NH* not observed; δ_C (125 MHz; CDCl₃) 157.8 (CO), 139.1 (phenyl C-1), 138.9 (naphthalenyl C-8a), 130.2 (naphthalene C-4), 129.4 (naphthalenyl C-2), 129.3 (phenyl C-2 and C-6), 127.9 (naphthalenyl C-4a), 127.8 (naphthalenyl C-5), 126.7 (naphthalenyl C-7), 126.1 (naphthalenyl C-8), 124.5 (phenyl C-4), 122.6 (naphthalenyl C-6), 121.9 (phenyl C-3 and C-5), 118.2 (naphthalenyl C-3), 105.3 (naphthalenyl C-1), 60.9 (C-4), 51.8 (C-5), 44.2 (4-CH₂), 36.2 (ethyl C-1), 19.5 (Me), 13.4 (ethyl C-2); *m/z* (ES) 360.1 (100%, [M+H]⁺); HRMS Found: 382.1909 (C₂₃H₂₅N₃O, requires M+Na 382.1890).

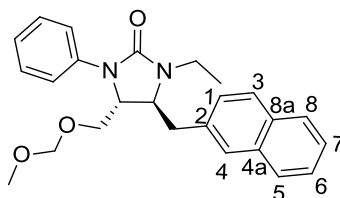
(*E*)-*N*-(2-(3-ethyl-1-phenylureido)-4-(naphthalen-2-yl)but-3-enyl)-2-nitrobenzenesulfonamide **59¹⁰⁰**



The *title compound* **59** was obtained from the allyl urea **55** (0.1 g, 0.19 mmol) and 2-bromonaphthalenyl (90 mg, 0.38 mmol) following **general procedure C**¹⁰⁰ and stirring for 2 days. The crude product was purified by flash chromatography (98.5:1.5 CH₂Cl₂–MeOH) followed by mass directed chromatography to give a yellow oil (13.6 mg, 13%). *R_F*: 0.25 (60:30, petrol–EtOAc); $\nu_{\max}/\text{cm}^{-1}$ (film); 3063, 2930, 1649, 1541, 1513, 1362, 1276, 970, 731; δ_H (500 MHz; CDCl₃) 8.30 (1H, dd *J* 7.7 and 1.5, Ns 3-H), 7.80 (1H, dd, *J* 7.8 and 1.5, Ns 5-H), 7.76 (1H, d, *J* 8.4, naphthalenyl 5-H or 8-H), 7.73 (1H, d, *J* 8.5, naphthalenyl 3-H or 4-H), 7.69 (1H, td, *J* 7.7 and 1.3, Ns 4-H), 7.64 (1H,

td, J 7.7 and 1.3, Ns 6-H), 7.60 (1H, s, naphthalenyl 1-H), 7.48-7.40 (7H, m, 5 x phenyl CH, naphthalenyl 5-H or 8-H and 3-H or 4-H), 7.24 (2H, dd, J 8.0, 1.2, naphthalenyl 6- and 7-H), 6.59 (1H, d, J 15.9, 4-H), 6.16 (1H, dd, J 15.9 and 8.6, 3-H), 6.15 (1H, t, J 5.5, NHNs), 5.01 (1H, app.td, J 8.8 and 5.5, 2-H), 4.06 (1H, app t, J 5.6, NHEt), 3.66 (1H, ddd, J 12.5, 9.0 and 5.6, 1-H_A), 3.41 (1H, dt, J 12.5 and 5.5, 1-H_B), 3.25-3.16 (2H, m, ethyl 1-H₂), 1.01 (3H, t, J 7.2, ethyl 2-H₃); δ_C (125 MHz; CDCl₃) 157.7 (CO), 148.2, 139.5 (Ar C), 134.3 (4-C), 134.1, 133.8, 133.6 (Ar C), 133.5 (Ar CH), 133.3 (Ar C), 132.8 (Ar CH), 131.0 (Ns C-3), 130.4 (phenyl C-2 and C-6), 130.3 (phenyl C-3- and C-5), 128.8, 128.4 128.2, 127.8 (Ar CH), 126.9 (naphthalene C-1), 126.5, 126.3 (Ar CH), 125.8 (C-3), 125.5 (Ns C-5), 123.6 (Ar CH), 59.5 (C-2), 46.3 (C-1), 35.7 (ethyl C-1), 15.5 (ethyl C-2); m/z (ES) 522.1 (100%, fragment [M-NO₂+Na]⁺; HRMS Found: 545.1864 (C₂₉H₂₈N₄O₅S, requires M+H 545.1853).

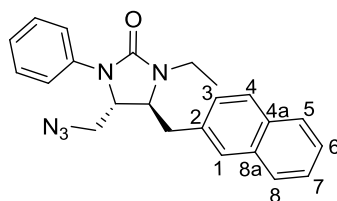
(4*R, 5*S**)-1-Ethyl-4-((methoxymethoxy)methyl)-5-(naphthalen-2-ylmethyl)-3-phenylimidazolidin-2-one **60**¹⁰⁰**



The *title compound* **60** was prepared from the allyl urea (55 mg, 0.2 mmol) **56** and 2-bromonaphthalenyl (91 mg, 2.2 mmol) according to **general procedure C**,¹⁰⁰ stirring for 3 days. The crude product was purified by flash chromatography (petrol–EtOAc 80:20 → 70:30) to give a yellow oil (33 mg, 35%). R_F : 0.25 (50:50, petrol–EtOAc); $\nu_{\max}/\text{cm}^{-1}$ (film); 3057, 2928, 2825, 1703, 1598, 1425, 1261, 1044, 918, 751; δ_H (500 MHz; CDCl₃) 7.82-7.79 (3H, m, naphthalenyl 7-, 6- and 4-H), 7.69 (1H, s, naphthalenyl 1-H), 7.51-7.44 (2H, m, naphthalenyl 3- or 5-H and 8-H), 7.39 (2H, d, J 8.5 phenyl 2- and 6-H), 7.35 (1H, d, J 7.5, naphthalenyl 3- or 5-H), 7.24 (2H, d, J 8.5 phenyl 3- and 5-H), 7.00 (1H, app. t, J 7.4, phenyl 4-H), 4.37 (1H, d, J 6.5, OCH_AH_BO), 4.35 (1H, d, J 6.5, OCH_AH_BO), 4.08 (1H, dt, J 6.3 and 3.1, 4-H), 4.03 (1H, ddd, J 8.3, 4.8 and 3.0, 5-H), 3.75 (1H, dq, J 14.0 and 7.5, ethyl 1-H_AH_B), 3.46 (1H, dd, J 10.4 and 6.3, 4-CH_AH_B), 3.28-3.26 (2H, m, 4-CH_AH_B and 5-CH_AH_B), 3.12 (3H, s, OCH₃), 3.13-3.09

(1H, m, ethyl 1- H_AH_B), 2.92 (1H, dd, J 13.7 and 8.3, 5- CH_AH_B), 1.22 (3H, t, J 7.2, ethyl 2- H_3); δ_C (125 MHz; $CDCl_3$) 156.6 (CO), 139 (phenyl C-1), 134 (naphthalenyl C-4a), 133.5 (naphthalenyl C-2), 132.3 (naphthalenyl C-8a), 128.8 (phenyl C-2 and C-6), 128.4 (naphthalenyl C-7- or C-6- or C-4), 128.0 (naphthalenyl C-1), 127.7 (naphthalenyl C-7- or C-6- or C-4), 127.5 (naphthalenyl C-7- or C-6- or C-4), 127.3 (naphthalenyl C-3 or C-5), 126.3 (naphthalenyl C-3 or C-5), 125.7 (naphthalenyl C-8), 123.1 (phenyl C-4), 120 (phenyl C-2 and C-6), 96.4 (OCH_AH_BO), 66.1 (4- CH_2), 57.9 (C-4), 55.8 (C-5), 55.2 (OCH_3), 39.2 (5- CH_2), 36.3 (ethyl C-1), 13.1 (ethyl C-2); m/z (ES) 427.1 (100%, $[M+Na]^+$); HRMS Found: 427.2000 ($C_{25}H_{28}N_2O_3$ requires $M+Na$ 427.1992).

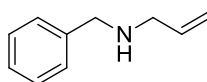
(4*S, 5*S**)-4-(Azidomethyl)-1-ethyl-5-(naphthalen-2-ylmethyl)-3-phenyl imidazolidin-2-one **61**¹⁰⁰**



The *title compound* **61** was prepared from the allyl urea **57** (70 mg, 0.27 mmol) and 2-bromonaphthalenyl (0.17 g, 0.80 mmol) according to **general procedure C**,¹⁰⁰ stirring for 3 days. The crude product was purified by flash chromatography (petrol–EtOAc 80:20 → 70:30) to give a yellow oil (6 mg, 5%). R_F : 0.6 (50:50, petrol–EtOAc); ν_{max}/cm^{-1} (film); 2925, 2105, 1704, 1501, 1423, 1260, 800, 752; δ_H (500 MHz; $CDCl_3$) 7.85–7.81 (3H, m, naphthalenyl 7-, 6- and 4-H), 7.69 (1H, s, naphthalenyl 1-H), 7.52–7.46 (2H, m, naphthalenyl 3- and 8-H), 7.36–7.33 (3H, m, phenyl 2- and 6-H, naphthalenyl 5-H), 7.30–7.28 (2H, m, phenyl 3- and 5-H), 7.05 (1H, tt, J 7.5 and 1.0, phenyl 4-H), 4.08 (1H, app. dt, J 5.7 and 3.0, 5-H), 3.96 (1H, ddd, J 8.3, 4.2 and 3.0, 4-H), 3.78 (1H, dq, J 14.6 and 7.2, ethyl 1- H_A), 3.37–3.32 (2H, m, 4- CH_AH_B and 5- CH_AH_B), 3.18 (1H, dq, J 14.0 and 7.0, ethyl 1- H_B), 2.89–2.82 (2H, m, 4- CH_AH_B and 5- CH_AH_B), 1.27 (3H, t, J 7.2, ethyl 2- H_3); δ_C (125 MHz; $CDCl_3$) 159.4 (CO), 138.1 (phenyl C-1), 133.6 (naphthalenyl C-4a), 133.4 (naphthalenyl C-2), 132.5 (naphthalenyl C-8a), 129.1 (phenyl C-2 and C-6), 128.8 (naphthalenyl C-7 or C-6 or C-4), 128.1

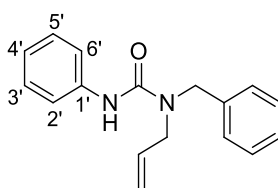
(naphthalenyl C-1), 127.8 (naphthalenyl C-7 or C-6 or C-4), 127.6 (naphthalenyl C-7 or C-6 or C-4), 127.1 (naphthalenyl C-5), 126.5 (naphthalenyl C-3), 125.9 (naphthalenyl C-8), 123.9 (phenyl C-4), 120.7 (phenyl C-3 and C-5), 57.6 (C-5), 55.9 (C-4), 51.1 (5-CH₂), 39.2 (4-CH₂), 36.4 (ethyl C-1), 13.1 (ethyl C-2); *m/z* (ES) 408.1 (100%, [M+Na]⁺); HRMS Found: 408.1799 (C₂₃H₂₃N₅O requires M+Na 408.1795).

***N*-Benzylprop-2-en-1-amine **70**¹⁵⁰**



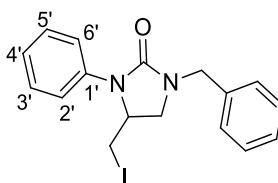
The title compound **70** was prepared according to the method of Mukherjee *et al.*¹⁵⁰ Benzylbromide (2.1 mL, 17.7 mmol) was added *via* syringe pump over 1 h to a suspension of K₂CO₃ (2.9 g, 21.0 mmol) in allyl amine (10.5 mL, 140.1 mmol) and the resulting mixture was stirred at r.t. for 2 days. The reaction mixture was filtered through Celite[®] eluting with CH₂Cl₂; the filtrate was concentrated under reduced pressure and the crude product was purified by flash chromatography (petrol–EtOAc 50:50) to give a yellow oil (1.20 g, 47%). *R*_F: 0.5 (10:90, petrol–EtOAc); *v*_{max}/cm⁻¹ (film) 3311, 3027, 2813, 1948, 1810, 1643, 1455, 1106, 918, 736; *δ*_H (500 MHz; CDCl₃); 7.34–7.27 (4H, m, phenyl 2-, 6-, 3- and 5-H), 7.23 (1H, dd, *J* 8.7 and 1.4, phenyl 4-H), 5.87 (1H, ddt, *J* 17.1, 10.3 and 6.0, 2-H), 5.13 (1H, dd, *J* 17.1 and 1.4, 3-H_A), 5.04 (1H, dd, *J* 10.3 and 1.4, 3-H_B), 3.79 (1H, s, benzyl CH₂), 3.28 (2H, dt, *J* 6.0 and 1.4, 1-H₂), 1.39 (1H, br. s, NH); *m/z* (ES) 148.2 (100%, [M+H]⁺). Spectra corresponds to the one reported in the literature.¹⁵⁰

1-Allyl-1-benzyl-3-phenylurea **71**^{100,151}



The title compound **71** was prepared according to **general procedure B**¹⁰⁰ from phenylisocyanate (1.4 mL, 12.4 mmol) and the amine **70** (1.21 g, 8.2 mmol) in CH₂Cl₂ stirring for 2 days. The crude product was purified by flash chromatography (petrol–EtOAc 70:30) to give a yellow oil (2.1 g, 95%). *R*_F: 0.7 (50:50 petrol–EtOAc); $\nu_{\max}/\text{cm}^{-1}$ (film) 3031, 2984, 2922, 2278, 1645, 1441, 1231, 928, 754, 696; δ_{H} (500 MHz; CDCl₃) δ 7.41–7.25 (m, 9H, Ar), 7.03 (1H, t, *J* 7.1, Ar), 6.45 (s, 1H, NH), 5.89 (1H, ddd, *J* 15.8, 11.9 and 5.4, allyl 2-H), 5.37–5.31 (2H, m, allyl 3-H_A and 3-H_B), 4.62 (2H, s, benzyl CH₂), 3.98 (2H, d, *J* 5.4 Hz, allyl 1-H); δ_{C} (125 MHz; CDCl₃) 157.8 (CO), 139.0, 137.6 (Ar C-1 and C-1'), 133.9 (C-2), 128.9, 128.8, 127.7, 127.5, 123.0, 119.7 (Ar CH), 117.5 (C-3), 50.7 (benzyl CH₂), 50.1 (C-1); *m/z* (ES) 267.1 (100%, [M+H]⁺); HRMS Found: 267.1485 (C₁₇H₁₈N₂O requires M+H 267.1470). Characterisation data consistent with those reported in literature.¹⁵¹

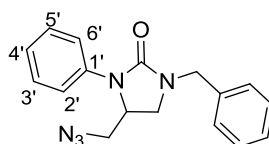
1-Benzyl-4-(iodomethyl)-3-phenylimidazolidin-2-one **73**¹²⁴



Triethylamine (0.25 mL, 2.2 mmol) was added slowly to a solution of the benzyl allyl urea **71** (0.30 g, 1.1 mmol) in CH₂Cl₂ (5 mL) followed by trimethylsilyltrifluoromethanesulfonate (0.40 mL, 2.0 mmol). The resulting mixture was stirred for 1 h at r.t. and concentrated under reduced pressure. The crude material was dissolved in THF (7.0 mL) and I₂ (0.57 g, 2.0 mmol) was added. The resulting mixture was stirred at r.t. overnight, then it was poured into an aqueous solution of Na₂S₂O₃ (20%, w/v, 40 mL) and extracted with EtOAc (3.0 × 20 mL). The combined organic phases were dried (MgSO₄) and concentrated under reduced pressure to give a crude

product which was purified by flash chromatography (petrol–EtOAc 60:40) to give the *title compound 73* as a pale yellow oil (0.24 g, 53%). R_F : 0.7 (60:40, petrol–EtOAc); $\nu_{\max}/\text{cm}^{-1}$ (film) 2923, 2098, 1698, 1655, 1500, 1441, 1260, 1138, 1028, 755, 696, 525; δ_H (500 MHz; CDCl_3) 7.46 (2H, dd, J 8.1 and 1.1, Ar CH), 7.39–7.30 (7H, m, Ar CH), 7.14 (1H, dd, J 7.3 and 1.2, Ar CH), 4.56 (1H, d, J 14.9, benzyl CH_AH_B), 4.41 (1H, d, J 14.9, benzyl CH_AH_B), 4.35 (1H, app tdd, J 8.9, 4.7 and 2.5, 4-H), 3.54 (1H, app. t, J 9.2, 5- H_A), 3.33 (1H, dd, J 10.3 and 2.5, 4- CH_AH_B), 3.16 (1H, dd, J 9.3 and 4.7, 5- H_B), 3.15 (1H, dd, J 10.3 and 8.8, 4- CH_AH_B); δ_C (125 MHz; CDCl_3) 157.4 (CO), 137.8, 136.5 (Ar C-1 and C-1'), 129.2, 128.7, 128.3 (Ar CH), 127.7, 124.3 (Ar C-4 and C-4'), 121.4 (Ar CH), 54.12 (C-4), 48.1 (C-5), 47.9 (benzyl CH_2), 8.0 (4- CH_2); m/z (ES) 393.2 (100%, $[\text{M}+\text{H}]^+$); HRMS Found: 393.0456 ($\text{C}_{17}\text{H}_{17}\text{N}_2\text{OI}$ requires $\text{M}+\text{H}$ 393.0458).

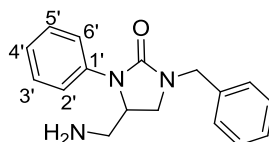
4-(Azidomethyl)-1-benzyl-3-phenylimidazolidin-2-one **74**^{137, 151}



Sodium azide (0.05 g, 0.8 mmol) was added portionwise at 0 °C to a solution of the the imidazolidinone **73** (0.10 g, 0.25 mmol) in DMF (2.5 mL) and the resulting mixture was stirred at r.t overnight. EtOAc (5.0 mL) was added to the reaction mixture, the resulting mixture was washed with water (2 × 5.0 mL) and brine (2 × 50 mL). The combined organic phases were dried (MgSO_4) and concentrated under reduced pressure to give the title compound **74** as a white amorphous solid which was used without further purification (3 mg, 37%). R_F : 0.7 (40:60, petrol–EtOAc); $\nu_{\max}/\text{cm}^{-1}$ (film) 2250, 2106, 1651, 1441, 1357, 1259, 1087, 907, 713, 695; δ_H (500 MHz; CDCl_3) 7.47 (2H, dd, J 8.7 and 1.1, Ar CH), 7.40–7.34 (7H, m, Ar CH), 7.31 (1H, dd, J 7.5 and 2.3, Ar CH), 4.51 (1H, dd, J 15.0, benzyl CH_AH_B), 4.46 (1H, dd, J 15.0, benzyl CH_AH_B), 4.38 (1H, dddd, J 9.3, 6.4, 4.6 and 3.1, 4-H), 3.49 (1H, dd, J 6.4 and 1.2, 4- CH_AH_B), 3.48 (1H, app. t, J 9.2, 5- H_A), 3.38 (1H, dd, J 12.7 and 3.1, 4- CH_AH_B), 3.24 (1H, dd, J 9.2 and 4.6, 5- H_B); δ_C (125 MHz; CDCl_3) 157.5 (CO), 137.9, 136.6 (Ar C-1 and C-1'), 129.2, 128.7, 128.2 (Ar CH), 127.7, 124.3 (Ar C-4 and C-4'), 121.2 (Ar CH), 52.4 (4- CH_2), 51.4 (C-4), 48.0 (benzyl CH_2), 45.0 (C-5); m/z (ES) 308.2 (100%, $[\text{M}+\text{H}]^+$);

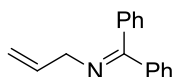
HRMS Found: 330.1325 ($C_{17}H_{17}N_5O$ requires $M+H$ 330.35). Characterisation data were consistent with those reported in literature.¹⁵¹

4-(Aminomethyl)-1-benzyl-3-phenylimidazolidin-2-one **75**¹³⁸



Triphenylphosphine (19 mg, 58 μ mol) was added to a solution of the imidazolinone **74** (15 mg, 48 μ mol) in THF-H₂O (550 μ L of THF, 50 μ L of H₂O) and the resulting mixture was stirred at 45 °C overnight. The solvent was removed to give a crude product which was purified by flash chromatography (petrol-EtOAc 50:50, then CH₂Cl₂-EtOH-NH₄OH 84.7:13.6:1.7) to give the *title imidazolidinone 75* as a pale yellow oil (11 mg, 81%). R_F : 0.7 (70:30, CH₂Cl₂-MeOH); ν_{max}/cm^{-1} (film) 3384, 2920, 1697, 1598, 1500, 1439, 1261, 956, 756; δ_H (500 MHz; CDCl₃) 7.5 (2H, dd, J 8.7 and 1.0, Ar CH), 7.36-7.28 (7H, m, Ar CH), 7.1 (1H, tt, J 7.8 and 1.0, Ar CH), 4.53 (1H, d, J 14.9, benzyl CH_AH_B), 4.42 (1H, d, J 14.9, benzyl CH_AH_B), 4.31-4.27 (1H, m, 4-H), 3.47 (1H, app. t, J 9.0, 5-H_A), 3.27 (1H, dd, J 9.0 and 5.1, 5-H_B), 2.93 (1H, dd, J 13.4 and 6.3, 4- CH_AH_B), 2.83 (1H, app. d, J 13.4, 4- CH_AH_B), 1.61 (2H, br. s, NH₂); δ_C (125 MHz; CDCl₃) 158.1 (CO), 138.6, 136.8 (Ar C-1 and C-1'), 129.0, 128.7, 128.3 (Ar CH), 127.6, 123.9 (Ar C-4 and C-4'), 121.1 (Ar CH), 54.7 (C-4), 48.4 (benzyl CH₂), 44.9 (C-5), 42.4 (4-CH₂); m/z (ES) 282.2 (100%, $[M+H]^+$); HRMS Found: 282.1603 ($C_{17}H_{19}N_3O$ requires $M+H$ 282.1601).

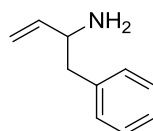
N-(Diphenylmethylene)prop-2-en-1-amine **78**¹²⁶



The title compound **78** was prepared according to the general method of Blacker *et al.*¹²⁶ Allyl amine (4.0 g, 77.0 mmol) was added to a solution of benzophenone (8.6 g,

47.0 mmol) in toluene (45 mL) at r.t., followed by titanium isopropoxide (9.4 mL, 32.0 mmol) and the resulting mixture was stirred at 80 °C overnight. After cooling down at r.t., water (2.0 mL) and toluene (35 mL) were added and the reaction mixture was stirred for 2 h at r.t., filtered through Celite[®], washed with toluene (2 × 20 mL). The organic phases were concentrated under reduced pressure to give the title compound **78** as a yellow oil that was used without further purification (10.4 g, 98%). R_F : 0.8 (20:80, petrol–EtOAc); $\nu_{\max}/\text{cm}^{-1}$ (film) 3059, 3024, 2912, 1957, 1661, 1622, 1491, 1446, 1314, 1287, 1179, 1074, 918, 780; δ_H (500 MHz; CDCl₃) 7.64 (2H, dd, J 8.4 and 1.3, Ar CH), 7.48–7.36 (4H, m, Ar CH), 7.32–7.31 (2H, m, Ar CH), 7.18 (2H, dd, J 7.7 and 1.6, Ar CH), 6.06 (2H, ddt, J 17.2, 10.5 and 5.4, 2-H), 5.18 (1H, dq, J 17.2 and 1.8, 3-H_A), 5.11 (1H, dq, J 10.5 and 1.8, 3-H_B), 4.04 (2H, dt, J 5.4 and 1.8, 1-H₂); δ_C (75 MHz; CDCl₃) 168.8 (N=CPh₂), 139.8, 136.7 (Ar C), 136.6 (Ar CH), 130.0 (C-2), 129, 128.5, 128.3, 128.1, 127.7 (Ar CH), 115.1 (C-3), 56.4 (C-1); HRMS Found: 222.1281 (C₁₆H₁₅N requires M+H 222.1107). Characterisation data were consistent with those reported in literature.¹²⁶

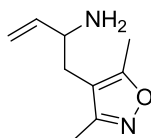
1-phenylbut-3-en-2-amine **76**¹²⁶



The title compound **78** was prepared according to the general method of Blacker *et al.*¹²⁶ The amine **76** (4.0 g, 18.1 mmol) and benzylchloride (2.1 mL, 18.1 mmol) were mixed in the presence of *n*-butyl lithium (11.3 mL, 18.1 mmol) according to **general procedure D**. The crude product was purified by flash chromatography (petrol–EtOAc 80:20 → 70:30) to give a yellow oil (0.85 g, 50%). R_F : 0.15 (99.5:0.5, CH₂Cl₂–MeOH); $\nu_{\max}/\text{cm}^{-1}$ (film) 3910, 3758, 2107, 1644, 1495, 1454, 1371, 1260, 1078, 994, 746; δ_H (500 MHz; CDCl₃) 7.3 (2H, t, J 7.3, Ar), 7.26–7.19 (3H, m, Ar), 5.89 (1H, ddd, J 17.0, 10.3, 6.4, 3-H), 5.14 (1H, d, J 17.0, 4-H_A), 5.04 (1H, d, J 10.3, 4-H_B), 3.6 (1H, ddd, J 8.3, 6.4 and 5.4, 2-H), 2.83 (1H, dd, J 13.3 and 5.4, 1-H_A), 2.62 (1H, dd, J 13.3 and 8.3, 1-H_B), 1.47 (2H, br. s., NH₂); δ_C (75 MHz; CDCl₃) 142.4 (phenyl C-1), 138.8 (phenyl C-4), 129.4 (phenyl C-2 and C-6 or C-3 and C-5), 128.4 (phenyl C-2 and C-6 or C-3 and C-5), 126.3 (C-4), 113.6 (C-3), 55.5 (C-2), 44.4 (C-1); HRMS Found: 148.1147

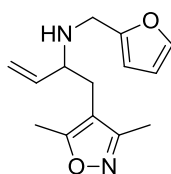
(C₁₀H₁₃N, M+H requires 148.1121). Characterisation data were consistent with those reported in literature.¹²⁶

1-(3,5-dimethylisoxazol-4-yl)but-3-en-2-amine **77**¹²⁶



The *title compound* **77** was prepared from the amine **78** (6.4 g, 29.0 mmol) and 4-chloromethyl-3,5-dimethylisoxazolyl (3.6 mL, 29.0 mmol) in the presence of *n*-Butyl lithium (11.6 mL, 29.0 mmol) according to **general procedure D**.¹²⁶ A yellow oil (2.4 g, 49%) was obtained and used without further purification. R_F : 0.1 (99.5:0.5, CH₂Cl₂–MeOH); $\nu_{\max}/\text{cm}^{-1}$ (film) 3698, 2962, 1956, 1637, 1577, 1492, 1450, 1260, 1195, 1015, 923, 745; δ_H (500 MHz; CDCl₃) 5.80 (1H, ddd, J 17.2, 10.3 and 6.6, 3-H), 5.11 (1H, dt, J 17.2 and 1.2, 4-H_A), 5.05 (1H, dt, J 10.3 and 1.2, 4-H_B), 3.45 (1H, app. q, J 6.6, 2-H), 2.43 (1H, app. d, J 6.6, 1-H_A), 2.42 (1H, app. d, J 7.2, 1-H_B), 2.33 (3H, s, isoxazolyl 5-CH₃), 2.23 (3H, s, isoxazolyl 3-CH₃), 1.49 (2H, br. s., NH₂); δ_C (75 MHz; CDCl₃) 166.0 (isoxazolyl C-5), 159.9 (isoxazolyl C-3), 141.8 (C-3), 114.5 (C-4), 110.5 (isoxazolyl C-4), 54.5 (C-2), 30.8 (C-1), 11.3 (isoxazolyl 5-CH₃), 10.5 (isoxazolyl 3-CH₃); HRMS Found 167.1190 (C₉H₁₄N₂O requires M+H 167.1179).

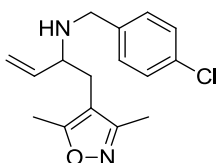
1-(3,5-Dimethylisoxazol-4-yl)-*N*-(furan-2-ylmethyl)but-3-en-2-amine **80**¹³⁶



The *title compound* **80** was prepared from the amine **77** (1.3 g, 7.9 mmol) and furanylaldehyde (0.8 mL, 9.5 mmol) according to **general procedure E**,¹³⁶ stirring for 4 h at r.t., before adding NaBH₄ (2.0 eq.). A yellow oil (1.9 g, 98%) was obtained and

used without further purification. R_F : 0.2 (99:1, CH_2Cl_2 -MeOH); $\nu_{\text{max}}/\text{cm}^{-1}$ (film) 3307, 2978, 2931, 1651, 1636, 1455, 1424, 1195, 1148, 1011, 922, 742; δ_{H} (500 MHz; CDCl_3) 7.33 (1H, dd, J 1.8 and 0.8, furanyl 5-H), 6.29 (1H, dd, J 3.1 and 1.8, furanyl 4-H), 6.10 (1H, dd, J 3.1 and 0.8, furanyl 3-H), 5.60 (1H, ddd, J 17.1, 10.2 and 8.2, 3-H), 5.14 (1H, ddd, J 10.2, 1.5 and 0.5, 4- H_A), 5.08 (1H, ddd, J 17.1, 1.5 and 0.8, 4- H_B), 3.80 (1H, d, J 14.6, $\text{CH}_A\text{H}_B\text{N}$), 3.64 (1H, d, J 14.6, $\text{CH}_A\text{H}_B\text{N}$), 3.12 (1H, app. dq, J 7.1 and 0.5, 2-H), 2.48 (1H, d, J 14.4 and 7.0, 1- H_A), 2.71 (1H, d, J 14.4 and 7.1, 1- H_B), 2.27 (3H, s, isoxazolyl 5- CH_3), 2.15 (3H, s, isoxazolyl 3- CH_3), 1.56 (1H, br. s, NH); δ_{C} (75 MHz; CDCl_3) 166.2 (isoxazolyl C-5), 159.9 (isoxazolyl C-3), 153.6 (furanyl C-2), 141.8 (furanyl C-5), 139.6 (C-3), 117.5 (C-4), 110.2 (isoxazolyl C-4), 110.1 (furanyl C-4), 106.9 (furanyl C-3), 60.3 (C-2), 43.6 (CH_2NH), 29.0 (C-1), 11.2 (isoxazolyl 5- CH_3), 10.3 (isoxazolyl 3- CH_3); m/z (ES) 247.1 (100%, $[\text{M}+\text{H}]^+$); HRMS Found: 247.1439 ($\text{C}_{14}\text{H}_{18}\text{N}_2\text{O}_2$, $\text{M}+\text{H}$ requires 247.1441).

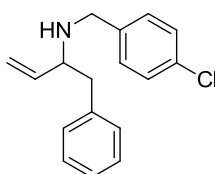
N*-(4-Chlorobenzyl)-1-(3,5-dimethylisoxazol-4-yl)but-3-en-2-amine **81*¹³⁶



The *title compound* **81** was prepared from the amine **77** (1.3 g, 7.6 mmol) and *p*-chlorobenzaldehyde (2.6 mL, 18.2 mmol) according to **general procedure E**,¹³⁶ stirring at reflux overnight, before adding NaBH_4 (6.0 eq.). The crude product was dissolved in EtOAc (15 mL), extracted with a aqueous solution of HCl (2.0 M) (3.0 x 10 mL), then the combined water phases were basified with an aqueous solution of NaOH (50% w/v) until pH 10-11, and extracted with EtOAc (3.0 x 20 mL). The organic phases were dried (MgSO_4) and concentrated under reduced pressure to give a yellow oil (0.99 g, 45%). R_F : 0.6 (95:5, CH_2Cl_2 -MeOH); $\nu_{\text{max}}/\text{cm}^{-1}$ (film) 3354, 2926, 1637, 1491, 1449, 1196, 1089, 1014, 924, 800; δ_{H} (500 MHz; CDCl_3) 7.27 (2H, d, J 8.3, phenyl 3- and 5-H), 7.17 (2H, d, J 8.3, phenyl 2- and 6-H), 5.61 (1H, ddd, J 17.1, 10.1 and 8.2, 3-H), 5.15 (1H, d, J 10.1, 4- H_A), 5.06 (1H, d, J 17.1, 4- H_B), 3.79 (1H, d, J 13.6, benzyl CH_AH_B), 3.59 (1H, d, J 13.6, benzyl CH_AH_B), 3.09 (1H, app. q, J 7.2, 2-H), 2.48 (1H, dd, J 14.4 and 6.9, 1- H_A), 2.43 (1H, dd, J 14.4 and 6.9, 1- H_B), 2.27 (3H, s, isoxazolyl 5-

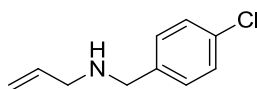
CH₃), 2.15 (3H, s, isoxazolyl 3-CH₃); δ_C (75 MHz; CDCl₃) 166.0 (isoxazolyl C-5), 159.9 (isoxazolyl C-3), 139.7 (phenyl C-1), 132.7 (C-3), 129.3 (phenyl C-2- and C-6), 128.5 (phenyl C-3- and C-5), 128.3 (phenyl C-4), 117.2 (C-4), 110.3 (isoxazolyl C-4), 60.8 (C-2), 50.4 (benzyl CH₂), 29.1 (C-1), 11.3 (isoxazolyl 5-CH₃), 10.4 (isoxazolyl 3-CH₃); m/z (ES) 291.3 (100%, [M+H]⁺); HRMS Found 291.1259 (C₁₆H₁₉ClN₂O, M+H requires 291.1272).

***N*-(4-Chlorobenzyl)-1-phenylbut-3-en-2-amine **82**¹⁵²**



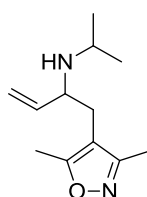
p-Chlorobenzaldehyde (0.7 g, 5.0 mmol) was added to a solution of the amine **76** (0.49 g, 3.3 mmol) in MeOH (0.25 M), followed by molecular sieves (4 Å) and the mixture was stirred at reflux overnight. The reaction was filtered through Celite[®], concentrated under reduced pressure and resuspended in dry MeOH. NaBH₄ (2.0 eq.) was then added at 0 °C and the mixture was left stirring at r.t. overnight. The reaction mixture was quenched with water (5.0 mL), diluted with CH₂Cl₂ (20 mL) and the phases were separated. The aqueous phase was extracted with CH₂Cl₂ (3 x 10 mL) and the combined organic phases were dried (MgSO₄) and concentrated under reduced pressure to give a crude product, which was purified by flash chromatography (80:20 hexane–EtOAc) to give the *title amine* **82** as a colourless oil (0.6 g, 65%). *R*_F: 0.4 (50:50, petrol–EtOAc); $\nu_{\max}/\text{cm}^{-1}$ (film) 3346, 2922, 2849, 1491, 1455, 1090, 1014, 700; δ_H (500 MHz; CDCl₃) 7.34–7.26 (4H, m, Ar CH), 7.22 (2H, dd, *J* 8.0 and 2.0 Ar CH), 7.16 (2H, d, *J* 6.8, Ar CH), 7.08 (1H, d, *J* 8.2 Ar CH), 5.70 (1H, ddd, *J* 17.1, 10.3, 8.0, 3-H), 5.13 (1H, ddd, *J* 10.3, 1.6 and 0.6, 4-H_A), 5.09 (1H, ddd, *J* 17.1, 1.6 and 0.8, 4-H_B), 4.68 (1H, br. s., NH), 3.78 (1H, d, *J* 13.8 benzyl CH_AH_B), 3.57 (1H, d, *J* 13.8 benzyl CH_AH_B), 3.27 (1H, app. td, *J* 8.0 and 5.7, 2-H), 2.81 (1H, dd, *J* 13.5 and 5.7, 1-H_A), 2.75 (1H, dd, *J* 13.5 and 8.0, 1-H_B); δ_C (75 MHz; CDCl₃) 140.5 (Ar C), 138.4 (C-3), 132.5 (Ar C), 129.4, 129.3 (Ar CH), 128.7 (Ar C), 128.3, 126.5, 126.5 (Ar CH), 116.5 (C-4), 61.8 (C-2), 50.3 (benzyl CH₂), 42.5 (C-1); m/z (ES) 271.4 (100%, [M+H]⁺); HRMS Found 272.1194 (C₁₇H₁₈ClN, M+H requires 272.1200).

N*-(4-Chlorobenzyl)prop-2-en-1-amine **83*^{136, 153}



The title compound **83** was prepared from allylamine (0.4 mL, 5.2 mmol) and *p*-chlorobenzaldehyde (0.6 mL, 4.3 mmol) according to **general procedure E**,¹³⁶ stirring at reflux for 4 h, before adding NaBH₄ (4 eq.). A yellow oil (0.33 g, 43%) was obtained and used without further purification. *R*_F: 0.4 (95:5, CH₂Cl₂–MeOH); $\nu_{\text{max}}/\text{cm}^{-1}$ (film) 3368, 2927, 1643, 1491, 1462, 1407, 1090, 10115, 819; δ_{H} (500 MHz; CDCl₃) 7.28 (2H, d, *J* 8.4, phenyl 3- and 5-H), 7.25 (2H, d, *J* 8.4, phenyl 2- and 6-H), 5.91 (1H, ddd, *J* 17.1, 10.2 and 6.0, 2-H), 5.22 (1H, dd, *J* 17.1 and 1.5, 3-H_A), 5.18 (1H, dt, *J* 10.2 and 1.1, 3-H_B), 3.79 (2H, s, benzyl CH₂), 3.25 (2H, dd, *J* 6.0 and 1.1, 1-H₂), 1.55 (2H, br. s., NH₂); δ_{C} (75 MHz; CDCl₃) 138.9 (C-3), 136.7 (phenyl C-1), 132.8 (phenyl C-4), 129.6 (phenyl C-3 and C-5), 128.6 (phenyl C-2 and C-6), 116.3 (C-4), 52.6 (benzyl CH₂), 51.8 (C-2); *m/z* (ES) 181.9 (100%, [M+H]⁺); HRMS Found 182.0730 (C₉H₁₄N₂O requires M+H 182.0731). Characterisation data were consistent with those reported in literature.¹⁵³

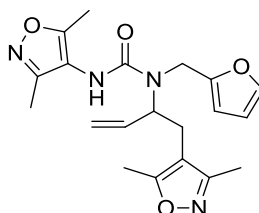
1-(3,5-Dimethylisoxazol-4-yl)-*N*-isopropylbut-3-en-2-amine **84**¹⁵⁴



Acetone (0.17 mL, 2.4 mmol) was added to a solution of the amine **77** (0.2 g, 1.2 mmol) in EtOH (0.8 M, 1.5 mL), followed by MgSO₄ (15 mg) and the mixture was stirred at r.t. for 8 h; then NaBH₄ (0.1 g, 7.2 mmol) was added and the mixture was left stirring at r.t. overnight. The reaction mixture was quenched with an aqueous solution of NaOH (1.0 M, 2.0 mL), EtOH was removed under reduced pressure and the remaining solution was extracted with EtOAc (3 x 10 mL). The combined organic phases were washed with brine (2 x 5.0 mL), dried (Na₂SO₄) and concentrated under reduced pressure to give the *title amine* **84** as a pale yellow oil (0.15 g, 61%). *R*_F: 0.2 (99.5:0.5,

CH₂Cl₂–MeOH); $\nu_{\max}/\text{cm}^{-1}$ (film) 3365, 2962, 1660, 1638, 1454, 1426, 1195, 996, 921, 744; δ_{H} (500 MHz; CDCl₃) 5.56 (1H, ddd, J 17.1, 10.1 and 8.4, 3-H), 5.06 (1H, dd, J 10.1 and 1.1, 4-H_A), 4.99 (1H, dd, J 17.1 and 1.1, 4-H_B), 3.22 (1H, app. td, J 8.1, and 6.1, 2-H), 2.84 (1H, m, *isopropyl CH*), 2.50 (1H, dd, J 13.7 and 6.1, 1-H_A), 2.38 (1H, dd, J 13.7 and 7.8, 1-H_B), 2.33 (3H, s, isoxazolyl 5-CH₃), 2.22 (3H, s, isoxazolyl 3-CH₃), 1.06 (3H, d, J 6.1, *isopropyl CH₃*), 0.97 (3H, d, J 6.2, *isopropyl CH₃*); δ_{C} (75 MHz; CDCl₃) 165.9 (isoxazolyl C-5), 159.9 (isoxazolyl C-3), 140.3 (C-3), 120.9 (C-4), 110.6 (isoxazolyl C-4), 59.1 (C-2), 45.7 (*isopropyl C-1*), 29.4 (C-1), 24.0 (*isopropyl CH_{3A}*), 22.0 (*isopropyl CH_{3B}*), 11.3 (isoxazolyl 5-CH₃), 10.5 (isoxazolyl 3-CH₃); m/z (ES) 209.1 (100%, [M+H]⁺); HRMS Found: 209.1648 (C₁₂H₂₀N₂O, M+H requires 209.1651).

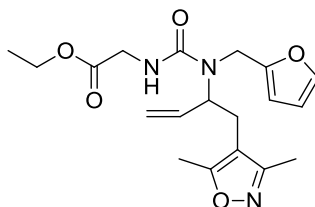
3-(3,5-Dimethylisoxazol-4-yl)-1-(1-(3,5-dimethylisoxazol-4-yl)but-3-en-2-yl)-1-(furan-2-ylmethyl)urea **85¹⁰⁰**



The *title compound* **85** was prepared from the amine **80** (0.5 g, 2.1 mmol) and 4-isocyanato-3,5-dimethylisoxazolyl (0.7 mL, 6.45 mmol) in CH₂Cl₂ stirring at 35 °C for 1 day, according to **general procedure B**.¹⁰⁰ The crude product was purified by flash chromatography (50:50, petrol–EtOAc) to give a yellow oil (0.60 g, 77%). R_{F} : 0.3 (60:40, petrol–EtOAc); $\nu_{\max}/\text{cm}^{-1}$ (film) 3320, 2928, 1722, 1660, 1651, 1645, 1515, 1456, 1427, 1241, 1012, 917, 734 ; δ_{H} (500 MHz; CDCl₃) 7.41 (1H, dd, J 1.9 and 0.8, furanyl 5-H), 6.40 (1H, dd, J 3.2 and 1.9, furanyl 4-H), 6.27 (1H, dd, J 3.2 and 0.8, furanyl 3-H), 5.60 (1H, ddd, J 17.3, 10.5 and 6.1, 3-H), 5.92 (1H, br. s., *NH*), 5.26 (1H, ddd, J 10.5, 1.5 and 1.1, 4-H_A), 5.21 (1H, ddd, J 17.3, 1.5 and 1.1, 4-H_B), 4.73 (1H, app. td, J 7.7 and 6.1, 2-H), 4.37 (1H, d, J 17.0, *CH_AH_BN*), 4.33 (1H, d, J 17.0, *CH_AH_BN*), 2.78 (1H, d, J 14.6 and 7.8, 1-H_A), 2.70 (1H, d, J 14.6 and 7.5, 1-H_B), 2.30 (3H, s, isoxazolyl 5-CH₃), 2.23 (3H, s, isoxazolyl 5'-CH₃), 2.22 (3H, s, isoxazolyl 3-CH₃), 2.08 (3H, s, isoxazolyl 3'-CH₃); δ_{C} (75 MHz; CDCl₃) 166.3 (isoxazolyl C-5), 163.5

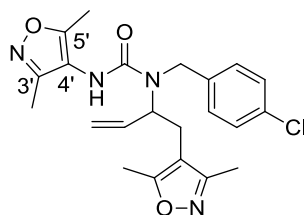
(isoxazolyl C-3), 160.1 (isoxazolyl C-5'), 158.26 (isoxazolyl C-3'), 156.0 (CO), 151.2 (furanlyl C-2), 143.2 (furanlyl C-5), 136.8 (C-3), 118.5 (C-4), 114.8 (isoxazolyl C-4'), 111.3 (furanlyl C-4), 110.3 (isoxazolyl C-4), 108.9 (furanlyl C-3), 59.1 (C-2), 42.8 (CH₂N), 25.7 (C-1), 11.6 (isoxazolyl 5-CH₃), 11.3 (isoxazolyl 5'-CH₃), 10.7 (isoxazolyl 3-CH₃), 9.8 (isoxazolyl 3'-CH₃); m/z (ES) 385.1 (100%, [M+H]⁺); HRMS Found: 407.1702 (C₂₀H₂₄N₄O₄, M+Na requires 407.1690).

Ethyl 2-(3-(1-(3,5-dimethylisoxazol-4-yl)but-3-en-2-yl)-3-(furanlyl-2-ylmethyl)ureido)acetate **86¹⁰⁰**



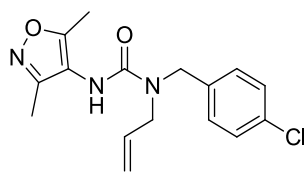
The *title compound* **86** was prepared from the amine **80** (0.5 g, 2.0 mmol) and ethyl 2-isocyanatoacetate (0.7 mL, 6.1 mmol) in CH₂Cl₂ stirring at 35 °C for 3 days, according to **general procedure B**.¹⁰⁰ The crude product was purified by flash chromatography (99.5:0.5, CH₂Cl₂-MeOH) to give a yellow oil (0.52 g, 70%). *R*_F: 0.45 (95:5, CH₂Cl₂-MeOH); *v*_{max}/cm⁻¹ (film) 3383, 2982, 1748, 1644, 1526, 149, 1377, 1195, 1023, 933, 746; *δ*_H (500 MHz; CDCl₃) 7.37 (1H, d, *J* 1.8, furanlyl 5-H), 6.33 (1H, dd, *J* 3.2 and 1.8, furanlyl 4-H), 6.25 (1H, dd, *J* 3.2, furanlyl 3-H), 5.92 (1H, ddd, *J* 17.3, 10.5 and 6.3, 3-H), 5.26 (1H, t, *J* 4.9 NH), 5.19 (1H, d, *J* 10.5, 4-H_A), 5.13 (1H, d, *J* 17.3, 4-H_B), 4.43 (1H, app. q, *J* 7.1, 2-H), 4.37 (1H, d, *J* 17.0, CH_AH_BN), 4.25 (1H, d, *J* 17.0, CH_AH_BN), 4.20 (2H, q, *J* 7.2, ethyl 1-H₂), 3.99 (2H, d, *J* 4.9, CH₂CO), 2.81 (1H, d, *J* 14.5 and 7.1, 1-H_A), 2.70 (1H, d, *J* 14.5 and 8.1, 1-H_B), 2.27 (3H, s, isoxazolyl 5-CH₃), 2.20 (3H, s, isoxazolyl 3-CH₃), 1.27 (3H, t, *J* 7.2 ethyl 2-H₃); *δ*_C (75 MHz; CDCl₃) 170.9 (CO₂Et), 166.0 (NCON), 159.7 (isoxazolyl C-5), 157.5 (isoxazolyl C-3), 151.0 (furanlyl C-2), 142.6 (furanlyl C-5), 136.0 (C-3), 117.9 (C-4), 110.7 (furanlyl C-4), 110.4 (isoxazolyl C-4), 108.4 (furanlyl C-3), 61.5 (ethyl C-1), 59.7 (C-2), 43.2 (CH₂NCONH), 43.0 (CH₂CO₂Et), 25.6 (C-1), 14.3 (ethyl C-2), 11.0 (isoxazolyl 5-CH₃), 10.4 (isoxazolyl 3-CH₃); m/z (ES) 398.1 (100%, [M+Na]⁺); HRMS Found: 376.1882 (C₁₉H₂₅N₃O₅, M+H requires 379.1867).

1-(4-Chlorobenzyl)-3-(3,5-dimethylisoxazol-4-yl)-1-(1-(3,5-dimethylisoxazol-4-yl)but-3-en-2-yl)urea **87¹⁰⁰**



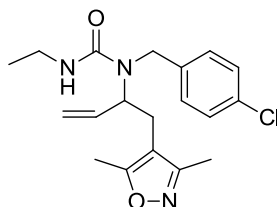
The *title compound* **87** was prepared from the amine **81** (0.3 g, 1.2 mmol) and 4-isocyanato-3,5-dimethylisoxazolyl (0.4 mL, 3.6 mmol) in CH₂Cl₂ stirring at 35 °C for 1 day, according to **general procedure B**.¹⁰⁰ The crude product was dissolved in EtOAc (~10 mL), petrol was added until the precipitation was completed and the precipitate was removed by filtration. The filtrate was concentrated under reduced pressure to give a yellow oil (0.3 g, 58%). *R*_F: 0.4 (95:5, CH₂Cl₂-MeOH); *v*_{max}/cm⁻¹ (film) 3286, 2925, 1663, 1643, 1492, 1463, 1242, 1091, 932, 751; δ _H (500 MHz; CDCl₃) 7.35 (2H, d, *J* 8.4, phenyl 3- and 5- H), 7.20 (2H, d, *J* 8.4, phenyl 2- and 6-H), 5.93 (1H, ddd, *J* 17.1, 10.7 and 6.6, 3-H), 5.44 (1H, br. s., NH), 5.25-5.18 (2H, m, 4-H_A and 4-H_B), 4.85 (1H, dt, *J* 8.0 and 6.8, 2-H), 4.51 (1H, d, *J* 13.6, benzyl CH_AH_B), 4.30 (1H, d, *J* 13.6, benzyl CH_AH_B), 2.75 (1H, dd, *J* 14.5 and 8.0, 1-H_A), 2.67 (1H, dd, *J* 14.5 and 7.3, 1-H_B), 2.27 (3H, s, isoxazolyl 5-CH₃), 2.21 (3H, s, isoxazolyl 5'-CH₃), 2.06 (3H, s, isoxazolyl 3-CH₃), 1.90 (3H, s, isoxazolyl 3'-CH₃); δ _C (75 MHz; CDCl₃) 165.9 (isoxazolyl C-5), 163.4 (isoxazolyl C-5'), 159.7 (isoxazolyl C-3), 157.9 (isoxazolyl C-3'), 155.7 (CO), 135.8 (C-3), 135.3 (phenyl C-1), 134.0 (phenyl C-4), 129.3 (phenyl C-3 and C-6), 127.8 (phenyl C-2 and C-6), 119.0 (C-4), 114.1 (isoxazolyl C-4'), 110.3 (isoxazolyl C-4), 58.5 (C-2), 47.9 (benzyl CH₂), 25.6 (C-1), 11.2 (isoxazolyl 5-CH₃), 10.7 (isoxazolyl 3-CH₃), 10.3 (isoxazolyl 5'-CH₃), 9.4 (isoxazolyl 3'-CH₃); *m/z* (ES) 451.4 (100%, [M+Na]⁺); HRMS Found 451.1523 (C₂₂H₂₅ClN₄O₃, M+Na requires 451.1507).

1-Allyl-1-(4-chlorobenzyl)-3-(3,5-dimethylisoxazol-4-yl)urea **88**¹⁰⁰



The *title compound* **88** was prepared from the amine **83** (0.3 g, 1.8 mmol) and 4-isocyanato-3,5-dimethylisoxazolyl (0.6 mL, 5.3 mmol) in CH₂Cl₂ stirring at 35 °C for 2 days, according to **general procedure B**.¹⁰⁰ The crude product was dissolved in EtOAc (~10 mL), petrol was added until the precipitation was completed and the precipitate was removed by filtration. The filtrate was concentrated under reduced pressure to give a yellow oil (0.47 g, 82%). *R*_F: 0.7 (80:20, petrol–EtOAc); *v*_{max}/cm⁻¹ (film) 3295, 2926, 1723, 158, 1635, 1515, 1492, 1248, 1092, 1014, 795; *δ*_H (500 MHz; MeOD-*d*₄) 7.38 (2H, d, *J* 8.6, phenyl 3- and 5-H), 7.31 (2H, d, *J* 8.6, phenyl 2- and 6-H), 5.88 (1H, ddd, *J* 17.1, 10.3 and 5.1, 2-H), 5.25 (1H, d, *J* 10.3 and 1.4, 3-H_A), 5.23 (1H, dd, *J* 17.1, 3-H_B), 4.89 (2H, s, benzyl CH₂), 4.00 (1H, d, *J* 5.1, 1-H₂), 2.28 (3H, s, isoxazolyl 5-CH₃), 2.15 (3H, s, isoxazolyl 3-CH₃); *δ*_C (75 MHz; MeOD-*d*₄) 165.8 (isoxazolyl C-5), 160.4 (isoxazolyl C-3), 158.8 (CO), 138.1 (phenyl C-1) 134.3 (C-2), 134.2 (phenyl C-4), 134.2 (phenyl C-2 and C-6), 130.1 (phenyl C-3 and C-5), 117.1 (C-3), 116.4 (isoxazolyl C-4), 50.4 (benzyl CH₂), 10.6 (isoxazolyl 5-CH₃), 9.3 (isoxazolyl 3-CH₃); *m/z* (ES) 342.7 (100%, [M+Na]⁺) HRMS Found 320.1168 (C₁₆H₁₉ClN₃O₂ requires MH⁺ 320.1160).

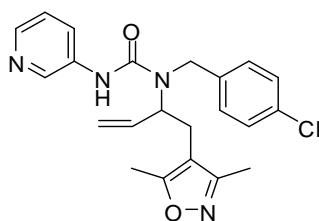
1-(4-Chlorobenzyl)-1-(1-(3,5-dimethylisoxazol-4-yl)but-3-en-2-yl)-3-ethylurea **89**¹⁰⁰



The *title compound* **89** was prepared from the amine **81** (0.28 g, 1.0 mmol) and ethylisocyanate (0.23 mL, 3.0 mmol) in CH₂Cl₂ stirring at 35 °C for 1 day, according to **general procedure B**.¹⁰⁰ The crude product was dissolved in EtOAc (~15 mL), washed

with an aqueous saturated solution of NaHCO₃ (2 x 7.0 mL) and brine (2 x 7.0 ml). The organic phase was dried (MgSO₄) and concentrated under reduced pressure to give a yellow oil (0.3 g, 87%). *R*_F: 0.3 (94:6, CH₂Cl₂-MeOH); $\nu_{\max}/\text{cm}^{-1}$ (film) 3357, 2972, 2930, 1633, 1530, 1450, 1293, 114, 929, 746; δ_{H} (500 MHz; CDCl₃) 7.30 (2H, d, *J* 8.3, phenyl 3- and 5- H), 7.12 (2H, d, *J* 8.3, phenyl 2- and 6-H), 5.88 (1H, ddd, *J* 17.2, 10.4 and 6.7, 3-H), 5.16 (1H, dd, *J* 17.2 and 1.0 4-H_A), 5.12 (1H, dd, *J* 10.4 and 1.0 4-H_B), 4.55 (1H, app. q, *J* 7.0, 2-H), 4.38 (1H, d, *J* 17.4, benzyl CH_AH_B), 4.19 (1H, br. s., NH), 4.15 (1H, d, *J* 17.4, benzyl CH_AH_B), 3.18 (2H, m, ethyl 1-H₂), 2.79 (1H, dd, *J* 14.3 and 7.1, 1-H_A), 2.60 (1H, dd, *J* 14.3 and 8.1, 1-H_B), 2.26 (3H, s, isoxazolyl 5-CH₃), 2.19 (3H, s, isoxazolyl 3-CH₃), 1.00 (3H, t, *J* 7.2, ethyl 2-H₃); δ_{C} (75 MHz; CDCl₃) 165.9 (isoxazolyl C-5), 159.7 (isoxazolyl C-3), 157.9 (CO), 136.2 (phenyl C-1), 136.1 (C-3), 133.4 (phenyl C-4), 129.1 (phenyl C-3 and C-5), 127.9 (phenyl C-2 and C-6), 118.2 (C-4), 110.2 (isoxazolyl C-4), 59.2 (C-2), 48.5 (benzyl CH₂), 35.6 (ethyl C-1), 25.7 (C-1), 15.4 (ethyl C-2), 11.1 (isoxazolyl 5-CH₃), 10.3 (isoxazolyl 3-CH₃); *m/z* (ES) 384.5 (100%, [M+Na]⁺); HRMS Found 362.1634 (C₁₉H₂₄ClN₃O₂, M+H requires 362.1629).

1-(4-Chlorobenzyl)-1-(1-(3,5-dimethylisoxazol-4-yl)but-3-en-2-yl)-3-(pyridin-3-yl)urea 90¹⁰⁰

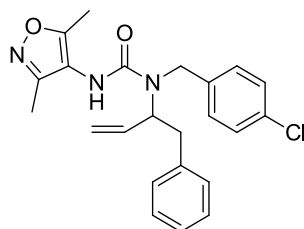


The *title compound* **90** was prepared from the amine **81** (0.4 g, 1.4 mmol) and 3-isocyanatopyridine (0.5 g, 4.5 mmol) in CH₂Cl₂ stirring at 35 °C for 1 day, according to **general procedure B**.¹⁰⁰ The crude product was purified by flash chromatography (99:1, CH₂Cl₂-MeOH) to give a yellow oil (0.5 g, 80%). *R*_F: 0.6 (95:5, CH₂Cl₂-MeOH); $\nu_{\max}/\text{cm}^{-1}$ (film) 3588, 2923, 1731, 1655, 1533, 1483, 1421, 1227, 1089, 931, 801; δ_{H} (500 MHz; CDCl₃) 8.26 (1H, d, *J* 3.9, py 4-H), 8.16 (1H, s, py 2-H), 7.86-7.84 (1H, m, py 6-H), 7.30 (2H, d, *J* 8.3, phenyl 3- and 5- H), 7.29-7.26 (1H, m, py 5-H)^a,

^a Signal overlapping with δ_{H} 7.3

7.12 (2H, d, *J* 8.3, phenyl 2- and 6-H), 5.88 (1H, ddd, *J* 17.2, 10.4 and 6.7, 3-H), 5.16 (1H, dd, *J* 17.2 and 1.0, 4-H_A), 5.12 (1H, dd, *J* 10.4 and 1.0, 4-H_B), 4.55 (1H, app. q, *J* 7.0, 2-H), 4.38 (1H, d, *J* 17.4, benzyl CH_AH_B), 4.19 (1H, br. s., *NH*), 4.15 (1H, d, *J* 17.4, benzyl CH_AH_B), 2.79 (1H, dd, *J* 14.2 and 7.1, 1-H_A), 2.60 (1H, dd, *J* 14.2 and 8.1, 1-H_B), 2.26 (3H, s, isoxazolyl 5-CH₃), 2.19 (3H, s, isoxazolyl 3-CH₃); δ_C (75 MHz; CDCl₃) 166.2 (isoxazolyl C-5), 162.9 (isoxazolyl C-3), 159.6 (CO), 155.14 (py C), 144.65, 141.65, (py CH), 138.6 (phenyl C-1), 135.9 (C-3), 135.2 (phenyl C-4), 129.5 (phenyl C-3 and C-5), 128.1 (phenyl C-2 and C-6), 127.3, 123.6 (py CH), 119.1 (C-4), 109.8 (isoxazolyl C-4), 59.6 (C-2), 49.3 (benzyl CH₂), 25.5 (C-1), 11.2 (isoxazolyl 5-CH₃), 10.3 (isoxazolyl 3-CH₃); *m/z* (ES) 411.2 (100%, [M+H]⁺); HRMS Found 411.1614 (C₂₂H₂₃ClN₄O₂, M+H requires 411.1631).

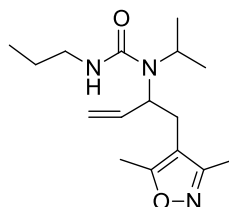
1-(4-chlorobenzyl)-3-(3,5-dimethylisoxazol-4-yl)-1-(1-phenylbut-3-en-2-yl)urea
91¹⁰⁰



The *title compound 91* was prepared from the amine **82** (0.35 g, 1.3 mmol) and 4-isocyanato-3,5-dimethylisoxazolyl (0.4 mL, 3.9 mmol) in CH₂Cl₂ stirring at 35 °C for 1 day, according to **general procedure B**.¹⁰⁰ The crude product was purified by flash chromatography (70:30, petrol–EtOAc) to give a yellow oil (0.43 g, 81%). *R*_F: 0.4 (50:50, petrol–EtOAc); $\nu_{\max}/\text{cm}^{-1}$ (film) 3311, 1367, 1494, 1465, 1245, 1089, 929, 748; δ_H (500 MHz; CDCl₃) 7.33-7.27 (5H, m, Ar), 7.23 (2H, dd, *J* 8.0 and 6.7, Ar), 7.13 (2H, d, *J* 8.5, Ar), 6.0 (1H, ddd, *J* 17.3, 10.5, 5.6, 3-H), 5.31 (1H, ddd, *J* 17.3 4-H_A), 5.25 (1H, ddd, *J* 10.5, 4-H_B), 5.00 (1H, app. dt, *J* 7.8, 5.5, 2-H), 4.51 (1H, d, *J* 17.1 benzyl CH_AH_B), 4.11 (1H, d, *J* 17.1 benzyl CH_AH_B), 3.08 (1H, dd, *J* 12.7 and 7.8, 1-H_A), 3.04 (1H, dd, *J* 12.7 and 5.5, 1-H_B), 2.08 (3H, s, isoxazolyl 5-CH₃), 1.93 (3H, s, isoxazolyl 3-CH₃); δ_C (75 MHz; CDCl₃) 163.2 (isoxazolyl 5-C), 157.9 (isoxazolyl C-3), 155.8 (CO), 137.8 (C Ar), 137.0 (C-3), 136.0, 133.7 (Ar C), 129.2, 129.1, 128.6, 128.5, 126.7 (Ar CH), 117.7 (C-4), 114.3 (isoxazolyl C-4), 60.4 (C-2), 48.3 (benzyl CH₂), 38.0 (C-1)

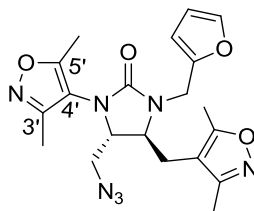
14.2 (isoxazolyl 5-CH₃), 10.8 (isoxazolyl 3-CH₃); HRMS Found 410.1637 (C₂₃H₂₄ClN₄O₂, M+H requires 410.1629).

1-(1-(3,5-dimethylisoxazol-4-yl)but-3-en-2-yl)-3-ethyl-1-isobutylurea 92¹⁰⁰



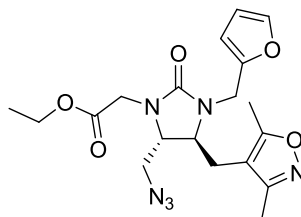
The *title compound 92* was prepared from the amine **84** (80 mg, 0.4 mmol) and ethylisocyanate (0.1 mL, 1.2 mmol) in CH₂Cl₂ stirring at 35 °C for 2 days, according to **general procedure B**.¹⁰⁰ The crude product was purified by flash chromatography (97.5:2.5, CH₂Cl₂–MeOH) to give a yellow oil (80 mg, 68%). *R*_F: 0.4 (95:5, CH₂Cl₂–MeOH); *v*_{max}/cm⁻¹ (film) 3372, 2963, 1633, 1531, 1455, 1325, 1195, 1000, 919, 744; *δ*_H (500 MHz; CDCl₃) 6.07 (1H, ddd, *J* 17.4, 10.5 and 5.4, 3-H), 5.14 (1H, dd, *J* 10.5 and 1.2, 4-H_A), 5.08 (1H, dd, *J* 17.4, 1.2, 4-H_B), 4.32 (1H, t, *J* 4.7, NH), 4.07-4.01 (1H, m, isopropyl CH), 3.71-3.67 (1H, m, 2-H), 3.13 (2H, dd, *J* 13.7 and 7.0, propyl 1-H₂), 2.90 (1H, dd, *J* 14.6 and 8.3, 1-H_A), 2.76 (1H, dd, *J* 14.6 and 7.0, 1-H_B), 2.23 (3H, s, isoxazolyl 5-CH₃), 2.16 (3H, s, isoxazolyl 3-CH₃), 1.47-1.43 (2H, m, *J* 6.1, propyl 2-H₂), 1.03 (3H, d, *J* 6.7, isopropyl CH_{3A}), 0.86 (3H, t, *J* 7.4, propyl 3-H₃), 0.97 (3H, d, *J* 6.27, isopropyl CH_{3B}); *δ*_C (75 MHz; CDCl₃) 166.3 (isoxazolyl C-5), 159.7 (isoxazolyl C-3), 157.3 (CO), 138.7 (C-3), 116.5 (C-4), 111.2 (isoxazolyl C-4), 55.9 (C-2), 47.2 (isopropyl C-1), 42.5 (propyl C-1), 25.3 (C-1), 23.4 (propyl C-2), 21.3 (isopropyl CH_{3A}), 21.1 (isopropyl CH_{3B}), 11.5 (isoxazolyl 5-CH₃), 11.0 (propyl C-3), 10.3 (isoxazolyl 3-CH₃); *m/z* (ES) 294.1 (100%, [M+H]⁺); HRMS Found: 316.1987 (C₁₆H₂₇N₃O₂, M+Na requires 316.1995).

(4*S, 5*S**)-4-(Azidomethyl)-3-(3,5-dimethylisoxazol-4-yl)-5-((3,5-dimethylisoxazol-4-yl) methyl)-1-(furan-2-ylmethyl)imidazolidin-2-one **93**^{124,137}**



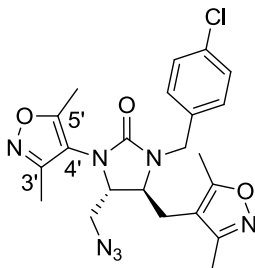
The *title compound* **93** was prepared from the allyl urea **85** (1.6 mmol) according to **general procedure F**.^{124,137} The crude product was purified by flash chromatography (98.5:1.5, CH₂Cl₂–MeOH) to give a yellow oil (108 mg, 16% over two steps). *R*_F: 0.6 (94:6, CH₂Cl₂–MeOH); $\nu_{\max}/\text{cm}^{-1}$ (film) 2932, 2109, 1711, 1441, 1254, 1011, 750; δ_{H} (500 MHz; CDCl₃) 7.43 (1H, dd, *J* 1.9 and 0.9, furanyl 5-H), 6.39 (1H, dd, *J* 3.2 and 1.9, furanyl 4-H), 6.29 (1H, dd, *J* 3.2 and 0.9, furanyl 3-H), 4.91 (1H, d, *J* 15.8, NCH_AH_B), 4.05 (1H, d, *J* 15.8, NCH_AH_B), 3.55 (1H, ddd, *J* 7.7, 5.4 and 4.3, 5-H), 3.46 (1H, ddd, *J* 5.8, 4.3 and 3.6, 4-H), 3.13 (1H, dd, *J* 12.5 and 5.8, 4-CH_AH_B), 3.05 (1H, dd, *J* 12.5 and 3.6, 4-CH_AH_B), 2.82 (1H, dd, *J* 14.8 and 5.4, 5-CH_AH_B), 2.55 (1H, dd, *J* 14.8 and 7.7, 5-CH_AH_B), 2.34 (3H, s, isoxazolyl 5-CH₃), 2.31 (3H, s, isoxazolyl 5'-CH₃), 2.21 (3H, s, isoxazolyl 3-CH₃), 2.15 (3H, s, isoxazolyl 3'-CH₃); δ_{C} (75 MHz; CDCl₃) 166.5 (isoxazolyl C-5), 166.3 (CO), 159.3 (isoxazolyl C-3), 158.1 (furanyl C-2), 157.0 (isoxazolyl C-5'), 149.7 (isoxazolyl C-3'), 142.8 (furanyl C-5), 113.2 (isoxazolyl C-4'), 110.7 (furanyl C-4), 109.2 (furanyl C-3), 108.4 (isoxazolyl C-4), 59.4 (C-5), 55.1 (C-4), 52.0 (5-CH₂), 39.5 (CH₂NCO), 26.5 (4-CH₂), 11.3 (isoxazolyl 5-CH₃), 11.1 (isoxazolyl 5'-CH₃), 10.4 (isoxazolyl 3-CH₃), 9.4 (isoxazolyl 3'-CH₃); *m/z* (ES) 448.2 (100%, [M+Na]⁺); HRMS Found: 448.1720 (C₂₀H₂₃N₇O₄, M+Na requires 448.1704).

Ethyl 2-((4*S, 5*S**)-5-(azidomethyl)-4-((3,5-dimethylisoxazol-4-yl)methyl)-3-(furan-2-yl methyl)-2-oxoimidazolidin-1-yl)acetate **95**^{124,137}**



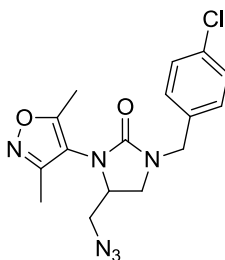
The *title compound* **95** was prepared from the allyl urea **86** (1.4 mmol) according to **general procedure F**.^{124,137} The crude product was purified by flash chromatography (99.5:0.5, CH₂Cl₂-MeOH) to give a yellow oil (116 mg, 20% over two steps). *R*_F: 0.6 (94:6, CH₂Cl₂-MeOH); $\nu_{\max}/\text{cm}^{-1}$ (film) 2934, 2107, 1742, 1704, 1457, 1202, 1015, 754; δ_{H} (500 MHz; CDCl₃, 325 K) 7.37 (1H, dd, *J* 1.8 and 0.8, furanyl 5-H), 6.34 (1H, dd, *J* 3.2 and 1.8, furanyl 4-H), 6.23 (1H, dd, *J* 3.2 and 0.8, furanyl 3-H), 4.85 (1H, d, *J* 15.8, 3-CH_AH_B), 4.43 (1H, d, *J* 18.1, CH_AH_BCO₂Et), 4.20 (2H, qd, *J* 7.1 and 3.3 ethyl 1-H₂), 4.04 (1H, d, *J* 15.8, 3-CH_AH_B), 3.69 (1H, d, *J* 18.1, CH_AH_BCO₂Et), 3.37 (1H, app. td, *J* 5.3 and 4.1, 4-H), 3.29 (1H, ddd, *J* 9.1, 5.1 and 4.1, 5-H), 3.09 (1H, dd, *J* 12.6 and 5.2, 4-CH_AH_B), 3.04 (1H, dd, *J* 12.6 and 5.6, 4-CH_AH_B), 2.81 (1H, dd, *J* 14.4 and 5.1, 5-CH_AH_B), 2.54 (1H, dd, *J* 14.4 and 9.1, 5-CH_AH_B), 2.32 (3H, s, isoxazolyl 5-CH₃), 2.17 (3H, s, isoxazolyl 3-CH₃), 1.29 (3H, t, *J* 7.1, ethyl 2-H₃); δ_{C} (75 MHz; CDCl₃) 169.6 (CO₂Et), 166.5 (isoxazolyl C-5), 159.4 (isoxazolyl C-3), 158.5 (NCON), 150.1 (furanyl C-2), 142.6 (furanyl C-5), 110.6 (furanyl C-4), 108.8 (furanyl C-3), 108.6 (isoxazolyl C-4), 61.4 (ethyl C-1), 57.6 (C-4), 55.5 (C-5), 51.4 (4-CH₂), 43.5 (CH₂CO₂Et), 38.9 (3-CH₂), 26.0 (5-CH₂), 14.2 (ethyl C-2), 11.1 (isoxazolyl 5-CH₃), 10.3 (isoxazolyl 3-CH₃); *m/z* (ES) 439.4 (100%, [M+Na]⁺). HRMS Found: 439.2204 (C₁₉H₂₄N₆O₅, M+Na requires 439.2197).

(4*S, 5*S**)-4-(Azidomethyl)-1-(4-chlorobenzyl)-3-(3,5-dimethylisoxazol-4-yl)-5-((3,5-dimethyl isoxazol-4-yl)methyl)imidazolidin-2-one **98**^{124,137}**



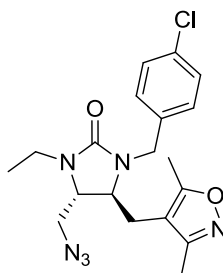
The *title compound* **98** was prepared from the allyl urea **87** (0.7 mmol) according to **general procedure F**.^{124,137} The crude product was purified by flash chromatography (99.5:0.5, CH₂Cl₂–MeOH) to give a yellow oil (65 mg, 20% over two steps). *R*_F: 0.3 (95:5, CH₂Cl₂–MeOH); $\nu_{\max}/\text{cm}^{-1}$ (film) 2926, 2109, 1688, 1492, 1440, 1424, 1218, 1200, 1062, 733; δ_{H} (500 MHz; CDCl₃) 7.37 (2H, d, *J* 8.3, phenyl 3- and 5-H), 7.26 (2H, d, *J* 8.3, phenyl 2- and 6-H), 5.03 (1H, d, *J* 14.9, benzyl CH_AH_B), 4.12 (1H, d, *J* 14.9, benzyl CH_AH_B), 4.11 (1H, app. q, *J* 4.5, 5-H), 3.53 (1H, app. dt, *J* 8.6 and 5.0, 4-H), 3.32 (1H, dd, *J* 13.5 and 4.3, 5-CH_AH_B), 3.04 (1H, dd, *J* 13.5 and 4.1, 5-CH_AH_B), 2.72 (1H, dd, *J* 14.8 and 5.2, 4-CH_AH_B), 2.44 (1H, dd, *J* 14.8 and 8.6, 4-CH_AH_B), 2.25 (3H, s, isoxazolyl 5-CH₃), 2.24 (3H, s, isoxazolyl 5'-CH₃), 2.15 (3H, s, isoxazolyl 3-CH₃), 2.09 (3H, s, isoxazolyl 3'-CH₃); δ_{C} (75 MHz; CDCl₃) 166.3 (isoxazolyl C-5), 158.9 (isoxazolyl C-3), 156.6 (isoxazolyl C-5'), 153.1 (CO), 134.3 (phenyl C-4), 134.1 (phenyl C-1), 129.6 (phenyl C-3 and C-5), 129.1 (phenyl C-2 and C-6), 107.8 (isoxazolyl C-4), 79.4 (C-5), 56.9 (C-4), 52.5 (5-CH₂), 46.8 (benzyl CH₂), 25.8 (4-CH₂), 11.2 (isoxazolyl 5-CH₃), 11.1 (isoxazolyl 5'-CH₃), 10.3 (isoxazolyl 3-CH₃), 9.9 (isoxazolyl 3'-CH₃), isoxazolyl C-3' and isoxazolyl C-4 not observed; *m/z* (ES) 470.4 (100%, [M+H]⁺); HRMS Found: 470.1709 (C₂₂H₂₄ClN₇O₃, M+H requires 470.1702).

4-(Azidomethyl)-1-(4-chlorobenzyl)-3-(3,5-dimethylisoxazol-4-yl)imidazolidin-one
100^{124,137}



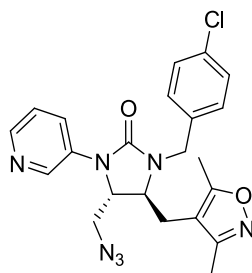
The *title compound* **100** was prepared from the allyl urea **88** (1.5 mmol) according to **general procedure F**.^{124,137} The crude product was purified by flash chromatography (20:80, hexane–EtOAc) to give a yellow oil (97 mg, 18% over two steps). R_F : 0.7 (96.5:3.5, CH₂Cl₂–MeOH); $\nu_{\max}/\text{cm}^{-1}$ (film) 3404, 3226, 2107, 1682, 1443, 1254, 1045, 814; δ_H (500 MHz; CDCl₃) 7.35 (2H, d, J 8.5, phenyl 3- and 5-H), 7.31 (2H, d, J 8.5, phenyl 2- and 6-H), 4.65 (1H, app. ddt, J 8.5, 6.3 and 4.4, 4-H), 4.54 (2H, s, benzyl CH₂), 3.58 (1H, dd, J 13.3 and 4.3, 4-CH_AH_B), 3.50 (1H, app. t, J 8.5, 5-H_A), 3.42 (1H, dd, J 13.3 and 4.5, 4-CH_AH_B), 3.27 (1H, dd, J 8.6 and 6.3, 5-H_B), 2.26 (3H, s, isoxazolyl 5-CH₃), 2.17 (3H, s, isoxazolyl 3-CH₃); δ_C (75 MHz; CDCl₃) 156.8 (isoxazolyl C-5), 156.4 (isoxazolyl C-3), 153.2 (CO), 134.6 (phenyl C-1), 133.8 (phenyl C-4), 129.5 (phenyl C-3 and C-5), 129.0 (phenyl C-2 and C-6), 122.9 (isoxazolyl C-4), 74.0 (C-4), 52.8 (benzyl CH₂), 48.4 (C-5), 47.6 (4-CH₂), 11.0 (isoxazolyl 3-CH₃), 9.9 (isoxazolyl 5-CH₃); m/z (ES) 361.3 (100%, [M+H]⁺); HRMS Found: 361.1180 (C₁₆H₁₇ClN₆O₂, M+H requires 361.1179).

(4*S, 5*S**)-4-(azidomethyl)-1-(4-chlorobenzyl)-5-((3,5-dimethylisoxazol-4-yl)methyl)-3-ethyl imidazolidin-2-one **102**^{124,137}**



The *title compound* **102** was prepared from the allyl urea **89** (0.9 mmol) according to **general procedure F**.^{124,137} The crude product was purified by flash chromatography (99.5:0.5, CH₂Cl₂–MeOH) to give a yellow oil (25 mg, 7% over two steps). *R*_F: 0.8 (96:4, CH₂Cl₂–MeOH); $\nu_{\text{max}}/\text{cm}^{-1}$ (film) 3456, 2930, 2109, 1696, 1495, 1087, 936; δ_{H} (500 MHz; CDCl₃) 7.30 (2H, dd, *J* 8.2, phenyl 3- and 5-H), 6.92 (2H, d, *J* 8.2, phenyl 2- and 6-H), 4.30 (1H, app. td, *J* 4.7 and 2.6, 5-H), 4.11 (1H, d, *J* 14.7, benzyl CH_AH_B), 4.04 (1H, d, *J* 14.7, benzyl CH_AH_B), 3.64 (1H, dd *J* 12.7 and 2.6, 5-CH_AH_B), 3.42 (1H, m, 4-H), 3.39 (1H, dd, *J* 12.7 and 6.1, 5-CH_AH_B), 3.18–3.12 (3H, m, 4-CH_AH_B and ethyl 1-H₂), 2.75 (1H, dd, *J* 14.5 and 4.5, 4-CH_AH_B), 2.21 (3H, s, isoxazolyl 5-CH₃), 2.18 (3H, s, isoxazolyl 3-CH₃) 1.00 (3H, t, *J* 6.7, ethyl 2-H₃); δ_{C} (75 MHz; CDCl₃) 166.2 (isoxazolyl C-5), 159.6 (isoxazolyl C-3), 157.7 (CO), 134.7 (phenyl C-4), 134.1 (phenyl C-1), 129.4 (phenyl C-3 and C-5), 127.9 (phenyl C-2 and C-6), 110.5 (isoxazolyl C-4), 64.9 (C-5), 53.0 (C-4), 39.7 (benzyl CH₂), 35.6 (5-CH₂), 29.7 (ethyl C-1), 22.5 (4-CH₂), 15.3 (ethyl C-3), 10.9 (isoxazolyl 5-CH₃), 10.2 (isoxazolyl 3-CH₃); *m/z* (ES) 403.2 (100%, [M+H]⁺); HRMS Found: 403.1650 (C₁₉H₂₃ClN₆O₂, M+H requires 403.1649).

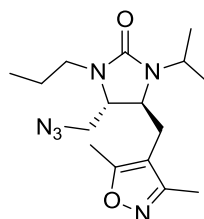
(4*S, 5*S**)-4-(azidomethyl)-1-(4-chlorobenzyl)-5-((3,5-dimethylisoxazol-4-yl)methyl)-3-(pyridin-3-yl)imidazolidin-2-one **103**^{124,137}**



The *title compound* **103** was prepared from the allyl urea **90** (1.1 mmol) according to **general procedure F**.^{124,137} The crude product was purified by flash chromatography (99.2:0.8, CH₂Cl₂–MeOH) to give a yellow oil (89 mg, 18% over two steps). *R*_F: 0.2 (96:4, CH₂Cl₂–MeOH); $\nu_{\text{max}}/\text{cm}^{-1}$ (film) 2930, 2103, 1698, 1485, 1243, 1150, 1080, 801; δ_{H} (500 MHz; CDCl₃) 8.49 (1H, app. s, py 4-H), 8.41 (1H, s, py 2-H), 8.24 (1H, app. d, *J* 3.9, py 6-H), 7.38 (2H, dd, *J* 8.4, phenyl 3- and 5-H), 7.36–7.33 (1H, app. m, py 5-H), 7.28 (2H, d, *J* 8.4, phenyl 2- and 6-H), 5.11 (1H, d, *J* 15.3, benzyl CH_AH_B), 4.19 (1H, app. dd, *J* 5.1 and 4.3, 5-H)^a, 4.15 (1H, d, *J* 15.3, benzyl CH_AH_B), 3.99 (1H, app. dt, *J* 9.0 and 5.1, 4-H), 3.35 (1H, dd, *J* 13.4 and 4.1, 5-CH_AH_B), 3.01 (1H, dd, *J* 13.4 and 4.2, 5-CH_AH_B), 2.76 (1H, dd, *J* 14.7 and 5.3, 4-CH_AH_B), 2.44 (1H, dd, *J* 14.7 and 9.0, 4-CH_AH_B), 2.25 (3H, s, isoxazolyl 5-CH₃), 2.07 (3H, s, isoxazolyl 3-CH₃); δ_{C} (75 MHz; CDCl₃) 166.3 (isoxazolyl C-5), 160.3 (isoxazolyl C-3), 159.0 (CO), 154.4, 145.7, 143.5 (py CH), 140.6 (py C-1) 134.2 (phenyl C-4), 130.2 (phenyl C-1), 129.7 (phenyl C-3 and C-5), 129.6 (phenyl C-2 and C-6), 107.9 (isoxazolyl C-4), 79.4 (C-5), 56.4 (C-4), 52.6 (5-CH₂), 46.8 (benzyl CH₂), 25.9 (4-CH₂), 11.2 (isoxazolyl 5-CH₃), 10.3 (isoxazolyl 3-CH₃); *m/z* (ES) 452.2 (100%, [M+H]⁺); HRMS Found: 452.1601 (C₂₂H₂₂ClN₇O₂, M+H requires 452.1596).

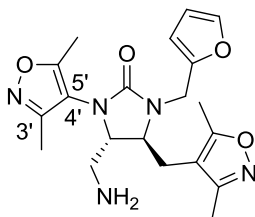
^a Overlapping with signal at δ_{H} 4.15

(4*S, 5*S**)-4-(azidomethyl)-5-((3,5-dimethylisoxazol-4-yl)methyl)-3-isopropyl-1-propyl imidazolidin-2-one **107**^{124,137}**



The *title compound* **107** was prepared from the allyl urea **92** (0.3 mmol) according to **general procedure F**.^{124,137} The crude product was purified by flash chromatography (50:50, petrol–EtOAc) to give a yellow oil (13 mg, 13% over two steps). R_F : 0.1 (99:1, CH₂Cl₂–MeOH); $\nu_{\max}/\text{cm}^{-1}$ (film) 2962, 2930, 2106, 1699, 1635, 1455, 1198, 1035, 931, δ_H (500 MHz; CDCl₃) 4.12 (1H, hept, J 6.9, *isopropyl CH*), 3.97 (1H, app. td, J 5.2 and 3.0, 5-H), 3.55 (1H, app. dt J 10.5 and 3.5, 4-H), 3.20-3.16 (2H, m, propyl 1-H₂), 3.12-3.05 (2H, m, 5-CH_AH_B and 5-CH_AH_B), 2.77 (1H, dd, J 14.6 and 3.9, 4-CH_AH_B), 2.43 (1H, dd, J 14.6 and 10.5, 4-CH_AH_B), 2.37 (3H, s, isoxazolyl 5-CH₃), 2.26 (3H, s, isoxazolyl 3-CH₃), 1.54-1.47 (2H, m, propyl 2-H₂), 1.31 (1H, d, J 6.8, *isopropyl CH_{3A}*), 1.26 (1H, d, J 6.9, *isopropyl CH_{3B}*), 0.9 (3H, t, J 7.4, propyl-3H₃); δ_C (75 MHz; CDCl₃) 170.3 (isoxazolyl C-5), 166.7 (isoxazolyl C-3), 159.2 (CO), 108.9 (isoxazolyl C-4), 77.8 (C-5), 55.7 (C-4), 53.1 (5-CH₂), 48.3 (propyl C-1), 46.0 (*isopropyl CH*), 28.3 (4-CH₂) 25.3 (propyl C-2), 22.0, 19.3 (*isopropyl CH_{3A}* and *CH_{3B}*) 15.6 (propyl C-3), 11.3 (isoxazolyl 5-CH₃), 10.6 (isoxazolyl 3-CH₃); m/z (ES) 335.0 (100%, [M+H]⁺); HRMS Found: 335.2202 (C₁₆H₂₆N₆O₂, M+H requires 335.2190).

(4*S, 5*S**)-4-(Aminomethyl)-3-(3,5-dimethylisoxazol-4-yl)-5-((3,5-dimethylisoxazol-4-yl) methyl)-1-(furan-2-ylmethyl)imidazolidin-2-one **94**¹³⁸**

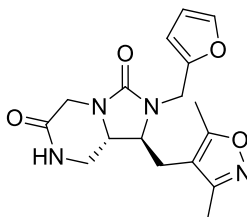


The *title compound* **94** was prepared from the azide **93** (0.1 mmol) and trimethylphosphine (solution 1 M in THF, 0.16 mL, 0.16 mmol), according to **general procedure G**.¹³⁸ The crude product was purified by HPLC (5:95, MeCN–H₂O in 45 minutes) to give a yellow oil (8.0 mg, 18%). *R*_F: 0.3 (95:5, CH₂Cl₂–MeOH)^a; δ_H (500 MHz; CDCl₃) 7.43 (1H, d, *J* 1.9, furanyl 5-H), 6.33 (1H, dd, *J* 3.1 and 1.9, furanyl 4-H), 6.27 (1H, d, *J* 3.1 furanyl 3-H), 4.70 (1H, d, *J* 15.8, 3-CH_AH_B), 4.10 (1H, d, *J* 15.8, 3-CH_AH_B), 3.60 (1H, app. td, *J* 5.6 and 3.8, 5-H), 3.31 (1H, app. dt, *J* 7.6 and 3.6, 4-H), 2.73 (1H, app. d, *J* 5.8, 5-CH_AH_B), 2.72 (1H, app. d, *J* 5.4, 5-CH_AH_B)^b, 2.49 (1H, dd, *J* 13.1 and 3.4, 4-CH_AH_B), 2.35 (1H, dd, *J* 13.1 and 7.6, 4-CH_AH_B), 2.29 (3H, s, isoxazolyl 5-CH₃), 2.11 (6H, s, isoxazolyl 5'-CH₃ and isoxazolyl 3-CH₃), 1.97 (3H, s, isoxazolyl 3'-CH₃), NH₂ not observed; δ_C (75 MHz; CDCl₃) 168.6 (isoxazolyl C-5), 168.2 (isoxazolyl C'-5), 161.5 (CO) 160.1 (isoxazolyl C-3), 159.8 (isoxazolyl C-3'), 151.5 (furanyl C-2), 144.2 (furanyl C-5), 111.7 (isoxazolyl C-4), 111.6 (furanyl C-4), 110.7 (isoxazolyl C-4'), 110.2 (furanyl C-3), 63.5 (C-5), 57.3 (C-4), 44.2 (5-CH₂), 40.3 (3-CH₂), 26.7 (4-CH₂), 11.3 (isoxazolyl 5-CH₃), 11.0 (isoxazolyl 5'-CH₃), 10.5 (isoxazolyl 3-CH₃), 9.7 (isoxazolyl 3'-CH₃); *m/z* (ES) 400.32 (100%, [M+H]⁺); HRMS Found: 400.1988 (C₂₀H₂₅N₅O₄ M+H requires 400.1979).

^a Insufficient quantity to perform the I.R. analysis

^b Signal overlapping with the one at 2.73

(1*S, 8*aS**)-1-((3,5-Dimethylisoxazol-4-yl)methyl)-2-(furan-2-ylmethyl) tetrahydroimidazo[1,5-*a*]pyrazine-3,6(5*H*,7*H*)-dione **97**¹³⁸**

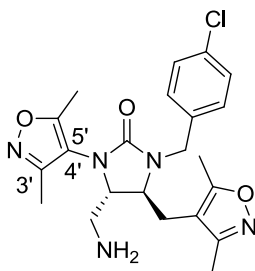


The *title compound* **97** was prepared from the azide **95** (0.07 mmol) and trimethylphosphine (solution 1M in THF, 0.1 mL, 0.1 mmol), according to **general procedure G**.¹³⁸ The crude product was purified by HPLC (5:95, MeCN–H₂O in 45 minutes) to give a yellow oil (2.0 mg, 8%). *R*_F: 0.2 (94:6, CH₂Cl₂–MeOH)^a; δ_H (500 MHz; CDCl₃) 7.39 (1H, dd, *J* 1.2 and 0.5, furanyl 5-H), 6.36 (1H, dd, *J* 2.8 and 1.2, furanyl 4-H), 6.27 (1H, dd, *J* 2.8 and 0.5, furanyl 3-H), 4.88 (1H, d, *J* 15.7, 2-CH_AH_B), 4.49 (1H, d, *J* 18.1, 5-*H*_A), 4.03 (1H, d, *J* 15.7 2-CH_AH_B), 3.73 (1H, d, *J* 18.1, 5-*H*_B), 3.36 (1H, app. dt *J* 10.6 and 3.7, 9-H), 3.12 (1H, app. dt, *J* 9.3, and 3.5, 1-H), 3.07 (1H, app. t, *J* 11.2, 8-*H*_A), 2.90 (1H, dd, *J* 11.5 and 4.5, 8-*H*_B), 2.85 (1H, dd, *J* 14.6, 5.3, 1-CH_AH_B), 2.45 (1H, dd, *J* 14.6, 9.3, 1-CH_AH_B), 2.33 (3H, s, isoxazolyl 5-CH₃), 2.17 (3H, s, isoxazolyl 3-CH₃), NH not observed; δ_C (75 MHz; MeOD-*d*4)^b 168.9 (CO₂NH), 166.9 (isoxazolyl C-5), 160.1 (isoxazolyl C-3), 159.1 (NCON), 150.9 (furanyl C-2), 144.3 (furanyl C-5), 111.6 (furanyl C-4), 110.3 (furanyl C-3), 109.0 (isoxazolyl C-4), 57.6 (ethyl C-1), 54.6 (C-9), 45.2 (1-CH₂), 44.8 (C-5), 39.7 (2-CH₂), 25.7 (C-8), 17.4 (isoxazolyl 5-CH₃), 16.9 (isoxazolyl 3-CH₃); *m/z* (ES) 367.1 (100%, [M+Na]⁺); HRMS Found: 367.1379 (C₁₇H₂₀N₄O₄, M+Na requires 367.1377).

^a Quantity was not sufficient to perform the I.R. analysis

^b Quaternary carbons assigned through HMBC experiment

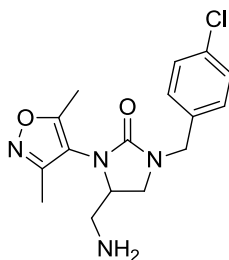
(4*S, 5*S**)-4-(aminomethyl)-1-(4-chlorobenzyl)-3-(3,5-dimethylisoxazol-4-yl)-5-((3,5-dimethyl isoxazol-4-yl)methyl)imidazolidin-2-one **99**¹³⁸**



The *title compound* **98** was prepared from the azide **99** (0.11 mmol) and trimethylphosphine (solution 1 M in THF, 0.17 mL, 0.17 mmol), according to **general procedure G**.¹³⁸ The crude product was purified by mass directed chromatography (5:95, MeOH–H₂O) to give a yellow oil (4.6 mg, 9%). *R*_F: 0.2 (95:5, CH₂Cl₂–MeOH)^a; δ_{H} (500 MHz; MeOD-*d*₄) 7.55–7.46 (4H, m, phenyl 3-, 5-, 2- and 6-H), 5.01 (1H, d, *J* 15.5, benzyl CH_AH_B), 4.61 (app. dt, *J* 8.8 and 4.3, 5-H), 4.47 (1H, d, *J* 15.5, benzyl CH_AH_B), 3.79 (1H, app. dt *J* 6.4 and 4.9, 4-H), 3.02 (1H, dd, *J* 14.0 and 8.8, 5-CH_AH_B), 2.99 (1H, d, *J* 14.0 and 4.1, 5-CH_AH_B), 2.95 (1H, dd, *J* 15.1 and 4.9, 4-CH_AH_B), 2.50 (1H, dd, *J* 15.1 and 6.4, 4-CH_AH_B), 2.41 (3H, s, isoxazolyl 5-CH₃), 2.26 (3H, s, isoxazolyl 5'-CH₃), 2.23 (3H, s, isoxazolyl 3-CH₃), 2.15 (3H, s, isoxazolyl 3'-CH₃), NH₂ not observed; δ_{C} (75 MHz; MeOD-*d*₄) 168.8 (isoxazolyl C-5), 161.1 (isoxazolyl C-3), 158.2 (isoxazolyl C-5'), 158.1 (CO), 154.4 (isoxazolyl C-3'), 135.3 (phenyl C-4), 131.0 (phenyl C-2 and C-6), 130.5 (phenyl C-1), 130.3 (phenyl C-3 and C-5), 114.2 (isoxazolyl C-4), 109.4 (isoxazolyl C-4'), 79.8 (C-5), 60.3 (C-4), 47.4 (benzyl CH₂), 43.0 (5-CH₂), 25.2 (4-CH₂); 11.3 (isoxazolyl 5-CH₃), 10.9 (isoxazolyl 5'-CH₃), 10.4 (isoxazolyl 3-CH₃), 9.9 (isoxazolyl 3'-CH₃); *m/z* (ES) 444.3 (100%, [M+H]⁺); HRMS Found: 444.1800 (C₂₂H₂₆ClN₅O₃, M+H requires 444.1797).

^a Insufficient quantity to perform the I.R. analysis

4-(Aminomethyl)-1-(4-chlorobenzyl)-3-(3,5-dimethylisoxazol-4-yl)imidazolidin-2-one **101**¹³⁸

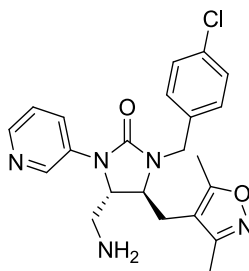


The *title compound* **101** was prepared from the azide **100** (0.27 mmol) and trimethylphosphine (solution 1 M in THF, 0.41 mL, 0.41 mmol), according to **general procedure G**¹³⁸. The crude product was purified by HPLC (5:95, MeCN–H₂O in 45 minutes) to give a yellow oil (2.6 mg, 7%). *R*_F: 0.4 (95:5, CH₂Cl₂–MeOH)^a; δ_H (500 MHz; DMSO-*d*₆) 7.44 (2H, d, *J* 8.5, phenyl 3- and 5-H), 7.41 (2H, d, *J* 8.5, phenyl 2- and 6-H), 4.84 (1H, app. ddt, *J* 8.5, 7.7 and 4.0, 4-H), 4.52 (1H, d, *J* 15.3, benzyl CH_AH_B), 4.47 (1H, d, *J* 15.3, benzyl CH_AH_B), 3.59 (1H, app. t, *J* 8.5, 4-CH_AH_B), 3.25 (1H, app d, *J* 8.5, 4-CH_AH_B)^b, 3.16 (1H, dd, *J* 13.8 and 4.0, 5-H_A), 3.08 (1H, dd, *J* 13.8 and 7.7, 5-H_B), 2.18 (3H, s, isoxazolyl 5-CH₃), 2.03 (3H, s, isoxazolyl 3-CH₃), NH₂ not observed; δ_C (75 MHz; DMSO-*d*₆) 156.2 (isoxazolyl C-5), 155.4 (isoxazolyl C-3), 153.0 (CO), 135.6 (phenyl C-4), 132.0 (phenyl C-1), 129.9 (phenyl C-2 and C-6), 128.5 (phenyl C-3 and C5), 95.9 (isoxazolyl C-4), 73.2 (C-4), 48.0 (4-CH₂), 47.4 (benzyl CH₂), 40.1 (C-5), 10.9 (isoxazolyl 5-CH₃), 9.7 (isoxazolyl 3-CH₃); *m/z* (ES) 335.1 (100%, [M+H]⁺); HRMS Found: 669.2457 (C₁₆H₁₉ClN₄O₂, M₂+H requires 669.2465).

^a Insufficient quantity to perform the I.R. analysis

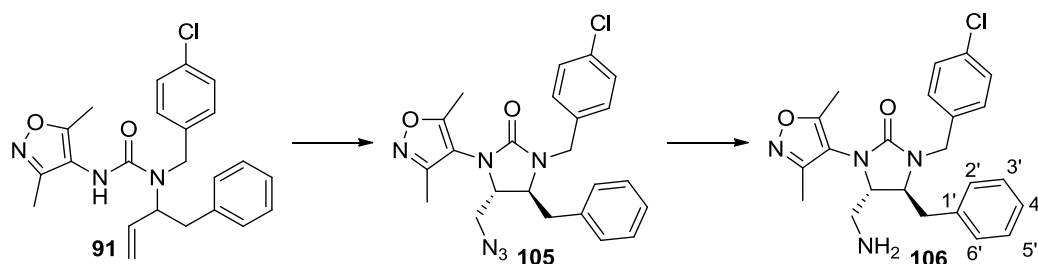
^b Signal masked by solvent

(4*S, 5*S**)-4-(Aminomethyl)-1-(4-chlorobenzyl)-5-((3,5-dimethylisoxazol-4-yl)methyl)-3-(pyridin-3-yl)imidazolidin-2-one **104**¹³⁸**



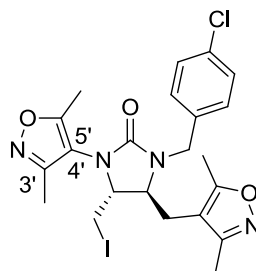
The *title compound* **104** was prepared from the azide **103** (0.23 mmol) and triphenylphosphine (90 mg, 0.34 mmol), according to **general procedure G**.¹³⁸ The crude product was purified by flash chromatography (99:1, CH₂Cl₂-MeOH); to give a yellow oil (28 mg, 27%). *R*_F: 0.4 (92:8, CH₂Cl₂-MeOH); *v*_{max}/cm⁻¹ (film) 3407, 2922, 1695, 1488, 1432, 1252, 1086, 739; δ _H (500 MHz; CDCl₃) 8.61 (1H, d, *J* 2.5 py 2-H), 8.34 (1H, dd, *J* 4.5 and 1.1, py 4-H), 8.12 (1H, ddd, *J* 8.4, 2.5 and 1.1, py 6-H), 7.34 (2H, dd, *J* 8.4, phenyl 3- and 5-H), 7.30 (1H, dd, *J* 8.4 and 4.5, py 5-H), 7.21 (2H, d, *J* 8.4, phenyl 2- and 6-H), 4.96 (1H, d, *J* 15.3, benzyl CH_AH_B), 4.02 (1H, d, *J* 15.3, benzyl CH_AH_B), 3.74 (1H, app. dt *J* 6.3 and 3.2, 4-H), 3.59 (1H, ddd, *J* 8.5, 5.6 and 3.2, 5-H), 2.73 (1H, dd, *J* 14.7 and 5.6, 5-CH_AH_B), 2.69 (1H, dd, *J* 13.5 and 6.3, 4-CH_AH_B), 2.59 (1H, dd, *J* 13.3 and 3.0, 4-CH_AH_B), 2.44 (1H, dd, *J* 14.7 and 8.5, 5-CH_AH_B), 2.27 (3H, s, isoxazolyl 5-CH₃), 2.11 (3H, s, isoxazolyl 3-CH₃), NH₂ not observed; δ _C (75 MHz; CDCl₃) 166.2 (isoxazolyl C-5), 159.3 (isoxazolyl C-3), 156.6 (phenyl C-1), 144.6 (py C-1), 140.5, (py C-5), 135.5 (phenyl C-4), 134.0 (CO), 133.9 (py C-4) 129.6 (phenyl C-3 and C-5), 129.0 (phenyl C-2 and C-6), 127.5 (py C-2), 123.7 (py C-6), 108.3 (isoxazolyl C-4), 59.8 (C-4), 54.2 (C-5), 45.5 (benzyl CH₂), 41.8 (5-CH₂), 26.8 (4-CH₂), 11.2 (isoxazolyl 5-CH₃), 10.4 (isoxazolyl 3-CH₃); *m/z* (ES) 426.2 (100%, [M+H]⁺); HRMS Found: 426.1704 (C₂₂H₂₂ClN₅O₂, M+H requires 426.1691).

(4*S, 5*S**)-4-(Aminomethyl)-5-benzyl-1-(4-chlorobenzyl)-3-(3,5-dimethylisoxazol-4-yl) imidazolidin-2-one **106**^{124,137, 138}**



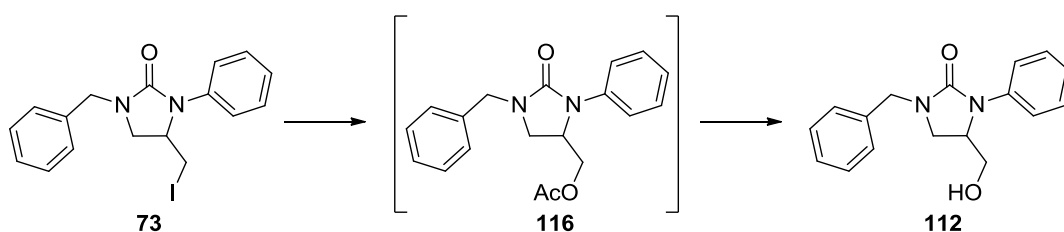
The azide **105** (0.08 mmol) was prepared from the allyl urea **91** (1.0 mmol) according to **general procedure F**.^{124,137} After elution through a silica plug (40:60, petrol–EtOAc) and evaporation under reduced pressure, the azide **105** was mixed with triphenylphosphine (0.03 g, 0.13 mmol) according to **general procedure G**¹³⁸ and the crude product was purified by flash chromatography (50:50 → 100:0, petrol–EtOAc); to give the *title imidazolidinone* **106**, as a yellow oil (11 mg, 2.5% over three steps). R_F : 0.1 (10:90, petrol–EtOAc); $\nu_{\max}/\text{cm}^{-1}$ (film) 2922, 1717, 1678, 1446, 1408, 1247, 1091, 1064, 725; δ_H (500 MHz; CDCl_3) 7.44 (3H, app. s, Ar CH), 7.39–7.36 (3H, m, Ar CH), 7.32–7.29 (1H, m, Ar CH), 7.28 (2H, dd, J 6.8 and 1.3, Ar CH), 4.95 (1H, d, J 15.7, benzyl CH_AH_B), 4.45 (1H, d, J 15.7, benzyl CH_AH_B), 4.41 (1H, app. dt J 6.9 and 4.7, 4-H), 3.99 (1H, app. dt, J 6.7 and 4.7, 5-H), 3.07 (1H, dd, J 13.8 and 4.5, 5- CH_AH_B), 2.99 (1H, dd, J 13.8 and 6.7, 5- CH_AH_B), 2.54 (1H, dd, J 13.7 and 6.9, 4- CH_AH_B), 2.47 (1H, dd, J 13.7 and 4.6, 4- CH_AH_B), 2.15 (3H, s, isoxazolyl 5- CH_3), 2.04 (3H, s, isoxazolyl 3- CH_3), NH_2 not observed; δ_C (75 MHz; CDCl_3) 158.5 (isoxazolyl C-5), 158.3 (isoxazolyl C-3), 156.8 (CO), 137.2 (phenyl C-1), 137.0 (phenyl C-1'), 134.7 (phenyl C-4), 130.9, 130.8, 129.9 (Ar CH) 129.5 (phenyl C-4'), 128.3 (Ar CH), 125.4 (isoxazolyl C-4), 83.9 (C-4), 61.4 (C-5), 46.8 (benzyl CH_2), 45.5 (4- CH_2), 38.8 (5- CH_2), 10.8 (isoxazolyl 5- CH_3), 9.8 (isoxazolyl 3- CH_3); m/z (ES) 425.2 (100%, $[\text{M}+\text{H}]^+$); HRMS Found: 425.1744 ($\text{C}_{23}\text{H}_{25}\text{ClN}_4\text{O}_2$, $\text{M}+\text{H}$ requires 425.1738).

(4*R, 5*S**)-1-(4-chlorobenzyl)-3-(3,5-dimethylisoxazol-4-yl)-5-((3,5-dimethylisoxazol-4-yl) methyl)-4-(iodomethyl)imidazolidin-2-one **111****¹²⁴



To a solution of the allyl urea **87** (0.1 mmol) in CH₂Cl₂ (0.22 M), trimethyltrifluoromethanesulfonate (0.1 mL, 0.56 mmol) was added, followed by DBU (90 μ L, 0.6 mmol) and the resulting mixture was stirred at r.t. for 1h and half. The solvent was removed under reduced pressure, the crude material was dissolved in dry THF (0.16 M), iodine was added (2.0 eq.) and the mixture was left stirring at r.t overnight, then at reflux for 3 h. The reaction mixture was poured in an aqueous saturated solution of Na₂S₂SO₄ (2.0 mL) and extracted with EtOAc (3 x 1.0 mL); the combined organic phases were dried (MgSO₄) and concentrated under reduced pressure. The crude product was purified by mass directed chromatography (5:95, CH₃CN-H₂O) to give the *imidazolidinone* **111** as a yellow oil (6 mg, 12%). *R*_F: 0.7 (10:10:80, toluene–petrol–EtOAc); $\nu_{\max}/\text{cm}^{-1}$ (film) 2926, 2853, 1686, 1632, 1424, 1261, 1088, 614; δ_{H} (500 MHz; CDCl₃) 7.37 (2H, d, *J* 8.3, phenyl 3- and 5-H), 7.26 (2H, d, *J* 8.3, phenyl 2- and 6-H), 5.02 (1H, d, *J* 15.2, benzyl CH_AH_B), 4.09 (1H, d, *J* 15.2, benzyl CH_AH_B), 4.04 (1H, app. dt *J* 6.5 and 4.5, 5-H), 3.54 (1H, ddd, *J* 8.2, 5.4 and 4.4, 4-H), 3.02-2.99 (2H, m, 5-CH_AH_B and 5-CH_AH_B), 2.71 (1H, dd, *J* 14.7 and 5.4, 4-CH_AH_B) 2.50 (1H, dd, *J* 14.7 and 8.2, 4-CH_AH_B), 2.28 (3H, s, isoxazolyl 5-CH₃), 2.27 (3H, s, isoxazolyl 5'-CH₃), 2.17 (3H, s, isoxazolyl 3-CH₃), 2.12 (3H, s, isoxazolyl 3'-CH₃); δ_{C} (75 MHz; CDCl₃) 166.4 (isoxazolyl C-5), 159.1 (isoxazolyl C-3), 156.6 (isoxazolyl C-5'), 156.4 (CO), 152.4 (isoxazolyl C-3'), 134.3 (phenyl C-4), 129.6 (phenyl C-2 and C-6), 129.2 (phenyl C-3 and C-5), 120.3 (phenyl C-1), 108.1 (isoxazolyl C-4), 105.0 (isoxazolyl C-4'), 79.6 (C-5), 60.2 (C-4), 46.8 (benzyl CH₂), 25.8 (5-CH₂), 11.3 (isoxazolyl 5-CH₃), 11.3 (isoxazolyl 5'-CH₃), 10.4 (isoxazolyl 3-CH₃), 10.2 (isoxazolyl 3'-CH₃), 5.2 (4-CH₂); *m/z* (ES) 555.0 (100%, [M+H]⁺); HRMS Found: 555.0664 (C₂₂H₂₄ClIN₄O₃, M+H requires 555.0670).

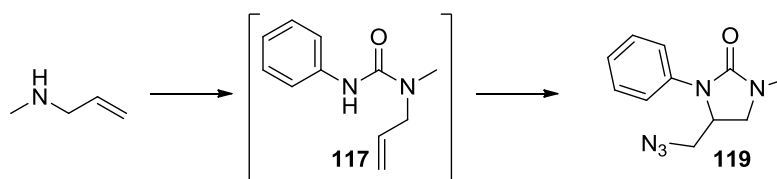
1-Benzyl-4-(hydroxymethyl)-3-phenylimidazolidin-2-one, **112**¹⁵⁵



AgOAc (70 mg, 0.4 mmol) was added to a solution of the iodide **73** (70 mg, 0.17 mmol) in AcOH (1.7 mL) and the resulting mixture was stirred at 70 °C for three days. The mixture was allowed to reach r.t., then CH₂Cl₂ (15 mL) and an aqueous saturated solution of NaHCO₃ (15 mL) were added portion wise. The phases were separated and the organic phase was washed with H₂O (2 x 8.0 mL) and brine (2 x 8.0 mL), dried (MgSO₄) and concentrated under reduced pressure to give a crude product **116** which was used without further purification.

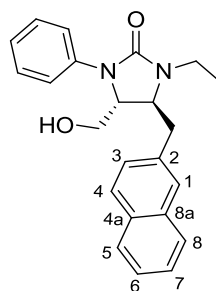
K₂CO₃ (30 mg, 0.22 mmol) was added to a solution of **116** (35 mg, 0.1 mmol) in MeOH (2.0 mL) and the resulting mixture was stirred at r.t. for 36 hours. The solvent was removed and the crude material was partitioned between CH₂Cl₂ (5.0 mL) and H₂O (5.0 mL); the phases were separated and the organic phase was washed with brine (2 x 2.0 mL), dried (MgSO₄) and concentrated under reduced pressure. The crude product was purified by flash chromatography (50:50, hexane–EtOAc) to give the *title imidazolidione* **112** as a yellow oil (13.6 mg, 28% over two steps). *R*_F: 0.35 (40:60, petrol–EtOAc); *v*_{max}/cm⁻¹ (film) 3369, 2961, 2927, 1681, 1446, 1260, 1088, 800; *δ*_H (500 MHz; CDCl₃) 7.50 (2H, d *J* 8.3, Ar CH), 7.42-7.27 (7H, m, Ar CH), 7.11 (1H, t, *J* 7.5, Ar CH), 4.54 (1H, d, *J* 15.0, benzyl CH_AH_B), 4.42 (1H, d, *J* 15.0, benzyl CH_AH_B), 4.35 (1H, app. dtd, *J* 9.2, 5.1 and 3.0, 4-H), 3.77 (1H, dd, *J* 11.3 and 5.2, 4-CH_AH_B), 3.64 (1H, dd, *J* 11.3 and 3.0, 4-CH_AH_B), 3.47 (1H, app. t, *J* 9.2, 5-H_A), 3.36 (1H, dd, *J* 8.9 and 5.1, 5-H_B), OH not observed; *δ*_C (75 MHz; CDCl₃) 158.0 (CO), 129.1, 128.7, 128.2 (Ar 3 x CH), 127.6, 124.0 (Ar 2 x C), 121.1 (Ar CH), 61.3 (4-CH₂), 54.3 (C-4), 48.0 (benzyl CH₂), 44.4 (C-5); *m/z* (ES) 305.0 (100%, [M+Na]⁺); HRMS Found: 305.1262 (C₁₇H₁₈N₂O₂ M+Na requires 305.1260).

4-(Azidomethyl)-1-methyl-3-phenylimidazolidin-2-one, compound **119**^{100, 124,137}



The urea **117** was prepared from methyl allyl amine (70 μ L, 0.7 mmol) and phenylisocyanate (0.15 mL, 1.4 mmol) with stirring overnight according to **general procedure B**.¹⁰⁰ The reaction mixture was filtered and concentrated under reduced pressure to give a crude product which was used without further purification for the preparation of the azide **119** according to **general procedure F**^{124,137}. The crude product was purified by flash chromatography (70:30, hexane–EtOAc) to give the *title azide* **119** as a white solid (22 mg, 14% over three steps). R_F : 0.2 (50:50, petrol–EtOAc); m.p. 62–65 °C; $\nu_{\max}/\text{cm}^{-1}$ (film) 2933, 2868, 2094, 1687, 1494, 1427, 1377, 1248, 1160, 747; δ_H (500 MHz; CDCl₃) 7.44 (2H, m, phenyl 2- and 6-H), 7.36 (2H, m, phenyl 4-H), 7.12 (1H, tt, J 7.4 and 1.1, phenyl 3- and 5-H), 4.39 (1H, dddd, J 9.9, 6.6, 4.6 and 3.2, 4-H), 3.59 (1H, app. t, J 9.1, 5-H_A), 3.50 (1H, dd, J 12.6 and 6.6, 4-CH_AH_B), 3.44 (1H, dd, J 12.6 and 3.2, 4-CH_AH_B), 3.36 (1H, dd, J 9.1 and 4.6, 5-H_B), 2.9 (3H, s, CH₃); δ_C (75 MHz; CDCl₃) 157.9 (CO), 138.1 (phenyl C-1), 129.2 (phenyl C-2 and C-6), 124.2 (phenyl C-4), 121.1 (phenyl C-3 and C-5), 51.3 (C-4), 47.9 (4-CH₂), (C-5), 31.0 (CH₃); m/z (ES) 254.0 (100%, [M+Na]⁺); HRMS Found: 232.1202 (C₁₁H₁₃N₅O M+H requires 232.1193).

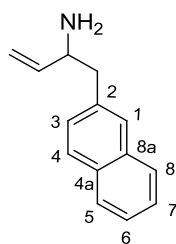
(4*R, 5*S**)-1-Ethyl-4-(hydroxymethyl)-5-(naphthalen-2-ylmethyl)-3-phenyl imidazolidin-2-one, **114**¹⁵⁶**



A few drops of hydrochloric acid (12 M) were added to a solution of the imidazolidinone **60** (40 μ mol) in MeOH (0.6 mL) and the resulting mixture was stirred at r.t. for 2 days. Water (1.0 mL) was added and the mixture was extracted with EtOAc; the organic phase was washed with brine (2 x 1.0 mL), dried (MgSO_4) and concentrated under reduced pressure to give a crude product which was purified by flash chromatography to give the *title imidazolidinone* **114** as an amorphous solid (6 mg, 42%). R_F : 0.25 (40:60, petrol–EtOAc); $\nu_{\text{max}}/\text{cm}^{-1}$ (film) 3385, 2931, 1677, 1501, 1431, 1261, 1060, 909, 750; δ_H (500 MHz; CDCl_3) 7.85–7.79 (3H, m, naphthalenyl 3-, 4- and 5- or 8-H), 7.65 (1H, s, naphthalenyl 1-H), 7.51–7.45 (2H, m, naphthalenyl 6- and 7-H), 7.39–7.34 (3H, m, naphthalenyl 5- or 8-H and phenyl 2- and 6-H), 7.28–7.28 (2H, m, phenyl 3- and 5-H),^a 7.03 (1H, app.t, J 7.5, phenyl 4-H), 4.09 (1H, app. dt, J 8.8 and 4.5, 5-H), 3.99 (1H, app. dt, J 7.1 and 4.5, 4-H), 3.73 (1H, dq, J 14.7 and 7.3, ethyl 1- H_A), 3.57 (1H, dd, J 11.7 and 4.7, 4- CH_AH_B), 3.34 (1H, dd, J 13.7 and 4.7, 5- CH_AH_B), 3.25–3.09 (2H, m, ethyl 1- H_B and 4- CH_AH_B), 2.88 (1H, dd, J 13.7 and 8.8, 5- CH_AH_B), 1.24 (3H, t, J 7.1, ethyl 2- H_3); δ_C (75 MHz; CDCl_3) 157.1 (CO), 138.8 (phenyl C-1), 133.7 (naphthalenyl C-2), 133.5, 132.4, (naphthalene C-1a and C-8a), 128.9 (phenyl C-3 and C-5), 128.6, 128.1, 127.7, 127.5, 127.2, 126.4, 125.8 (naphthalene 7 x CH), 123.6 (phenyl C-4), 120.5 (phenyl C-2 and C-6), 61.2 (4- CH_2), 59.6 (C-4), 55.2 (C-5), 39.5 (5- CH_2), 36.5 (ethyl C-1), 13.1 (ethyl C-2); m/z (ES) 383.2 (100%, $[\text{M}+\text{Na}]^+$); HRMS Found: 383.1736 ($\text{C}_{23}\text{H}_{24}\text{N}_2\text{O}_2$ M+Na requires 383.1729).

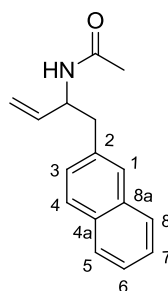
^a Signal masked by the solvent peak

1-(Naphthalen -2-yl)but-3-en-2-amine, **120**¹²⁶



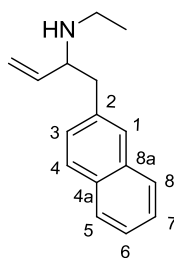
The *title compound* **120** was prepared from diphenyl methylene propenamine **78** (4.1 g, 18.4 mmol) and 2-chloromethylnaphthalenyl (3.2 mL, 18.4 mmol) in the presence of *n*-Butyl lithium (7.4 mL, 18.4 mmol) according to **general procedure D**.¹²⁶ A yellow oil was obtained and used without further purification (0.3 g, 20%). R_F : 0.1 (90:10, petrol–EtOAc); $\nu_{\max}/\text{cm}^{-1}$ (film) 3054, 2922, 1598, 1506, 1435, 1367, 994, 918, 814, 748; δ_H (500 MHz; CDCl_3) 7.83-7.78 (3H, m, naphthalenyl 3-, 4- and 5- or 8-H), 7.66 (1H, s, naphthalenyl 1-H), 7.48-7.43 (2H, m, naphthalenyl 6- and 7-H), 7.35 (1H, dd, J 8.4 and 1.6, naphthalenyl 5- or 8-H), 5.94 (1H, ddd, J 17.1, 10.3 and 6.26, 3-H), 5.17 (1H, dd, J 17.1 and 1.4, 4- H_A), 5.06 (1H, dd, J 10.3 and 1.4, 4- H_B), 3.74-3.69 (1H, m, 2-H), 3.00 (1H, dd, J 13.3 and 5.6, 1- H_A), 2.79 (1H, dd, J 13.3 and 8.3, 1- H_B), 1.5 (2H, br. s, NH_2); δ_C (75 MHz; CDCl_3) 142.4 (C-3), 136.2 (naphthalenyl C-4a), 133.4 (naphthalenyl C-2), 132.1 (naphthalenyl C-8a), 127.9, 127.8, 127.7, 127.6, 127.5, 125.9, 125.3 (naphthalene 7 x CH), 113.6 (C-4), 55.3 (C-2), 44.5 (C-1); HRMS Found: 198.1277 ($\text{C}_{14}\text{H}_{15}\text{N}$ $M+H$ requires 198.1275).

N*-(1-(Naphthalen-2-yl)but-3-en-2-yl)acetamide, **121*¹⁵⁷



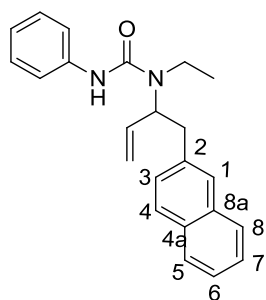
Triethylamine (0.8 ml, 6.2 mmol) and acetylchloride (0.5 mL, 7.3 mmol) were added at 0 °C to a solution of the amine **120** (0.70 g, 3.7 mmol) in CH₂Cl₂ and the resulting mixture was stirred at r.t. overnight. The mixture was filtered and concentrated under reduced pressure; the crude material was dissolved in the minimum amount of CH₂Cl₂, acetone was added until precipitation was completed and the precipitate was removed by filtration. The filtrate was concentrated under reduced pressure to give a crude product which was purified by flash chromatography (50:50, petrol–EtOAc) to yield the *title acetamide* **121** as yellow oil (0.48 g, 54%). *R*_F: 0.2 (40:60, petrol–EtOAc); $\nu_{\max}/\text{cm}^{-1}$ (film) 3282, 3052, 1655, 1542, 1432, 1369, 1278, 990, 816; δ_{H} (500 MHz; CDCl₃) 7.83–7.77 (3H, m, naphthalenyl 3-, 4- and 5- or 8-H), 7.62 (1H, s, naphthalenyl 1-H), 7.49–7.42 (2H, m, naphthalenyl 6- and 7-H), 7.33 (1H, dd, *J* 8.3 and 1.0, naphthalenyl 5- or 8-H), 5.86 (1H, ddd, *J* 16.2, 10.2 and 5.4, 3-H), 5.38 (1H, d, *J* 6.8, *NH*), 5.11 (1H, d, *J* 16.2, 4-H_A), 5.10 (1H, d, *J* 10.2, 4-H_B), 4.89 (1H, app. dq, *J* 6.8 and 5.4, 2-H), 3.04 (1H, d, *J* 6.8, 1-H_A), 3.03 (1H, d, *J* 6.1, 1-H_B), 1.95 (3H, s, CH₃); δ_{C} (75 MHz; CDCl₃) 169.3 (CO), 137.5 (C-3), 134.7 (naphthalenyl C-4a), 133.4 (naphthalenyl C-2), 132.3 (naphthalenyl C-8a), 128.8, 128.0, 127.8, 127.6, 127.5, 126.1, 125.6 (naphthalene 7 x CH), 115.3 (C-4), 52.0 (C-2), 41.1 (C-1), 23.4 (CH₃); *m/z* (ES) 262.1 (100%, [M+Na]⁺); HRMS Found: 262.1205 (C₁₆H₁₇NO M+Na requires 262.1202).

N*-Ethyl-1-(naphthalen-2-yl)but-3-en-2-amine, **122*¹⁵⁷



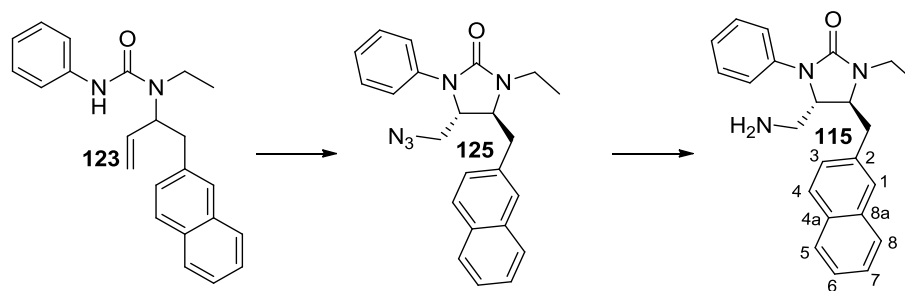
LiAlH₄ (0.45 g, 12.0 mmol) was added at 0 °C to a solution of the amide **121** (0.48 g, 2.0 mmol) in THF, and the resulting mixture was allowed to warm to r.t. and stirred for 5 h, then at reflux overnight. An aqueous solution of NaOH (15% w/v) was added at 0 °C dropwise, then the mixture was filtered through Celite[®], washed with THF and the filtrate concentrated under reduced pressure to give the *title amine* **122** as a yellow oil (0.4 g, 88%). *R*_F: 0.2 (92:8, CH₂Cl₂-MeOH); *v*_{max}/cm⁻¹ (film) 3059, 2968, 1685, 1494, 1284, 1119, 747; *δ*_H (500 MHz; CDCl₃) 7.85-7.74 (3H, m, naphthalenyl 3-, 4-, and 5- or 8-H), 7.65 (1H, s, naphthalenyl 1-H), 7.49-7.41 (2H, m, naphthalenyl 6- and 7-H), 7.34 (1H, dd, *J* 8.4 and 1.5, naphthalenyl 5- or 8-H), 5.75 (1H, ddd, *J* 16.8, 10.5 and 8.1, 3-H), 5.09 (1H, d, *J* 16.8, 4-H_A), 5.08 (1H, d, *J* 10.5, 4-H_B), 3.44 (1H, app. q, *J* 7.4, 2-H), 3.02 (1H, dd, *J* 13.4 and 7.3, 1-H_A), 2.97 (1H, dd, *J* 13.4 and 6.6, 1-H_B), 2.73 (1H, dq, *J* 11.8 and 7.1, ethyl 1-H_A), 2.52 (1H, dq, *J* 11.8 and 7.1, ethyl 1-H_B), 1.06 (3H, t, *J* 7.1, ethyl 2-H₃), *NH* not observed; *δ*_C (75 MHz; CDCl₃) 140.0 (C-3), 135.8 (naphthalenyl C-4a), 133.5 (naphthalenyl C-2), 132.3 (naphthalenyl C-8a), 128.0, 127.9, 127.7, 127.6, 127.5, 126.0, 125.4, (naphthalene 7 x CH), 116.8 (C-4), 62.9 (C-2), 42.3 (C-1), 41.6 (ethyl C-1), 14.8 (ethyl C-2); *m/z* (ES) 226.1 (100%, [M+H]⁺). HRMS Found: 226.1598 (C₁₆H₁₉N M+H requires 262.1590).

1-Ethyl-1-(1-(naphthalen-2-yl)but-3-en-2-yl)-3-phenylurea, **123**¹⁰⁰



The *title compound* **123** was prepared from the amine **122** (0.14 g, 0.6 mmol) and phenylisocyanate (0.15 mL, 1.3 mmol) in CH₂Cl₂ stirring at 35 °C for 3 hours, according to **general procedure B**.¹⁰⁰ The crude product was purified by flash chromatography (70:30, petrol–EtOAc) to give a yellow oil (80 mg, 47%). *R*_F: 0.7 (40:60, petrol–EtOAc); $\nu_{\max}/\text{cm}^{-1}$ (film) 2933, 2870, 1686, 1586, 1494, 1428, 1255, 1016, 696; δ_{H} (500 MHz; CDCl₃) 7.85-7.76 (3H, m, naphthalenyl 3-, 4- and 5- or 8-H), 7.68 (1H, s, naphthalenyl 1-H), 7.49-7.41 (2H, m, naphthalenyl 6- and 7-H), 7.39 (1H, dd, *J* 8.4 and 1.5, naphthalenyl 5- or 8-H), 7.23 (2H, d, *J* 7.2, phenyl 2- and 6-H), 7.21 (2H, d, *J* 7.2, phenyl 3- and 5-H), 7.00 (1H, dd, *J* 7.2 and 1.8, phenyl 4-H), 6.20 (1H, s, NH), 6.08 (1H, ddd, *J* 17.4, 10.5 and 5.2, 3-H), 5.31 (1H, d, *J* 17.4, 4-H_A), 5.29 (1H, d, *J* 10.5, 4-H_B), 4.79 (1H, app. q, *J* 6.8, 2-H), 3.35 (1H, dq, *J* 14.3 and 7.1, ethyl 1-H_A), 3.29 (1H, dd, *J* 13.6 and 7.0, 1-H_A), 3.19 (1H, dd, *J* 13.6 and 6.9, 1-H_B), 3.09 (1H, dq, *J* 14.3 and 7.1, ethyl 1-H_B), 1.13 (3H, t, *J* 7.1, ethyl 2-H₃); δ_{C} (75 MHz; CDCl₃) 155.0 (CO), 139.1 (phenyl C-1), 137.6 (C-3), 135.8 (naphthalenyl C-4a), 133.6 (naphthalenyl C-2), 132.3 (naphthalenyl C-8a), 128.8 (phenyl C-2 and C-6), 128.2, 127.8, 127.7, 127.6, 126.5, 126.1, 125.5 (naphthalene 7 x CH), 122.9 (phenyl C-4), 119.8 (phenyl C-3 and C-5), 117.0 (C-4), 60.5 (C-2), 40.5 (ethyl C-1), 38.5 (C-1), 15.0 (ethyl C-2); *m/z* (ES) 711.4 (100%, [2M+Na]⁺); HRMS Found: 367.1793 (C₂₃H₂₄N₂O M+Na requires 367.1780).

(4S*, 5S*)-4-(aminomethyl)-1-ethyl-5-(naphthalen-2-ylmethyl)-3-phenyl imidazolidin-2-one, compound 115^{124,137, 138}



The azide **125** was prepared from the allyl urea **123** (1.0 mmol), according to **general procedure F**.^{124,137} After elution through a silica plug (40:60, petrol–EtOAc) and evaporation under reduced pressure, the azide **125** was mixed triphenylphosphine (30 mg, 0.13 mmol) and stirred for 3 days according to **general procedure G**.¹³⁸ The crude product was purified by flash chromatography (50:50 → 100:0, petrol–EtOAc) to give the *title amine* **115**, as a yellow oil (22 mg, 25% over three steps). R_F : 0.1 (96:4, CH₂Cl₂–MeOH); $\nu_{\max}/\text{cm}^{-1}$ (film) 3053, 2929, 1666, 1590, 1243, 1020, 754; δ_H (500 MHz; CDCl₃) 7.85–7.76 (3H, m, naphthalenyl 3-, 4-, and 5- or 8-H), 7.65 (1H, s, naphthalenyl 1-H), 7.52–7.44 (2H, m, naphthalenyl 6- and 7-H), 7.31 (1H, dd, J 8.4 and 1.2, naphthalenyl 5- or 8-H), 7.22–7.19 (2H, m, phenyl 2- and 6-H), 7.03–7.01 (2H, m, phenyl 3- and 5-H), 6.94–6.91 (1H m, phenyl 4-H), 4.22 (1H, app. dt, J 6.3 and 4.7, 4-H), 3.86 (1H, app. dt, J 9.1 and 4.7, 5-H), 3.79 (1H, dq, J 14.5 and 7.2, ethyl 1-H_A), 3.33 (1H, dd, J 13.6 and 4.4, 5-CH_AH_B), 3.28 (1H, dq, J 14.5 and 7.2, ethyl 1-H_B), 2.87 (1H, dd, J 13.6 and 9.1, 5-CH_AH_B), 2.54 (1H, dd, J 13.6 and 4.2, 4-CH_AH_B), 2.47 (1H, dd, J 13.6 and 6.3, 4-CH_AH_B), 1.28 (3H, t, J 7.1, ethyl 2-H₃); δ_C (75 MHz; CDCl₃) 151.9 (CO), 147.9 (phenyl C-1), 133.6 (naphthalenyl C-4a), 133.5 (naphthalenyl C-2), 132.4 (naphthalenyl C-8a), 128.7 (naphthalene CH), 128.5 (phenyl C-2 and C-6), 128.0, 127.7, 127.5, 127.1, 126.4, 125.9 (naphthalene 6 x CH), 123.5 (phenyl C-3 and C-5), 121.7 (phenyl C-4), 82.0 (C-5), 58.9 (C-4), 44.8 (5-CH₂), 39.0 (4-CH₂), 37.6 (ethyl C-1), 12.3 (ethyl C-2); m/z (ES) 360.2 (100%, [M+H]⁺); HRMS Found: 360.2082 (C₂₃H₂₅N₃O M+H requires 360.2070).

5.4 General procedure for biological fluorimetric assay

Individual compounds were assayed using a BACE fluorimetric assay,¹⁵⁸ performed in 96 well plates. The following materials were employed. Quenched fluorescent peptide substrate: Swedish mutant APP sequence (SEVNLDAEFK) tagged with FAM and TAMRA (FAM-SEVNLDAEFK-TAMRA). Enzymes: recombinant BACE-1 (R&D System),¹⁵⁹ or recombinant BACE-2 (R&D System).¹⁵⁹ Inhibitor: β -secretase Inhibitor IV (Merck Chemicals).¹⁶⁰

The assay protocol was adapted from Hussain *et al.*¹⁵⁸ Recombinant BACE-1 (26.0 nM) or recombinant BACE-2 (3.0 nM) were diluted in enzyme buffer [100.0 mM sodium acetate, pH 4.5, 40.0 mM sodium chloride, 10% (v/v) glycerol, 0.2% (w/v) CHAPS]. The enzyme was incubated in the presence or absence of β -secretase Inhibitor IV (for positive control, at 0.01 mM for assaying BACE-1 and at 0.1 mM for assay BACE-2), DMSO (for negative control, 5% or 10%) or compounds (for assay compound activity) with shaking for 10 min at 25 °C. For detection of enzyme activity, the quenched fluorescent peptide substrate (5.0 μ M) was diluted in substrate buffer [100.0 mM sodium acetate, pH 4.5, 0.06% Triton x-100]. Enzyme buffer and substrate buffer were used at 1:1 ratio in each well to a total volume of 100 μ L. The fluorescence was measured using a Synergy HT Bio-Tek fluorimeter using KC4 software, with excitation and emission wavelengths set to 485 nm and 585 nm, respectively. Kinetic measurements over 20 minutes at 2 minutes intervals were performed, 2 duplicate readings were obtained and the results of each measurement were averaged during data processing. Each assay was performed at least three times. A representative 96-well plate layout is shown below (Figure 65).

	1	2	3	4	5	6	7	8	9	10	11	12
A	fluorescent quenched substrate only		negative control		positive control							
B	compounds at 100 μ M concentration in duplicates or compounds in serial dilution in duplicates											
F												
D												
E												
F												
G												
H												

Figure 65. 96 well plate layout of assessing BACE-1 and BACE-2 inhibition.

The compounds were configured as follow for the assay: for single concentration tests, a solution of 100 μ M of compound in enzyme buffer containing 5% or 10% DMSO (depending on compound solubility) was used, for dose response of selected compounds, an initial compound solution of 2000 μ M or 1000 μ M solution in DMSO (depending on compound solubility) was used and then serial diluted in DMSO in 5-9 steps, as low as 2.0 μ M.

The data were processed as follows: the average value of fluorescence unit (FU) of wells A1 and A2 was deducted from the average value of fluorescent unit obtained from each measurement corresponding to either the individual compound, the negative or the positive control. The overall kinetic measurements for each well were plotted in a graph FU vs time. A linear fit was applied to the measurement points and slopes corresponding to individual compounds, negative or positive control were derived. The compound inhibition % was calculated as:

$$\frac{\text{compound slope} - \text{positive control slope}}{\text{negative control slope} - \text{positive control slope}} \times 100$$

The results were reported as mean \pm SEM. Dose response data, expressed as percentage inhibition vs log[M], were fitted with a sigmoidal dose response model by using Origin Pro 8.6.

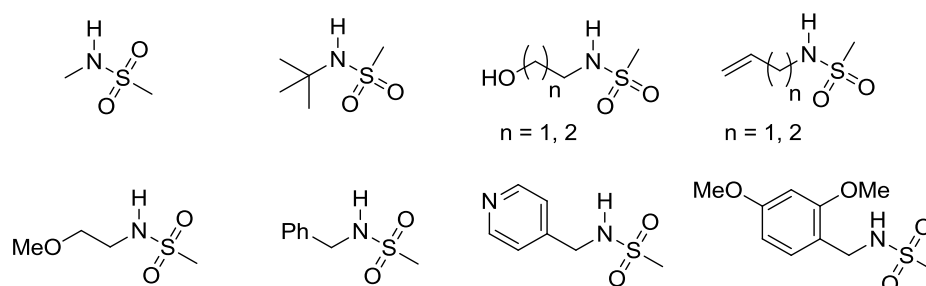
5.4.1 Protocol to assess the optimal concentration of BACE-2 to use in a fluorimetric assay

In order to optimise the recombinant BACE-2 for the assay, four different concentrations were assayed. The assay was performed according to the protocol described in Section 1.4, with the following exceptions. Recombinant BACE-2 was used in 30.0 nM, 17.2 nM, 8.6 nM and 3.0 nM diluted in an enzyme buffer, and the samples were incubated in the absence or in the presence of β -secretase Inhibitor IV (at 0.01 mM for BACE-1 and at 0.1 mM for BACE-2). A layout of the 96 well plate prepared is shown below (Figure 66).

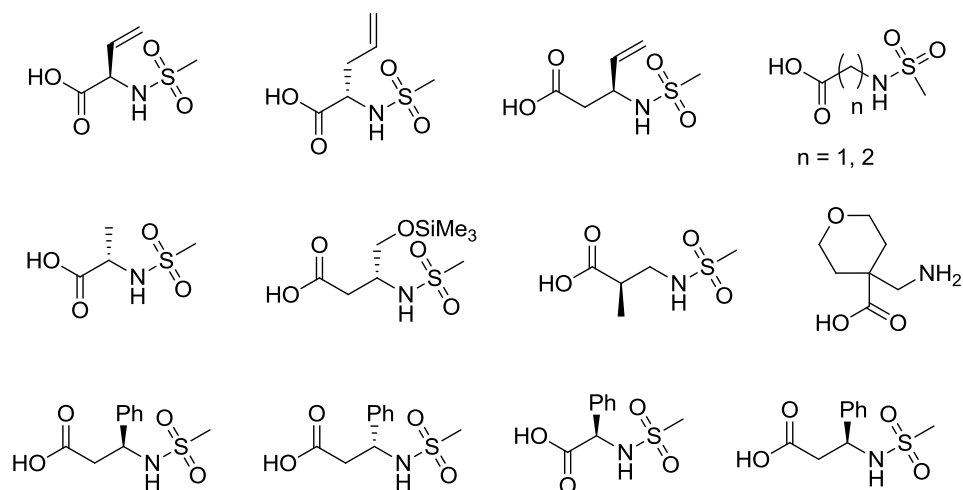
	1	2	3	4	5	6	7	8	9	10	11	12
A	fluorescent quenched substrate only		recombinant BACE-1 (26.0 nM)		recombinant BACE-1 (26.0 nM) + inhibitor							
B	recombinant BACE-2 (30.0 nM)		recombinant BACE-2 (17.2 nM)		recombinant BACE-2 (8.6 nM)		recombinant BACE-2 (3.0 nM)					
C	recombinant BACE-2 (30.0 nM)+ inhibitor		recombinant BACE-2 (17.2 nM) + inhibitor		recombinant BACE-2 (8.6 nM)+ inhibitor		recombinant BACE-2 (3.0 nM)+ inhibitor					

Figure 66. 96 well plate prepared to assess the optimal concentration of BACE-2.

Sulfonamides (methylsulfonyl is a virtual protecting group)

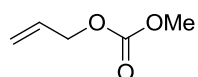
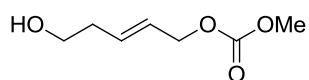
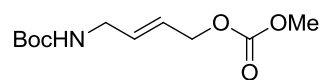
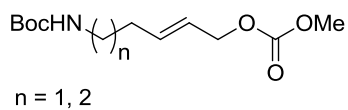
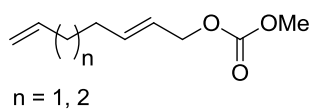


Amino acids derivatives (trimethyl silyl and methylsulfonyl are virtual protecting groups)

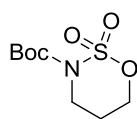
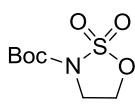
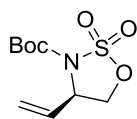
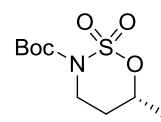
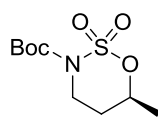
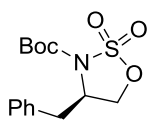
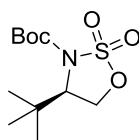
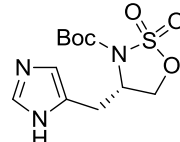
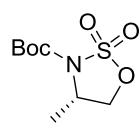
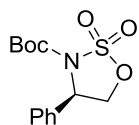
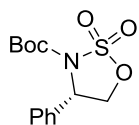
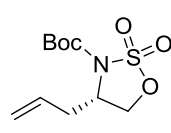
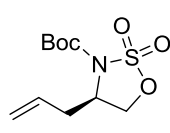
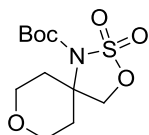
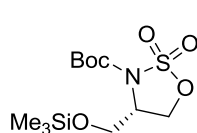


1.1.2 Electrophile building blocks

Allyl carbonates (*tert*-Butoxycarbonyl is a virtual protecting group)

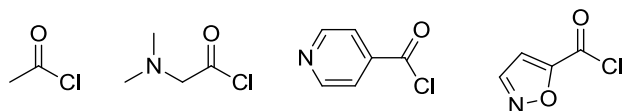


Cyclic sulfamidates (*tert*-Butoxycarbonyl is a virtual protecting group)

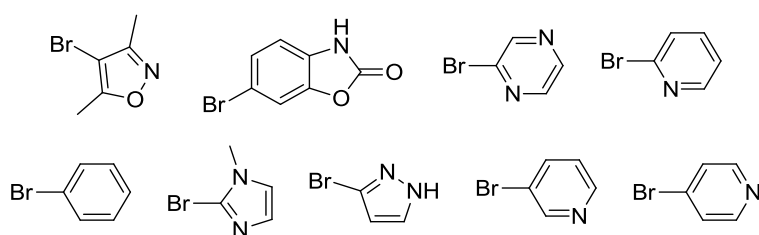


1.1.3 Derivatisation reagents

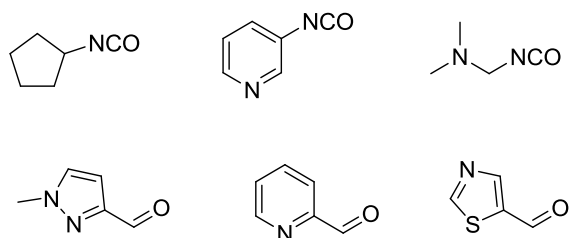
Acyl chlorides



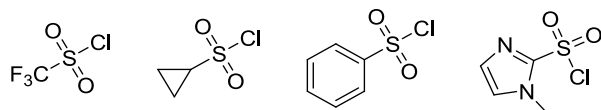
Aryl bromides



Isocyanates and aryl aldehyde

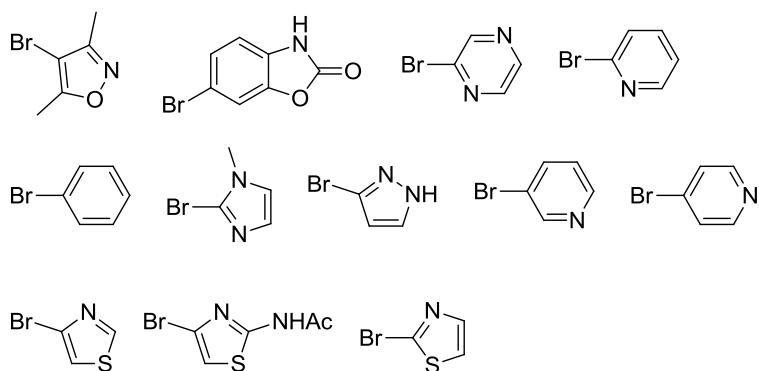


Sulfonyl chlorides

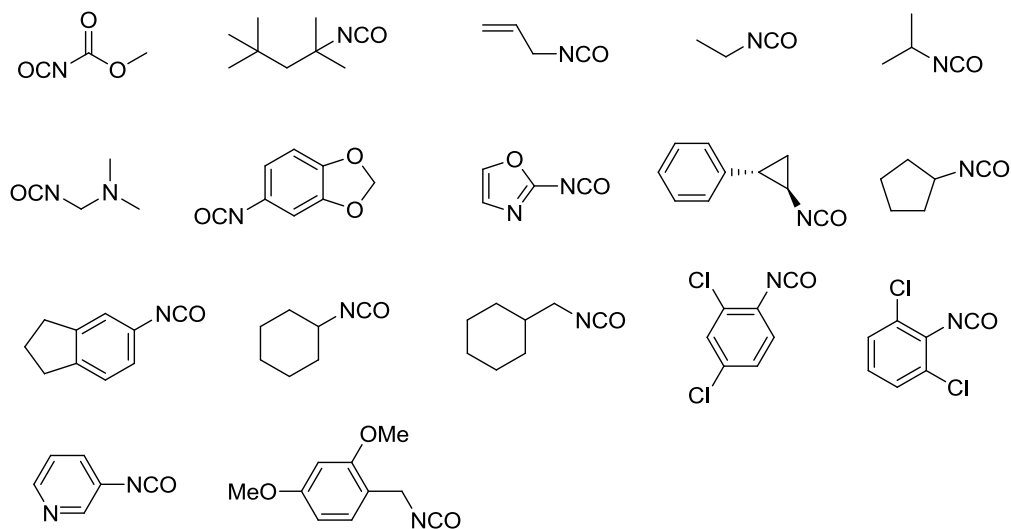


1.2 Virtual reactants employed in the virtual synthesis protocol to enumerate virtual *library B* (Section 2.3.2)

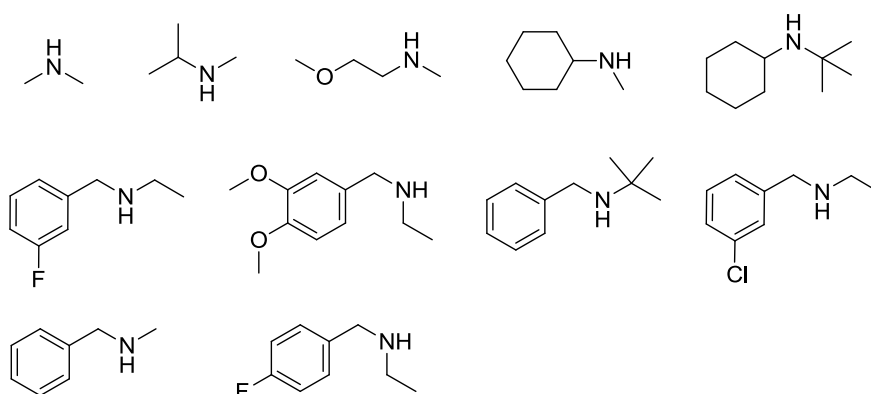
Aryl bromides



Isocyanates



Secondary amines



Other derivatisation reagents employed were the acyl chlorides, aryl aldehyde and sulfonyl chlorides included in Appendix 1.1.3.

1.3 Virtual reactions employed in the virtual synthesis protocol for the enumeration of *libraries A* and *B* (Section 2.3 and 2.3.2)

Table 19. Virtual coupling reactions between initial nucleophiles and electrophiles

Entry	Virtual reaction	Scheme
1	Iridium-catalysed asymmetric allylic amination ⁹⁸ with primary or secondary amines	
2	Amide formation from primary or secondary amines ¹⁶¹	
3	Nucleophilic opening of cyclic sulfamidates ⁹⁷	

Table 20. Virtual cyclisation reactions.

Entry	Virtual reaction	Scheme
1	Formation of cyclic urea (5- ^{162,163} , 6- ^{162, 164} , 7- ⁴ membered ring)	
a) CDI b) ^t BuOK in THF, then HCl/H ₂ O		
2	Formation of keto-piperidine ¹⁶⁵ (6- and 7- membered ring)	
3	Formation of cyclic secondary amine ¹⁶⁶ (5-, 6- and 7- membered ring)	
X= N, CH ₂ , O, C=O		
4	Ring-closing metathesis ⁹⁹ (5- and 6- membered ring)	
X= N, CH ₂ , O, C=O		

Table 21. Virtual Pd-catalysed cyclisation reactions.

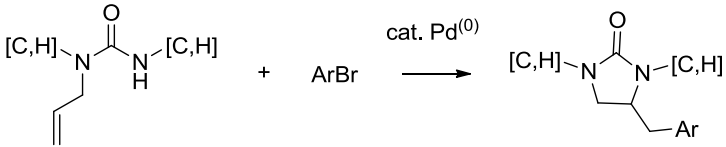
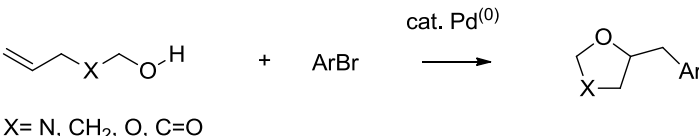
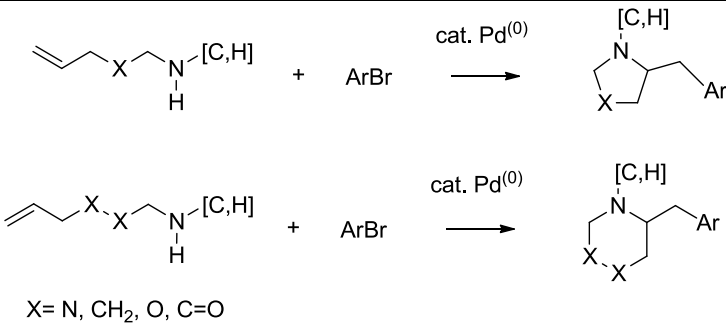
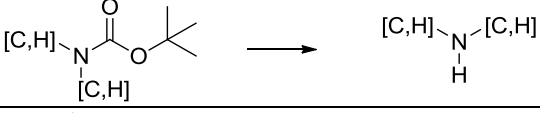
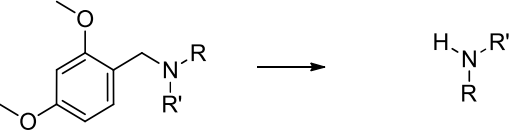
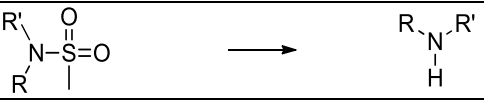
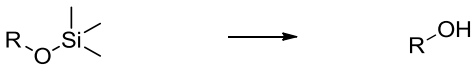
Entry	Virtual reaction	Scheme
1	Pd-catalysed urea intramolecular amino arylation ¹⁰⁰	
2	Pd-catalysed intramolecular oxyarylation ¹⁶⁷	 <p>X= N, CH₂, O, C=O</p>
3	Pd-catalysed intramolecular aminoarylation ¹⁶⁸ from primary or secondary amines (5- and 6- membered ring)	 <p>X= N, CH₂, O, C=O</p>

Table 22. Derivatisation reactions.

Entry	Virtual reaction	Scheme
1	Acylation of primary or secondary amines ^{161, 157}	
2	Reductive amination of primary or secondary amines ¹³⁶	
3	Arylation of primary or secondary amines ^{169, 170}	
4	Urea formation from secondary amines and isocyanates ¹⁰⁰ or <i>N</i> -acyl chlorides ¹⁷¹	
5	Thiourea formation from secondary amines ¹⁷²	
6	Sulfonamide formation from secondary amines ¹⁷³	

Table 23. Protecting group removal reactions

Entry	Virtual reaction	Scheme
1	Removal of Boc group ^{174, 175}	
2	Removal of Dmob group ¹⁷⁶	
3	Removal of sulfonamide ¹⁷⁷	
4	Removal of TMS group ^{178, 179, 180}	

Appendix 2. Virtual screening supplementary information

2.1 Predicted binding pose of representative ligands in the BACE-1 catalytic site, free from water molecules (Section 2.4)

Predicted binding poses of representative putative inhibitors of the imidazolidinone and amino tetrahydropyridine families are illustrated herein (Figure 67). The predicted binding poses were obtained by docking *library B* against the BACE-1 structure which did not contain water molecules in the catalytic site. The ligands chosen in the following illustrations are the same as the one represented in Figures 40, Section 2.4. The binding poses show that H-bond interactions were predicted to be formed with the catalytic aspartate residues, Asp32 and Asp228, even without the intermediary involvement of water molecules. The primary amine of the ligands was predicted to be protonated in the catalytic site of BACE-1 (pH 4.5).

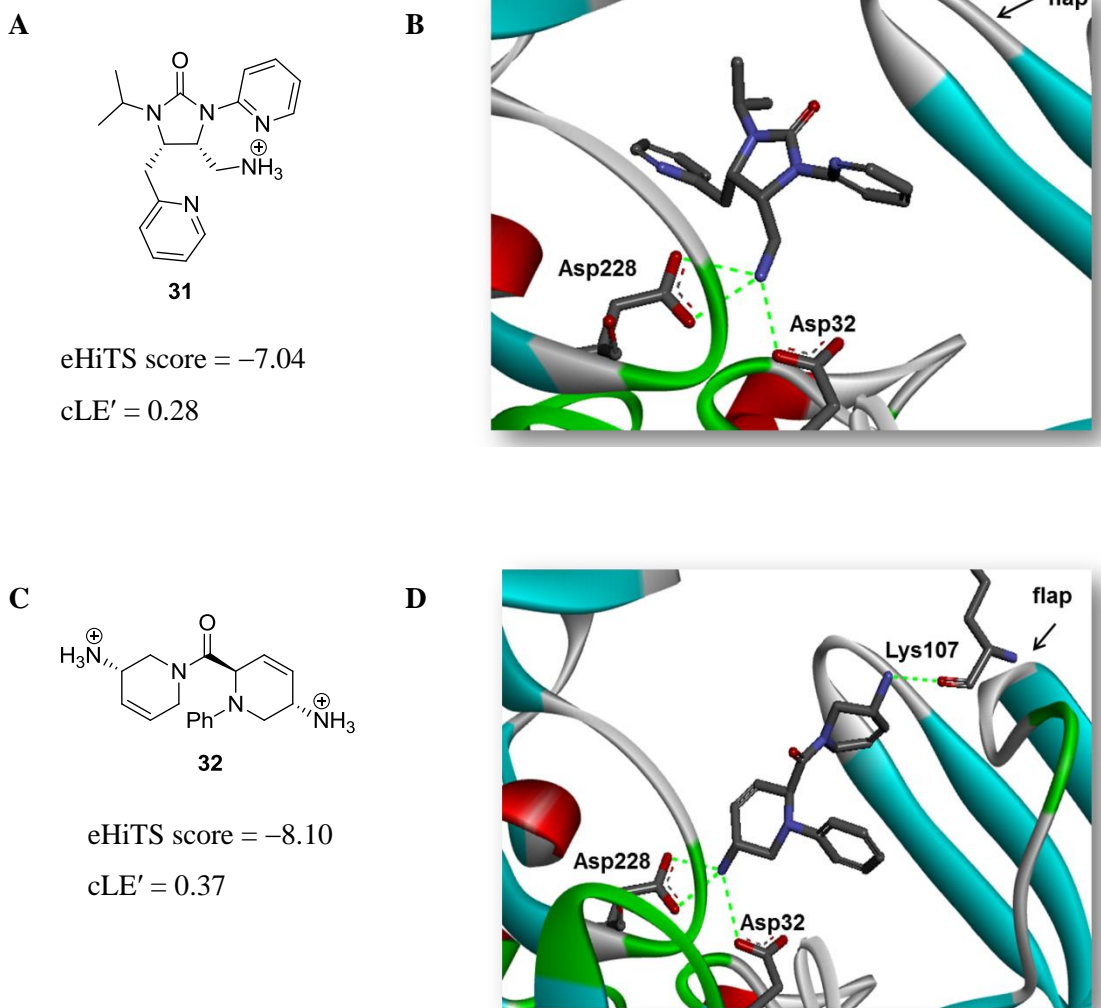


Figure 67. Predicted binding pose of representative members of the identified families of BACE-1 putative inhibitors. A) and C) 2D structure of the imidazolidinone putative inhibitor **31** (A) and of the amino tetrahydropyridine putative inhibitor **32** (C) in their protonated state. B) and D) 3D image of the predicted binding pose of the putative inhibitors **31** (B) and **32** (D) in the catalytic site of BACE-1. The predicted H-bond interactions are shown with green dotted lines. Asp32 and Asp228 form H-bonds with the protonated primary amine, NH_3^+ , of the putative inhibitor **31** (B). Asp32 and Asp228 form H-bonds with the protonated primary amine, NH_3^+ , of the putative inhibitor **32** (D), while Lys107, located in the flap region (Section 1.3.2), forms H-bond with the other protonated primary amine, NH_3^+ , of the putative inhibitor.

2.2 H-bond length evaluation (Section 2.4.1)

The length of the predicted H-bonds formed between the identified putative inhibitors and the BACE-1 catalytic site were measured and compared to the ones reported in X-ray crystal structures of BACE-1 complexes available in the literature. The length range was of 2.4-2.9 Å for H-bonds formed with Asp32 and Asp228, and 2.2-2.5 Å for the H-bonds formed with Wat1 and the other water molecules located in the catalytic site. These values were in agreement with the length range reported in the literature.^{82, 86} Examples are illustrated in Figure 68 and Figure 69.

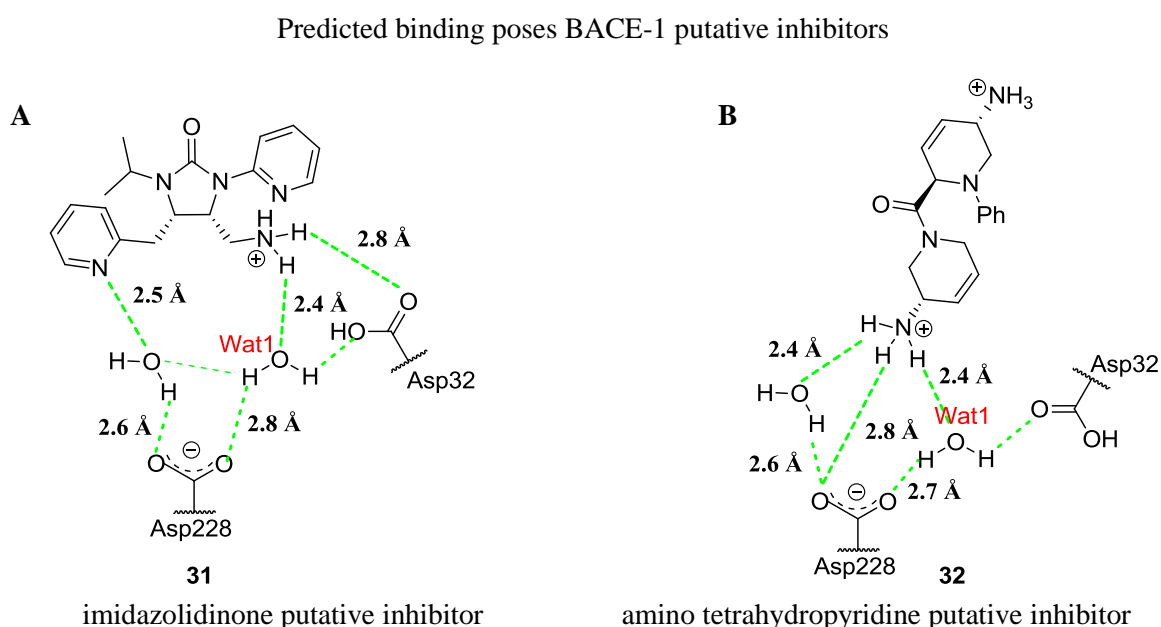


Figure 68. Length of H-bonds formed amongst putative inhibitors and aminoacidic residues in the catalytic site of BACE-1. Two-dimensional representation of the predicted H-bonds formed by the imidazolidinone putative inhibitors **31** (A) and the amino tetrahydropyridine putative inhibitors **32** (B). The H-bond lengths of the predicted H-bonds of the putative inhibitors is in the range of 2.4-2.8 Å.

X-ray crystal structures of known BACE-1

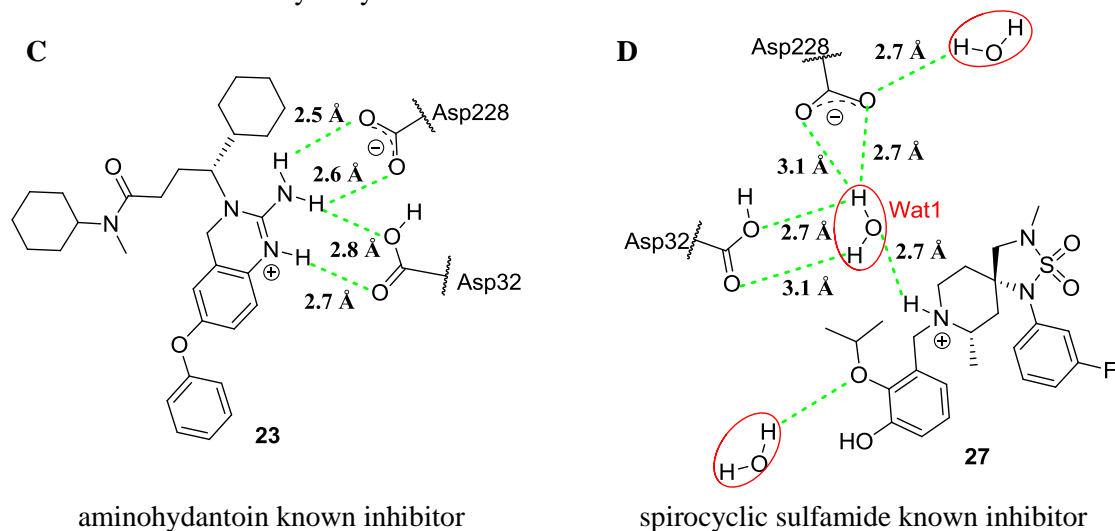


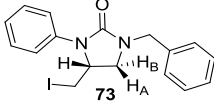
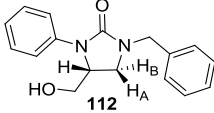
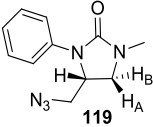
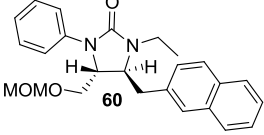
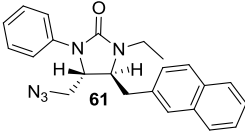
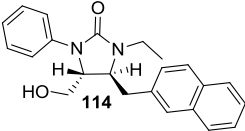
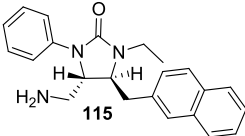
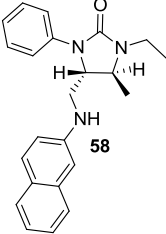
Figure 69. Length of H-bonds formed amongst known inhibitors and aminoacidic residues in the catalytic site of BACE-1. Two-dimensional representation of the predicted H-bonds formed by the known inhibitors **23**²⁸ (C) and **27**⁸⁶ (D) (Section 1.44 and 1.4.5). The H-bond lengths in the known X-ray crystal structures are in the range of 2.5-3.1 Å; of 2.4-2.8 Å.

Appendix 3. Stereochemical assignment of the synthesised imidazolidinones (Section 3.2.2.1 and 3.3.2.3)

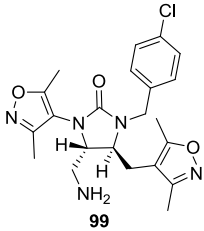
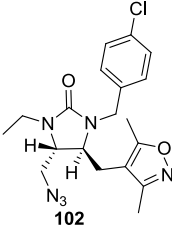
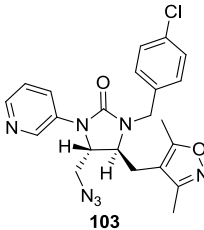
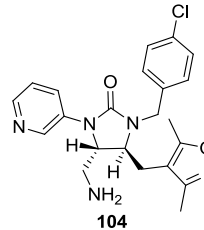
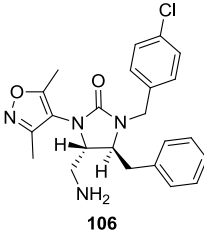
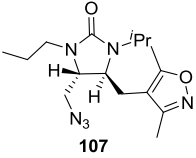
Table 24. Summary of the *J* values of the signals of the diagnostic protons of the urea ring system in the synthesised imidazolidinones.

R = H, CH₂Ar

Entry	Compound ^a	<i>J</i> (4-H/5-H)		Relative Configuration
		<i>syn</i>	<i>anti</i>	
1 ^b		8.9	6.0	-
2 ^b		<i>ca.</i> 9.0	5.1	-
3		7.7	4.0	-
4		8.5	6.3	-
5		9.2	4.6	-

Entry	Compound ^a	<i>J</i> (4-H/5-H)		Relative Configuration
		<i>syn</i>	<i>anti</i>	
6		8.9	4.7	-
7		9.2	5.2	-
8		9.1	4.6	-
9		-	3.0	<i>trans</i>
10		-	3.0	<i>trans</i>
11		-	4.5	<i>trans</i>
12		-	<i>ca.</i> 4.7	<i>trans</i>
13		-	<i>ca.</i> 5.2	<i>trans</i>

Entry	Compound ^a	<i>J</i> (4-H/5-H)		Relative Configuration
		<i>syn</i>	<i>anti</i>	
14	 93	-	4.3	<i>trans</i>
15	 94	-	ca. 3.8	<i>trans</i>
16	 95	-	4.1	<i>trans</i>
17	 97	-	ca. 3.7	<i>trans</i>
18	 111	-	4.4	<i>trans</i>
19	 98	-	ca. 5.0	<i>trans</i>

Entry	Compound ^a	<i>J</i> (4-H/5-H)		Relative Configuration
		<i>syn</i>	<i>anti</i>	
20	 99	-	ca. 4.6	<i>trans</i>
21	 102	-	ca. 4.7	<i>trans</i>
22	 103	-	ca. 5.1	<i>trans</i>
23	 104	-	3.2	<i>trans</i>
24	 106	-	4.7	<i>trans</i>
25	 107	-	3.0	<i>trans</i>

^aThe synthesised compounds were racemic, therefore the relative configuration is shown; ^bThe relative *syn* and *anti* relationship was confirmed by NOE experiment.

Appendix 4. Biological data supplementary information

4.1 Dose responses curves of active imidazolidinones (Section 4.2)

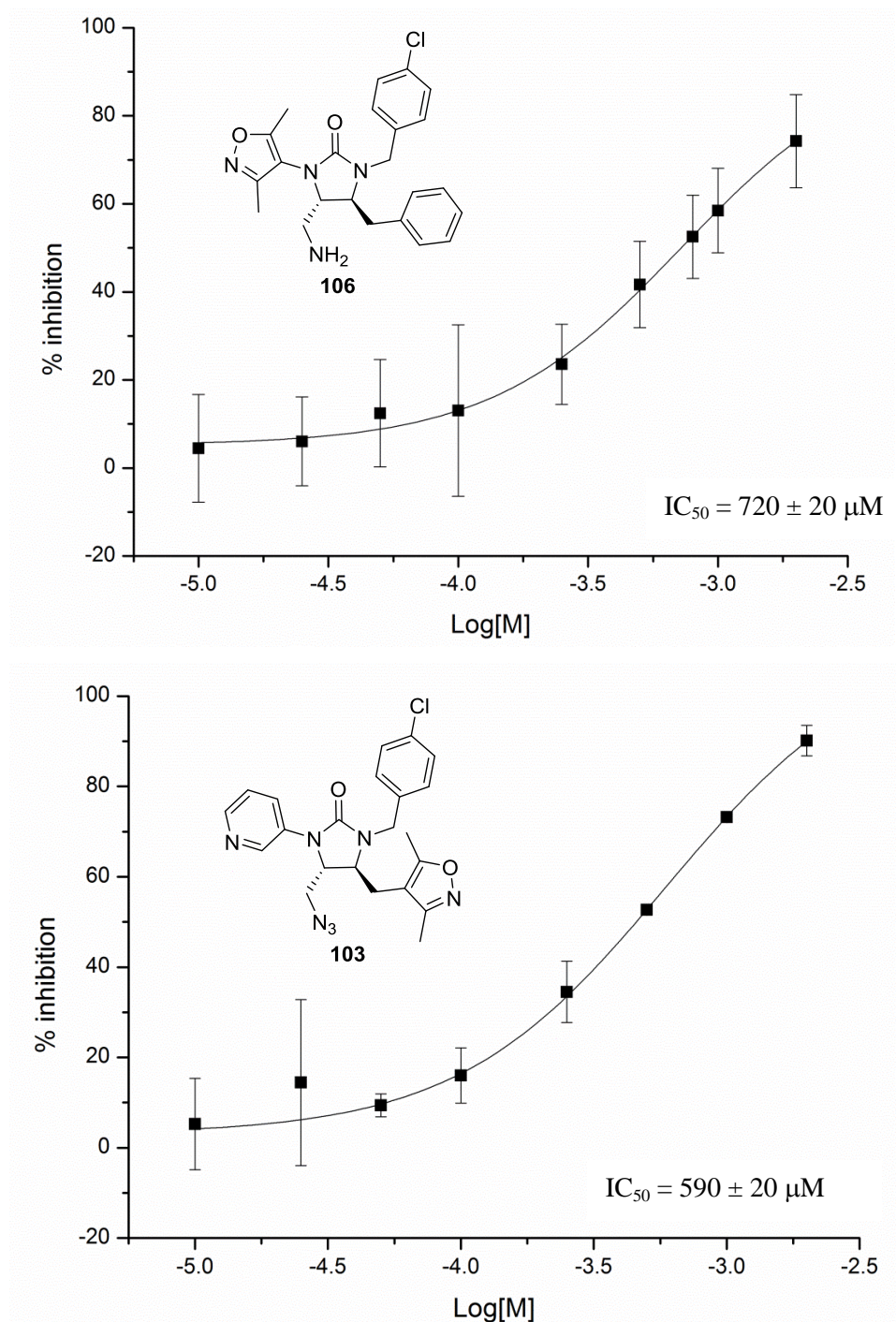


Figure 70. Dose response curves of the imidazolidinone 106 and 103. Compounds 106 and 103 were introduced in Section 4.2, Table 15, entry 2 and 9.

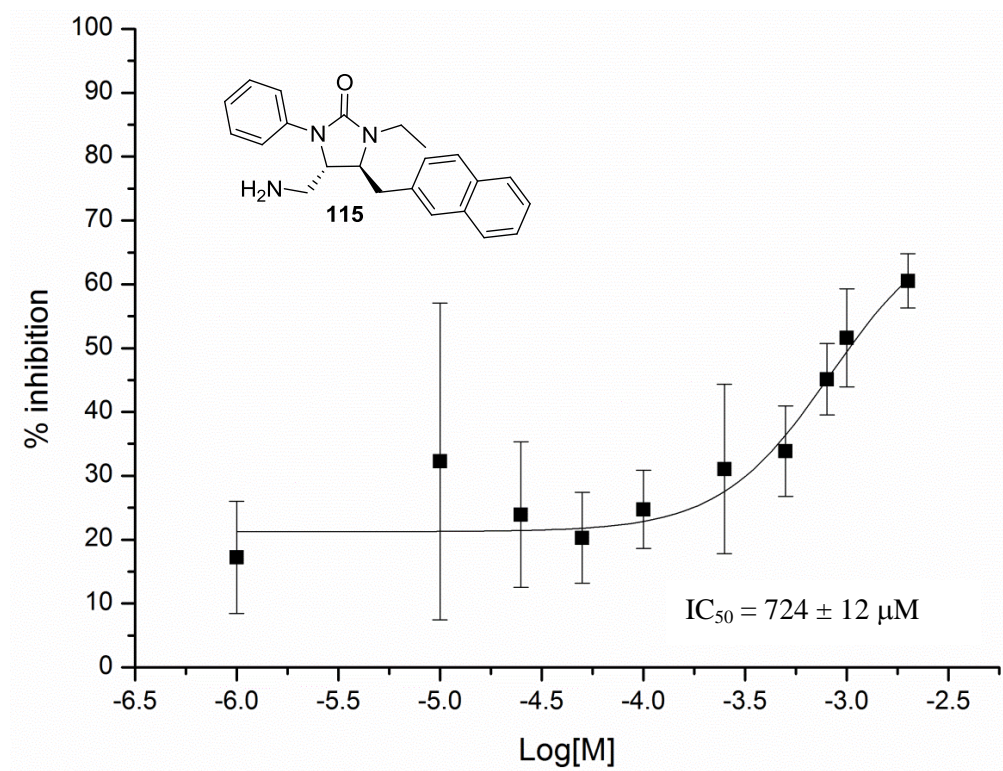


Figure 71. Dose response curves of the imidazolidinone 115. Compound 115 was introduced in Section 4.3.3, Table 17, entry 4.

4.2 Assessing the optimal concentration of BACE-2 for biological fluorimetric assay

In order to assay selected compounds against BACE-2 (Section 4.4.1), a homolog of BACE-1, the optimal concentration of BACE-2 to use in the fluorimetric assay was evaluated. The fluorescence resulting from BACE-2 cleavage of the peptide substrate was compared to that emitted by BACE-1 (26.0 nM). The signal was recorded over 20 minutes, at intervals of 2 minutes; the results are shown below (Figure 72).

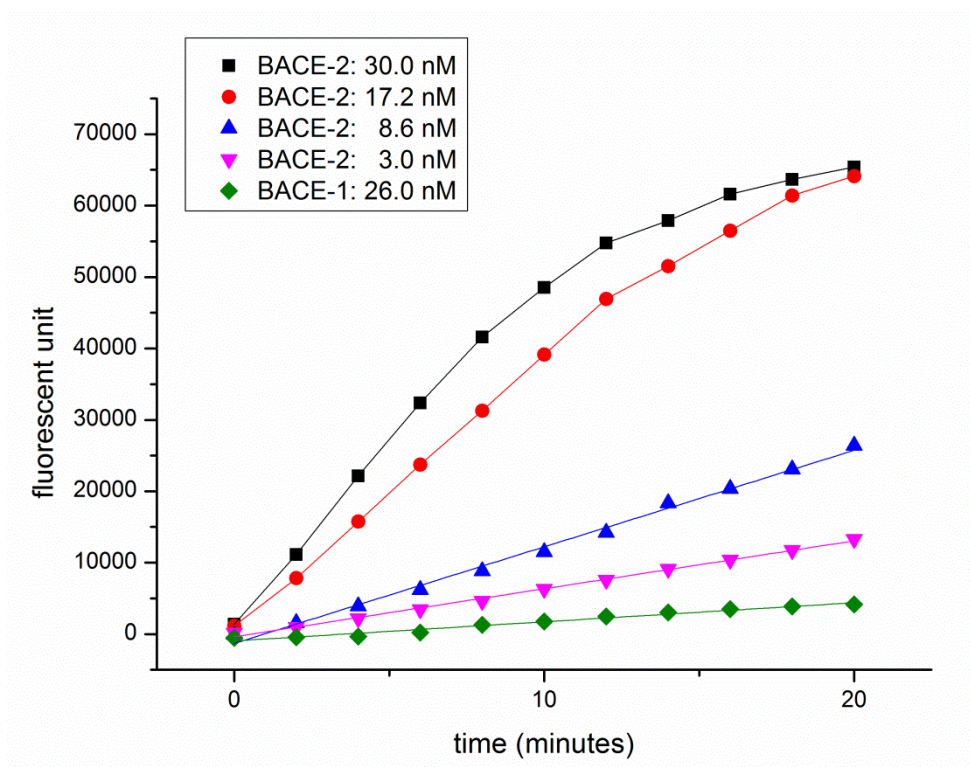


Figure 72. Fluorescence signal emitted by the fluorescent quenched peptide substrate, cleaved by BACE-2 enzyme. The most similar fluorescence emission trend, in comparison to BACE-1 at 26.0 nM (green line), was obtained using 3.0 nM of BACE-2 (pink line).

As shown in the graph, the relative fluorescence emission using *ca.* 10 times less BACE-2, 3.0 mM, (pink line) was similar to that seen with BACE-1, 26.0 nM, (green line). A higher quantity of BACE-2 (8.6, 17.2 and 30.0 nM) gave a much higher value of fluorescent emission. Inhibition of BACE-2 by β -secretase inhibitor IV was also assessed. β -secretase inhibitor IV was used at 0.01 nM to assay BACE-1 and at 0.1 mM to assay BACE-2^a. The signal was recorder over 20 minutes, at intervals of 2 minutes; the results are shown below (Figure 73).

^a Details of assay preparation are described in Section 5.4.1

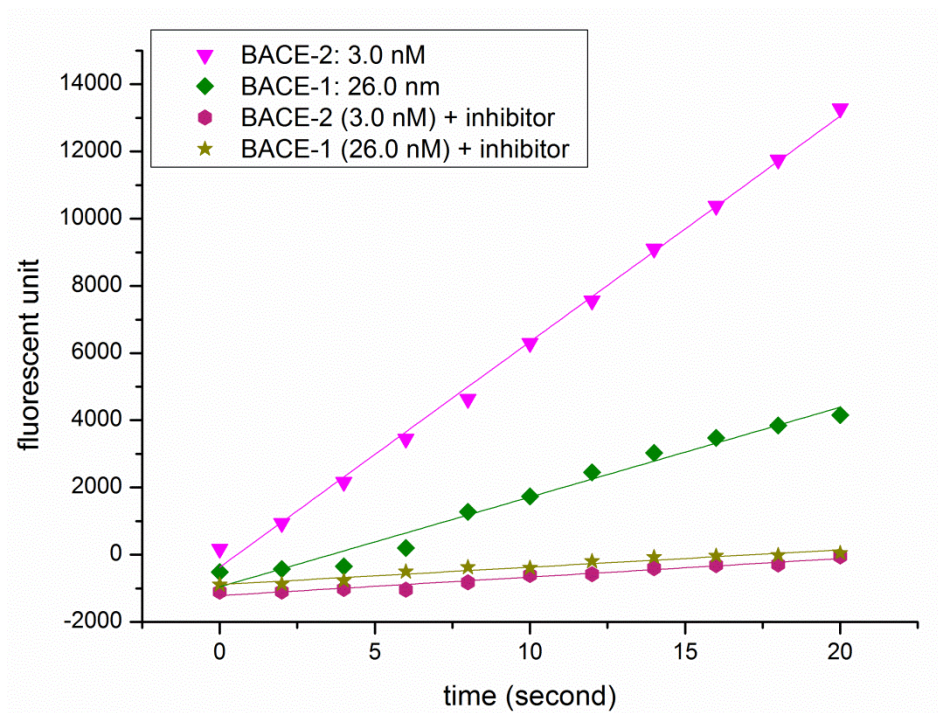


Figure 73. Inhibition of BACE-2 by β -secretase inhibitor IV. Yellow and purple lines show inhibition of BACE-1 (yellow line) and BACE-2 (purple line) by β -secretase inhibitor IV, compared to non-inhibited BACE-1 (green line) and BACE-2 (pink line) activity.

The reduced fluorescence signals obtained when BACE-1 or BACE-2 cleaves the substrate, in the presence of the β -secretase inhibitor IV, showed a similar linear trend (yellow and purple line). For BACE-2 assays a concentration of 3.0 nM was used to assay selected compounds (Section 4.4 and 5.4).

Reference

1. C. A. Lipinski, F. Lombardo, B. W. Dominy and P.J. Feeney, *Adv. Drug Deliver. Rev.*, 1997, **23**, 3-25.
2. A. Nadin, C. Hattotuwigama and I. Churcher, *Angew. Chem. Int. Edit.*, 2012, **51**, 1114-1122.
3. J. B. Baell, *J. Chem. Inf. Model.*, 2012, **53**, 39-55.
4. M. P. Gleeson, *J. Med. Chem.*, 2008, **51**, 817-834.
5. R. Mannhold and A. Petrauskas, *QSAR Comb. Sci.*, 2003, **22**, 466-475.
6. A. Monge, A. Arrault, C. Marot and L. Morin-Allory, *Mol. Divers.*, 2006, **10**, 389-403.
7. M. Congreve, R. Carr, C. Murray and H. Jhoti, *Drug Discov. Today*, 2003, **8**, 876-877.
8. T. Oprea, *J. Comput. Aid. Mol. Des.*, 2000, **14**, 251-264.
9. L. M. Mayr and D. Bojanic, *Curr. Opin. Pharmacol.*, 2009, **9**, 580-588.
10. M. Rossi, B. Rotblat, K. Ansell, I. Amelio, M. Caraglia, G. Misso, F. Bernassola, C. N. Cavasotto, R. A. Knight, A. Ciechanover and G. Melino, *Cell. Death Dis.*, 2014, **5**, e1203.
11. C. Madiraju, K. Welsh, M. P. Cuddy, P. H. Godoi, I. Pass, T. Ngo, S. Vasile, E. A. Sergienko, P. Diaz, S.-I. Matsuzawa and J. C. Ree, *J. Biomol. Screen.*, 2012, **17**, 163-176.
12. E. Siebring-van Olst, C. Vermeulen, R. X. de Menezes, M. Howell, E. F. Smit and V. W. van Beusechem, *J. Biomol. Screen.*, 2013, **18**, 453-461.
13. J. P. Overington, B. Al-Lazikani and A. L. Hopkins, *Nat. Rev. Drug Discov.*, 2006, **5**, 993-996.
14. P. J. Hajduk, J. Dinges, J. M. Schkeryantz, D. Janowick, M. Kaminski, M. Tufano, D. J. Augeri, A. Petros, V. Nienaber, P. Zhong, R. Hammond, M. Coen, B. Beutel, L. Katz and S. W. Fesik, *J. Med. Chem.*, 1999, **42**, 3852-3859.
15. S. D. Hanton, *Chem. Rev.*, 2001, **101**, 527-570.
16. D. A. Erlanson, A. C. Braisted, D. R. Raphael, M. Randal, R. M. Stroud, E. M. Gordon and J. A. Wells, *P. Natl. Acad. Sci. USA*, 2000, **97**, 9367-9372.

17. V. L. Nienaber, P. L. Richardson, V. Klighofer, J. J. Bouska, V. L. Giranda and J. Greer, *Nat. Biotechnol.*, 2000, **18**, 1105-1108.
18. P. J. Hajduk, A. Gomtsyan, S. Didomenico, M. Cowart, E. K. Bayburt, L. Solomon, J. Severin, R. Smith, K. Walter, T. F. Holzman, A. Stewart, S. McGaraughty, M. F. Jarvis, E. A. Kowaluk and S. W. Fesik, *J. Med. Chem.*, 2000, **43**, 4781-4786.
19. R. Nguyen and I. Huc, *Angew. Chem. Int. Edit.*, 2001, **40**, 1774-1776.
20. B. J. Rachele, ed., *Library Design, Search Methods, and Applications of Fragment-Based Drug Design*, American Chemical Society, 2011.
21. T. J. Marrone, J. M. Briggs and J. A. McCammon, *Annu. Rev. Pharmacol.*, 1997, **37**, 71-90.
22. D. B. Kitchen, H. Decornez, J. R. Furr and J. Bajorath, *Nat. Rev. Drug Discov.*, 2004, **3**, 935-949.
23. Z. Zsoldos, D. Reid, A. Simon, B. S. Sadjad and A. P. Johnson, *Curr. Protein Pept. Sc.*, 2006, **7**, 421-435.
24. A. Srinivas Reddy, S. Priyadarshini Pati, P. Praveen Kumar, H. N. Pradeep and G. Narahari Sastry, *Curr. Protein Pept. Sc.*, 2007, **8**, 329-351.
25. R. M. Christoph Sotriffer (Editor), Hugo Kubinyi, Gerd Folkers, *Virtual Screening*, Wiley-VCH, Weinheim, Germany, 2011.
26. G. M. Morris, D. S. Goodsell, R. S. Halliday, R. Huey, W. E. Hart, R. K. Belew and A. J. Olson, *J. Comput. Chem.*, 1998, **19**, 1639-1662.
27. C. Abad-Zapatero, *Expert Opin. Drug Dis.*, 2007, **2**, 469-488.
28. R. A. E. Carr, M. Congreve, C. W. Murray, and D. C. Rees, *Drug Discov. Today*, 2005, **10**, 987-992.
29. C. W. Murray and D. C. Rees, *Nat. Chem.*, 2009, **1**, 187-192.
30. C. H. Reynolds, B. A. Tounge and S. D. Bembenek, *J. Med. Chem.*, 2008, **51**, 2432-2438.
31. C. Yung-Chi and W. H. Prusoff, *Biochem. Pharmacol.*, 1973, **22**, 3099-3108.
32. A. L. Hopkins, G. M. Keseru, P. D. Leeson, D. C. Rees and C. H. Reynolds, *Nat. Rev. Drug Discov.*, 2014, **13**, 105-121.

33. W. R. J. D. Galloway, A. Isidro-Llobet and D. R. Spring, *Nat. Commun.*, 2010, **1**, 80.
34. S. J. Haggarty, *Curr. Opin. Chem. Biol.*, 2005, **9**, 296-303.
35. W. H. B. Sauer and M. K. Schwarz, *J. Chem. Inf. Comp. Sci.*, 2003, **43**, 987-1003.
36. D. Pizzirani, T. Kaya, P. A. Clemons and S. L. Schreiber, *Org. Lett.*, 2010, **12**, 2822-2825.
37. I. U. Khand, G. R. Knox, P. L. Pauson, W. E. Watts and M. I. Foreman, *J. Chem. Soc., Perkin Trans. 1*, 1973, 977-981.
38. T. James, P. MacLellan, G. M. Burslem, I. Simpson, J. A. Grant, S. Warriner, V. Sridharan and A. Nelson, *Org. Biomol. Chem.*, 2014, **12**, 2584-2591.
39. S. K. Maurya, M. Dow, S. Warriner and A. Nelson, *Beilstein J. Org. Chem.*, 2013, **9**, 775-785.
40. S. L. Cole and R. Vassar, *J. Biol. Chem.*, 2008, **283**, 29621-29625.
41. C. E. Hunt and A. J. Turner, *FEBS J.*, 2009, **276**, 1845-1859.
42. L.-F. Lue, Y.-M. Kuo, A. E. Roher, L. Brachova, Y. Shen, L. Sue, T. Beach, J. H. Kurth, R. E. Rydel and J. Rogers, *Am. J. Pathol.*, 1999, **155**, 853-862.
43. R. von Bernhardi and G. Ramirez, *Biological Research*, 2001, **34**, 123-128.
44. J. Avila, J. J. Lucas, M. Pérez and F. Hernández, *Physiol. Rev.*, 2004, **84**, 361-384.
45. S. Sankaranarayanan, E. A. Price, G. Wu, M.-C. Crouthamel, X.-P. Shi, K. Tugusheva, K. X. Tyler, J. Kahana, J. Ellis, L. Jin, T. Steele, S. Stachel, C. Coburn and A. J. Simon, *J. Pharmacol. Exp. Ther.*, 2008, **324**, 957-969.
46. F. M. Laird, H. Cai, A. V. Savonenko, M. H. Farah, K. He, T. Melnikova, H. Wen, H.-C. Chiang, G. Xu, V. E. Koliatsos, D. R. Borchelt, D. L. Price, H.-K. Lee and P. C. Wong, *J. Neurosci.*, 2005, **25**, 11693-11709.
47. D. De Pietri Tonelli, M. Mihailovich, A. Di Cesare, F. Codazzi, F. Grohovaz and D. Zacchetti, *Nucl. Acids Res.*, 2004, **32**, 1808-1817.
48. ProteinDataBank, www.rcsb.org/pdb/home/home.do, accessed January 2011.
49. J. Yuan, S. Venkatraman, Y. Zheng, B. M. McKeever, L. W. Dillard and S. B. Singh, *J. Med. Chem.*, 2013, **56**, 4156-4180.

50. L. Hong, R. T. Turner, G. Koelsch, D. Shin, A. K. Ghosh and J. Tang, *Biochemistry-US*, 2002, **41**, 10963-10967.
51. L. Hong, G. Koelsch, X. Lin, S. Wu, S. Terzyan, A. K. Ghosh, X. C. Zhang and J. Tang, *Science*, 2000, **290**, 150-153.
52. L. Hong and J. Tang, *Biochemistry-US*, 2004, **43**, 4689-4695.
53. B. Clarke, L. Cutler, E. Demont, C. Dingwall, R. Dunsdon, J. Hawkins, C. Howes, I. Hussain, G. Maile, R. Matico, J. Mosley, A. Naylor, A. O'Brien, S. Redshaw, P. Rowland, V. Soleil, K. J. Smith, S. Sweitzer, P. Theobald, D. Vesey, D. S. Walter and G. Wayne, *Bioorg. Med. Chem. Lett.*, 2010, **20**, 4639-4644.
54. L. Touloukhou, W. J. Metzler, M. R. Witmer, R. A. Copeland and J. Marcinkeviciene, *J. Biol. Chem.*, 2003, **278**, 4582-4589.
55. N. Yu, Hayik SA, B. Wang, N. Liao, C. H. Reynolds and K. M. Merz, *J. Chem. Theory Comp.*, 2006, **2**, 1057.
56. X. Cai, T. Golde and S. Younkin, *Science*, 1993, **259**, 514-516.
57. M. Citron, D. B. Teplow and D. J. Selkoe, *Neuron*, 1995, **14**, 661-670.
58. J. M. Sauder, J. W. Arthur and R. L. Dunbrack Jr, *J. Mol. Biol.*, 2000, **300**, 241-248.
59. R. Postina, A. Schroeder, I. Dewachter, J. Bohl, U. Schmitt, E. Kojro, C. Prinzen, K. Endres, C. Hiemke, M. Blessing, P. Flamez, A. E. Godaux, F. van Leuven, and F. Fahrenholz, *J. Clin. Invest.*, 2004, **113**, 1456-1464.
60. G. B. McGaughey and M. K. Holloway, *Expert Opin. Drug Dis.*, 2007, **2**, 1129-1138.
61. A. K. Ghosh, D. Shin, G. Koelsch, X. Lin, J. Ermolieff and J. Tang, *J. Am. Chem. Soc.*, 2000, **122**, 3522-3523.
62. J. Marcinkeviciene, Y. Luo, N. R. Graciani, A. P. Combs and R. A. Copeland, *J. Biol. Chem.*, 2001, **276**, 23790-23794.
63. V. John, J. P. Beck, M. J. Bienkowski, S. Sinha and R. L. Heinrikson, *J. Med. Chem.*, 2003, **46**, 4625-4630.
64. E. W. Baxter and A. B. Reitz, *Annual Reports in Medicinal Chemistry*, 2005, **40**, 35-48.

65. F. Wångsell, F. Russo, J. Sävmarker, Å. Rosenquist, B. Samuelsson and M. Larhed, *Bioorg. Med. Chem. Lett.*, 2009, **19**, 4711-4714.
66. F. Wångsell, K. Gustafsson, I. Kvarnström, N. Borkakoti, M. Edlund, K. Jansson, J. Lindberg, A. Hallberg, Å. Rosenquist and B. Samuelsson, *Eur. J. Med. Chem.*, 2010, **45**, 870-882.
67. W. Yang, W. Lu, Y. Lu, M. Zhong, J. Sun, A. E. Thomas, J. M. Wilkinson, R. V. Fucini, M. Lam, M. Randal, X.-P. Shi, J. W. Jacobs, R. S. McDowell, E. M. Gordon and M. D. Ballinger, *J. Med. Chem.*, 2006, **49**, 839-842.
68. S. J. Stachel, C. A. Coburn, T. G. Steele, K. G. Jones, E. F. Loutzenhiser, A. R. Gregro, H. A. Rajapakse, M.-T. Lai, M.-C. Crouthamel, M. Xu, K. Tugusheva, J. E. Lineberger, B. L. Pietrak, A. S. Espeseth, X.-P. Shi, E. Chen-Dodson, M. K. Holloway, S. Munshi, A. J. Simon, L. Kuo and J. P. Vacca, *J. Med. Chem.*, 2004, **47**, 6447-6450.
69. A. Ghosh, S. Gemma and J. Tang, *Neurotherapeutics*, 2008, **5**, 399-408.
70. R. Machauer, S. Veenstra, J.-M. Rondeau, M. Tintelnot-Blomley, C. Betschart, U. Neumann and P. Paganetti, *Bioorg. Med. Chem. Lett.*, 2009, **19**, 1361-1365.
71. J. E. Meredith, L. A. Thompson, J. H. Toyn L. Marcin, D. M. Barten, J. Marcinkeviciene, L. Kopcho, Y. Kim, A. Lin, V. Guss, C. Burton, L. Iben, C. Polson, J. Cantone, M. Ford, D. Drexler, T. Fiedler, K. A. Lentz, J. E. Grace, J. Kolb, J. Corsa, M. Pierdomenico, K. Jones, R. E. Olson, J. E. Macor and C. F. Albright., *J. Pharmacol. Exp. Ther.*, 2008, **326**, 502-513.
72. S. Hanessian, G. Yang, J.-M. Rondeau, U. Neumann, C. Betschart and M. Tintelnot-Blomley, *J. Med. Chem.*, 2006, **49**, 4544-4567.
73. A. Lerchner, R. Machauer, C. Betschart, S. Veenstra, H. Rueeger, C. McCarthy, M. Tintelnot-Blomley, A.-L. Jaton, S. Rabe, S. Desrayaud, A. Enz, M. Staufenbiel, P. Paganetti, J.-M. Rondeau and U. Neumann, *Bioorg. Med. Chem. Lett.*, 2010, **20**, 603-607.
74. K. P. Moore, H. Zhu, H. A. Rajapakse, G. B. McGaughey, D. Colussi, E. A. Price, S. Sankaranarayanan, A. J. Simon, N. T. Pudvah, J. H. Hochman, T. Allison, S. K. Munshi, S. L. Graham, J. P. Vacca and P. G. Nantermet, *Bioorg. Med. Chem. Lett.*, 2007, **17**, 5831-5835.
75. M. S. Malamas, K. Barnes, M. Johnson, *et al.*, *Bioorg. Med. Chem. Lett.*, 2010, **18**, 630-639.
76. M. S. Malamas, A. Robichaud, J. Erdei, D. Quagliato, W. Solvibile, P. Zhou, K. Morris, J. Turner, E. Wagner, K. Fan, A. Olland, S. Jacobsen, P. Reinhart, D. Riddell and M. Pangalos, *Bioorg. Med. Chem. Lett.*, 2010, **20**, 6597-6605.

77. M. S. Malamas, J. Erdei, I. Gunawan, K. Barnes, Y. Hui, M. Johnson, A. Robichaud, P. Zhou, Y. Yan, W. Solvibile, J. Turner, K. Y. Fan, R. Chopra, J. Bard and M. N. Pangalos, *Bioorg. Med. Chem. Lett.*, 2011, **21**, 5164-5170.
78. M. Congreve, D. Aharony, J. Albert, O. Callaghan, J. Campbell, R. A. E. Carr, G. Chessari, S. Cowan, P. D. Edwards, M. Frederickson, R. McMenemy, C. W. Murray, S. Patel and N. Wallis, *J. Med. Chem.*, 2007, **50**, 1124-1132.
79. Y.-S. Wang, C. Strickland, J. H. Voigt, M. E. Kennedy, B. M. Beyer, M. M. Senior, E. M. Smith, T. L. Nechuta, V. S. Madison, M. Czarniecki, B. A. McKittrick, A. W. Stamford, E. M. Parker, J. C. Hunter, W. J. Greenlee and D. F. Wyss, *J. Med. Chem.*, 2009, **53**, 942-950.
80. S. W. Gerritz, W. Zhai, S. Shi, S. Zhu, J. H. Toyn, J. E. Meredith, L. G. Iben, C. R. Burton, C. F. Albright, A. C. Good, A. J. Tebben, J. K. Muckelbauer, D. M. Camac, W. Metzler, L. S. Cook, R. Padmanabha, K. A. Lentz, M. J. Sofia, M. A. Poss, J. E. Macor and L. A. Thompson, *J. Med. Chem.*, 2012, **55**, 9208-9223.
81. D. C. Cole, J. R. Stock, R. Chopra, R. Cowling, J. W. Ellingboe, K. Y. Fan, B. L. Harrison, Y. Hu, S. Jacobsen, L. D. Jennings, G. Jin, P. A. Lohse, M. S. Malamas, E. S. Manas, W. J. Moore, M.-M. O'Donnell, A. M. Olland, A. J. Robichaud, K. Svenson, J. Wu, E. Wagner and J. Bard, *Bioorg. Med. Chem. Lett.*, 2008, **18**, 1063-1066.
82. E. W. Baxter, K. A. Conway, L. Kennis, F. Bischoff, M. H. Mercken, H. L. De Winter, C. H. Reynolds, B. A. Tounge, C. Luo, M. K. Scott, Y. Huang, M. Braeken, S. M. A. Pieters, D. J. C. Berthelot, S. Masure, W. D. Bruinzeel, A. D. Jordan, M. H. Parker, R. E. Boyd, J. Qu, R. S. Alexander, D. E. Brenneman and A. B. Reitz, *J. Med. Chem.*, 2007, **50**, 4261-4264.
83. M. S. Malamas, J. Erdei, I. Gunawan, K. Barnes, M. Johnson, Y. Hui, J. Turner, Y. Hu, E. Wagner, K. Fan, A. Olland, J. Bard and A. J. Robichaud, *J. Med. Chem.*, 2009, **52**, 6314-6323.
84. I. V. Efremov, F. F. Vajdos, K. A. Borzilleri, S. Capetta, H. Chen, P. H. Dorff, J. K. Dutra, S. W. Goldstein, M. Mansour, A. McColl, S. Noell, C. E. Oborski, T. N. O'Connell, T. J. O'Sullivan, J. Pandit, H. Wang, B. Wei and J. M. Withka, *J. Med. Chem.*, 2012, **55**, 9069-9088.
85. J. C. Barrow, S. R. Stauffer, K. E. Rittle, P. L. Ngo, Z. Yang, H. G. Selnick, S. L. Graham, S. Munshi, G. B. McGaughey, M. K. Holloway, A. J. Simon, E. A. Price, S. Sankaranarayanan, D. Colussi, K. Tugusheva, M.-T. Lai, A. S. Espeseth, M. Xu, Q. Huang, A. Wolfe, B. Pietrak, P. Zuck, D. A. Levorse, D. Hazuda and J. P. Vacca, *J. Med. Chem.*, 2008, **51**, 6259-6262.
86. M. A. Brodney, G. Barreiro, K. Ogilvie, E. Hajos-Korcsok, J. Murray, F. Vajdos, C. Ambroise, C. Christoffersen, K. Fisher, L. Lanyon, J. Liu, C. E. Nolan, J. M. Withka, K. A. Borzilleri, I. Efremov, C. E. Oborski, A. Varghese and B. T. O'Neill, *J. Med. Chem.*, 2012, **55**, 9224-9239.

87. W. Xu, G. Chen, W. Zhu and Z. Zuo, *Bioorg. Med. Chem. Lett.*, 2010, **20**, 5763-5766.
88. W. Xu, G. Chen, W. Zhu and Z. Zuo, *Bioorg. Med. Chem. Lett.*, 2010, **20**, 6203-6207.
89. N. Y. Mok, J. Chadwick, K. A. B. Kellett, E. Casas-Arce, N. M. Hooper, A. P. Johnson and C. W. G. Fishwick, *J. Med. Chem.*, 2013, **56**, 1843-1852.
90. J. Viklund, K. Kolmodin, G. Nordvall, B.-M. Swahn, M. Svensson, Y. Gravenfors and F. Rahm, *Acs Med. Chem. Lett.*, 2014, **5**, 440-445.
91. J. K. Atwal, Y. Chen, C. Chiu, D. L. Mortensen, W. J. Meilandt, Y. Liu, C. E. Heise, K. Hoyte, W. Luk, Y. Lu, K. Peng, P. Wu, L. Rouge, Y. Zhang, R. A. Lazarus, K. Scarce-Levie, W. Wang, Y. Wu, M. Tessier-Lavigne and R. J. Watts, *Sci. Transl. Med.*, 2011, **3**, 84ra43.
92. A. K. Ghose, V. N. Viswanadhan and J. J. Wendoloski, *J. Phys. Chem. A*, 1998, **102**, 3762-3772.
93. J. M. Stevenson and P. D. Mulready, *J. Am. Chem. Soc.*, 2003, **125**, 1437-1438.
94. PipelinePilot, <http://accelrys.com/products/pipeline-pilot/>, accessed April 2011.
95. Corina, <http://www.molecular-networks.com/products>, accessed April 2011.
96. H. F. G. Velec, H. Gohlke and G. Klebe, *J. Med. Chem.*, 2005, **48**, 6296-6303.
97. A. J. Williams, S. Chakthong, D. Gray, R. M. Lawrence and T. Gallagher, *Org. Lett.*, 2003, **5**, 811-814.
98. P. Tosatti, A. Nelson and S. P. Marsden, *Org. Biomol. Chem.*, 2012, **10**, 3147-3163.
99. D. Rix, F. Caijo, I. Laurent, F. Boeda, H. Clavier, S. P. Nolan and M. Mauduit, *J. Org. Chem.*, 2008, **73**, 4225-4228.
100. J. A. Fritz, J. S. Nakhla and J. P. Wolfe, *Org. Lett.*, 2006, **8**, 2531-2534.
101. Maestro, <http://www.schrodinger.com/products/14/12/>, accessed June 2011.
102. SPROUT, <http://www.simbiosys.ca/sprout/>, accessed February 2011.
103. P. A. Johnson, Z. Zsoldos, V. Aniko, *et al.*, 'Computational tools for fragment based drug design', in ACS National Meeting, 22-26/03/2009, Salt Lake City, UT, United States, 2009.

104. R. Silvestri, *Med. Res. Rev.*, 2009, **29**, 295-338.
105. J. Albert, G. Chessari and P. Edwards, '*Novel 2-Aminopyrimidine derivatives and their use*', WO2007058581, 05/24/2007
106. G. R. Bhisetti, S. D. Britt, J. H. Come, D. D. Deninger, C. A. Lepre, M. A. Murcko, J. O. Saunders and T. Wang, '*Inhibitors of bace*', WO2002088101 A2, 07/11/2002
107. J. A. Fritz and J. P. Wolfe, *Tetrahedron*, 2008, **64**, 6838-6852.
108. C. Gnamm, G. Franck, N. Miller, T. Stork, K. Brödner and G. Helmchen, *Synthesis*, 2008, **2008**, 3331-3350.
109. J. R. Parikh and W. v. E. Doering, *J. Am. Chem. Soc.*, 1967, **89**, 5505-5507.
110. G. Wittig and U. Schöllkopf, *Chem. Ber.*, 1954, **87**, 1318-1330.
111. T. Moriwake, S.-I. Hamano, D. Miki, S. Saito and S. Torii, *Chem. Lett.*, 1986, **15**, 815-818.
112. D. R. Anton and R. H. Crabtree, *Organometallics*, 1983, **2**, 621-627.
113. I. S. Mikhel, H. Rügger, P. Butti, F. Camponovo, D. Huber and A. Mezzetti, *Organometallics*, 2008, **27**, 2937-2948.
114. C. A. Kiener, C. Shu, C. Incarvito, and J. F. Hartwig, *J. Am. Chem. Soc.*, 2003, **125**, 14272-14273.
115. P. Tosatti, A. J. Campbell, D. House, A. Nelson and S. P. Marsden, *J. Org. Chem.*, 2011, **76**, 5495-5501.
116. N. R. Candeias, F. Montalbano, P. M. S. D. Cal, and P. M. P. Gois, *Chem. Rev.*, 2010, **110**, 6169-6193.
117. T. Fukuyama, C.-K. Jow and M. Cheung, *Tetrahedron Lett.*, 1995, **36**, 6373-6374.
118. J. M. Weiss, H. N. Jimenez, G. Li, M. April, M. A. Uberti, M. D. Bacolod, R. M. Brodbeck and D. Doller, *Bioorg. Med. Chem. Lett.*, 2011, **21**, 4891-4899.
119. R. F. Heck, *J. Am. Chem. Soc.*, 1968, **90**, 5526-5531.
120. M. Anteunis and D. Danneels, *Org. Magn. Resonance*, 1975, **7**, 345-348.
121. V. H. Rawal and M. P. Cava, *Tetrahedron Lett.*, 1985, **26**, 6141-6142.

122. N. J. Tom, W. M. Simon, H. N. Frost and M. Ewing, *Tetrahedron Lett.*, 2004, **45**, 905-906.
123. N. R. Candeias, P. M. S. D. Cal, V. André, M. T. Duarte, L. F. Veiros and P. M. P. Gois, *Tetrahedron*, 2010, **66**, 2736-2745.
124. C. J. Moody, P. A. Hunt and C. Smith, *ARKIVOC*, 2000, 698-706.
125. H. Staudinger and J. Meyer, *Helv. Chim. Acta*, 1919, **2**, 635-646.
126. A. J. Blacker, M. Roy, S. Hariharan, A. Upare, A. Jagtap, K. Wankhede, S. K. Mishra, D. Dube, S. Bhise, S. Vishwasrao and N. Kadam, *Org. Process Res. Dev.*, 2010, **15**, 331-338.
127. G. Clayden, Warren and Wothers, *Organic Chemistry*, 1st edn., Oxford University press, Oxford, 2001.
128. X. Sun, Y. Wang, H. Qing, M. A. Christensen, Y. Liu, W. Zhou, Y. Tong, C. Xiao, Y. Huang, S. Zhang, X. Liu and W. Song, *FASEB J.*, 2005, **19**, 739-749.
129. R. Yan, J. B. Munzner, M. E. Shuck and M. J. Bienkowski, *J. Biol. Chem.*, 2001, **276**, 34019-34027.
130. R. R. Ahmed, C. J. Holler, R. L. Webb, F. Li, T. L. Beckett and M. P. Murphy, *J. Neurochem.*, 2010, **112**, 1045-1053.
131. S. J. Stachel, T. G. Steele, A. Petrocchi, S. J. Haugabook, G. McGaughey, M. Katharine Holloway, T. Allison, S. Munshi, P. Zuck, D. Colussi, K. Tugasheva, A. Wolfe, S. L. Graham and J. P. Vacca, *Bioorg. Med. Chem. Lett.*, 2012, **22**, 240-244.
132. P. Ferrara, H. Gohlke, D. J. Price, G. Klebe and C. L. Brooks, *J. Med. Chem.*, 2004, **47**, 3032-3047.
133. M. Feher and C. I. Williams, *J. Chem. Inf. Model.*, 2009, **49**, 1704-1714.
134. M. L. Verdonk, G. Chessari, J. C. Cole, M. J. Hartshorn, C. W. Murray, J. W. M. Nissink, R. D. Taylor and R. Taylor, *J. Med. Chem.*, 2005, **48**, 6504-6515.
135. W. C. Still, M. Kahn and A. Mitra, *J. Org. Chem.*, 1978, **43**, 2923-2925.
136. Y. Qiao, J. Gao, Y. Qiu, L. Wu, F. Guo, K. Kam-Wing Lo and D. Li, *Eur. J. Med. Chem.*, 2011, **46**, 2264-2273.
137. S. Knapp and A. T. Levorse, *J. Org. Chem.*, 1988, **53**, 4006-4014.

138. L. Banfi, G. Guanti, M. Paravidino and R. Riva, *Org. Biomol. Chem.*, 2005, **3**, 1729-1737.
139. P. Tosatti, J. Horn, A. J. Campbell, D. House, A. Nelson and S. P. Marsden, *Adv. Synth. Catal.*, 2010, **352**, 3153-3157.
140. F. R. Pinacho Crisóstomo, R. Carrillo, L. G. León T. Martín, J. M. Padrón and V. S. Martín, *J. Org. Chem.*, 2006, **71**, 2339-2345.
141. C. F. Gnamm, G. Franck, N. Miller, T. Stork, K. Brödner and G. Helmchen, *Synthesis*, 2008, 3331– 3350.
142. S. Chaffins, M. Brettreich and F. Wudl, *ChemInform*, 2002, **33**, 104-104.
143. J. Bornhöft, J. Siegwarth, C. Näther and R. Herges, *Eur. J. Org. Chem.*, 2008, **2008**, 1619-1624.
144. C. R. Smith, D. J. Mans, T. V. RajanBabu, S. E. Denmark and S. T. Nguyen, *Org. Synth.*, 2008, **85**, 238-247.
145. A. Rimkus and N. Sewald, *Org. Lett.*, 2002, **5**, 79-80.
146. L. A. Arnold, R. Imbos, A. Mandoli, A. H. M. de Vries, R. Naasz and B. L. Feringa, *Tetrahedron*, 2000, **56**, 2865-2878.
147. C. Zhong, Y. Wang, A. W. Hung, S. L. Schreiber and D. W. Young, *Org. Lett.*, 2011, **13**, 5556-5559.
148. Y. Kawaguchi, S. Yamauchi, K. Masuda, H. Nishiwaki, K. Akiyama, M. Maruyama, T. Sugahara, T. Kishida and Y. Koba, *Biosci. Biotech. Bioch.*, 2009, **73**, 1806-1810.
149. R. P. Trump, J. E. Cobb, B. G. Shearer, M. H. Lambert, R. T. Nolte, T. M. Willson, R. G. Buckholz, S. M. Zhao, L. M. Leesnitzer, M. A. Iannone, K. H. Pearce, A. N. Billin and W. J. Hoekstra, *Bioorg. Med. Chem. Lett.*, 2007, **17**, 3916-3920.
150. S. Mukherjee and B. List, *J. Am. Chem. Soc.*, 2007, **129**, 11336-11337.
151. F. C. Sequeira, B. W. Turnpenny and S. R. Chemler, *Angew. Chem. Int. Edit.*, 2010, **49**, 6365-6368.
152. W. F. McCalmont, J. R. Patterson, M. A. Lindenmuth, T. N. Heady, D. M. Haverstick, L. S. Gray and T. L. Macdonald, *Bioorg. Med. Chem.*, 2005, **13**, 3821-3839.

153. K. A. Tehrani, T. NguyenVan, M. Karikomi, M. Rottiers and N. De Kimpe, *Tetrahedron*, 2002, **58**, 7145-7152.
154. D. D. Dore, J. R. Burgeson, R. A. Davis and S. R. Hitchcock, *Tetrahedron Asymmetry*, 2006, **17**, 2386-2392.
155. S. G. Davies, J. A. Lee, P. M. Roberts, J. E. Thomson and C. J. West, *Tetrahedron*, 2012, **68**, 4302-4319.
156. J. A. Marshall and M. R. Palovich, *J. Org. Chem.*, 1998, **63**, 3701-3705.
157. T. Oka, T. Yasusa, T. Ando, M. Watanabe, F. Yoneda, T. Ishida and J. Knoll, *Bioorg. Med. Chem.*, 2001, **9**, 1213-1219.
158. I. Hussain, J. Hawkins, D. Harrison, C. Hille, G. Wayne, L. Cutler, T. Buck, D. Walter, E. Demont, C. Howes, A. Naylor, P. Jeffrey, M. I. Gonzalez, C. Dingwall, A. Michel, S. Redshaw and J. B. Davis, *J. Neurochem.*, 2007, **100**, 802-809.
159. R&DSsystem, www.rndsyste.ms.com, accessed October 2012.
160. Merk, <http://www.merckmillipore.co.uk/chemicals>, accessed June 2012.
161. J. L. Falcó, M. Piqué, M. González, I. Buirá, E. Méndez, J. Terencio, C. Pérez, M. Príncipe, A. Palomer and A. Guglietta, *Eur. J. Med. Chem.*, 2006, **41**, 985-990.
162. T. Fujimoto, Y. Imaeda, N. Konishi, K. Hiroe, M. Kawamura, G. P. Textor, K. Aertgeerts and K. Kubo, *J. Med. Chem.*, 2010, **53**, 3517-3531.
163. D. A. Favor, D. S. Johnson, J. T. Repine and A. D. White, 'Tetrahydro-pyridoazepin-8-ones and related compounds for the treatment of schizophrenia', WO2006103559, 05/10/2006
164. P. Thanigaimalai, K.-C. Lee, S.-C. Bang, J.-H. Lee, C.-Y. Yun, E. Roh, B.-Y. Hwang, Y. Kim and S.-H. Jung, *Bioorg. Med. Chem.*, 2010, **18**, 1135-1142.
165. K. Gáll-Istók, L. Sterk, G. Tóth, and G. Deák, *J. Heterocyclic Chem.*, 1984, **21**, 1045-1048.
166. K. Kitahara, T. Toma, J. Shimokawa, and T. Fukuyama, *Org. Lett.*, 2008, **10**, 2259-2261.
167. M. B. Hay, A. R. Hardin and J. P. Wolfe, *J. Org. Chem.*, 2005, **70**, 3099-3107.
168. J. E. Ney and J. P. Wolfe, *Angew. Chem. Int. Edit.*, 2004, **116**, 3689-3692.

169. H. Xu and C. Wolf, *Chem. Commun.*, 2009, 1715-1717.
170. J. F. Hartwig, M. Kawatsura, S. I. Hauck, K. H. Shaughnessy and L. M. Alcazar-Roman, *J. Org. Chem.*, 1999, **64**, 5575-5580.
171. A. El-Faham, S. N. Khattab, M. Abdul-Ghani, and F. Albericio, *Eur. J. Org. Chem.*, 2006, **2006**, 1563-1573.
172. Y. Nate, S. Yasuo, Y. Honma, H. Nakai, H. Wada, M. Takeda, H. Yabana and T. Nagao, *Chem. Pharm. Bull.*, 1987, **35**, 1935-1968.
173. G. Zhou, P. Ting, R. Aslanian and J. J. Piwinski, *Org. Lett.*, 2008, **10**, 2517-2520.
174. J. B. Springer, Y. H. Chang, K. I. Koo, O. M. Colvin, M. E. Colvin, M. E. Dolan, S. M. Delaney, J. L. Flowers and S. M. Ludeman, *Chem. Res. Toxicol.*, 2004, **17**, 1217-1226.
175. G. W. Kabalka, N.-S. Li and R. D. Pace, *Synthetic Comm.*, 1995, **25**, 2135-2143.
176. T. Yamauchi, K. Higashiyama, H. Kubo and S. Ohmiya, *Tetrahedron Asymmetry*, 2000, **11**, 3003-3015.
177. E. Alonso, D. J. Ramón and M. Yus, *Tetrahedron*, 1997, **53**, 14355-14368.
178. S. Murata, M. Suzuki and R. Noyori, *J. Am. Chem. Soc.*, 1979, **101**, 2738-2739.
179. J. Otera, Y. Niibo, S. Chikada and S. Ohmiya, *Synthesis*, 1988, **1988**, 328-329.
180. T. Schmittberger and D. Uguen, *Tetrahedron Lett.*, 1995, **36**, 7445-7448.